

Biomechanics at the workplace under hypogravity conditions

Présentée le 14 juin 2022

Faculté des sciences et techniques de l'ingénieur
Institut de génie électrique et électronique
Programme doctoral en génie civil et environnement

pour l'obtention du grade de Docteur ès Sciences

par

Tatiana VOLKOVA

Acceptée sur proposition du jury

Prof. D. Tuia, président du jury
Prof. V. Gass, directeur de thèse
Dr T. Reiter, rapporteur
Prof. M. Landgraf, rapporteur
Prof. K. Aminian, rapporteur

Learning never exhausts the mind.
— Leonardo da Vinci (1452-1519)

To all current and future astronauts...

Acknowledgements

This thesis was realized thanks the kind support of many people. I would like to express my sincere gratitude to all of them. Firstly, I would like to thank my supervisor Prof. Dr. Volker Gass, and my scientific advisor Prof. Dr. Claude Nicolier, who made this work possible. Their guidance and advice helped me through all the stages of writing my dissertation. I also want to thank Claude for the first time in my life, he awakened in me a burning desire not only to design working environments on the Moon / Mars, but also to become an astronaut myself. And also for his inspiration to learn how to fly an airplane.

I would also like to express my gratitude to my wonderful family and my beloved and supportive fiancée in general for their continued support and understanding in conducting my research and writing my dissertation. Your prayers for me have supported me every minute of this long journey.

I am deeply indebted to the Hofmann family for allowing me to install a swimming pool in their garden to conduct my first experiments on human performance in reduced gravity. I am also deeply indebted to the Grandshamps family for allowing me to continue experimenting on the grounds of their Swissub professional dive center. A big thanks to the Meyer family who also allowed me to do experiments out of the water at their home when it was not possible to do it at EPFL. Special thanks to all the participants (or "astronauts") of the experiments. Without you and your valuable data, this study would not have been possible.

I want to express my deep gratitude for the patience of Leonardo Citraro, who explained to me the basics of computer vision, which became one of my main research methods. Many thanks and appreciation to all my Space Innovation and eSpace colleagues (Martine, Yannick, Gilles, Gregoire, Tatiana, Julien, Michael, Candice), as well as Emma Sorrentino from the administration of the EDCE EPFL doctoral school for providing the necessary information for the successful preparation of this dissertation. Finally, I would like to thank God for accompanying me and protecting me throughout this difficult journey.

Lausanne, 10 May 2022

Abstract

Future short- and long-term missions to the Moon or Mars give rise to new technical and biomechanical issues that need to be addressed. These include requirements on the working and living conditions of astronauts under hypogravity, between 0 and 1G, as on Mars ($\frac{1}{3}$ G) and the Moon ($\frac{1}{6}$ G). One of these challenges involves the design of a workplace for astronauts on the surface of the Moon and Mars under hypogravity conditions. The main goal of this thesis is to establish guidelines for workplace design based on human biomechanics: specifically sitting workplaces and handling areas under hypogravity conditions. Such a workplace could be used in long-term space missions in order to maximize worker performance and minimize the risks of musculoskeletal injuries. The recommendations for design, maintenance, and usage of this workplace for static, dynamic, and repetitive tasks in different gravity conditions (1G, $\frac{1}{3}$ G, $\frac{1}{6}$ G) are provided.

Four methods were combined in these studies: direct, indirect, subjective, and observation. Studies of workplace performance for repetitive tasks, tasks with joystick, assembling, and handwriting showed a highly significant ($p < 0.01$)^I increase in overall mental workload with increasing gravity and a moderate increase ($p < 0.05$) in overall mental workload for tasks with the keyboard. Postural studies were conducted because force exertions should always be considered in relation to posture. The results on body position change show that there is a tendency for the upper limbs of the human body and the trunk to tilt backward in the sitting position when performing static and dynamic tasks under hypogravity. Gravity change resulted in a significant ($p < 0.01$) change in torso inclination, as well as upper extremities inclination. The use of the marker-less tracking method allowed to capture these trends, invisible to the eye, at the end of the task, when the participant began to be tired, as this deviation occurred gradually.

Fatigue experiments have revealed two trends. First, a significant relationship ($p < 0.01$) was found between endurance time and gravity levels: with an increase in gravity, endurance

^I*** $p < 0.01$ - results are highly significant, ** $p < 0.05$ - results have moderate significance, * $p < 0.10$ - results have marginal significance.

decreases for all participants conducting a static task. Second, there is a marginal relationship ($p < 0.1$) between the subjective weighted workload and the level of gravity: with an increase in gravity, the weighted workload for all participants increases when performing the same task. The same trend was observed for dynamic and repetitive tasks for both males and females. In summary, the proposed objective method, combined with subjective assessment, is useful for the study of human fatigue.

Experiments on comfort in a sitting position and performing static and dynamic tasks, showed that there is a significant comfort increase in different parts of the body, especially the back ($p < 0.01$), neck ($p < 0.01$), upper and lower back ($p < 0.01$) with decreasing gravity level.

The combination of multidisciplinary data can expand the ergonomics of the hypogravity workspace in general. Because it takes into account physical fatigue in the model, such a design of the workplace will require less effort from the worker. In addition, it can reduce overuse injuries and musculoskeletal disorders that are common in many workplace situations and lead to absence and auxiliary expenses.

Furthermore, digital human simulation based on experimental data for modeling and further predictions can be enriched with collected data for new simulations and optimization problems. Consequently, this will lead not only to the emergence of new knowledge, but also to the development of empirical data-based guidelines and standards for the design of workplaces under hypogravity.

Keywords: workplace, posture study, fatigue, comfort at the workplace, human-centered design, Moon exploration, Mars exploration, task performance, reduced gravity, digital human modeling, markerless motion capture.

Résumé

Les futures missions de courte et longue durée vers la Lune ou Mars soulèvent des questions techniques et biomécaniques nouvelles. Cela concerne en particulier les exigences sur les conditions de travail et de vie des astronautes en hypogravité, entre 0 et 1G, notamment sur Mars ($\frac{1}{3}G$) et la Lune ($\frac{1}{6}G$). Un de ces défis concerne la conception d'un environnement de travail pour les astronautes à la surface de la Lune et de Mars dans des conditions d'hypogravité.

L'objectif principal de cette thèse est d'établir des recommandations, basées sur la biomécanique humaine, pour la conception d'environnements de travail : en particulier les postes assis et les zones de manutention dans des conditions d'hypogravité. De tels environnements pourraient être utilisés lors de missions spatiales de longue durée afin de maximiser les performances des astronautes, et minimiser les risques de blessures musculo-squelettiques. Des recommandations sont formulées pour la conception, l'entretien et l'utilisation de ces environnements de travail sur des tâches statiques, dynamiques et répétitives dans différentes conditions de gravité (1G, $\frac{1}{3}G$, $\frac{1}{6}G$).

Quatre méthodes ont été combinées dans ces études : directe, indirecte, subjective et d'observation. Des études sur les performances en environnement de travail pour les tâches répétitives, les tâches faisant appel à la manipulation de joysticks, l'assemblage, et l'écriture manuscrite, ont montré une augmentation très significative ($p < 0.01$)^{II} de la charge mentale globale avec une gravité croissante, et une augmentation modérée ($p < 0.05$) de la charge mentale globale liée à l'usage d'un clavier. Des études posturales ont été menées, les efforts devant être toujours être considérés en relation avec la posture. Les résultats concernant le changement de position du corps montrent qu'il existe une tendance pour les membres supérieurs du corps humain et le tronc à s'incliner vers l'arrière en position assise lors de l'exécution de tâches statiques et dynamiques en hypogravité. Le changement de gravité provoque un changement significatif ($p < 0.01$) de l'inclinaison du torse, ainsi que de l'inclinaison des

^{II***} $p < 0.01$ les résultats sont hautement significatifs, ^{**} $p < 0.05$ les résultats ont une signification modérée, ^{*} $p < 0.10$ les résultats ont une signification marginale

membres supérieurs. L'utilisation de la méthode de suivi sans marqueur a permis de capter ces tendances, invisibles à l'œil nu, à la fin de la tâche, lorsque le participant commence à ressentir de la fatigue, car cette déviation se produit progressivement.

Des expériences d'étude de la fatigue ont révélé deux tendances associées à la différence de capacités physiques entre hommes et femmes. La première est une relation significative ($p < 0.01$) entre l'endurance à l'effort et le niveau de gravité, avec une pente négative pour tous les participants pour une tâche statique. Il existe par ailleurs une relation marginale ($p < 0.1$) entre la charge mentale globale et le niveau de gravité avec une pente positive pour tous les participants, pour la même tâche. La même tendance a été observée pour les tâches dynamiques et répétitives. Il a été conclu que la méthode objective proposée, en combinaison avec une évaluation subjective, est utile pour l'étude de la fatigue humaine.

Des expériences sur le confort en position assise et la réalisation de tâches statiques et dynamiques, ont montré qu'il y a une augmentation significative du confort dans différentes parties du corps, en particulier le dos ($p < 0.01$), la nuque ($p < 0.01$), le haut et le bas du dos ($p < 0.01$) avec un niveau de gravité décroissant.

Une approche pluridisciplinaire permet d'étudier l'ergonomie des environnements de travail en hypogravité. Un tel environnement de travail nécessitera moins d'efforts pour les travailleurs en raison de la prise en compte de la fatigue physique dans le modèle. En outre, cela permet potentiellement de réduire les microtraumatismes répétés, et les troubles musculo-squelettiques, qui sont courants dans de nombreuses situations de travail. De plus, la Modélisation Humaine Numérique, qui nécessite des données expérimentales pour la modélisation, peut être enrichie avec des données collectées pour de nouvelles simulations et des problèmes d'optimisation. Cela conduira au développement de nouvelles connaissances et à l'élaboration de lignes directrices et de normes pour la conception des environnements de travail en hypogravité.

Mots clés : poste de travail, étude de la posture, fatigue, confort au travail, conception centrée sur l'humain, exploration de la Lune, exploration de Mars, exécution de tâches, gravité réduite, modélisation humaine numérique, capture de mouvement sans marqueur

Contents

Acknowledgements	i
Abstract (English/Français)	iii
List of figures	xi
List of tables	xv
List of abbreviations	xvii
List of definitions	xix
1 Introduction	1
1.1 Motivation	2
1.2 Broadening the scope	3
1.2.1 Impact of gravity on life	3
1.2.2 Sitting biomechanics	4
1.2.3 Physiology of muscle work	10
1.2.4 Health and Performance during space missions	13
1.2.5 Comfort at workplace	14
1.2.6 Workplace under different gravity conditions	20
1.2.7 Assessment methods	26
1.2.8 Workplace design standardization	30
1.2.9 Filling the gap in the field	34
1.3 Objectives and main contributions	35
1.4 Structure of the thesis	36
2 Biomechanical modeling	39
2.1 Anthropometry in occupational biomechanics	39
2.2 3D kinematics of motions and camera calibration	46
2.3 Methodology for biomechanical calculations	52
2.3.1 Biomechanical modelling of static posture	54
2.3.2 Human motion dynamics theory	59
3 Data collection and analysis	67
3.1 Overview of data collection	67

3.2	Statistical methods	70
3.3	Performance at the workplace	72
3.3.1	Observational methods	73
3.3.2	Subjective Methods	74
3.4	Postural study	75
3.4.1	Indirect methods	75
3.5	Fatigue study	86
3.5.1	Direct methods	86
3.5.2	Subjective method	87
3.6	Pushing/pulling study	88
3.6.1	Direct methods	88
3.7	Seated discomfort study	89
3.7.1	Indirect methods	90
3.7.2	Subjective methods	90
3.7.3	Observational methods	90
4	Results	91
4.1	Camera calibration results	91
4.2	Performance at the workplace	95
4.3	Postural study	99
4.3.1	Joint angles assessment	100
4.3.2	Joint forces and torques assessment	103
4.3.3	Workload of the elbow/shoulder	104
4.3.4	CoM assessment	105
4.4	Fatigue study	110
4.5	Pushing and pulling study	117
4.6	Seated discomfort study	119
4.6.1	Average of all body parts	119
4.6.2	Analysis for each body part comfort	122
4.6.3	Effect of backrest angles on comfort	122
4.7	Combinatorial study	125
4.7.1	ISO standards selection	125
4.7.2	Full variable analysis	127
5	Baseline for workplace design	131
5.1	Interpretation of results	131
5.1.1	Performance at the workplace	131
5.1.2	Postural study	132
5.1.3	Fatigue study	135
5.1.4	Pushing and pulling study	138
5.1.5	Seated discomfort study	138
5.1.6	Combinatorial study	139
5.1.7	Markerless motion capture	139

CONTENTS

5.2	Optimization approach for workplace design under $\frac{1}{6}G$ and $\frac{1}{3}G$ conditions . . .	140
5.3	Extension of the 1G standards for HG conditions	148
5.4	Workplace design recommendations	150
6	Discussions and conclusions	155
6.1	General discussion	155
6.2	Synthesis of research	156
6.3	Limitations of this thesis	158
6.3.1	Performance at the workplace	159
6.3.2	Postural study	159
6.3.3	Fatigue study	159
6.3.4	Pushing and pulling study	160
6.3.5	Combinatorial study	160
6.3.6	Seated discomfort study	160
6.4	Ethical issues	161
6.5	Future works	161
6.5.1	The whole habitat experiments under HG	161
6.5.2	Parabolic flight experiments for validation purposes	163
6.5.3	Neutral posture under HG identification	168
6.5.4	Computer vision in underwater conditions	168
6.5.5	New methods of HG simulation	168
6.5.6	Workplace optimization based on fatigue and postural study	168
A	An appendix	171
A.1	Supplementary figures and tables	171
A.1.1	Camera calibration	181
A.1.2	Statistical analysis	182
A.2	Supplementary results	185
A.3	Parabolic flight campaign	196
A.4	Codes/scripts	198
A.5	Matlab script	199
	Bibliography	211
	Curriculum Vitae	229

List of Figures

1.1 Gravity "shapes" life. Author's vision.	3
1.2 Seat design elements (Keegan, 2005)	7
1.3 Disc-pressure findings in unsupported sitting)	8
1.4 The effect of changing the angle between the thigh and torso)	8
1.5 Fatigue failure model adapted by Seo et al., 2016 from (McGill, 1997)	11
1.6 Stress-strain model (Rohmert, 1984)	12
1.7 Static versus dynamic work (Rohmert, 1984)	12
1.8 A cockpit comfort level	15
1.9 Outside view of Concordia research station	16
1.10 Recommendations for habitable volume design under HG	16
1.11 Three suggested body adaptations to inclined seats.	17
1.12 Seats in vehicles	19
1.13 Specific research field elements for the workplace design	20
1.14 (A) Scheme of Munich Space Chair. (B) The food table restraints and foot loops in Skylab, (C) Chairs in the MIR station mock-up	24
1.15 Subject inside the Lunar Module	25
1.16 Biomechanical human models. Sitting posture (Song et al., 2010)	27
1.17 Worldwide and national human factors and ergonomics standards	30
1.18 Human factor - standards groups relation	31
1.19 OCRA checklist components	33
2.1 Segmentation of human body (Plagenhoef et al., 1983)	40
2.2 Locomotion energetics	44
2.3 (A) Hypothetical normal standing postures. (B) Individual postures	45
2.4 Hypothesized normal sitting postures	46
2.5 The Euclidean transformation	48
2.6 Radial distortions	48
2.7 Zhang's approach demonstration.	49
2.8 Example a minimal tree	51
2.9 Ballasts distribution on the participants body)	53
2.10 (A) The 2D free body diagram. (B) OpenPose skeleton	56
2.11 2-DOF kinematic skeleton of an arm with a plane of motion	61
3.1 Experimental set up for performance at the workplace study	73

3.2	Details of the experimental set up for performance at the workplace study . . .	73
3.3	Experimental site for postural studies	75
3.4	(A) Experimental setup. (B) Participant 3D scan example	76
3.5	White balance adjustment and creating new resolution	77
3.6	The scheme of data processing for 3D biomechanical computations	77
3.7	3D skeleton model used for data processing	84
3.8	Block diagram for electronics box	84
3.9	(A) Experimental set up for pushing/pulling (B) Block diagram	88
3.10	Side view of the experimental chair configurations	89
4.1	Intrinsic parameters computation visual results.	92
4.2	Relative poses results.	92
4.3	Bundle adjustment output.	93
4.4	Global registration results. View cam 3.	93
4.5	Global registration results. View cam 1 and cam 2.	94
4.6	Body tilts angles results	95
4.7	WWL % for 1G and for $\frac{1}{2}$ G. Performance tasks	96
4.8	Spine/vertical mean angle for females	101
4.9	Spine/vertical mean angle for males.	101
4.10	Upper arm/vertical mean angle for females	102
4.11	Upper arm/vertical mean angle for males.	102
4.12	Hip torques values for different levels of gravity	104
4.13	The whole body center of mass location	105
4.14	CoM mean values for Y - axis for static tasks for females	106
4.15	CoM mean values for Z - axis for static tasks for females	106
4.16	CoM mean values for Y - axis for static tasks for males	107
4.17	CoM mean values for Z - axis for static tasks for males	107
4.18	The ET power models (N = 520 studies, 6 task intensities (A)-(G)	112
4.19	Endurance time for Earth, Moon and Mars. (B) Weighted workload (WWL,%)	116
4.20	Pushing/pulling force data box plot for 1G and $\frac{1}{2}$ G	118
4.21	Overall body comfort under 1 G and $\frac{1}{2}$ G	119
4.22	Backrest impact on overall body comfort under 1G (Left) and HG (Right)	123
4.23	Maximum acceptable endurance time/trunk inclination	125
5.1	Workplace optimization	142
5.2	Optimal solution area for backrest inclination, 1G	147
5.3	Optimal solution area for backrest inclination, $\frac{1}{2}$ G	147
5.4	Proposed standard extension.	149
5.5	Pushing scheme under 1G (Left). Pushing scheme under HG (Right).	150
5.6	(A) Neutral posture under MG, 1G and HG	152
6.1	(A) A general view of the chair. (B) Sensor distribution on the seat.	165
6.2	General view of the rack with two mounted chairs with explanation	166

LIST OF FIGURES

6.3	Layout of cameras on the rack and around the rack	167
A.1	The international road map of artificial gravity research.	171
A.2	Chairs comparison (Vogler, 2005	172
A.3	The description of the subjective demands of the NASA-TLX survey.	179
A.4	NASA-TLX 100 points rating scale (Rubio et al., 2004)	179
A.5	Scheme of electronic for sitting part reaction force recording	180
A.6	The 2020 Physical Activity Readiness Questionnaire (PAR-Q+)	180
A.7	Template for comfort survey (Corlett, 1976)	180
A.8	Landmarks preparation step	182
A.9	Weighted workload (WWL,%) for static task (S1)	187
A.10	Forearm/vertical mean angle for females	188
A.11	Spine/thigh mean angle for females	188
A.12	Forearm/vertical mean angle for males	189
A.13	Spine/thigh mean angle for females	189

List of Tables

1.1	Advantages disadvantages of biomechanics and ergonomics methods	6
1.2	Methods for evaluating the functional qualities of industrial seats	9
1.3	Summary of seat-back inclination before 1972 (Harrison et al., 1999)	18
1.4	Research field - gravity level summary	21
2.1	Segment masses as percentages of total body mass	41
2.2	Ballast masses for static experiments	54
3.1	Experiments summary	72
4.1	Bundle adjustment calibration errors	94
4.2	Global registration errors	94
4.3	Summary of NASA-TLX parameters for the performance tasks	97
4.4	Statistical analysis of the repetitive tasks	98
4.5	Statistical analysis of the task with joystick and handwriting	98
4.6	Statistical analysis of the tasks with keyboard and assembling	99
4.7	Markerless motion capture errors	99
4.8	Forces and torques for shoulder and elbow for static task (S1)	103
4.9	Workload results.	105
4.10	Power model coefficients for Males/Females	111
4.11	Hand and back-leg-chest strength under 1G, ½G, ¼G for Males/Females.	113
4.12	Summary of the calculated NASA-TLX parameters	115
4.13	The ET (min) and WWL% under 1G, ½G, ¼G	117
4.14	Maximum action pulling force descriptive statistics	118
4.15	Maximum action pushing force descriptive statistics	119
4.16	Time and conditions factors impact on participants' body comfort	120
4.17	A post-hoc analysis: body comfort	120
4.18	The effect of time factor study of the participant' comfort	121
4.19	Impact of HG on the participants' body comfort	121
4.20	Impact of HG on the participants' body comfort	121
4.21	Gravity impact on the different body part comfort	122
4.22	Backrest angle impact on overall body comfort	124
4.23	Backrest factor impact on the body segments comfort	124
4.24	Spine/vertical mean angle for static and dynamic tasks together	127
4.25	Shoulder/vertical mean angle for static and dynamic tasks together	128

4.26 Mean CoM coordinate Z- axis pelvic for static and dynamic tasks together . . .	128
4.27 Mean CoM coordinate Y- axis pelvic for static and dynamic tasks together . . .	129
A.1 Cons and pros of markerless motion capture method	173
A.2 Organizational Structure of ISO TC 159	174
A.3 Organizational Structure of CEN/TC 122	175
A.5 Part of published CEN standards for ergonomics.	176
A.6 ISO Standards for ergonomics guiding principles	177
A.7 Functional factors in sitting (Corlett et al., 1995)	178
A.8 Descriptive statistics for the main characteristics of the participant.	183
A.9 Shapiro-Wilk normality test results. Performance study experiment	184
A.10 Shapiro-Wilk normality test results. Postural study experiment	184
A.11 Summary of the calculated NASA-TLX parameters for the performance tasks . .	185
A.12 Statistical analysis of the performance study tasks - Part I	186
A.13 Statistical analysis of the performance study tasks - Part II	186
A.14 Mean angle between spine and vertical for males and females separately	190
A.15 Spine/vertical mean angle for males and females together	190
A.16 Spine/tight mean angle for static and dynamic tasks together	191
A.17 Spine/tight mean angle for males and females separately	191
A.18 Spine/tight mean angle for males and females together	192
A.19 Shoulder/vertical mean angle for males and females separately	192
A.20 Shoulder/vertical mean angle for males and females together	193
A.21 Forearm/vertical mean angle for males and females separately	193
A.22 Forearm/vertical mean angle for males and females together	194
A.23 Mean CoM coordinate Z- axis pelvic for males and females separately	194
A.24 Mean CoM coordinate Z- axis pelvic for males and females together	195
A.25 Mean CoM coordinate Y- axis pelvic for males and females separately	195
A.26 Mean CoM coordinate Y- axis pelvic for males and females together	196

List of abbreviations

AG	Artificial gravity	MD	Mental demand
ANOVA	Analysis of variance	MF	Muscle fatigue
BA	Bundle adjustment	MG	Microgravity
BLC	Back-leg-chest	MN	Mean
BMD	Bone mineral density	MPJPE	Mean joint position errors
BMI	Body mass index	MSD	Musculoskeletal disorder
BS	Body segment	NASA-TLX	National aeronautics and space administration Task Load Index
CEN	European Committee for Standardization	NBL	Neutral buoyancy laboratory
CoM	Center of mass	NPP	Neutral position of the body
CG	Center of gravity	OCRA	Occupational repetitive action
CI	Confidence interval	OWAS	Working Posture Analysing System
D	Dynamic task	P	Performance
DHM	Digital human modelling	PCK	Percentage of correct keypoints
DOF	Degree of freedom	PD	Physical demand
EF	Effort	PE	Potential energy
EMG	Electromyography	R	Repetitive task
ESA	European space agency	REBA	Rapid entire body assessment
ET	Endurance time	RULA	Rapid upper limb assessment
EVA	Extra vehicular activity	S	Static task
FA	Forearm	SWAT	Subjective assessment technique
FR	Frustration	TC	Technical committee
G	Acceleration of gravity	TD	Temporal demand
HG	Hypogravity	TH	Thigh
HIDH	Human Integration Design Handbook	TR	Torso
ICE	Isolated, confined, extreme	UA	Upper arm
ISO	International organization standardization	WWL	Weighted workload
ISS	International Space Station	WP	Workload Profile
KE	Kinetic energy		
LD	Long duration		

List of definitions

Carrying manually - moving an object held in one or both hands, OR positioned on one or both shoulders.

Extreme body joint position occurs near the end of the range of motion, when the passive components such as ligaments are subjected to a significant mechanical load.

Good posture is one that creates the least postural tension in a static body position, when the muscles do the least work to counteract the action of gravity and other forces.

Holding time is the length of time in which a static working position is maintained.

Maximum holding time- the longest period of time that a static Working posture may be maintained continuously from a resting condition.

Manual handling - an activity that needs the use of human force to move an object.

Lifting/Lowering manually - moving an object from its initial position upwards/downwards manually (i.e. without the use of a mechanical aid).

Overall mental workload- perceived workload for aspects of performance.

Recovery time - Time available for recovery, i.e. the length of time that a body segment is fully supported or maintained in a neutral posture.

Working posture is maintained for a longer period of time; this refers to minor or non-existent fluctuations in the force delivered by muscles and other bodily components around a fixed force level.

1 Introduction

The successful Apollo mission to the Moon demonstrated that humans could work and live on another planetary body for a short time period. During the six Apollo missions, all twelve astronauts, spent a total of about 80 hours on the Moon for Extravehicular activity (EVA) and 290 hours inside the Lunar Module. Future missions to the Moon will likely involve longer stays and may include a permanent human presence. With this in mind, human activity – both mental and physical - is expected to play a critical role in mission success. Nevertheless, very little is known about the impact of hypogravity (HG) on working and living conditions^I. HG is defined as gravity conditions between ($0 < G < 1$). On Mars, one third of the Earth's gravity would be experienced ($\frac{1}{3}G$), and on the Moon one sixth ($\frac{1}{6}G$). These environmental conditions will certainly affect human health, motions, habits and workplaces. Knowledge of HG effects on human movement is currently limited to experiments on walking, running, and skipping, but no data is available regarding sitting and working. Also, little is known about the impact of HG on short-term (SD) and long-term (LD) missions and there is an evident gap in recommendations for structure design and habitat optimization.

This research is devoted to workplace design based on human biomechanics in HG conditions. The aim of this thesis is to develop guidelines for designing sedentary (sitting) workplaces and handling areas^{II} in HG. Such workplaces could be used in LD missions to optimize worker performance, in minimizing physical fatigue and risks of musculoskeletal disorders (MSD), while increasing comfort.

This activity is in line with the space agencies' accelerated plans to return to the Moon and land humans on its surface again before the end of this decade and later go on to Mars. New standards and corresponding technological advances will be needed to set up a sustainable living and working environment for humans. The problems related to workplace design in confined and extreme conditions found on Earth or in near-Earth facilities were addressed.

^IReduced gravity (RG), partial gravity (PG), hypogravity (HG) are synonyms and hereinafter the term HG is used

^{II}Handling area is a zone on a workplace that allows the worker to reach every point vertically or horizontally with both hands without leaving seat. All working materials, tools and parts are located in this area.

Human-centered design strategies and biomechanical issues for creating an effective workplace design for LD missions are considered. The recommendations for design, maintenance, and usage of this workplace in different gravity conditions are made. Numerical simulations including anthropometric data and 3D scan are used first to obtain input data. Then, laboratory based experiments are conducted in two environments to collect the final data. Based on this data the final model can be built. Underwater experiments are necessary to reduce the effects of gravity providing data points simulating Moon and Mars conditions. This research may lead to new ways to consider workplace design for space missions that could also be useful on Earth.

1.1 Motivation

During missions to the Moon and future missions to Mars, the effects of HG on the human body will play a critical role, especially as most will be LD missions. HG crucially affects astronauts' health, comfort, as well as their ability to perform tasks. It also has an effect on the risk of injury. Our knowledge of the effects on human movement under HG is currently limited. This research intends to fill a critical knowledge gap in terms of workplace design in HG, and will focus on the sitting posture as it is omnipresent and represents a large portion of tasks (Zemp et al., 2016).

In general, the risk of poor workplace design is related to the lack of a human-centered approach. A good human-centered design will increase the efficiency and function of all workplace components and should consequently also have a positive impact on operational costs. One of the ways to provide such a design is to examine the biomechanics of different types of behaviors. This contributes to ergonomics which includes numerous other fields, such as physiology, engineering, statistics, and anthropometry. However, the use of biomechanics provides a deep understanding of the human body and can reveal results that cannot be studied with ergonomics. Optimization of the biomechanical environment may tend to focus on one body part to the detriment of others (Salvendy, 2012b). However, biomechanical principles can be taken into account as a function of work environments and design variables as well as constraints. These biomechanical concepts translate constraints into mathematical equations and functions describing how risk factors affect the human body (Salvendy, 2012b). Thus, such a model allows for an evaluation of risk associated with the workplace using quantitative methods.

Critical parameters in biomechanical assessments which are the primary focus of this research include upper body muscle fatigue (MF), defined as the loss of the ability to generate force after muscle activity (Kirk et al., 2019), as well as comfort, performance and center of mass (CoM), and postural study. The analyses of these parameters should be conducted in early stages of the workplace design.

Although environmental conditions (temperature, lighting, noise, air quality, vibration) in the workplace affect health, safety, and task performance, they were not taken into account

in the experiments to simplify the analysis, but they were carefully documented. Therefore, only the specific added constraint of hypogravity will be considered. The aim is to develop a baseline for integrating a good ergonomic design with biomechanical modeling. This also includes human fatigue recommendations, and human performance concerns, as well as related comfort and productivity. In this research, direct methods and indirect methods as well as subjective methods were applied as they provide a usable and appropriate level of accuracy.

1.2 Broadening the scope

1.2.1 Impact of gravity on life

One of the fundamental physical forces is the gravitational one. Its intensity and direction are constant, but it is not clear enough what role this force can play in life. Studies began only after the launch of a Sputnik satellite in October 1957.

The weight of each object is determined by the gravitational load that affects masses on Earth. 1G for the Earth, $\frac{1}{6}$ G for the Moon, and $\frac{1}{3}$ G for Mars can be used as a reference. Many chemical, biological, and ecological processes, as well as their variations on the planet, are governed by weight. Since gravity creates biological modifications, then it must be the dominant physical force in the environment affecting life on Earth, according to (Morey-Holton, 2003).

Gravity, despite being nearly constant on Earth surface, played a crucial role in evolution when animals arose from the sea and began to colonize land. Terrestrial organisms evolved by shifting their orientation or raising their height in response to the shift in gravity's vector (Morey-Holton, 2003), as seen in Figure 1.1. This relates to overcoming direction shifts and moving fluids and structures against such loads, according to (Morey-Holton, 2003). An adaptation of biological systems can be investigated by altering the gravitational effect.

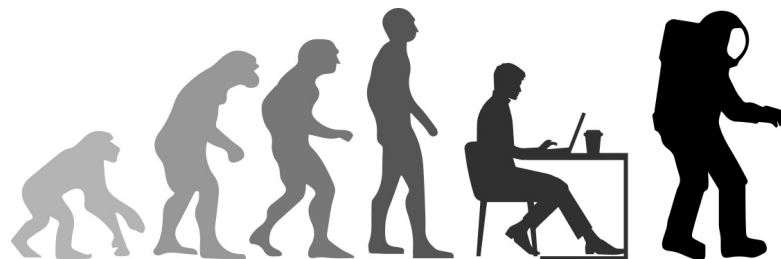


Figure 1.1: Gravity "shapes" life. Author's vision.

It becomes obvious from researching reduced gravity in spaceflight that both gravity as well as the absence of gravity with its physical changes can significantly impact the evolution of species. According to experiments conducted in space on these species, gravity is important for development of vertebrates; however, these studies were short-term (Laws et al., 2016).

The subtleties of non-terrestrial gravity's effect on the body are difficult to grasp in short-term trials. Only parabolic flight, suspended systems, or water can be used to study low gravity on land. If the goal is to establish a conducive environment for changed gravity, it is vital to understand and appreciate the distinctions between the Earth's physical environment and habitats in space. Many anatomical systems, including fluids and support structures, have been found to be affected by the absence of gravitational forces. When reentering the atmosphere and being impacted by gravitational forces, a human becomes vulnerable.

In this dissertation the focus is on biomechanical aspects and problems using examples related to the vestibular and musculoskeletal systems. The vestibular apparatus, is in charge of eye movements, balance, and posture. It has been proven that after working in changing gravity conditions, brain confusion arises, resulting in postural instability and cardiovascular issues when standing (Merfeld, 1996; Oman et al., 1996). The magnitude of the impact is proportional to the mission's duration.

The musculoskeletal system is extremely sensitive to load variations. The muscles and bones related to posture and load become weaker without gravity loading. When returning to Earth, the previous adaptation to space causes problems. Standing issues, disorientation, and muscle weakness occur after landing. Appropriate countermeasures must be created for improved adaption to any non-1G environment.

1.2.2 Sitting biomechanics

The origin of chairs and seats is not fully known. Evidence of the first chair dates back to 100 BC and was found in the ruins of Toro, 130 kilometers southwest of Tokyo, Japan (R. Lueder and Noro, 1994). By the Middle Ages, chairs were used by high-status samurai, as well as by priests during religious ceremonies. In the Western world, seating was first documented for use by the royal family and significantly, during the reign of Louis XIV (Chéronnet, 1950).

There is an almost endless variety of shapes, designs and materials available for chairs depending on their purpose and functionality. Chairs are also constantly being modified and improved, becoming lighter, "smarter", safer, more durable and environmentally friendly. In recent years, questions related to the influence of chairs and sitting posture on our health have increasingly been raised. Kilbom, 1987 and Lueder, 1992 stated that one of the biggest hazards to health is lack of movement, and static posture while seated is no exception.

Nonetheless, stress from static posture is currently considered to be only one element on par with physical and psychological stress in the work environment (Chou and Shekelle, 2010). Despite the fact that prolonged static sitting has been related to an increased risk of back, neck, shoulder, arm, and leg musculoskeletal diseases (Naqvi, 1994; Winkel and Rgensen, 1986), other authors a (e.g. Hartvigsen et al., 2000; Kwon et al., 2011; Lis et al., 2007; Roffey et al., 2010) didn't find a link between sitting and the occurrence of low back pain. At the same time, 60 percent of all workers in European Union countries (data from 2010-2015) report MSD

(De Kok et al., 2019).

To investigate sedentary behavior and comfort, various methods and equipment can be applied. It was not until the late 1960s that ergonomics began to develop methods for assessing comfort and at this time, electromyographic (EMG) studies of muscle activity in various postures emerged. At the moment, the most common approaches for quantifying strength and posture are: pressure sensors (Meyer et al., 2010; Dunk and Callaghan, 2005), optoelectronic motion analysis (Dunk and Callaghan, 2005), accelerometers (Ryan et al., 2011), surveys and video analysis (Womersley and May, 2006). Table 1.1 shows the various ergonomics and biomechanical methods with their advantages and disadvantages.

Many researchers do not trust subjective data and questionnaires and consider these to be unscientific research methods (Salvendy, 2012a). Yet some scientists are proponents of such methodology (Annett, 2002) and argue that subjective ratings can be efficient for evaluating the mechanisms underlying performance of e.g., interface design. Subjective measures include the following examples: Cooper-Harper rating scale, National aeronautics and space administration Task Load index (NASA-TLX), Subjective workload assessment technique (SWAT). Physiological measures can be conducted with dynamometer or force plate for force measures, electromyogram, electroencephalographic measure, electrocardiogram, eye fixation, to name a few examples. In certain cases, indirect physiological measures can be implemented when some parameters can be estimated numerically through software simulations or biomechanical calculations, as described in the next chapter.

Table 1.1: Advantages and disadvantages of biomechanics and ergonomics methods adapted from (X. Li et al., 2018)

Method	Example	Advantages	Limitations
Observation, self report	Direct observation, indirect observation, questionnaire, interview, etc.	Minimal disruption, Minimal instrumentation	Time-consuming, Error-prone, Subjective results
Direct physiological measurements	Goniometers, force sensors, accelerometers, EMG, optimal markers, etc.	High level of accuracy, Objective results	High experimental cost, Controlled environment, technical issues, ethical issue, interference with the work, human subject required to imitate the task
Indirect physiological measurements	Kinect range camera, computer vision-based approach, etc.	Objective results, easy experimental setting	High accuracy, illumination changes, view points, occlusion
Laboratory setting for both direct and indirect physiological measurements	EMG, optimal markers, Kinect range camera	Minimal disruption, reasonable level of detail and accuracy	Space limitation, ethical, technical, and cost issues, time-consuming data post-processing, number of human subjects required

Note: Copyright (American Society of Civil Engineers, © 1983) From (Journal of Construction Engineering and Management, 3D Visualization-Based Ergonomic Risk Assessment and Work Modification Framework and Its Validation for a Lifting Task) by (Li, Xinming et al. (2018)/American Society of Civil Engineers). Reproduced by permission of Taylor and Francis Group, LLC

The seated posture is also attracting more and more attention from experts such as orthopedists, anatomists, physiologists and medical professionals, even though a clear understanding and consensus of the correct working posture is not evident (Morabito et al., 2021). This has created a demand for the development of new studies and the creation of new physiological (biomechanical) and behavioral research methods.

Sitting posture studies have a long history, with extensive research published in Germany and then later in Sweden. Staffel, 1884 created a standard for the seated posture, which was often used (Fick, 1911, Straßer, 1913, and Schede, 1935). Yet, as early as 1911, there was controversy about the normal position of the spine while sitting (kyphosis or lordosis). Williams et al., 1991 provided a review of sedentary positions and pain, and lordosis has been reported to be preferable to kyphosis. In the late 1800s and early 1900s, Parow, 1864 and von Meyer, 1853 concluded that the ischial tuberosities, also known as the sit bones, were the main points of support in the seated position due to posterior pelvic rotation.

By 1929 seats in Siemens factories had backrests that were adjustable to reduce pressure on the area under the thighs, (Drescher, 1929). Keegan, 2005 and Keegan, 1962 wrote a review discussing a herniated lower lumbar disc that occurred while sitting on radiographs. Knutsson et al., 1966 performed an EMG assessment of the sacrospinal muscles while sitting. Kroemer, 1971 analyzed various elements of the workplace, including footrests, office equipment, consoles in the factories. Another study Corlett et al., 1995 stated that a work seat is for working from, hence function must impact the form. The users' behavior and subjective judgments must be considered in the evaluation, and using dimensions alone is insufficient. Table 1.2 depicts the methods used by several industrial workers to assess some of the chair's features. The method of choice can be determined by the study objective.

Some of the workplace variables studied prior to 1950 are shown in Figure 1.2. These variables include: 1, lumbar support; 2, backrest angle (minimum 105 degrees); 3, space for the sacrum and buttocks; 4 - convex chest support up to the lower shoulder blades; 5, shoulder 105 degree support; 6, adjustable backrest swivel; 7 - the length of the bottom of the seat; 8 - seat height above the floor; 9, the bottom of the seat is bent down under the knees; 10, free space for leg; and 11, tilt the bottom of the seat. Other workplace parameters are described in Appendix Table A.7.

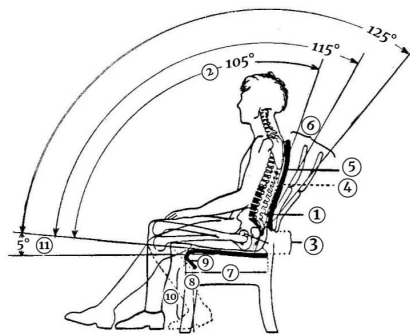


Figure 1.2: Seat design elements (Keegan, 2005). *Reprinted from Journal of Manipulative and Physiological Therapeutics, Vol 22 /Issue 9, Donald H. et al. (1999). Sitting biomechanics Part I: Review of the Literature, Pages No.16, Copyright (2022), with permission from Elsevier.*

In general, a work seat must transmit forces other than body weight through the occupant and therefore to the ground. For example, the backrest transmits force, especially pushing forces. In this case, part of the weight of the body and head is transferred to the back (E. Corlett and Eklund, 1984).

Nachemson, 1970 installed pressure gauges into the discs of living subjects and found that the sitting posture resulted in higher disk pressure than standing or lying down. Andersson, 1974 investigated seven unsupported and supported sitting positions. He discovered that in the unsupported sitting posture, the internal pressure in the disc was much higher than in the standing position. In the supported sitting posture, an increase in back tilt and lumbar support was linked to a reduction in disc pressure. In both standing and relaxed sitting without

support, myoelectric activity was nearly identical. The activity levels were highest in the front seat and lowest in the back seat, according to EMG data. The backrest should be tilted at least 100 degrees, according to the scientists, to get low values for both EMG readings and disc pressure. The pressure on the disc in a standing position is depicted in Figure 1.3. Keegan, 1962 sought a relationship between lordosis and the angle of the hip and trunk. He took X-rays while lying on his side, changing only the angle of the hip and torso.

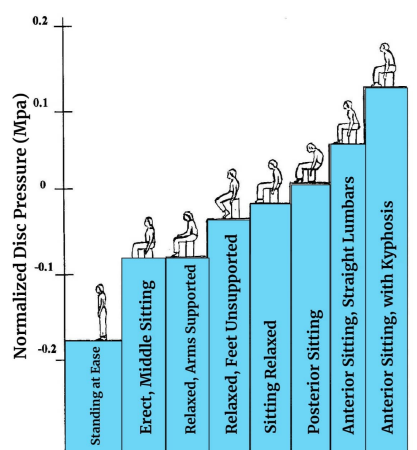


Figure 1.3: Disc-pressure findings in unsupported sitting (Andersson, 1974, Andersson, 1975). Reprinted from *Journal of Manipulative and Physiological Therapeutics*, Vol 22 /Issue 9, Donald H. et al. (1999). *Sitting biomechanics Part I: Review of the Literature*, Pages No.16, Copyright (2022), with permission from Elsevier.

Figure 1.4 shows that the pelvis turns back with a decrease in the angle of the thigh and trunk from 200 to 50 degrees and the lumbar lordosis becomes kyphotic.

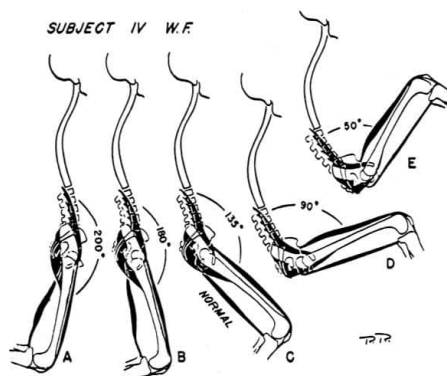


Figure 1.4: The effect of changing the angle between the thigh and torso in the supine position on the muscle tension (Keegan, 1962). Reprinted from *Journal of Manipulative and Physiological Therapeutics*, Vol 22 /Issue 9, Donald H. et al. (1999). *Sitting biomechanics Part I: Review of the Literature*, Pages No.16, Copyright (2022), with permission from Elsevier.

Table 1.2: Methods for evaluating the functional qualities of industrial seats (Corlett et al., 1995)

Functional factors	Dimensional measurements	Fitting trials	Force measurements	Biomechanics calculations	Observations	Subjective judgments overall	Subjective judgments body parts	Scaled Checklists	Cross-modality	Reach/force/stability	Stature changes
Seeing	✓	✓				✓					✓
Reaching	✓	✓		✓	✓		✓				✓
Seat	✓		✓	✓	✓	✓	✓	✓		✓	✓
Backrest	✓		✓	✓	✓	✓	✓	✓		✓	✓
Adjustments	✓	✓						✓		✓	
Ingress/egress	✓	✓		✓	✓	✓		✓			
Stability		✓		✓		✓				✓	
Support weight			✓	✓		✓	✓		✓	✓	
Under-thigh clearance	✓		✓			✓	✓	✓			✓
Trunk-thigh angle	✓			✓	✓						
Leg load			✓	✓		✓	✓	✓			✓
Neck/arm load					✓	✓	✓	✓			✓
Posture changes			✓		✓		✓	✓			
Long-term use					✓	✓	✓	✓			✓
Acceptability				✓		✓		✓			
Comfort			✓		✓	✓	✓	✓	✓		
Lumbar support	✓	✓	✓				✓	✓		✓	✓

Note: Copyright (Taylor & Francis Group, LLC © 2005) From (Evaluation of human work) by (John R. Wilson and Nigel Corlett). Reproduced by permission of Taylor and Francis Group, LLC, a division of Informa plc.

In the illustration, the anterior and posterior muscles of the thigh are highlighted with a thicker line to show their attachments. This figure also illustrates effect of the tension of these muscles on the pelvis. The same author identified a 135-degree hip-torso angle to be a neutral position of the muscles of the thigh. He found that posterior pelvic rotation and reduced lumbar lordosis are related to tension in the posterior thigh muscles.

Andersson, 1974 and Andersson, 1975 studied EMG measurements and pressure in seated discs for office, wheelchair, and driver's seats. Then, in 1980, a manual for car seats was published. Recent studies Wong et al., 2019 have shown that the sitting posture can affect the activity of the trunk muscles. The significantly lower activity of bilateral low trunk muscle activity during slouched sitting compared to upright sitting is consistent with previous observations (O'Sullivan et al., 2006).

It has been suggested that in postures with an average curvature of the spine, the lower back can take on the load of the upper body and hold the position against gravity (Dunk et al., 2009; O'Sullivan et al., 2006). Moreover, increased passive support in the sitting position to stabilize the body position can reduce muscle activation (O'Sullivan et al., 1997). The back of the seat distributes some of the weight of the upper body. It was established by the same author that muscle activity was significantly lower when sitting with support than when sitting in an upright position. At the same time, however, a decrease in muscle activity during sitting with support is not considered negative for biomechanical consequences. At present, sitting biomechanics is also actively being investigated. The current state of the art is presented in the sub-chapter 1.2.8. "Workplace under different gravity conditions".

1.2.3 Physiology of muscle work

Muscle strength, referring to the capacity of the muscle to produce the maximum strength, is difficult to maintain when performing physical tasks. This is because prolonged strength training causes muscle fatigue (MF), which causes a decrease in "muscle power output" if there is insufficient recovery (Andersson, 1975). Same author states that the degree of physical strain depends on the individual characteristics of the person (muscle mass), tasks intensity. It can also be related to the type of tasks performed (static, dynamic, repetitive). The relationship between force exertions and reduced muscle fatigue is shown in Figure 1.5, adapted from (McGill, 1997). To perform a manual handling task, muscles must be tensed by exerted force. In this case, the necessary forces for the task are lower than the physical capabilities of a person. If this task is done with repetitions, the muscles begin to fatigue. Further, this leads to a decrease in muscle strength, since the accumulation of substances causing fatigue occurs in the muscle fibers (dotted line in Figure 1.5). If pauses during the exercise are not provided, then muscle strength becomes lower than the force required to complete the task. This is referred to as fatigue failure (McGill, 1997) and it is limited by a time called endurance time (ET) (Chaffin et al., 2006). Muscle fatigue without adequate recovery results in the tissue's inability to withstand stress because of cellular changes. This can lead to MSD (Kumar, 2001).

One of the goals of ergonomics and biomechanics is to define acceptable muscle load limits that could be applied to prevent fatigue and MSD. Another goal is to develop a recommendation on the acceptable workload for manual handling of materials, taking into account the weight of the load, frequency of handling, range of motion, the distance from the load to the body and the physical characteristics of the person. Biomechanical analyses, aimed at minimizing repetitive and static tasks (static contractions), are certainly promising in this context.

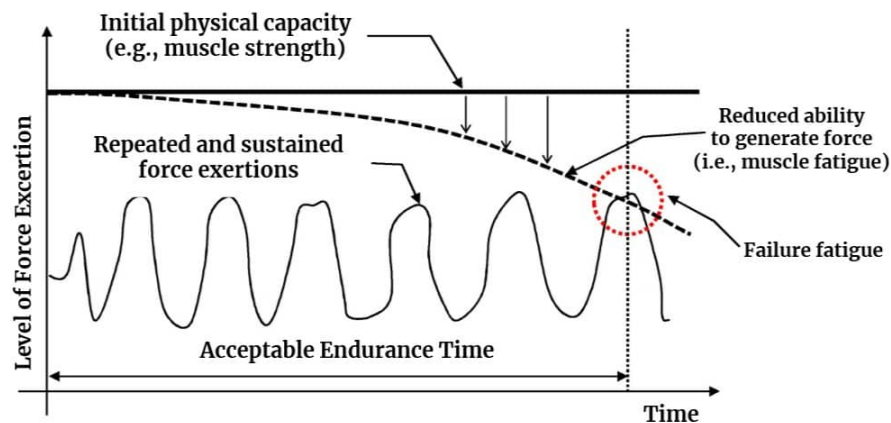


Figure 1.5: Fatigue failure model (adapted by Seo et al., 2016 from (McGill, 1997). *Republished with permission of American Society of Civil Engineers, from Simulation-Based Assessment of Workers' Muscle Fatigue and Its Impact on Construction Operations, American Society of Civil Engineers, 142(11), copyright 2022; permission conveyed through Copyright Clearance Center, Inc.*

Static muscle work

Static work leads to an increase in pressure inside the muscle and partial blockage of blood circulation. Further, muscle metabolism slows down. Therefore, with such work, the muscles get tired faster than with dynamic work (Rohmert, 1984). According to Laurig and Vedder, 1998, an important property of static work is an increase in pressure with an increase in the load intensity and duration. Larger muscle groups cause a stronger blood pressure response at the same intensity of work with respect to smaller ones. The ventilation process is nearly the same for both static and dynamic tasks. However, there are stronger metabolic changes in the muscles, which leads to a different reaction. This is well observed in the extended stress-strain model modified from (Rohmert, 1984), as shown below in Figure 1.6.

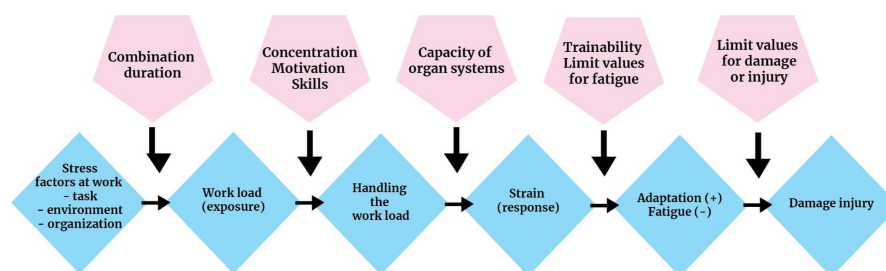


Figure 1.6: Stress-strain model (Rohmert, 1984). Extracted from “Encyclopedia of occupational Health and safety website”, 2011

Numerous empirical models can assess physical fatigue (Volkova et al., 2022). Such models use Intensity - Endurance time (ET) curves with exponential or power function (Rohmert, 1960; Monod and Scherrer, 1965; Huijgens, 1981; Rose et al., 2000; Garg et al., 2002; Imbeau, Farbos, et al., 2006, Frey Law and Avin, 2010; Ma et al., 2011), in order to calculate maximum holding time for any particular task. Different models apply to the various joint regions (shoulder, elbow, wrist), since energy transfer from the body to the muscles results in maximum strength being exponential (Volkova et al., 2022). According to Seo et al., 2016, these models are inappropriate for dynamic tasks studies with irregular pauses. This resulted in the development of dynamic fatigue models, one of which was described by (Liu et al., 2002) as a set of dynamic equations considering effect of muscle fatigue and recovery. As Volkova et al., 2022 have pointed out, Xia and Law, 2008 defined a muscle fatigue mathematical model for complex tasks.

Dynamic muscular work

Dynamic work leads to rhythmic contraction and relaxation of active skeletal muscles. According to metabolic demands, blood flow to the muscles increases. Work intensity affects heart rate and blood pressure, as well as oxygen extraction. Pulmonary ventilation is enhanced by deeper and faster breathing. According to Laurig and Vedder, 1998, lower active muscle mass (as in the hands) in dynamic work results in lower maximum work capacity and peak oxygen consumption compared to dynamic work with large muscles, as shown in Figure 1.7.

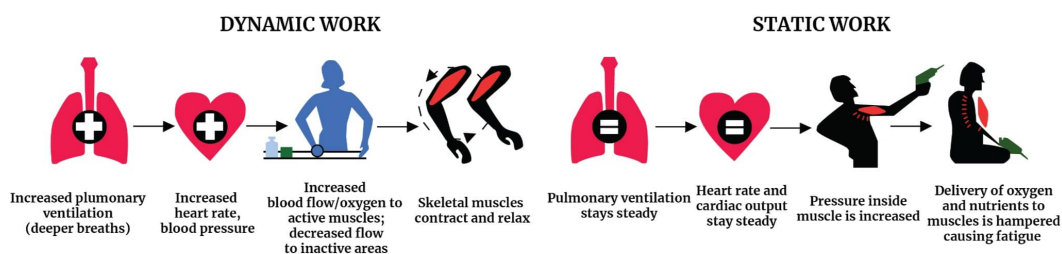


Figure 1.7: Static versus dynamic work (Rohmert, 1984). Extracted from “Encyclopedia of occupational Health and safety website”, 2011

1.2.4 Health and Performance during space missions

It is reasonable to send astronauts on a long journey across the solar system only if they arrive at their destination in good physical shape. Little is known about the short and long-term effects of HG, and this poses a huge risk to successful mission planning. Before sending people around the solar system, simulations and modeling on Earth must be conducted. Many countries conduct research activities to study the impact of artificial (AG) and HG. The international road map of artificial gravity research summarizes the current and future research activities of different countries on artificial AG, see Appendix Figure A.1. (Clément, 2017).

Studies are ongoing to increase knowledge about the possible effects of weightlessness and be able to counter it through drugs, diet, special exercises, or work regimes. For example, data from the previous MIR station, representing 90,000 hours of life in space, was made available to scientists (“ESA website”, 2022), of long stay as a source of data, and ISS for the moment counts around 185,420 occupied hours “ISS wikipedia”, 2022. Today, astronaut physiology and performance are on the list of priorities for aeronautical research.

It has been proven that despite hours of training, a prolonged stay in microgravity (MG) leads to a loss of real bone mineral density mass and muscles, including the heart, atrophy by about 1% per month (Orwoll et al., 2013). This is why astronauts need a thoughtful and individually tailored daily exercise program to reduce these effects, and this program should include static exercise in particular. This is only a small fraction of all the problems that can arise. After six months in LEO, most astronauts experience difficulty walking and must learn it again on Earth. This leads one to wonder what would happen on a trip to Mars and back that could last more than 18 months.

According to Reynolds, 2019 hypogravity can cause various physiological changes during space flight. But at the same time, daily sports training helps to mitigate the effects of non-terrestrial gravity on the body. The most important change is associated with cardiovascular deconditioning. This occurs due to prolonged periods of decreased cardiac workload and redistribution of body fluids in the body, including the circulatory system. Same author states that unlike terrestrial conditions, where gravity collects blood in the legs and feet, MG provides conditions in which the cardiovascular system can create a relatively even blood distribution between the upper and lower parts of the body. Then, after several hours at MG, body perception of increased volume of blood in the upper body such as hypervolemia ^{III} results in a reduction of the total volume of water in the body as a kind of compensation. Symptoms include e.g., orthostatic intolerance ^{IV} and decreased aerobic capacity, cardiac arrhythmias, and cardiac atrophy (Clément, 2011; Barratt and Pool, 2008; Hamilton, 2008). To date, it has not been established whether transient arrhythmias are caused by preexisting conditions or emerge as a result of changes following space flight (Lee et al., 2017; Lee, 2021).

^{III} Hypervolemia is a condition in which the blood contains too much fluid.

^{IV} Orthostatic intolerance is the onset of symptoms that are eased when reclining when standing upright.

It is assumed that there is a loss of potassium with a decrease in water content in the body during adaptation to MG (Nicogossian et al., 2016; Lee, 2021). The HG of the Moon may lead to a similar, or perhaps even less critical, result (Reynolds, 2019).

One review of Richter et al., 2017 showed improvement of a number of physiological measures of cardiopulmonary efficiency when gravity levels decreased, and that cardiac output increases with decreasing gravity. The period of time at which lunar gravity will weaken the disturbance of cardiac activity is still unknown.

In Volkova et al., 2022, mentioned Morey-Holton, 2003 concluded that in the context of extra-terrestrial missions under HG, both musculoskeletal and cardiovascular vestibular systems will be affected because of gravity changes. Body mineral density (BMD) is one of the key components used by ISS crewmembers to monitor bone health (Axpe et al., 2020). International Space Station (ISS) data was used by Axpe et al., 2020 who predicted a loss of bone mineral density at 32.4 - 36.8% in the femoral neck in a non-linear exponential model of six months of flight to Mars, as well as during long stays (Mars and on the Moon). Morey-Holton, 2003 showed that bone and muscle loss occurred in the lower limbs and upper limbs only, including the back.

In the same paper Volkova et al., 2022 it was stated that such findings may indicate that musculoskeletal system changes are local, but it is important to recall that upper extremities have not been in-depth investigated. It was highlighted that initial experiments on upper limb fatigue in weightlessness were conducted on parabolic flights (Bock, 1996) and on MIR (Gallasch et al., 1996), and were further developed in parabolic flight work by Nagatomo et al., 2014 where different levels of gravity (0G - 1.5G) were simulated. Blood flow of the upper and lower extremities of seated participants was compared, showing a normal level for microgravity in the upper extremities and a decrease in the lower extremities. Since these studies were conducted in 0G, a lack of analysis remains regarding long-duration effects of HG on upper limbs.

1.2.5 Comfort at workplace

Currently, the main indicator of the level of comfort of spacecraft is the free volume of the pressurized cabin per crew member (Minenko et al., 2017). To achieve the maximum level of comfort, the free volume of the spacecraft compartments must correspond to the set of functions performed by the crew or the increase in habitable volume spacecraft will be unjustified.

In Volkova et al., 2019 no assumptions were found dealing with issues related to workplace environment. However, various authors have tried to find gravity-dependence functions for habitable volumes.

Leading space agencies developed standards and baselines using:

- Historical examples of spacecraft pressurized volumes;
- Earth-based simulators in extreme environments;
- Volume "measurement/optimization" tools.

For historical spacecraft pressurized volumes the total habitable volume/subject requirements in "station-like" historical data ranges from 40 m³/person to 70 m³/person for a 180-day mission (Celentano et al., 1963; Fraser, 1966; Cente, 1966; Marton et al., 1971; Gore et al., n.d.; Sherwood and Capps, 1990; Petro, 2000; Perino, 2005; Rudisill et al., 2008; Sforza, 2015; Hofstetter et al., 2005; Davenport et al., 1963; Kennedy et al., 2007; Schwartz, 2005).

In the paper "A Cockpit comfort level of the descent capsule-shaped vehicles", Minenko et al., 2017 also concluded that the more diverse the subject's functionality in the spacecraft for the compartment under consideration, the greater the free habitable volume will be required for comfort. This can be seen in Figure 1.8.

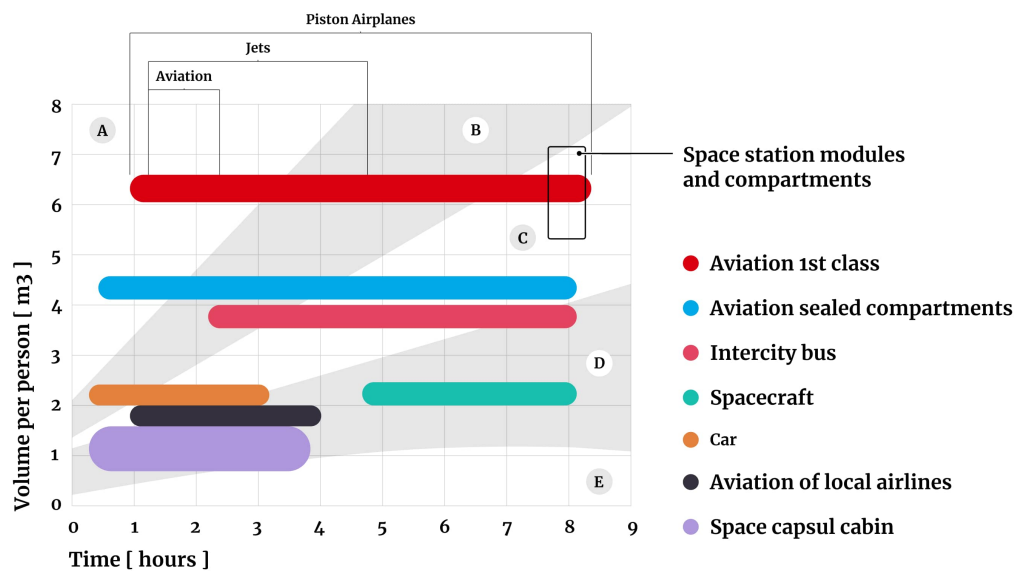


Figure 1.8: A cockpit comfort level of different vehicles, adapted from (Minenko et al., 2017). (A) - Luxury conditions, (B) - Comfortable conditions, (C) - Limited comfort, (D)- Critical level of comfort, (E) - Lack of comfort

Earth-based simulators also provide a number of baselines on volume requirements. Some of the most common simulators are Concordia Research station (see Figure 1.9), Mars-500 and Flashline Mars Arctic Research Station (FMARS).



Figure 1.9: Outside view of Concordia research station. Credit: French Polar Institute

Here, the pressurized habitat volume per person ranges from a minimum of 27m^3 to a maximum 425m^3 (M. M. Cohen, 2008). Few of these studies address the gravity dependency of the design, and those which do mainly relate to MG. A Boolean nature of gravity is suggested by the Human Integration Design Handbook (HIDH) (Christensen et al., n.d.) and using 1G volumes for all HG designs is recommended; see Figure 1.10.

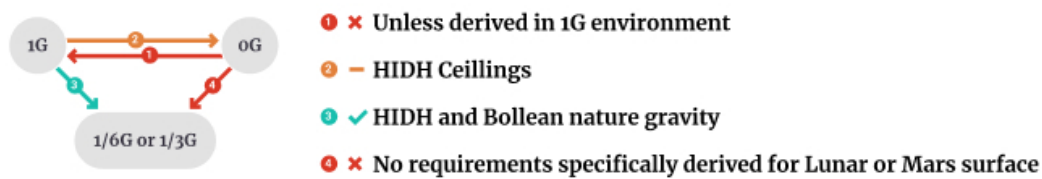


Figure 1.10: Recommendations for habitable volume design under HG adapted from(Christensen et al., n.d.) and (M. Simon et al., 2012). Credit to NASA Standard. *Reprinted from Acta astronautica, Vol 80, Simon et al. (2012). Historical volume estimation and a structured method for calculating habitable volume for in-space and surface habitats, Pages No.16, Copyright (2022), with permission from Elsevier Science Technology Journals.*

In future design concepts for workplaces, speculative predictions must be avoided and instead, quantitative and repetitive models developed. This can be accomplished using evidence-based sizing methods, built on functional, mission, and operational requirements. Despite working volume being an important issue for comfort, it was not studied within the framework of this dissertation. In this thesis, comfort in the workplace depends on the design of the workplace. The next paragraph will provide more information about the history of workplace design parameters.

Effects of workplace design

Until 1970, most sedentary studies were based on theoretical concepts, comments of subjects, average anthropometric indicators of the population, or radiographic studies. Design elements such as the backrest, armrest, seat slope, seat shape, and the seating width and length were

studied. It was concluded that it is important to observe the state of the spine in a standing posture before analyzing the sitting one. The following shows the different common postural deviation, and their relation to the workplace design parameters.

Bendix and Biering-Sørensen, 1983 studied the effect of the seat slope with 4-level option on 10 subjects during 1-hour experiments, observing an increase in lumbar lordosis with increasing forward seat tilt and hypothesizing three ways the body potentially adapts to forward seat tilt. See Figure 1.11.

Since their subjects' lumbar angles increased by 4 degrees, they suggested that position Figure 1.11 (B) took place. The subjects in the experiment themselves reported 0 - 5 - degree inclines as being most comfortable. Bendix and Biering-Sørensen, 1983 recommended a forward slope. Other solutions have been proposed such as level and backward slope. Schulthess, 1907 had suggested a 3 to 5-degree backward slope.

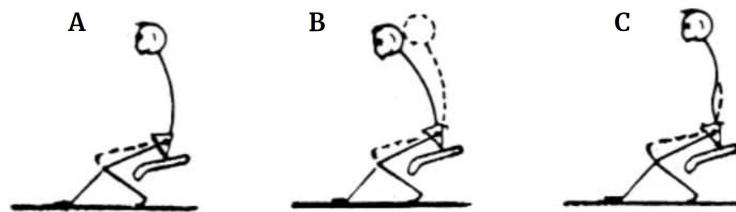


Figure 1.11: Three suggested body adaptations to inclined seats (Bendix and Biering-Sørensen, 1983). *Reprinted from Journal of Manipulative and Physiological Therapeutics, Vol 22 /Issue 9, Donald H. et al. (1999). Sitting biomechanics Part I: Review of the Literature, Pages No.16, Copyright (2022), with permission from Elsevier.*

Floyd and Roberts, 1958 proposed adjusting the tilt of the lower part of the seat to suit job requirements: freedom of movement would be provided by the horizontal seat, and tilting back helped the subject use the backrest for lumbar support.

The range of seat widths and lengths has also been extensively studied. In most references, the width and length were between 35 and 40 cm, respectively (Kroemer, 1971). Various propositions regarding seat shapes have included the saddle, molded for buttock fit and with posterior slope. Efforts to adjust the seat to the thighs have been unsuccessful, but an optimal solution of the flat surface has been suggested (Bennett, 1928). B, 1948; Keegan, 2005 and Kroemer, 1971 provided reviews on seat back design. Table 1.3 shows the recommended seat back inclinations from 90 to 125 degrees.

Table 1.3: Summary of seat-back inclination before 1972 (Harrison et al., 1999).

Author	Year	Suggested seat-back angle
Schulthess (Schulthess, 1907)	1905	100-105 degrees
Schede (Schede, 1935)	1935	Individual minimum
Lay and Fisher (Lay and Fisher, 1940)	1940	111-117 degrees
Morant (Morant, 1947)	1947	110 degrees for alert pilots, 110-125 degrees for rest position
Kroemer (Kroemer, 1971)	1971	90-120 degree range

Note: Reprinted from *Journal of Manipulative and Physiological Therapeutics*, Vol 22 /Issue 9, Donald H. et al. (1999). *Sitting biomechanics Part I: Review of the Literature*, Pages No.16, Copyright (2022), with permission from Elsevier.

Most sources recommended lumbar pad support in the range (3-5 cm) proposed by (Majeske and Buchanan, 1984). They argued that different joint angles were more adequate when sitting with lumbar support.

Williams et al., 1991 studied 210 subjects who, when they sat with lumbar support, reported significant reductions in pre-existing lower back pain and reductions in reflected leg pain.

It is also important to consider previously adopted guidelines on the formation of the design of the working space of several other environments, namely tanks, land vehicles, and airplanes. These can act as analogues to astronauts' workplaces.

Tanks are designed in such a way as to maximize the efficiency of crew members and the productivity of their labor during long periods in the tank. When designing a tanker's workplace, the main rule is to consider the location of the CoM relative to the fulcrum of the body and the reach of the limbs from this zone. The further the distance is, the faster fatigue will come due to increased muscle tension. Also, considering such parameters as visibility and reach of controls, creating conditions for short and long rest should be carefully studied and included at the design stage.

Civil land transport has the largest volume of free space in comparison with other analogues. Therefore, from the layout of the free volume in their design, the emphasis is transferred to the layout of the equipment. First, this applies to the seat: the correct shape is created thanks to special studies designed to calculate the main parameters as accurately as possible. The dimensions shown in Figure 1.12 (A) were determined by studying and comparing many different Soviet and foreign seats in vehicles.

A number of requirements relate to the **driver workplace**: safe entry and exit from the cab, control in any position, and the most comfortable body position during work. The minimum seat width should be 48 cm, with the option of adjusting seat position within ± 10 cm in the horizontal and ± 5 cm in the vertical planes. The backrest should have an appropriate slope;

its distance from the pedals should be 90-93 cm. The controls must be placed within reach of the motor field (see Figure 1.12 (B and (C)); the most important and regularly used controls should be within easy reach of the motor field. The location of the controls helps to effectively distribute the loads of both arms and legs of the human operator.

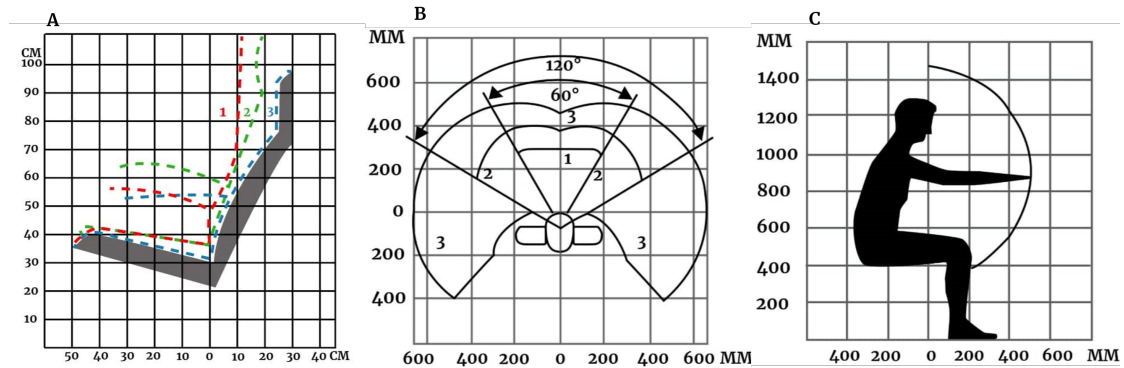


Figure 1.12: (A) Seats in vehicles (side view) (“Gardenweb”, 2022). (retrieved from <http://gardenweb.ru/rabochee-sidene> 1 - seat in aircraft of British airlines; 2 - seat in fast trains of Swiss railways; 3 - seat in passenger trains of British Railways, (B) 1 - area for placing the most frequently used and most important controls (optimal area of the motor field); 2 - area for placing frequently used controls (area of easy reach of the motor field); 3 - area for placement of rarely used controls (area of reach of the motor field), (C) The reach of the motor field in the vertical plane when working while sitting.; (Neufert and Neufert, 2012)

Compared to land transport, **pilot workplaces** are characterized by smaller working volumes and higher requirements for operational efficiency, making their requirements for ergonomic parameters during design even higher.

To date, no single international ergonomic standard for the design of a cockpit has been validated. Therefore, seating of pilots in aircraft of similar purpose - and even designed by the same designer – present significant differences. This is sometimes due to the design conditions, but in most cases such difficulties arise due to the lack of solid requirements and standards (Volkova, 2017).

Performance can thus be improved firstly by optimizing comfort and fatigue, using functional design considerations that accommodate physical and psychological needs. Currently, common extreme environment habitat designs aim primarily to satisfy technical requirements of a mission, notably in terms of essential life support for the crew, but to ensure well-being and productivity, prioritization of aesthetic and ergonomic aspects throughout the design process must occur. Secondly, safety and comfort considerations taking into account the hardware's structural and technical requirements must not be neglected and experiences in designing workplaces for workers in an office, in transport, and in aircraft can be effectively applied to develop guidelines for workplaces in new conditions.

It is vital to identify the gaps in methods and processes, which are used for human factors in data collection and investigation. This will make it possible to enhance advancement in space habitat design practices for the future.

1.2.6 Workplace under different gravity conditions

This sub-chapter is based on the conference paper "Defining best practices for safety and comfort in Moon and mars habitats" prepared for the International Astronautical Conference 2019 held in Washington DC, USA (Volkova et al., 2019). The best workplace design practices under various gravity conditions (1G, MG, HG) were analyzed and defined four types of research methodologies, describing behavioural (cognitive), psychological (social), physiological and biomechanical elements considered by ergonomists in workplace design in extreme environments. Figure 1.13 presents all elements considered by ergonomists in the design of alternative workplaces. Table 1.4 shows the gaps in the field with respect to the research fields and gravity level.

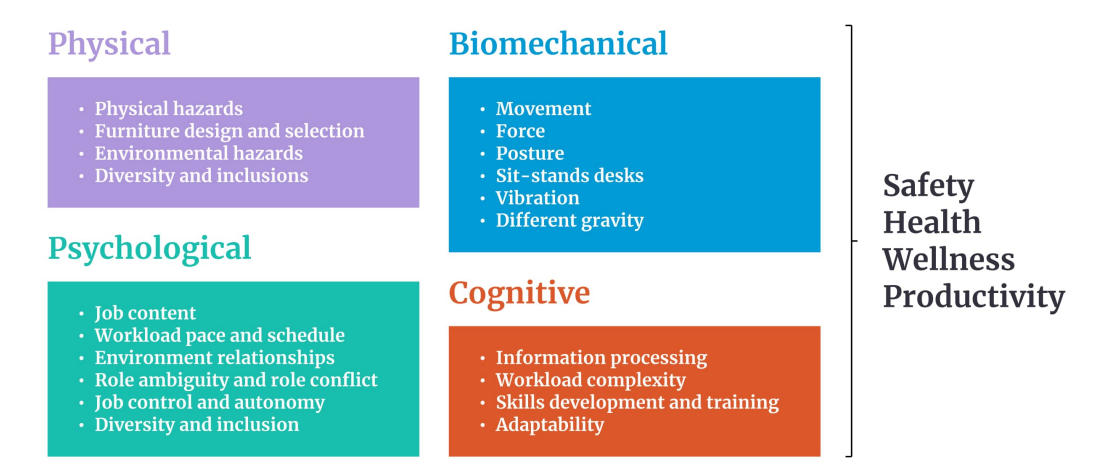


Figure 1.13: Specific research field elements considered by ergonomists in the workplace design in extreme environments. Adapted and supplemented from (McAtamney et al., 2016). Copyright (2022) From Challenges and Future Research Opportunities with New Ways of Working by McAtamney et al./Alan Hedge. Reproduced by permission of Taylor and Francis Group, LLC, a division of Informa plc.

Only the main research fields of direct relevance to this thesis are presented here. The focus is thus on the biomechanical^V and physical research aspects. Other research fields and elements are explained in and physical research filed.

^V *Biomechanical* research field is used to study human kinetics and kinematics, and estimate corresponding performance.

Other research fields and elements are explained in (Volkova et al., 2019).

Table 1.4: Research field - gravity level summary. Extracted and adapted from (Volkova et al., 2019)

	1G		HG		MG	
Research field	Regular work-place	Earth-based simulations	Simulation	Real mission	ISS, Shuttle, Skylab	MIR,
Cognitive	✓	✓*	?	?	✓*	
Psychological	✓	✓	?	?	✓	
Physiological	✓	-	-	?	✓	
Biomechanical	✓	-	-	?	✓*	

Note: ✓ - base of data exist in the research field, ✓* - sporadic data exist in this field of research, ? - a very small data set exist in the research field, " - " no data exist yet in the research field,

Workplaces in 1G

Physiological/Biomechanical

Earth-based simulators

There are very few studies related to the physiological, biomechanical user perspective in connection with isolated, confined, extreme (ICE) environments. Adams, 2002 proposed to study the subject's patterns of motions within a given environment of LMLSTP, Phase III. This method involved the capture of hard data and application of statistical analysis to the use of provided spaces for work and living. Tafforin and Bichi, 1996 collected video data and organized a global data set, which would respect the multidisciplinary effects (physiological, psychological, and operational) of LD isolation. One of the first data storage GLOBEMSI was created by ESA for ISEMSI-90, EXEMSI-92, and HUBES-94 analysis. They built the statistics of motions, postures, distances between subjects, and their social orientations. It could potentially be very useful for harmonization and then comparing the data for LD missions. Some interesting projects with digital tracking systems have more recently been proposed for Earth-based simulator monitoring. One example is the AllTraq Real-Time Location System implementation into the NEEMO project. It can measure real-time location and real-time inventory of assets; it can also monitor temperature, humidity, and motion, as well as generating alerts for unauthorized movement or sensor data and providing historical data and analytics.

Regular workplaces

Current research related to the physiological, biomechanical analysis propose the following solutions for "better" integration of the user to the architectural conceptions (Shapiro, 2019):

- Path integration-cues to self – motion optic flow (information from vision about move-

ment speed) (Lappe, Hoffmann, et al., 2000);

- Proprioception (information from muscles and the joints about the location of the limbs) (Zabihhosseinian et al., 2015);
- Motor efference (commands coming from the brain used to predict the locations of the limbs) (Fee, 2014);
- Vestibular information (information from the inner ear about balance and rotation).

There is also some innovative new research which will be soon implemented to the workplace process design related to human biomechanics. Several examples are discussed here.

Nishanth et al., 2015 performed posture assessment on employees to derive risk of MSD injury in a stator assembly shop. This was based on a Rapid Upper Limb Assessment score (RULA). The authors proposed to improve this study by analyzing employee psychosocial aspects, energy expenditure and heart rate variability based on discussion by Uusitalo et al., 2011 and Bouchard and Trudeau, 2007 for disease control and prevention. Bruno Garza and Young, 2015 reviewed aspects of performance and preference that relate to computer work. They focused on biomechanical risk factors of pointing devices, keyboards, as well as touch less gesturing and voice input in offices.

Kim et al., 2015 studied the impact of surface hardness on biomechanical stress, the pressure from the contact of the forearm with the surface, while using computer input devices. It was found that in the case of a surface covered by soft material, the body had more significant contact area with this surface in comparison with a surface covered by hard material. Many questions about the features of sitting-standing workstations remain (Karol and Robertson, 2015). The Karol and Robertson study was related to human comfort and performance analysis. The authors compared the effects of standing and sitting on the human body. They found that temporary standing during an 8-hour workday is better than continuous sitting. However, prolonged standing can lead to injury. According to the same authors there is currently not enough literature on the impact of sit and stand workstations on human productivity. Often, studies about sit and stand workstations focus on increasing physical performance and musculoskeletal comfort (Karol and Robertson, 2015).

To analyze and design human-built environment systems, different laws can be implemented; these include the Fitts model (Fitts, 1954) with all its variations adapted for different body parts. Applying these laws to the design process can make positive and impactful changes for the user.

New technologies can help to collect and analyse biomechanics data using sensors, motion capture with markers or markerless, new digital applications. Such technologies can increase the efficiency of experiments and speedup the data collection, processing and analysis.

Workplaces in MG

Physiological/Biomechanical

According to NASA Spinoff measurements ("NASA. Ergonomic chair website", 2022), the most unstressed and relaxed state of subjects in MG occur when there is a 128-degree trunk-to-thigh angle, a 122-degree angle between shoulder and forearm, a 36-degree angle between shoulder and back, and finally a 111-degree shank to foot angle. The same authors "NASA. Ergonomic chair website", 2022 state that such "posture fosters a non-stressed muscle system, enhanced circulation" (p.20) correctly aligned vertebrae, improved digestion, and encouraged better breathing.

The effectiveness of subjects performing tasks on the ISS mainly depends on pre-designed procedures (Rando and Schuh, 2008). This study showed that the subject's task performance, evaluated after scheduled activities within the allotted time, was affected by the poor design of procedures for station tasks. It is crucial to perform the task in time, which is directly related to well-designed procedures.

The task performance designed for the 1G setting can be decreased in the MG or HG environment. It follows that fixation systems and all interfaces must be designed with respect to the environments and gravity in which they would be used (Ippel, 1996) because of vestibular and sensory adaptation. Over time the human body learns to live in MG, made possible by means of adaptive bodily responses such as fluid shifts and neuromotor adjustments.

During a separate mission on Skylab, MIR, ISS a different solution for workplace design was applied and tested (Häuplik-Meusburger, 2011). In MG, restraint systems are one of the most essential elements of the workplace. Several examples of restraint systems and workplaces (Vogler, 2005 and Häuplik-Meusburger, 2011) are presented in Figure 1.14. It is important to note that the restraint system plays a significant role during space missions. The comparison of workplace design for space-related projects is presented in Appendix Figure A.2.

Video recording of subjects is one way to carry out biomechanical analysis; this was done, for example at Skylab (Leach and Rambaut, 1977). Due to the architectural construction of the experimental and forward compartments, it was situated in a 1G orientation. The following data were recorded:

- The velocity of motions;
- Translating and completing the translation of body parts, including feet, head, etc..

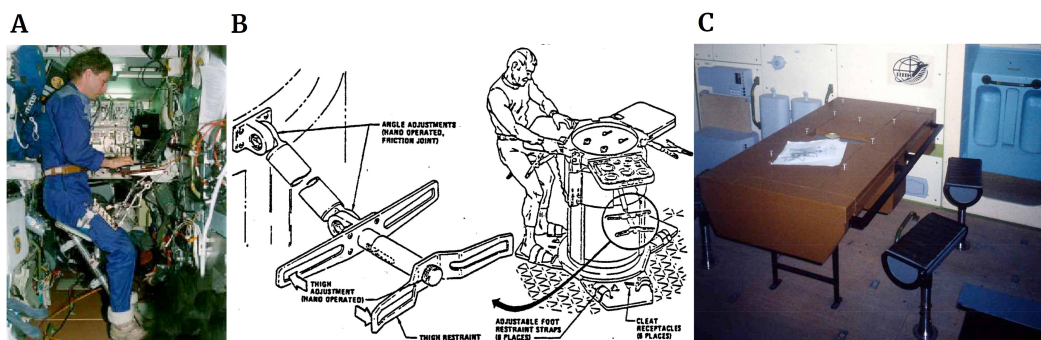


Figure 1.14: (A) Scheme of Munich Space Chair. (B) The food table restraints and foot loops in Skylab, (C) Chairs in the MIR station mock-up at the European Astronauts Center in Cologne (Vogler, 2005). Republished with permission of SAE International, from Design study for an Astronaut's workstation, Vogler, Andreas, SAE Technical paper series, 2005-01-3050, copyright 2022; permission conveyed through Copyright Clearance Center, Inc.

ICE space and the wardroom appeared to cause the motions of the subject almost in a 1G orientation. For example, some troubles were discovered in such a workplace. Motions around the worktable showed to be to some degree an issue for the subjects (Leach and Rambaut, 1977).

Operational challenges happen at the beginning of spaceflight as the subject has troubles with gaze transition (reading, perceiving the information on the screens). Human factors for spaceflight ought to consider the suggestions of these neurovestibular changes for eye-head coordination and motions.

McPhee and Charles stated that "designers of cursor control devices have to consider a number of environmental factors, including g-forces, vibration, and gloved operations, as well as task specificity" (2009,p.20). The experiment with cursor control shows that during several flight studies, the computer mouse would not work in MG (Holden et al., 1991). The same authors tested cursor control devices operated with and without gloves using various devices. The trackball devices performed better (timing, precision) in comparison with the roll bar device, joystick, track pad mouse, and optical mouse. Holden et al., 1991 conclude that it is better to have different devices for different tasks.

Workplaces in HG ($\frac{1}{6}G$ - $\frac{1}{3}G$)

Physiological/Biomechanical

HG workplaces have only been designed as part of the Apollo program. Apollo's lunar module was confined to an interior space of approximately 6.2 m³ designed for the subjects for three men. The duration of all missions was only several days. Physical movement inside the lunar module was extremely restricted. For ergonomic safety, a restraint system and floor covered with velcro were integrated into the module. There was no privacy in the module. This module

was adapted for rest and work with most subjects working on the lunar surface outside this module. There were not any seats for the subjects; during flight periods they were fixed into place by spring-loaded cables attached to the floor, as seen in Figure 1.15. Subjects slept on slung hammocks, like bunk beds, crossing one over another. The lunar module had been designed to operate in an HG or MR environment (Kelly, 1964).

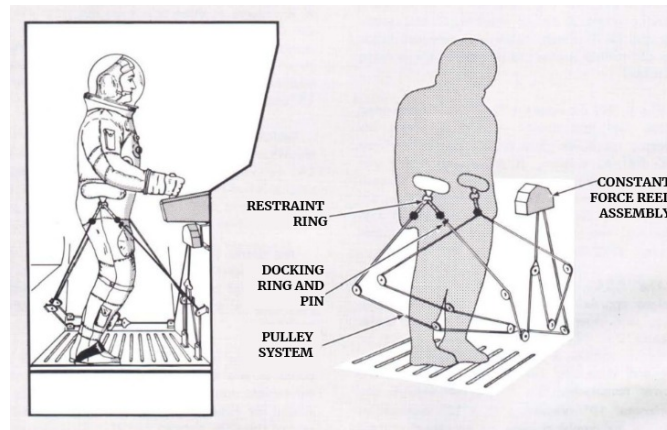


Figure 1.15: Subject inside the Lunar Module. NASA, Lunar module documentation (“NASA. Apollo news reference. Section: Crew personal equipment CPE1-16”, 1972). Credit to NASA/ALSJ.

All computing equipment and joysticks were designed with respect to lunar inertia (Blackshear and Gapcynski, 1977). In the instructions for equipment, designers described the limitations of the necessary forces and angles to manipulate the equipment. According to “ApolloSaturn website”, 2017 the astronauts had Velcro on the floor, armrests, and handrails.

The armrests, at each subject station, were integrated for stability during the operation of the thrust/propulsion control unit, as well as the attitude control unit. They were also used to restrain the subject laterally. The adjustable armrests could be moved in two ways: by exerting downward pressure or by pressing latch buttons. The maximum strength limit of the armrest was 1332 N (“ApolloSaturn website”, 2017).

Multiple *Handholds* at current stations help attenuate movements in the desired direction. The handholds are abundant in the module, which may help prevent non-desirable displacement (“ApolloSaturn website”, 2017).

Restraint Assembly is a complex system of ropes, restraint rings, and a constant- force reel system. Altogether, it ensures that the task is performed with the lowest possible physical effort and lowest potential for injuries (“ApolloSaturn website”, 2017).

For lunar, as well as planetary missions, the interactive systems, such as Phienix Science Interface (PSI) or other analogs, will be required. Such interfaces are good examples of human-computer interaction, which can efficiently support human decision-making (Aghevli et al.,

2006).

Many scientists predict that analysis of work under $\frac{1}{6}G$ still requires further research (Häuplik-Meusburger, 2011). Such analysis and experiments can be validated by means of suspension systems, under water experiments in neutral buoyancy laboratory (NBL) and parabolic flights. Currently, parabolic flight simulation is recognized as the gold standard for HG simulations.

1.2.7 Assessment methods

In the following paragraphs, various existing research methods will be listed, with an explanation of human biomechanics in the workplace. It will also be clarified which methods were used in this thesis.

Direct assessment methods

This subsection was extracted from Volkova et al., 2022 peer-reviewed Frontier in Physiology publication Volkova et al., 2022 devoted to "An empirical and subjective model of upper extremity fatigue under hypogravity". Various tools have been used to measure physiological parameters for upper extremity physical fatigue and workload investigation. As indicated by Volkova et al., 2022 these include dynamometer (Romero-Franco et al., 2019, Alizadehkhayat et al., 2007), EMG (Chany et al., 2007, Lalitharatne et al., 2012), electroencephalographic measure (Wang et al., 2021) and electrocardiogram (Redgrave et al., 2018). Various monitoring approaches have been applied: posture sway (Davidson et al., 2004), joint kinematics (Riley and Bilodeau, 2002), perceived discomfort/fatigue (Balci and Aghazadeh, 2004). In this thesis, hand as well as back-chest-leg dynamometers were used. For some experiments, a timer was used to record the duration of the participant's work.

Indirect assessment methods

The biomechanical models are based on typical human postures. To analyze the forces and torques acting on the joints, different biomechanical modes can be applied. The most common methods for deriving the equations of motions are described below (Aritan, 2012):

The total energy of the body in motion is used to specify the **Lagrangian equation of motion**. Forces between bodies are not taken into account in this formulation because they do not add energy to the system. Despite motion equations often being simple to define, this method is unsuitable for inverse dynamics calculations (Aritan, 2012).

Newton-Euler equations. For complicated systems, all forces applied to each body must be evaluated, making this method challenging and time-consuming. Any suitable inertial reference frame can be used to write the overall equations of motion. This approach is useful for inverse dynamics since it has both recursive and non-recursive formulations (Newton, 2009).

D'Alembert principle: The equation of motion includes all applied forces acting on each

accelerated body. The equilibrium equation is then solved. The limitation of this strategy is that it can only be utilized for slow-moving systems (d'Alembert, 1743).

Kane's dynamics This method based on the Lagrange form of D'Alembert's principle group of methods. By multiplying the Newton-Euler equations by vectors, scalar forces acting on each body are built. In this case, closed kinematic chains can be calculated directly (Kane and Levinson, 1985).

The following example from Song et al., 2010 describes the pilot posture. This model allows calculations of the influential waist factors through the mechanical, human model. In this case, the biomechanical model represents the simplified skeleton of the human body, shown in Figure 1.16. Two directions of motions were analyzed: forward-backward and right-left. Some forces e.g., F_m on the same Figure 1.16, represent back muscle strength, which helps to tilt forward or back lean.

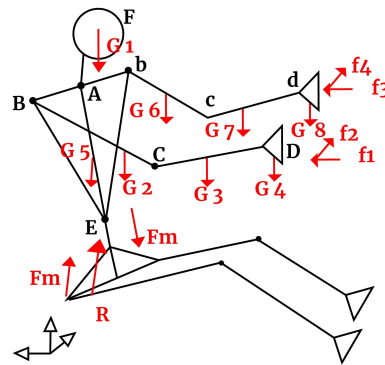


Figure 1.16: Biomechanical human models. Sitting posture (Song et al., 2010). Copyright © 2010 IEEE

The mechanical analysis of these positions was done under the assumptions that gravity and manipulation forces are known, but joint forces and muscle forces are unknown.. After solving balance these equations for human body, necessary forces could be found. The detailed studies can be found in (Song et al., 2010). The verification of the results can be undertaken using digital human modeling (DHM) softwares such as JACK (Blanchonette, 2010) or its analog.

In this thesis, D'Alembert's principle, as well as Lagrange equations of motions were used for biomechanical modeling. D'Alembert's principle was used for preliminary study of static motions for simplified 2-DOF biomechanical model. Lagrange equations were used for dynamic motions study.

Other examples of the dependence of human body and biomechanical parameters from design variables are listed below:

- Biomechanical analysis is essential for estimation handling activity. Tichauer, 1971

proposed to determine the moment of load relative to the disk of the vertebral column L5/S1 to establish the limit of lifting and carrying loads;

- According to Pynt, 2015, the effect of backrest recline 100 ± 110 and its effects of body posture defined. In the same research, the impact of forwarding tilt seating, listed the improvements in the forward tilt sitting design;
- Another study shows the weight load influencing factors (Hedge, 2016).

Other methods to investigate workplace design impact on human are motion-capture systems (Chaffin, 2007), as well as virtual reality, augmented reality (Ong et al., 2007), DHM (Ozsoy et al., 2015 Summerskill et al., 2016), game elements (Kosmadoudi et al., 2013) and finite element methods (Abouelkhair and Duprey, 2012), and artificial neural networks (Baque et al., 2018) are used for workplace design investigation. DHM evaluates the physical workload via joint moments by assuming a rigid link model for the human body. Many of these methods do not allow us to fully take into account the altered gravitational conditions; this could either be because of the complexity of the software or because of the need to use sensors attached to the body, which restrains motion or measurement. Computer vision provides significant benefits because of its ease of use and non-invasiveness (for example, in the case of markerless methods - see pros and cons for motion capture with marker and markerless methods in Appendix Table A.1). Existing methods based on only one camera can reconstruct a three-dimensional pose relative to the camera; however, this would not provide information about the global position and speed of the astronaut. Therefore, in this thesis, the aim was to evaluate the global three-dimensional posture of the human at each point; this was realized by evaluating video frames from several cameras located around the track. One method to obtain these poses is to manually annotate each frame and recreate a 3D structure from it. However, since manual annotation is time-consuming, it was decided instead to predict 2D joint locations with OpenPose (Osokin, 2018; Nakano et al., 2020) without the need to wear markers on the body. Usually, posture estimation algorithms have only been trained using databases of human posture, which do not contain images of astronauts working in an underwater environment. Existing data sets with underwater image data processing (Ma et al., 2009, Jian et al., 2017) are very limited in the number of human postures and their locations, which is why methods trained using them cannot be generalized well.

Subjective assessment methods

This subsection was extracted and adapted from Volkova et al., 2022 peer-reviewed Frontier in Physiology publication Volkova et al., 2022 devoted to "An empirical and subjective model of upper extremity fatigue under hypogravity". In Volkova et al., 2022 was stated that different subjective assessment methods can be implemented for mental workload study as well as ergonomic risk factors at workplace. Various subjective assessment methods can be implemented for mental workload study as well as ergonomic risk factors in the workplace. Some subjective assessment tools that could be applied to pilot or astronaut case studies include:

the Cooper-Harper Scale (Cooper and Harper, 1969), the Bedford Scale (Roscoe and Ellis, 1990), the Subjective assessment technique (SWAT) (Reid and Nygren, 1988) and the NASA Task Load Index (NASA-TLX) (Hart and Staveland, 1988), the Workload Profile (WP) (Tsang and Velazquez, 1996). NASA-TLX has the highest sensitivity.

According to one study (Rubio et al., 2004) NASA-TLX has the highest sensitivity, as well as strongest operator acceptance (Hill et al., 1992) compared to SWAT, WP. NASA-TLX's validity assessment, resulted in a positive correlation coefficient was found between the three tools and NASA-TLX shows a higher correlation with human performance than either SWAT and WP. Rubio et al., 2004 suggested that the SWAT and NASA-TLX is credible for composite natural world tasks. Rubio et al., 2004 the Subjective assessment technique and NASA-TLX may be credible for composite natural world tasks and if the goal is to predict task-specific human performance, NASA-TLX is recommended. In this thesis NASA-TLX method was applied for performance and fatigue studies.

Observational methods

The Ovako Working Posture Analysing System (OWAS) (Karhu et al., 1977), RULA (McAtamney and Corlett, 1993), and Rapid Entire Body Assessment (REBA) (Hignett and McAtamney, 2000), occupational repetitive action (OCRA) checklist/index are observational methods used to assess postural stress on the workers. All of the methods were created for distinct goals, and as a result, they are applied in a variety of settings (Kilbom, 1994). Each strategy offers a unique approach to operator classification that sets it apart from the others. Depending on the technique utilized, this can result in variations in the ultimate outcome for the operator's load.

Scientific studies have demonstrated the utility of such methodologies in monitoring worker posture in a variety of settings, including warehouses (Torres and Viña, 2012), construction (K. W. Li and Lee, 1999), and more.

Unstructured observational methods, conducted in an open manner are quite common for postural studies investigations. The length of observation periods plays an important role in research. If it concerns the study of human behavior or movement, then the duration is determined by the type of task performed by the participant in the experiment. Where dynamic operation is observed, long observation periods may be appropriate, for more static applications, short observation periods may be appropriate (Branton and Grayson, 1967; Shackel et al., 1969). There are also gender differences in sitting postures taken, as well as in the length of periods of sitting noted by (Shackel et al., 1969). In this thesis, the OCRA checklist was used for quick assessment of upper-limb exposure in repetitive labor and unstructured observational methods were used for sitting neutral posture investigations under HG and joint angles assessment when markerless motion capture method did not work well due to poor visibility.

1.2.8 Workplace design standardization

This sub-chapter provides an overview of "Human factors, ergonomics and biomechanics", with a particular focus on international and american perspectives. However, the main national standards will also be discussed.

Standards are essential for the collection and dissemination of technical information (Spivak and Brenner, 2018). Similarly, standards are needed for international quality control and to support legislation in ensuring equal opportunity and work. Standardization provides uniformity and interchangeability in certain applications; for example, standards can prevent unnecessary product variations by limiting the variety of sizes and shapes. Such measures reduce trade barriers, increase security, ensure compatibility of products, systems, and services (Wettig, 2002).

The basis of worldwide and national standardization related to the human factor and ergonomics are listed in Figure 1.17 below :

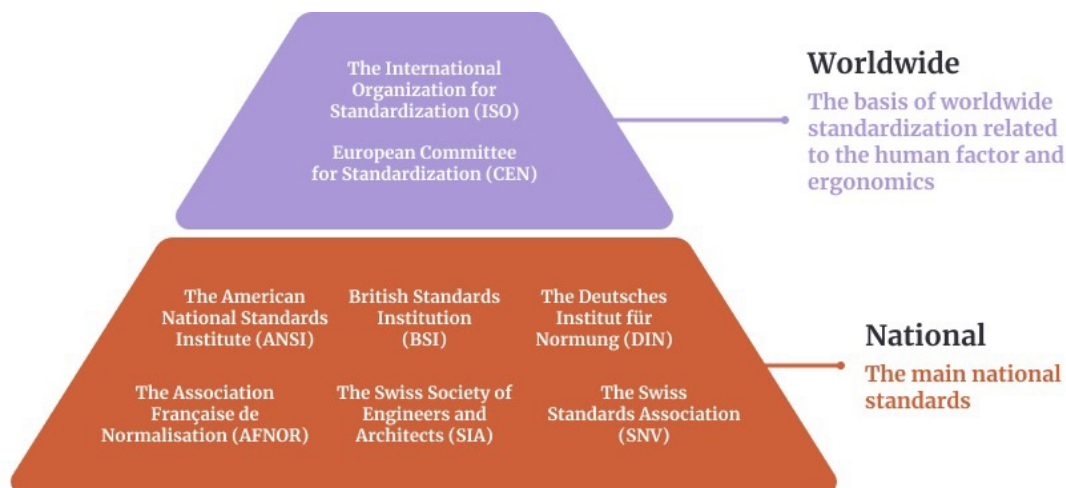


Figure 1.17: Worldwide and national human factors and ergonomics standards

In some cases, standards technical societies, labor organizations, customer organizations, government agencies may also prepare specific standards.

In Figure 1.18 the relation between physical performance parameters (human factor) and standards subjects is demonstrated.

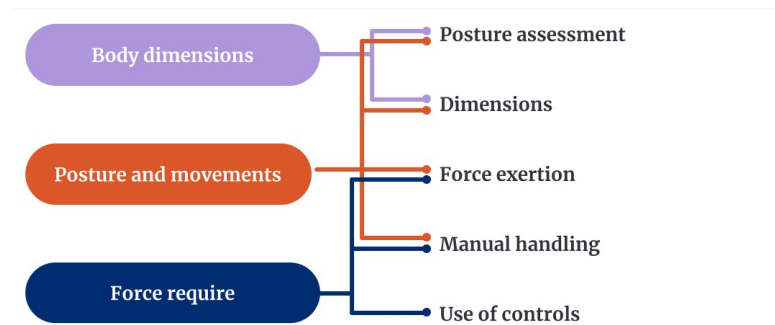


Figure 1.18: Human factor - standards groups relation

ISO standards for ergonomics According to Karwowski et al., 2021 ISO applied in 146 countries of national standards bodies. ISO promotes international interaction for the exchange of goods and services. ISO also contributes to the expansion of cooperation in the fields of scientific, economic and technological activities (Karwowski et al., 2021).

Since 1975, ISO has maintained Technical Committee (TC) 159 to create standards in the field of ergonomics (Parsons, 1995). The ISO technical committee also considers the fields of anthropometry and biomechanics to warrant optimal adaptation of working and living conditions to physiological and psychological capabilities of a person in a technological environment. Safety, health, well-being and efficiency are the primary goals of such standardization efforts (Parsons, 1995). The Ergonomics Standardization Group consists of four subcommittees: SC1, SC3, SC4 and SC5. There are two main committees focuses on the aspects studied in the frame of this thesis: "Ergonomic guiding principles" and "Anthropometry and biomechanics" ("ISO", 2004).

ISO standards for ergonomics guiding principles The ergonomics guiding principles are dealt with by Subcommittee TC159/SC1. This standard sets out ergonomic design principles for a work system, the application of which are relevant to human health and safety when designing working conditions (Parsons, 1995a). These include TC 159/SC 1/WG1 (see all standards of this committee in Appendix Table A.2, A.4, A.6).

ISO Standards for Anthropometry and biomechanics These standards are handled by subcommittee TC159/SC3. It consists of four working groups: "Anthropometry"; "Assessment of working postures", "Human physical strength" and "Manual work and heavy weights" ("ISO", 2004).

In this thesis, other standards from other committees were implemented, such as:

- ISO 11226-1:2000 - Ergonomics - Evaluation of static working postures ("ISO 11226.EPFL Cobaz site", 2000);

- ISO/CD 11228-2 Ergonomics - Manual handling - Part 2: Pushing and pulling ("ISO 11228-2. EPFL Cobaz site", 2007);
- ISO/CD 11228-3 Ergonomics-Manual handling - part 3: Handling of low loads at high frequency ("ISO 11228-3. EPFL Cobaz site", 2007).

In the appendix, the Organizational structure of ISO TC 159 "Ergonomics" and other ergonomics-related standards under development can be found Appendix Table A.3 - A.6.

Below are some details related to the selected standards.

ISO 11226:2000 - Ergonomics - Evaluation of static working postures

The first standard that can be directly related to the results obtained is the ISO 11226: 2000 standard. This standard determined the acceptability of static working postures. Posture evaluation adapted for the different body segments and joints. Initially, only body angles are taken into account (recommendations are largely based on the risks of overloading passive body structures). The rating may result in an "acceptable", "go to step 2" or "not recommended" result ("ISO 11226.EPFL Cobaz site", 2000). If the working posture is not acceptable, then adjustments must be made to approach a neutral working position. The duration of the working posture should be taken into account when assessing body position (using recommendations based on endurance data). Extreme joint positions should be assessed as "not recommended" Karwowski et al., 2021. In this dissertation, work postures were assessed using computer vision, inclinometers and goniometers.

Within the framework of this standard, different parts of the body, torso, upper limbs (forearm and shoulder) are studied. The angles of the neck and head were not taken into account due to the protrusion of the neck and head from the water and reduced visibility to recognize these body segments.

ISO/CD 11228-2 Ergonomics - Manual handling - Part 2: Pushing and pulling

There are few quantitative risk-assessment approaches for pushing and pulling on a formulaic basis ("ISO 11228-2. EPFL Cobaz site", 2007). Most likely because it requires less physical effort than lifting and hauling. This gap is filled, according to ISO 11228-2 ("ISO 11228-2. EPFL Cobaz site", 2007).

Pushing and pulling, unlike lifting and carrying, were thought to be unrelated to biomechanics (Mital et al., 2017). However, recent research by Jäger et al., 2001 has shown that pulling tasks might result in significant lumbar spine loads, particularly when the task is pulling. The appropriate posture and location of force exertion have a significant impact on maximum voluntary contraction when pushing and pulling things (Schaub et al., 1997). Depending on the operators' size, the biomechanical load condition for a given task may differ.

Risk assessment for pushing and pulling should consider: initial force used to overcome the

object inertia, posture a person adopt, frequency and duration of the applied force, distance over which operators move objects, moving object maneuverability, the surface over which the object moved, individual characteristics of operator. Considering biomechanical approach, force exertion in relation to both human physical capabilities and lumbar spine compression is considered for different age population. Also energy expenditure and fatigue limits are considered. And operator perception of acceptable efforts, force and discomfort are taken into account. The risk assessment include: 2 methods: simplified and detailed. These methods have 3 risk scores - green (acceptable), yellow (conditionally acceptable risk) and red- (not acceptable).

ISO/CD 11228-3 Ergonomics-Manual handling - part 3: Handling of low loads at high frequency

This standard specifies ergonomic recommendations for repeated job tasks that require manual handling of small loads on a regular basis. It provides guidance on assessing the risk factors typically associated with high-frequency, moderate-duty work (“ISO 11228-3. EPFL Cobaz site”, 2007). These recommendations are primarily based on experimental studies of musculoskeletal loading, pain and discomfort. This standard based on OCRA risk assessment. The OCRA index is the ratio of the number of all actions performed, , to the number of specific actions performed for each body part in a work shift (Occhipinti, 1998; Colombini, 2002). Figure 1.19 shows the main components of OCRA checklist.

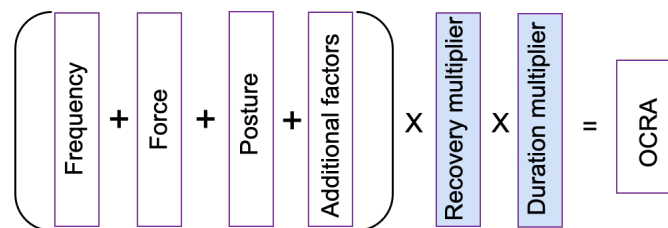


Figure 1.19: OCRA checklist components (“ISO 11228-3. EPFL Cobaz site”, 2007).

CEN standards for ergonomics CEN standards for ergonomics European standards development organizations cooperate with international bodies and national standards bodies in Europe (Wettig, 2002). According to (Dul et al., 1996), CEN established CEN TC122 Ergonomics as the body responsible for developing standards in the field of ergonomics in 1987. The organizational structure of CEN is shown in Appendix Table A.3 and A.5.

USA governmental human factors/ergonomics standards (Poston, 2004). A list of other state standards, including NASA-STD-3000 (Christensen et al., n.d.) relevant to the dissertation. NASA-STD-3000 contains general requirements for human space objects and associated equipment. This standard can be applied to almost all types of equipment.

According to this standard: "each program shall identify an anthropometry, biomechanics, range of motion, and strength data set for the ground support population to be accommodated in support of all requirements in this section of this NASA Technical Standard" (p.185). It is possible to use existing data sets from the HIDH. According to Christensen et al., n.d. new data sets will be required. To enable for essential repair, "maintenance, assembly, testing, or operational use by ground support" " (p.15) employees, technical systems must consider the physical capabilities and limitations of workers. Ground support personnel should not be forced to move, twist, or be in awkward positions as a result of system architecture or vehicle layout and tasks. Awkward positioning might raise the chances of making mistakes or injuring yourself and new standards and guidelines can reduce this risk.

1.2.9 Filling the gap in the field

The risk of poor workplace design is related to the lack of human-centered design. A human-centered design will increase the efficiency of safety and operation of all workplace components and should thus have a positive impact on cost. One goal is to reduce the concerns that have been identified: psychological and physiological or biomechanical factors, when taken into account, will have an impact on decreasing risk of injury and increasing human performance, whether at the workplace, working in confined space mines, on a moon base or in a Space station.

In this work, analyzing the root cause of the inefficiencies of current workplace design in HG conditions was considered. As seen earlier, the potential efficiency of subjective ratings in assessing mechanisms underlying performance is promising for interface design, in spite of a lack of confidence in subjective methods by certain researchers. Following the literature review, the NASA Task Load index subjective assessment technique was chosen, see details of this method in Appendix Figure A.3 and Figure A.4. Given the limits to the various methods presented in this section, one of the most efficient approaches is to create a good ergonomic design with integrated biomechanical modeling. This should also include safety and human performance concerns, as well as comfort, physical fatigue and productivity. Biomechanical measures can be obtained with motion capture methods, allowing one to collect the experimental data with coordinates, angles of the joints, torques/forces, CoM of the human body and its different postures (dynamic and static) in an efficient way. This would be based on the defined biomechanical models adapted to the workplace design, and collected experimental data for different gravity conditions.

In this study, Task Intensity - ET estimation and NASA-TLX were used in a combined approach. HG was assumed to increase participant productivity through reduction of both physical fatigue and of the mental workload of participants, compared to Earth's gravity. The relevance of this kind of assessment model of physiological limitations in a given workplace environment is clear for HG as well as 1G. For HG in particular, maximum admissible weight and forces can be designed for for some populations and using this data, cumulative trauma and motion-

specific disorders may be reduced.

Statistical multivariate regression/machine learning algorithms were applied to be able to integrate all data related to design and human physiology/biomechanics, including subjective assessment data, in the model and thus create the "best" design solution. Random Forest can be a good solution for regression analysis in order to find a suitable solution for workplace design due to its advantages: efficient data-processing with a large number of features and classes; insensitivity to feature values scaling; both continuous and discrete signs as equally valid processes; the possibility of narrowing solutions from data with missing feature values; high parallelizability and scalability; and finally, assessment of the significance of individual features of the model.

There is a dire lack of data collected about the time of real experiments. However, given motion simulations in HG conditions, a combination of machine learning to find the "best" design solutions with further digital human modeling (DHM) and various manual scenarios tested without real participants can help create a good foundation for workplace design.

Thus, it can be stated that the multi-level modeling of subjects' workplaces is still under development, this being related to the lack and homogenization of data derived from previous missions. On the other hand, the rich experience of the design of Earth-based simulators and living in confined conditions can serve as a design base from which extrapolation is possible. This can serve as a design base from which extrapolation is possible. Evidence based on HG experimental data were obtained to verify any model that must be reliable.

This work includes evidence based on HG experimental data, human biomechanics modeling in different gravity conditions, digital modeling as well as recommendations provided by Apollo astronauts. Looking to the future, human-centered design is essential to achieve the next step toward exploring the Moon, Mars, and beyond.

1.3 Objectives and main contributions

The main objective of this research is to establish guidelines for workplace design based on biomechanics - specifically sitting workplaces and handling areas – in HG conditions. Examples include computer workstations (e.g., desk) and hardware assembling stations (e.g., workbench), including manual handling operations.

Such workplaces would be available to astronauts in space missions and their optimized design could then contribute to maximize work performance and minimize the risks of musculoskeletal injuries. The issues found in workplace design in confined conditions of ground-based facilities in extreme environments as well as information gathered from our inhabited space stations will be addressed. This will be extrapolated to future workplaces on the Moon and Mars.

The following steps were taken to reach the objective:

- Data collection and methods definition;
- Measurement and simulation of human performance, postures, fatigue, comfort in various sitting positions and manual operations (identification of typical poses);
- Combinatorial study of the obtained results (statistical analysis);
- Optimization of the workplace design based on human biomechanics (motion capture, factor analysis, 3D simulation, optimization);
- Recommendations development towards extension of 1G standards for ergonomics and biomechanics at the workplace for HG environment.

As a result of this work, recommendations for design, maintenance, and usage of such workplaces in different gravity conditions (1G, $\frac{1}{2}$ G, $\frac{1}{3}$ G) are provided. The identification of features and parameters allowing design optimization based on human biomechanics is conducted using numerical models, with physical experiments carried out in a water tank to confirm these results. The outcome of this work may have an impact on workplace designs for both Earth and Space projects and lay down a number of important ground rules. This state-of-the-art research started with a literature review. For European Space Agency (ESA), National Aeronautics and Space Administration (NASA), and German Aerospace Center, Roscosmos internal data archives, the search strategy with a "Boolean logic" was applied in these databases. The focus has been on space-related topics, and for simplicity, the term astronaut will be used in this document for a description of actors in space.

Scientific originality The following elements demonstrate the scientific originality of this study:

- Measurement of human muscular fatigue as a function of workload in HG conditions and integration of the results into design models;
- Modeling of the biomechanics of human movements in such conditions;
- Development of corresponding workplace layout;
- Development of a numerical model of human motions under HG;
- Proposed extension of existing 1G standards for workplace design under HG.

1.4 Structure of the thesis

This thesis is composed of six chapters, including the introduction and conclusion. Broadening of the scope, including the literature review of sitting biomechanics, performance and fatigue

comfort at workplace aspects, assessment methods, objectives in this thesis are discussed in Chapter 1. This chapter is partially based on publication "Defining best design practices for safety and comfort in Moon and Mars habitats" presented at IAC-19 conference in Germany, Bremen (Volkova et al., 2019). Biomechanical modelling theory in sitting static posture, as well as dynamic motions at workplace are presented in Chapter 2, and are followed by the data collection and analysis in Chapter 3. These chapter is partially based on publication "Markerless motion capture method application for investigation of joint profiles in the workplace under simulated hypogravity" presented at IAC-21 conference in St. Petersburg, Russia, (Volkova et al., 2021) and conference poster devoted to "The study of upper extremity motions under partial gravity" at ESBiomech conference 2021 in Milan, Italy. The markerless motion capture solution was used for postural study, empirical and subjective models were applied for fatigue study, subjective methods were applied for seated discomfort and performance study. Chapter 4 covers the results of the thesis on all study methods, including performance studies, posture studies, workplace fatigue, pushing and pulling motions, and seated discomfort at the workplace. This chapter is partially based on publication "Multi-objective optimization for habitats in extreme environments" presented at IAC-2019 in Washington D.C., United States (Volkova et al., 2019) and peer-reviewed publication "An empirical and subjective model of upper extremity fatigue under hypogravity" published in *Frontiers in Physiology* journal (Volkova et al., 2022). Further interpretation of the results are discussed and a proposal to extend the standards for $\frac{1}{6}G$ with some recommendations for workplace design are described in Chapter 5. Chapter 6 includes studies synthesis, study limitations and directions for future work. Two additional peer-reviewed publications are under submission to the *Ergonomics*, Taylor Francis journal:

Publication: Volkova T., Prof. C. Nicollier, Prof. Dr. V. Gass, Hypogravity modeling of upper extremities when static and in motion: an investigation of joint profiles in workplace conditions", *Ergonomics*, Taylor Francis journal is under submission.

2 Biomechanical modeling

In this chapter the biomechanical modelling theory about sitting static posture, including static posture theory and human motion dynamics theory at the workplace is described.

2.1 Anthropometry in occupational biomechanics

Human biomechanical analysis considers the body as a system of mechanical links which are of known physical size and shape. Anthropometry determines these sizes and shapes, as well as various corresponding properties, such as length, volume, weight, location of the center of mass (CoM), and inertial properties. All these properties have been intensely studied and reported (K. H. Kroemer et al., 2010; Miller et al., 1975; Haslegrave, 1986; Lohman et al., 1988; Pheasant and Haslegrave, 1996; Plagenhoef et al., 1983).

Body-segment link length

The length of segments connecting joints can be easily identified and measured. For segments of the trunk, neck and head, however, this is more difficult. Anthropometrists have studied the length of segments and the position of the center of rotation of joints on cadavers (Braune, 1889; Dempster, 1955; Snyder et al., 1972; Chaffin et al., 1972) and living subjects. On living subjects, the approximate centers of rotation of the articulated joints can be projected by moving adjacent body segments along the range of motion of the joint. The intersection of two lines drawn parallel to the midline of the long axis of the segments during these movements defines the approximate center of rotation of the joint. This approach was effectively taken using radiographs (States, 1997; Cappozzo et al., 1996), by tracking carefully positioned markers on the surface of the segment. Currently, this can even be done by tracking joints with the markerless method (Colyer et al., 2018).

The simplified rotation system of major joint was developed over time by (Associates et al., 1978; Dempster, 1955; Snyder et al., 1972; Bush and Gutowski, 2003; Nussbaum and Zhang, 2000; Cerveri et al., 2004; Zatsiorsky, 1990; Plagenhoef et al., 1983). The following indications illustrate how the measurements of each segment are made. According to Plagenhoef et al.,

1983, the human body can be divided into 16 segments (including right/left body segments), as shown in Figure 2.1. Each body length segment can be defined as follows:

- Upper arm length: from the point of the upper arm to the forearm;
- Forearm length: from the point of the forearm to the wrist;
- Hand length: measured from the articulation point of the hand to the top of the middle finger;
- Head length: measured from the crown to the base of the neck;
- Torso length: measured from the base of the neck to the bottom of the body;
- Thigh length: measured from the hip to the knee joint;
- Shank length: measured from the knee joint to the floor.

This approach was adopted to measure the body-segment length of participants during the experiments of this thesis; all details are presented in Chapter 3.

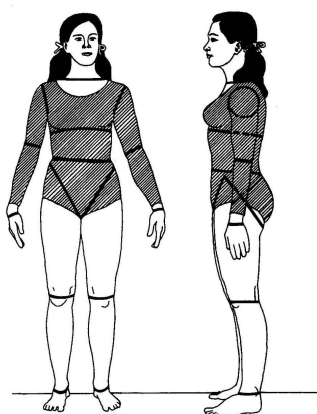


Figure 2.1: Segmentation of human body (Plagenhoef et al., 1983). Anatomical Data for Analyzing Human Motion, Plagenhoef, F. Gaynor Evans, Thomas Abdelnour, Research Quarterly for Exercise and Sport, copyright © the Society of Health and Physical Educators, www.shapeamerica.org, reprinted by permission of Taylor Francis Ltd, <http://www.tandfonline.com> on behalf of the Society of Health and Physical Educators, www.shapeamerica.org.

Body-segment volume and masses

The distribution of body weight in the human body is important in order to quantify the force of gravity affecting various musculoskeletal parts of the body, because in addition to external loads acting on body parts, the mass of segments and the force due to gravity create additional

stresses. In certain postures, such as outstretched arm task, these stresses can be quite large. Here the shoulder muscles quickly become fatigued, and it becomes difficult to maintain the posture over a longer period of time. The most widely used methods for assessing the volume of a body segment are water displacement and 3D scanning (Krzywicki and Chinn, 1967). The water displacement method is suitable for evaluating extremities by submerging the segment in water and measuring the displaced volume (for example hand, forearm and upper arm).

The masses and lengths of participants' body parts are measured in accordance with statistical data (Plagenhoef et al., 1983). The mass of each body segment can be determined by multiplying the body-specific coefficient given in Table 2.1 by the mass of the whole body.

Table 2.1: Segment masses as percentages of total body mass for males and females (Plagenhoef et al., 1983).

One segment	Men N=35	Women N=100
	Mean (SD)	Mean (SD)
Hand	0.65 (0.06)	0.5 (0.026)
Forearm	1.87 (0.2)	1.57 (0.1)
Upper arm	3.25 (0.49)	2.9 (0.32)
Foot	1.43 (0.13)	1.33 (0.02)
Shank	4.75 (0.53)	5.35 (0.47)
Thigh	10.5 (1.21)	11.75 (1.86)
Whole trunk	55.1 (2.75)	53.2 (4.64)
Head and neck	8.26	8.2
Thorax	20.1	17.2
Abdomen	13.06	12.24
Pelvis	13.66	15.96

Note: Anatomical Data for Analyzing Human Motion, Plagenhoef, F. Gaynor Evans Thomas Abdelnour, Research Quarterly for Exercise and Sport, copyright © the Society of Health and Physical Educators, www.shapeamerica.org, reprinted by permission of Taylor Francis Ltd, <http://www.tandfonline.com> on behalf of the Society of Health and Physical Educators, www.shapeamerica.org.

Segment mass values determined by other methods described in (Dempster, 1955; Associates et al., 1978; De Leva, 1996; Clauser et al., 1969).

As stated in the paper devoted to "An Empirical and Subjective Model of Upper Extremity Fatigue Under Hypogravity" Volkova et al., 2022, due to the non-invasive nature of the experiment for participants and the speed of measurements, the photogrammetrie approach can be utilized to assess the entire torso volume. However, in some situations, reconstructing the 3D volume of the hands necessitated a significant amount of mesh refinement and enhancement, therefore water displacement method can be chosen to quantify this volume.

Body - segment locations of CoM and inertial parameters

CoM assessment of the whole body plays an important role in biomechanical studies. In order to carry out a complete biomechanical analysis, in addition to the mass or weight of a body segment, one must know where its CoM is located. Several methods are thus used to calculate this essential element.

The first studies of the center of CoM were carried out nearly two-hundred years ago by (Weber and Weber, 1836; Harless, 1860; Braune and Fischer, 1889; Meeh, 1894; Bernstein et al., 1931; Bernstein, 1967; Dempster, 1955, Chandler et al. (1975), Plagenhoef et al., 1983). Most often, such studies were carried out both on living people and on cadavers.

The first method is performed using a force plate (AMTI OR6) to measure reaction forces. With the help of such a plate, the location of the CoM of the segment via computation of vertical, lateral and sagittal forces - is determined using the principle of static balance. The sum of the torques around any point in the force system is zero as long as the system is in equilibrium. The subject takes up various positions while supporting themselves on a force plate. This allows a very accurate estimation of the position of the CoM (Caron et al., 1997). By asking a person to take two different positions on the force plate and knowing the weight of the segment, one can locate the segment's CoM using the procedure described by (Le Veau, 1977) and (Zatsiorsky, 1990).

A second method is a variant of the immersion method. As detailed by Miller et al., 1975, the segment immerses into known discrete intervals and their volume is measured.

The inertial parameters of human segments can be determined through regression equations. Such equations have been extensively developed by (Winter, 2009; Dempster, 1955; De Leva, 1996; Zatsiorsky, 1990; Dumas et al., 2007; McConville et al., 1980; Young et al., 1983; Plagenhoef et al., 1983).

Dempster, 1955 and Plagenhoef et al., 1983 directly measured the inertial parameters using male cadavers using balance and pendulum methods. Zatsiorsky, 1990, indirectly measured such parameters using a frontal gamma scanner. They found the surface area of the body in subjects lying on their backs. Through this value, the masses and distances from the geometric centers of rectangular cuboids to the control anatomical landmarks were determined. Moreover, the CoM of the cuboids is located in their geometric centers, with the axes of inertia located in the axes of symmetry of the rectangular cuboids. McConville et al., 1980 and Young et al., 1983 measured inertial parameters using photogrammetry.

There are also non-linear methods for determining inertial parameters described by (Zatsiorsky, 1990). They are based on anthropometric measurements, but they are hardly used, probably because they include calipers and tape measures in addition to skin markers (Dumas and Wojtusich, 2018).

(Plagenhoef et al., 1983) is considered as the most accurate by the biomechanical community.

In this case, body parameters, such as the body mass and body segment CoM, are calculated from statistical data. Here the following assumptions are applied:

- In a uniform field of gravity the CoM coincides with CG. In the perpendicular plane to the main axis, CGs are not taken into account;
- Mass distribution as well as the volume of muscles remain constant regardless of the position of the body;
- The body is symmetrical with respect to the sagittal plane and divided into 16 segments;
- The overall anatomy does not change, regardless of body position. The body segment joints remain the same, providing the same spread with.

In consequence, the body segment start and end points remain the same, providing the same spread with any body position.

Steven (2013) hypothesized on increasing energy expenditure under lunar gravity conditions relative to Martian ones. They assumed that this can be related to the excess energy required for posture control and stability under reduced gravity. However, the reason for the "wasted energy" associated with the human motion under reduced gravity is still unclear. The authors made assumptions about the factors that should be considered for such analyses. These factors will allow to investigate inertial stability and metabolic cost. Additionally, the physiological impact that reduced gravity has on locomotion of astronauts under different gravity conditions still needs to be studied.

According to Bauby and Kuo, 2000, for maximization of astronaut performance, the rate of limited resource utilization needs to be minimized; the potential for a successful mission can be increased by means of system design optimization based on assessment of the factors affecting the astronaut's energy expenditure. They determined that in relation to the center of mass (CoM), stability is mainly controlled by foot position. With reduced gravity, due to less accurate orientation in space, the position of the foot can change; the EVA suit also contributes to this.

Some researchers assume that during constant velocity locomotion on the Moon, there is potential for inertial rotation about the center of mass (CoM) to be a significant factor that can impact the determination of metabolic cost (Chappell and Klaus, 2013; Saibene and Minetti, 2003).

The Figure 2.2 shows the factors that affect the energy of movement under hypogravity. The overall work consists of external and internal components. In the above example, adapted from Chappell and Klaus, 2013 for the sitting posture, the external work is the sum of the body's potential energy and kinetic energy changes, at the CoM. The adapted Chappell and Klaus, 2013 assumption for the sitting posture can be formulated as follows: internal work is

the sum of the kinetic energy changes of all segments of the body relative to the CoM, as well as the kinetic energy changes of the body rotating around the CoM.

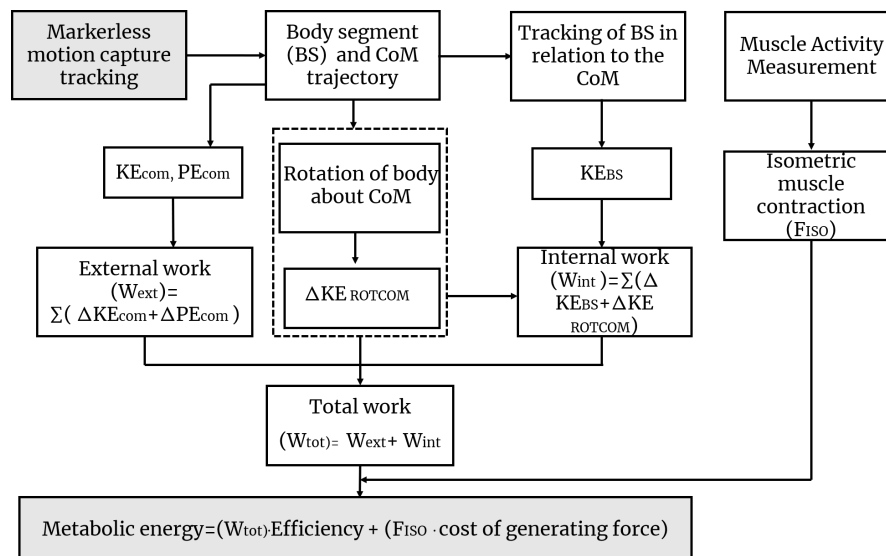


Figure 2.2: Locomotion energetics adapted from (Chappell and Klaus, 2013). Used by permission of Journal of Human Performance in Extreme Environments

To calculate energy, not only internal and external work is taken into account, but also the forces arising from isometric/opposite muscle contraction. Chappell and Klaus, 2013 suggest that the metabolic cost will be increased on Mars and the Moon, so more action will be required to create body stability. Further research into the concept of energy loss was recommended to address the problems of body stability during locomotion under hypogravity. In accordance with Chappell and Klaus, 2013 rotation of the body around the CoM, may contribute to an increase in metabolic costs of performing movement in conditions of reduced gravity (highlighted by a dotted line in the Figure 2.2).

To summarize the effects of lunar gravity:

- The body weight on the Moon is about six times less than that on Earth. The mass in both cases is the same and is determined by the amount of substance in the body;
- The astronaut must be able to move correctly. Such as with a lowered tempo and energy consumption for locomotion;
- Locomotion and the human body can be characterized by increased flexion in large joints; this allows for movement via jumping.

Normal Standing, sitting Postures^I Sitting postural control requires analysis of spinal changes occurring when seated. The neutral posture required for sitting, standing, and lying is the subject of a number of theoretical developments (Harrison et al., 1999).

To this date, there is no agreement regarding the use of the ideal reference position versus the average one. Most authors judge the location of the CoM along the vertical rack and the alignment of the CoM (Figure. 2.3 (A), d). In accordance with Kuchera, 1995, such a posture for a person in a standing position corresponds to drawing a single line between the ear, thigh, knee and ankle (Figure. 2.3, A, c). Although Woodhull et al., 1985 suggests that correct standing posture is determined by the fact that the body's CoM is located a little ahead to the talus of the ankle (Figure. 2.3 (A), b), another study (Kapandji and Kapandji, 2007) suggests that the key points of back of the head, back, and buttocks pass through the same vertical line (Figure. 2.3 (A), a). Figure 2.3 (B) shows examples of different curves of the spine. When evaluating the CoM of the body, it is necessary to take into account the characteristics of people's spine curve, such as lumbar lordosis, thoracic kyphosis, forward head etc.

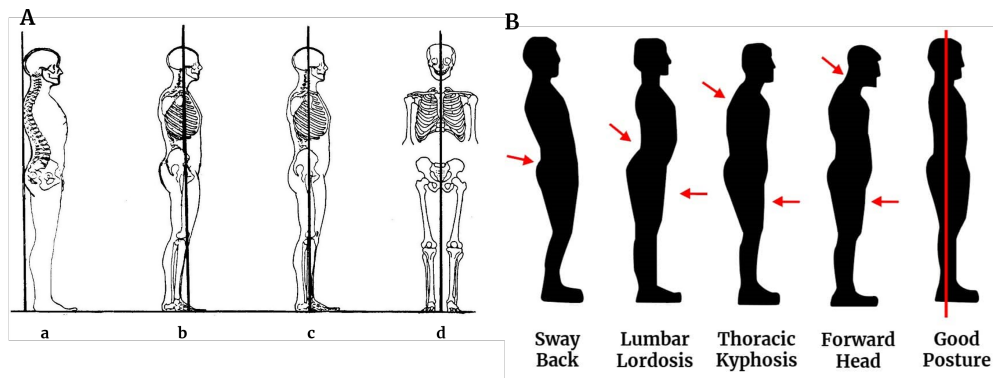


Figure 2.3: (A) Hypothetical normal standing postures (Kuchera, 1995). (B) Individual postures variations. Figure 2.3 (A) *Reprinted from Journal of Manipulative and Physiological Therapeutics, Vol 22 /Issue 9, Donald H. et al. (1999). Sitting biomechanics Part I: Review of the Literature, Pages No.16, Copyright (2022), with permission from Elsevier.*

According to (Schoberth, 2013), biomechanical analysis is best started with a classification of sitting posture according to the location of the body's CG. Figure 2.4 shows three sitting positions, with differences in shape of the lumbar spine. In the position of the body shown in Figure. 2.4 (B), the CoM is above the ischial tuberosities. In this position, with complete relaxation, the lumbar spine is either straight or slightly kyphotic. By turning the pelvis forward, once can move to the front position from the middle one (Figure. 2.4 (B) or without turning the pelvis, by bending and creating a kyphosis of the spine (Figure. 2.4 (A). In this position, the ischial tuberosities is behind of CG. In the posterior position, as shown in (Figure. 2.4 (D), the CoM is located above or behind the ischial tuberosities. This position can occur with

^IGood posture is one that creates the least postural tension in a static body position, when the muscles do the least work to counteract the action of gravity and other forces.

simultaneous rotation of the hip and kyphosis.

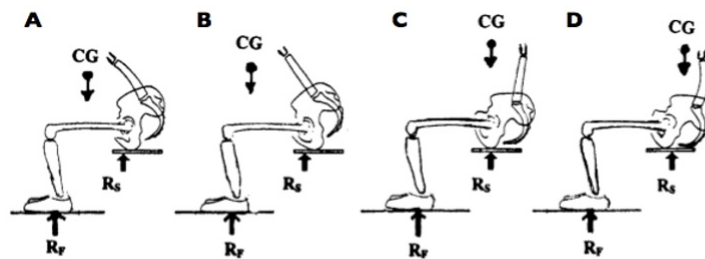


Figure 2.4: Hypothesized normal sitting postures (Schoberth, 2013): **(A)** CoM is above the ischial tuberosities - kyphosis of the spine. **(B)** CoM is above the ischial tuberosities, **(C)** The CoM is located inline with the ischial tuberosities, **(D)** The CoM is located behind the ischial tuberosities. *Reprinted from Journal of Manipulative and Physiological Therapeutics, Vol 22 /Issue 9, Donald H. et al. (1999). Sitting biomechanics Part I: Review of the Literature, Pages No.16, Copyright (2022), with permission from Elsevier.*

As participants under consideration are seated at a workplace and handling objects, it is important in this investigation to determine the sitting posture, in particular pelvic and thoracic tilt angles as they influence subjects' well-being. Side-view photographs are made of individuals subject as they sit. In addition, each subject is photographed in the standing position from a side view.

Anthropometry of participants and descriptive statistics

Different anthropometric measurements are taken for each male and female participant, including standing height, sitting height, upper limb, trunk and head length. The descriptive statistics of all participants is presented in Appendix, Table A.8.

2.2 3D kinematics of motions and camera calibration

Most of the experiments carried out as part of this dissertation involve 3D participant kinematics implemented using markerless motion capture. Thus, this subsection outlines the basic concept and mathematics used in computer vision, including methods used to estimate intrinsic and extrinsic parameters and methods for determining camera calibration errors. The camera calibration software written in the computer vision laboratory (CVLab) at EPFL is presented in "Github", 2022. The camera captures a visual image. The camera consists of a lens and a sensor. The lens directs (and distorts) the light, while the sensor captures it digitally. The mapping from three-dimensional to two-dimensional space occurs due to the lens, which is called projective transformation. To transform the restoration of the depth or position of objects in the scene, it is necessary to know the characteristics of the object. If the size of the object is known, then the distance from the object to the camera can be determined.

In general, the distance can be determined through triangulation of the positions of an object from multiple cameras. This operation requires camera characteristics such as intrinsic and extrinsic parameters. Estimating the intrinsic parameters is a fundamental step in eliminating lens nonlinearities. Extrinsic parameters allow one to project a three-dimensional point of the world onto the camera coordinate systems and vice versa. In this thesis, the camera is described by a Pinhole model.

The following equation were extracted from the report of computer vision expert ("Github", 2022) and (Hartley and Zisserman, 2003).

Projection model According to CVLab in most cases, the mathematical relationship between the 3D world and 2D is described by the Pinhole camera model ^{II}.

Within this model, according to Hartley and Zisserman, 2003 a point in space $\mathbf{X} = (X, Y, Z)^T$ is matched with a point on the image plane $\mathbf{x} = (x, y)^T$, where a line, called a ray, connecting the point \mathbf{X} with the projection center corresponds to the image plane.

$$(X, Y, Z)^T \mapsto (x, y)^T = (f_X / Z, f_Y / Z)^T \quad (2.1)$$

where f is the camera focal length ^{III}
 Z the depth of the object the camera center.

Thus, matrix form central projection can be written:

$$\begin{pmatrix} fX \\ fY \\ Z \end{pmatrix} = \begin{bmatrix} f & 0 & 0 \\ 0 & f & 0 \\ 0 & 0 & 1 \end{bmatrix} \begin{pmatrix} X \\ Y \\ Z \end{pmatrix} \quad (2.2)$$

To take into account that image is in pixels, the origin of the image is at the top left corner, the principal point is not necessary in the middle of the image coordinate maybe shifted, can be written:

$$\begin{pmatrix} uw \\ vw \\ w \end{pmatrix} = \begin{bmatrix} F_x & s & c_x \\ 0 & F_y & c_y \\ 0 & 0 & 1 \end{bmatrix} \begin{pmatrix} X \\ Y \\ Z \end{pmatrix} \quad (2.3)$$

$$\mathbf{x} = K\mathbf{X}_{\text{cam}} \quad (2.4)$$

^{II} **Pinhole camera model** describes the mathematical relationship between coordinates in 3D space

^{III} **Camera focal length**- distance from the camera center to the image plane

where $F_x = f m_x$ and $F_y = f m_y$ - focal length;
 m - number of pixels; K - intrinsic matrix.

Equation 2.4 (Hartley and Zisserman, 2003) describes a mapping between a camera coordinate system. This coordinate system is at the camera center of a 2D space defined in pixels. As the points in 3D are (see Figure 2.5), in general, defined in another reference system which is common to other cameras, the rotation R and translation t of the camera in this reference system must be taken into account. Thus, the following equation can be written:

$$\mathbf{x} = K[R|t]X \quad (2.5)$$

$[R|t]$ represents the extrinsic parameters. R is orthonormal.

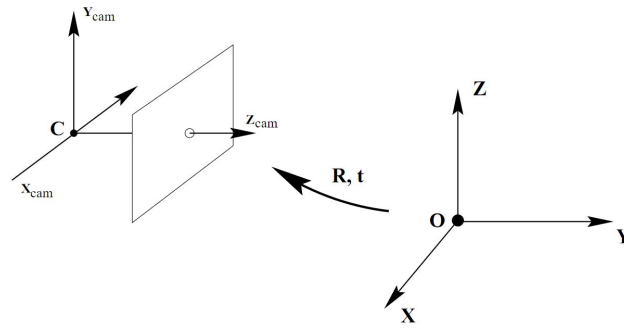


Figure 2.5: The Euclidean transformation (Hartley and Zisserman, 2013). *Reproduced from Multiple View Geometry in Computer Vision, Cambridge University Press with permission of The Licensor through PLSclear*

Distortion model An approximation of image distortion (seen in Figure 2.6), can be expressed as a combination of radial and tangential distortion functions. They are non-linear and are expressed by polynomials.

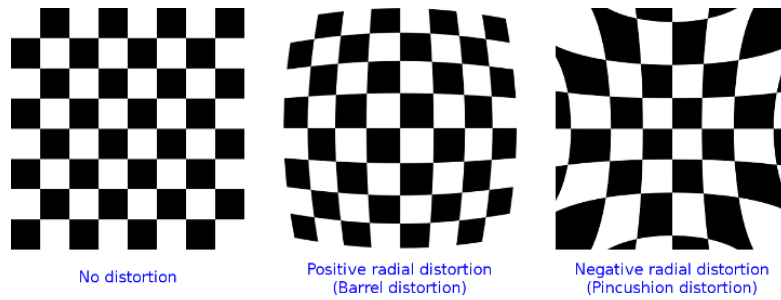


Figure 2.6: Radial distortions (Alqahtani et al., 2019). *Copyright (Alqahtani,Banks, Chandran, Zhang © 2019) From (Detection and tracking of faces in 3D using a stereo camera arrangements) by (Alqahtani et al.). Reproduced by permission of (International Association of Computer Science and Information Technology)*

Radial distortion can be described by the following equations (“Mathworkds website”, 2022):

$$u_{dist} = x \cdot (1 + k_1 \cdot r^2 + k_2 \cdot r^4 + k_3 \cdot r^6) \quad v_{dist} = y \cdot (1 + k_1 \cdot r^2 + k_2 \cdot r^4 + k_3 \cdot r^6) \quad (2.6)$$

where (x, y) is the position of a pixel/point in the normalized image coordinate system (undistorted) $r = \sqrt{x^2 + y^2}$ is the normalized distance of the pixel/point from the principal point which is (roughly) in the center of the image and k_1 , k_2 and K_3 are the distortion coefficients.

Tangential distortion can be described by the following equations (“Mathworkds website”, 2022):

$$u_{dist} = x + (2 \cdot p_1 \cdot x \cdot y + p_2 \cdot (r^2 + 2 \cdot x^2)) \quad (2.7)$$

$$v_{dist} = y + (2 \cdot p_2 \cdot x \cdot y + p_1 \cdot (r^2 + 2 \cdot y^2)) \quad (2.8)$$

where p_1 and p_2 are the distortion coefficients.

In OpenCV (Bradski, 2000), the intrinsic parameters are always in this order $[k_1 \ k_2 \ p_1 \ p_2 \ k_3]$.

Intrinsics estimation To estimate intrinsic parameters, such as the K matrix and distortion coefficients, in this work, the Zhang camera calibration approach (Zhang, 2000) is used (2.7). This approach employs a fixed pattern image and a black and white checkerboard, where the calibration points are the interior corners. A projection matrix estimate can be computed for each image, which is subsequently decomposed into a rotation R , a translation t , and an internal matrix K .

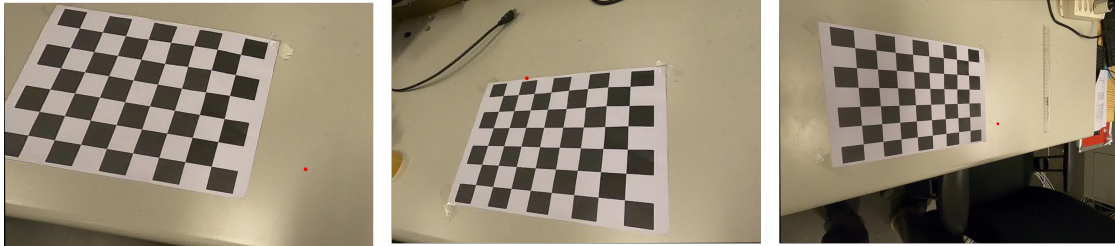


Figure 2.7: Zhang's approach demonstration. This calibration pattern has 6 inner(height) and 9 inner corners (width). The figure scenes are the result of the application of the Zhang's method by the author of this dissertation.

Intrinsics modification

If the camera recorded the video is in a position other than horizontal, the intrinsic parameters must be changed after they have been calculated. The following are the functions to rotate intrinsic 90 degrees counterclockwise, rotate intrinsic 90 degrees clockwise, and rotate intrinsic 180 degrees.

Listing 2.1: Rotation 90 degrees counterclockwise

```

1  fx, fy = K[[0,1],[0,1]]
2      cx, cy = K[[0,1],[2,2]]
3      k1, k2, p1, p2, k3 = dist
4
5      K_mod = np.array([
6          [fy, 0, cy],
7          [0, fx, w-cx],
8          [0, 0, 1]
9      ])
10     dist_mod = np.array([k1, k2, -p2, p1, k3])

```

Listing 2.2: Rotation 90 degrees clockwise

```

1  fx, fy = K[[0,1],[0,1]]
2      cx, cy = K[[0,1],[2,2]]
3      k1, k2, p1, p2, k3 = dist
4
5      K_mod = np.array([
6          [fy, 0, h-cy],
7          [0, fx, cx],
8          [0, 0, 1]
9      ])
10     dist_mod = np.array([k1, k2, p2, -p1, k3])

```

Listing 2.3: Rotation 180 degrees

```

1  fx, fy = K[[0,1],[0,1]]
2      cx, cy = K[[0,1],[2,2]]
3      k1, k2, p1, p2, k3 = dist
4
5      K_mod = np.array([
6          [fx, 0, w-cx],
7          [0, fy, h-cy],
8          [0, 0, 1]
9      ])
10     dist_mod = np.array([k1, k2, -p1, -p2, k3])

```

These functions are applied to modify intrinsic parameters necessary for an experiment.

Extrinsic estimation

To estimate external parameters, a method called Bundle Adjustment (BA) (Triggs et al., 1999) is used. BA is a technique that simultaneously reconstructs 3D structure (i.e. a set of 3D locations) and viewing parameters such as camera position, internal matrix and radial distortion from only a set of observations in images. This involves refining the set of initial estimates of the camera parameters and the design to find the set of parameters that provide the most accurate prediction of the location of the observed points in the set of available images. Due to the nature of the problem, the initial parameters must be set from a relatively good starting point to avoid a bad local minimum.

Bundle adjustment $\{R_i\}_{i=1}^N, \{t_i\}_{i=1}^N$ with optional intrinsic $\{K_i\}_{i=1}^N$ and the distortion parameters $\{D_i\}_{i=1}^N$ and some 3D object locations $\{X_j\}_{j=1}^M$ by minimizing the distance to their corresponding locations $\{x_j\}_{j=1}^M$ in the images.

$$\min_{C_i, X_i} \sum_i^N \sum_j^M m_{ij} \cdot d(\mathbf{Q}(C_i, X_j) - x_j)^2 \quad (2.9)$$

where $C_i = \{R_i, t_i, K_i, D_i\}$ refers to the camera parameters of view i ;

$\mathbf{Q}(\cdot)$ the projection function;

m_{ij} is a binary variable;

$d(\cdot)$ - is the Euclidean distance.

Relative poses Searching for relative camera poses is necessary to dwindle them and describe the position of each camera in the setup. Figure 2.8 shows the cameras as points, and the edges describe the relative poses between them. With this scheme, all poses can be calculated relative to one of the cameras. These poses can then be used as an initial solution for BA.

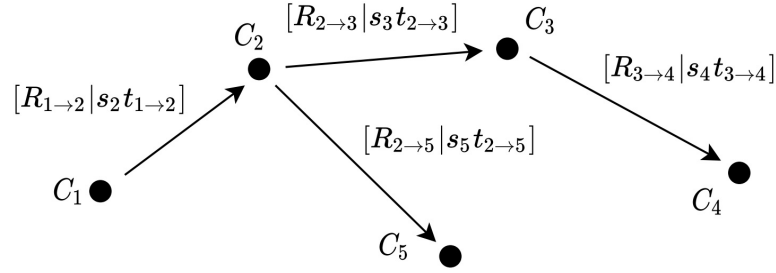


Figure 2.8: Example a minimal tree connecting every camera through relative poses(CVLab, 2021). Reprinted from Computer vision laboratory, EPFL report, Citraro, 2021 with permission of Citraro L..

If the position for camera l is defined as relative poses $C_{1 \rightarrow 2}$, and $C_{2 \rightarrow 3}$ the pose of C_3 can be defined with the following equations (CVLab, 2021):

$$R_2 = R_{1 \rightarrow 2} \cdot R_1 \quad (2.10)$$

$$t_2 = R_{1 \rightarrow 2} \cdot R_1 + t_{1 \rightarrow 2} \quad (2.11)$$

$$R_3 = R_{2 \rightarrow 3} \cdot R_2 \quad (2.12)$$

$$t_3 = R_{2 \rightarrow 3} \cdot R_2 + s \cdot t_{2 \rightarrow 3} \quad (2.13)$$

$$(2.14)$$

where s is the relative scale parameter. It can be calculated as the scale difference between common points of a triangle.

Global registration

To move poses to a global link systems with the correct scale, a hard transformation (rotation, scale and translation) between triangulated points and their true position in the world is evaluated. Once the transformation is found, the poses can be projected onto this new frame of reference. For this step, one finds a hard transformation (rotation, scale and translation) between two-point clouds with known dependencies. This is possible using Procrustes method (Gower and Dijksterhuis, n.d.), and further optimization to minimize the distance between two sets of points in the sense of least squares.

2.3 Methodology for biomechanical calculations

This sub-chapter, was partially extracted from Volkova et al., 2022 in peer-reviewed *Frontier in Physiology* publication Volkova et al., 2022 devoted to "An empirical and subjective model of upper extremity fatigue under hypogravity". Further sub-chapters review the various biomechanical modeling methods that were used in this dissertation. During the first experiments devoted to performance study at the workplace, D'Alembert's principle (Lanczos, 1970) was used. This allows for assessment of the direction of forward/backward deviation with respect to the vertical of the body while performing static tasks at the workplace. The torques in the elbow and shoulder joint were calculated. The computation of the torso inclination angles was done partially with computer vision methods and partially with goniometer when visibility underwater was insufficient for vision-based methods. Further, the recursive motion Lagrange equations were used for subsequent experiments devoted to postural studies. This method was applied to both static postures and dynamic motions problems, but was limited to calculating torques only in the elbow and shoulder joints due to complexity of the method and focus on upper extremity limbs analyses.

As the interest is to understand the biomechanics of activities at the workplace, all objects manipulated had to be characterized under normal and HG conditions. Additionally, as the experiment was conducted in a water tank, underwater conditions were utilized since Archimedes force counteracts the action of gravity. The required mass of ballasts to compensate these forces acting on limbs and torso was calculated. The ballasts are positioned close to CoM of the body segments, as shown in Figure 2.9.

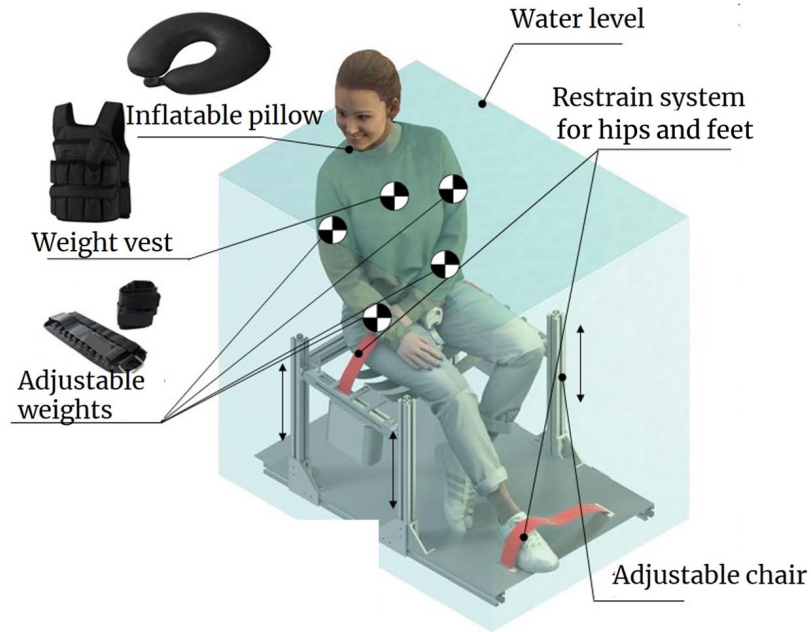


Figure 2.9: Ballasts distribution on the participants body). Adapted from (Volkova et al., 2022). Volkova, 2022. Creative Commons license

For the water tank experiments, ballasts were distributed to different segments of the participants' body in accordance with the segments buoyancy compensation model developed. Ballasts provided the required level of buoyancy, equivalent to gravity on the Moon ($G=1.626 \text{ [m/s}^2\text{]}$) and Mars ($G= 3.72076 \text{ [m/s}^2\text{]}$). The segments buoyancy compensation model can be calculated as follows (Volkova et al., 2022):

$$m_{b,p} \cdot g_m = (m_{b,p} + m_b) \cdot g_e - (V_{b,p} + \frac{m_b}{\rho_b}) \cdot g_e \cdot \rho_{H_2O} \quad (2.15)$$

where $m_{b,p}$ is the mass of the body part;

m_b - the mass of the ballast;

g_m - the acceleration of gravity on the surface of the Moon;

g_e - the acceleration of gravity on the surface of the Earth;

ρ_b - the density of ballast weights;

ρ_{H_2O} - the density of water.

Sand ($\rho_b = 2816.9 \text{ kg/ m}^3$) and lead ($\rho_b = 11340 \text{ kg/ m}^3$) and polystyrene ($\rho_b = 30 \text{ kg/ m}^3$) were used for ballast.

A limited number of tasks were performed by the participants: static weights (0.5kg, 1kg, 3kg, 5kg, 7kg) holding weights with an outstretched arm (S1), holding weights in an arm bent at the

elbow (S2), slow dynamic motion (D), and repetitive motion (R). Assembling and maintenance tasks, as well as tasks at workbench were investigated for the performance study. According to preliminary numerical analysis, the contribution of the moment of inertia of the ballasts to the dynamics of movements is negligible due to the insignificant weight of the ballasts necessary for simulating lunar gravity but is more significant for simulating Martian gravity. The contribution of the moment of inertia from the operational loads becomes significant when it is more than 3 kg. The weight of operational loads was compensated only by the force of Archimedes.

According to preliminary numerical analysis, the contribution of the moment of inertia of the ballasts to the dynamics of movements is negligible due to the insignificant weight of the ballasts necessary for simulating lunar gravity but is more significant for simulating Martian gravity. The contribution of the moment of inertia from the operational loads becomes significant when it is more than 3 kg. The weight of operational loads was compensated only by the force of Archimedes.

The results of solving the equation (2.15) for the initial data are summarized in Table 2.2.

Table 2.2: Ballast masses for static experiments for female.

Body part	Forearm	Upper arm	Trunk
Volume, [m ³]	0.0007148	0.001295	0.02841
Mass, [kg]	0.8635	1.595	29.260
Length, [mm]	247.1	235.9	690.1
Density, [kg/m ³]	1208.0	1231.7	1029.9
Archimede's force, [N]	7.0	12.7	278.7
Gravity force, [N]	8.45	15.6	287.0
Residual force, [N]	1.45	2.9	8.3
Moon gravity force, [N]	1.40	2.6	47.4
Ballast mass, [kg]	x	x	5.7

An analysis of Table 2.2 shows that participant 1 does not require the installation of ballast weights on the limbs. For example, for a participant with trunk volume of 28.41 dm³, and mass of trunk mass of 29.26 kg, ballast mass (lead) is 5.7 kg.

2.3.1 Biomechanical modelling of static posture

As discussed in sub-chapter 2.1, according to the available statistics the initial data was used, which represent the geometry and position of the CoM of parts of the human body. Measured data on the volume and mass of the trunk were also considered.

A static load caused by holding weights with an outstretched arm is one of the boundary

conditions for calculating the free body diagram of the participant. In general, the system is statically indeterminate, since the number of degrees of freedom of the human body significantly exceeds the number of equations of the static equilibrium. Since the rigidity of the human body under load is unknown, the use of classical methods of resistance of materials, involving the introduction of strain compatibility equations into the system, is practically impossible. The solution to this problem is to determine the geometry of the body of the participant using additional data, for example, obtained by 3D reconstruction and biomechanical modeling. In such a case, with a known geometry, the bodies of participants can be considered rigid and muscle loads can be determined from the equilibrium conditions of individual joints (hinges).

Static or quasi-static analyses are valid for movements that are relatively slow or that involve a single joint. For rapid motion or motion based on a kinetic chain of several joints, "interaction torques" or "motion dependent torques" must be taken into account. Quasi static analyses can be used, because of slow motions. The workload can be separately calculated for the shoulder and elbow joint of the right and left hands.

Calculating forces for free body diagram

Posture plays an important role at the workplace as individuals tire more rapidly if they are not comfortable, reducing work performance. Identification of different posture and fatigue profiles of participants with the help of biomechanical modeling, and recommendations to improve related workplace performance, are goals of this study. Results may have a positive influence on recreational behavior recommendations.

Biomechanical models differ significantly depending on the movements/postures performed during the experiment. Therefore, it is desirable to divide the free body diagram into the "upper arm" and the rest of the body (hereinafter referred to as the free body diagram). The 2D simplest free body diagram of the experiment is shown in Figure. 2.10 for 2D force and torques estimation. The blue circles show the main joints introduced into the analytical model, the extremities are shown by lines, the body by an arc and a chord, where the arc schematically shows the rounded back of the participant.

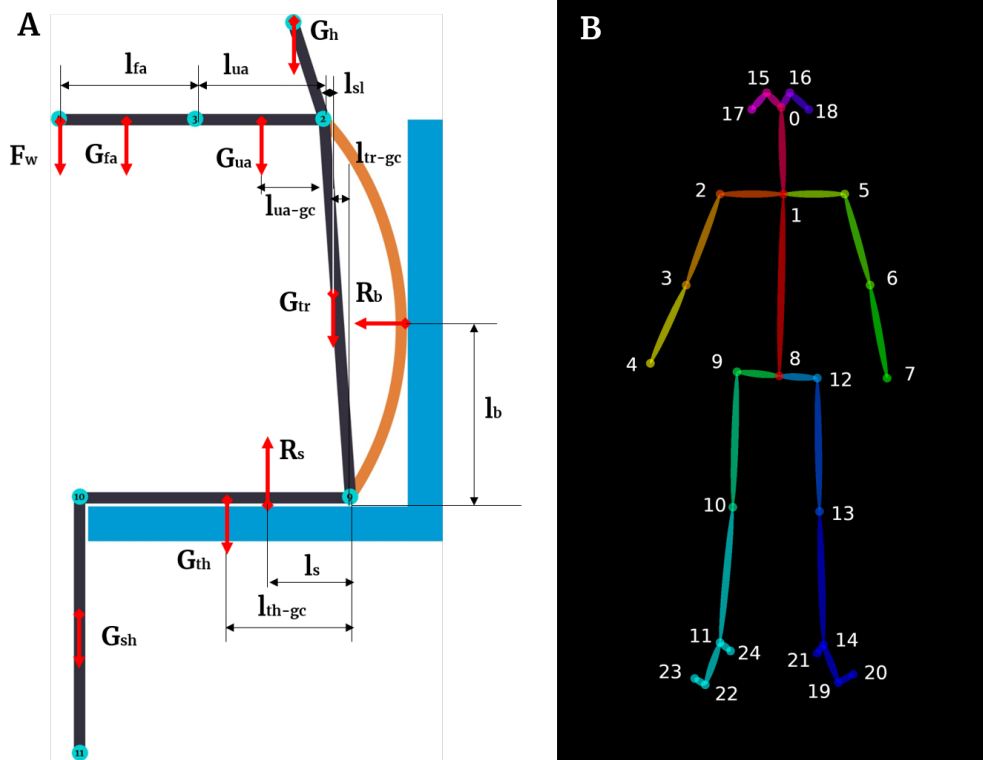


Figure 2.10: (A) The 2D simplest free body diagram of sitting posture, (B) OpenPose skeleton - 25 joints model (“CMUlab website”, 2022).

The strain on the participant is generated by the load held in their outstretched hand. The influence of head, torso and legs are compensated by ballasts, seat and footrest, thus isolating the arm from hand to shoulder. The weight of the participant and the load are balanced by the reactions of the seat and back of the chair, determined from the readings of the load cells. These sensors also allow the reactions at shoulder level to be determined. The equilibrium equation of the body with respect to each of the joints (hinges), allows the determination of forces and torques acting in it. A detailed description of the experimental setup can be found in Chapter 3. With data on the value of the moment, it is possible to compare the load on these muscles under experimental conditions with HG and with Earth gravity. It is also possible to directly compare this load impact on the body while performing the tasks in different postures.

The free body diagram of the wrist includes the mechanics of the movement of the fingers and the wrist joint. Fingers in the aggregate have several tens of degrees of freedom, which, combined with the mobility of the wrist joint, makes the task of modeling their movement practically unsolvable in the framework of this study. However, it can be shown that their functioning is not much different when working in terrestrial and reduced gravity, because the weight and inertia of the fingers are small compared with the effort they develop.

The rest of the body also has many degrees of freedom in various joints. The humerus relative

to the scapula has three degrees of freedom, the ulnar relative to the humerus has one, and the hand along with the radius along the forearm three degrees of freedom. Therefore, the wrist as a whole has seven degrees of freedom and, within the limits of the length of the arm, can move freely with respect to the body. In this case, the free body diagram can be determined only by accurately measuring the geometry of the body during the execution of the movement.

The range of possible hand movements without taking into account the motor skills of the hand is also excessively wide for the study of ergonomics with full induction. Therefore, it should be reduced to a set of elementary movements and poses, which can be investigated. The level of detail of the free body diagram of the body of the participant in determining the load on the muscles can vary. Its rational value is determined by the available accuracy of geometry measurements by 3D reconstruction.

In accordance with Figure 2.10 (A) for the shoulder and elbow joint, two equations of force projected in the vertical can be written:

$$F_{\text{shoulder}} = g \cdot (m_{ua} + m_{fa}) + F_w \quad F_{\text{elbow}} = g \cdot m_{fa} + F_w \quad (2.16)$$

where

m_{ua} – mass of upper arm, [kg];

m_{fa} – mass of forearm, [kg];

F_w – is the force acting on the participant from the load on the hand [N].

During experimentation, an interesting phenomenon showing that body stability is directly related to the pelvis rotation was observed (see free body diagram). This is why it was decided to analyze the torques and forces which occurred in the hip joint.

By analogy with the elbow and shoulder, similar dependencies can be applied for other joints. In the general case, the equivalent loads for different muscles and joints are different, which obviously leads to a different fatigue profile. One other important joint contributing to fatigue and posture in a sitting position is the hip joint, as rationalized below. For the simplest scheme for calculating the deviation of torso of participants during the execution of tasks, he calculations of the hip torque can be done. The sign of torque value will show where the body deviates, backward or forward.

According to d'Alembert, 1743 principle, for the hip joint, two equations can be written:

$$\sum F = 0$$

$$\sum M = 0$$

Since all the masses of body segments, as well as the weight of equipment and ballasts are

known, the first equation can be considered as a parity-check equation. This allows for identification of possible errors in the measurement of individual masses.

The second equation allows for the estimation of the CoM's positions in a specific posture, which is difficult to evaluate a priori. In accordance with Figure 2.10, thus, one can write:

$$F_w \cdot (l_{fa} + l_{ua-CG} + l_{sl}) + G_{fa-CG} \cdot (l_{ua-CG} + l_{ua-CG} + l_{sl}) + G_{ua-CG} \cdot (l_{ua-CG} + l_{sl}) - G_{tr-CG} \cdot l_{tr} + R_b \cdot l_b - R_s \cdot l_s + G_{th} G_{th-CG} \cdot l_{th-CG} = 0 \quad (2.17)$$

where

$F_w = (m_w - V_w \cdot \rho_{H2O}) \cdot g_e$ – (for underwater conditions) force acting on the participant from the side of the load in the hand;

$G_i = (m_i - V_i \cdot \rho_{H2O}) \cdot g_e$ – force arising from ballast weights and Archimedes force, the weight of the body parts of the participant; R_s – reaction force of the seat [N];

l_i – the lengths of the body parts [m];

l_{i-CG} – the distance to the CoM of the body part with the installed ballast weight [m];

l_b – the lever of the backrest of the chair [m];

l_s – the arm of the reaction of the seat [m];

l_{sl} – horizontal distance from the shoulder to the hip joints [m];

fa, ua, tr, th – indices of the forearm, upper arm, trunk and thigh, respectively.

Expressing l_{tr-CG} from expression (2.16), the distance between of the CoM and hip joint can be determined. From the condition of balance of the body of the participant (model included the joints from hand to hip joint), the following equation can be written:

$$\begin{aligned} M_{hip} &= R_s \cdot l_s = F_w \cdot (l_{fa-CG} + l_{ua-CG} + l_{sl}) \\ &\quad + G_{fa} \cdot (l_{fa-CG} + l_{ua-CG} + l_{sl}) + G_{ua-CG} \cdot (l_{ua-CG} + l_{sl}) \\ &\quad - G_{tr} \cdot l_{tr-CG} + R_b \cdot l_b - G_{th} \cdot l_{th-CG} \end{aligned} \quad (2.18)$$

$$F_{hip} = g \cdot (m_t + m_h + 2m_{ua} + 2m_{fa}) + F_w + F_R \quad (2.19)$$

Knowing the initial data, it is possible to calculate the value of the moment in the joint, which is a measure of the load on the muscles. A positive value corresponds to a forward tilt of the participant; this moment is created mainly by the gluteal muscles. With a negative value, the corresponding tilt is backward, and without backrest it involves the iliac-lumbar muscles. The

moment created in the hip joint by the gluteal muscles during sitting can be correlated with the moment created by leaning forward.

In the previously mentioned load case, holding a mass with outstretched arm, an error in determining the position of the arm at $\delta = 1[cm]$ implies an error in determining the moment applied at shoulder level:

$$a = \arctan \frac{\delta}{l_{sh} + l_{up}} = 2\%.$$

The error is approximately the same for determining the load on other muscles connecting the trunk to the limbs (the square muscle of the lower back, iliac-lumbar, etc.). However, it can be assumed that a geometrical measurement error of 1 cm is already too large to study the distribution of loads inside a body.

A change in the position of the chest relative to the pelvis is significant, since the mobility of the lumbar region is much higher than that of the chest; it has been shown (Rabinovich et al., 2007) that the maximum displacement of the upper chest of a person in a sitting position is 10 – 15[cm] without loss of posture stability. Therefore, while maintaining the measurement error of the geometry of 1[cm], the error in determining muscle effort increases to 7 – 10%.

Workload estimation

To estimate the joint workload, e.g., at the shoulder or elbow, the ratio of the joint torque and the joint capacity are examined. The following equation can be used for workload calculation (Database et al., 1996):

$$\text{Joint workload} = T_{\text{joint}} / J_{\text{capacity}},$$

where T_{joint} - is torque of the joint and J_{capacity} - is a physical joint capacity. Joint capacity can be estimated with the following equations (Database et al., 1996):

$$\begin{aligned} J_{\text{flexion}_{el}} &= -0.11 \cdot \text{age} + 10.63 \cdot \text{gender} + 0.05 \cdot \text{wh} + 19.66 \\ J_{\text{flexion}_{er}} &= -0.13 \cdot \text{age} + 12.24 \cdot \text{gender} + 0.07 \cdot \text{wh} + 22.78 \\ J_{\text{flexion}_{sl}} &= -0.12 \cdot \text{age} + 10.68 \cdot \text{gender} + 0.07 \cdot \text{wh} + 14.68 \\ J_{\text{flexion}_{sr}} &= -0.17 \cdot \text{age} + 16.26 \cdot \text{gender} + 0.07 \cdot \text{wh} + 23.35 \end{aligned} \quad (2.20)$$

where wh - is $\text{weight}/\text{height}^2$.

Other equations relate to the different part of body and different body segment positions in (Database et al., 1996). For gender values, 1 can be considered for males and 0 for females.

2.3.2 Human motion dynamics theory

Biomechanical modeling of dynamic movements was carried out taking into account three-dimensional kinematics. At this stage, it is important to explain the key theoretical elements

that were used to prepare the 3D kinematics.

Body-segment inertial property measurement methods

Data such as the location of the CoM of a body segment, its weight and link length are sufficient for a static analysis of forces and torques at each joint for a given posture to be performed. During dynamic activity, a person rotates body segments and a so-called "inertial property" of the segment must be taken into account, opposed to the rotation. This property is called the moment of inertia of the segment.

For dynamic experiments, the distribution of ballast weights is different than in static tests. With a relatively fast movement of the limbs, it is necessary to include the moments of inertia created by ballast weights, as well as the resistance of the water.

The moment of inertia of the upper arm/forearm with ballast (if it is installed), is

$$L_{b,p} = \frac{1}{3} \cdot m_{b,p} \cdot l_{b,p}^2 \quad (2.21)$$

An analysis of these dependencies shows that the systematic error coming from the ballast is in the order of units of percent.

More significant still are the water resistance forces. These forces can be roughly estimated obtained by presenting the forearm of the participant, moving rectilinearly and evenly in the water, as an equivalent cylinder, and then calculating the force of hydrodynamic resistance.

In this case, the diameter of the equivalent cylinder is

$$d = 2 \cdot \sqrt{\frac{V_{b,p}}{\pi \cdot l_{b,p}}}, \quad (2.22)$$

flow obstruction area $S = l_{b,p} \cdot d$, drag coefficient $C_x = 0.5$ (Savitsky, 1972). Then the resistance force is

$$F_{res} = C_x \cdot S \cdot \frac{\rho_{H2O} \cdot V^2}{2}. \quad (2.23)$$

It was decided to limit the speed of the forearm to $47[\frac{cm}{s}]$, in order to minimize this type of force, keeping it below 10 percent of the weight of the forearm $F_{fa} = m_{b,p} \cdot g_e$.

Inertial forces, as well as forces owing to gravity alone, act on a body segment when it pivots around the center of a joint. This can be depicted as two orthogonal forces in the plane of motion of the segment's motion and acting at the segment's CoM. Here Euler or Lagrange equations can be applied. The kinematic skeleton of the human body for calculations is

simplified to a set of articulated rigid bodies.

Dynamic motions computation It was assumed that only gravitational acceleration forces and joint torques and an external force (operational loads) are applied to human joints. In this thesis, the methods of recursive dynamics were applied, since they effectively simulate dynamic systems with a large degree of freedom, regardless of whether they are open or closed loop systems^{IV} (Saha and Schiehlen, 2001; Xiang et al., 2009). Recursive dynamics provides increased stability of numerical performance (Xiang et al., 2009). The range of possible hand movements was reduced to a set of elementary movements and postures, in particular, the movements of lifting and lowering. To take gravity into account vertical motions should be analyzed.

According to Xiang et al., 2009, after deriving the recursive Lagrange equations, a two-degree-of-freedom hand limited to movement in a vertical plane can be assessed (Figure 2.11). The arm with two degrees of freedom consists of two links, the lengths of which are equal to L_1 and L_2 , and the moments of inertia are equal to I_1 and I_2 , with l_1 and l_2 being the distances from the proximal joint to the CoM location of the limbs. The relative articulation angles are designated as q_1 and q_2 respectively, and are controlled by the actuation torques of the articulation τ_1 and τ_2 . Joint angles were measured using vision-based 3D motion analysis. Actuator moments (muscle actions) move the arm out of its initial position $q_1(0)$; $q_2(0)$ to the final position $(q_1)T$; $q_2(T)$. Where T is a time interval of a motion (Xiang et al., 2009).

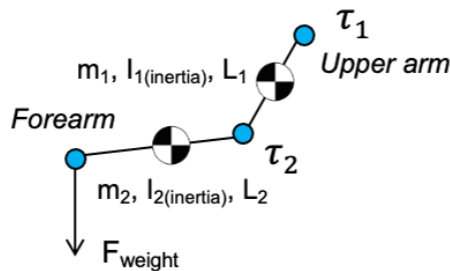


Figure 2.11: 2-DOF kinematic skeleton of an arm with a plane of motion

Lagrange's equation is used to derive the general form of the dynamic equation of motion. Only gravity forces and torque are considered. Then the Lagrange equation can be written as follows (Xiang et al., 2009):

$$\frac{d}{dt} \frac{\partial L}{\partial \dot{q}_i} - \frac{\partial L}{\partial q_i} = \tau_i, i = 1, \dots, n \quad (2.24)$$

where $L = T - V$ is the Lagrangian;

^{IV}Open loop system - serial manipulator mechanism; Close loop system - four/five-bar manipulator mechanism (Fu et al., 1987)

T - is the total kinetic energy;

V - is the total potential energy;

q_i - is the generalized coordinate of joint i;

τ_i - is the generalized torque of joint i;

n is the number of the total degree of freedom (DOF);

t - is the time.

A final version of equation of motion in vector-matrix form (Fu et al., 1987):

$$\tau = \underbrace{M(q)}_{\text{massinertia matrix}} \ddot{q} + \underbrace{V(q, \dot{q})}_{\text{Coriolis Centrifugal}} + \underbrace{\sum_i J_i^T m_i g}_{\text{gravity-forces}} + \underbrace{\sum_k J_k^T F_k}_{\text{external-forces}} + \underbrace{K(q - q^N)}_{\text{muscle-elasticity}} \quad (2.25)$$

Close-form Lagrange equations of motion for two-segment rigid arm can be written as follows (Hollerbach, 1980):

$$\begin{aligned} \tau_{\text{shoulder}} = & (I_1 + I_2 + m_1 \cdot l_1 \cdot l_1 + m_2 \cdot (L_1 \cdot L_1 + l_2 \cdot l_2 + 2 \cdot L_1 \cdot l_2 \cdot \cos(q_2))) \cdot \ddot{q}_1 + \\ & (I_2 + m_2 \cdot l_2 \cdot l_2 + m_2 \cdot L_1 \cdot l_2 \cdot \cos(q_2)) \cdot \ddot{q}_2 - \\ & 2 \cdot m_2 \cdot L_1 \cdot l_2 \cdot \dot{q}_1 \cdot \dot{q}_2 \cdot \sin(q_2) - \\ & m_2 \cdot L_1 \cdot l_2 \cdot \dot{q}_2 \cdot \dot{q}_2 \cdot \sin(q_2) + \dots \\ & m_2 \cdot g \cdot l_2 \cdot \cos(q_1 + q_2) + \dots \\ & m_1 \cdot g \cdot l_1 \cdot \cos(q_1) + \dots \\ & m_2 \cdot g \cdot L_1 \cdot \cos(q_1) + \dots \\ & f \cdot L_2 \cdot \cos(q_1 + q_2) + \dots \\ & f \cdot L_1 \cdot \cos(q_1) \end{aligned} \quad (2.26)$$

$$\begin{aligned} \tau_{\text{elbow}} = & (I_2 + m_2 \cdot l_2 \cdot l_2) \cdot \ddot{q}_2 + \\ & (I_2 + m_2 \cdot l_2 \cdot l_2 + m_2 \cdot L_1 \cdot l_2 \cdot \cos(q_2)) \cdot \ddot{q}_1 + \\ & m_2 \cdot L_1 \cdot l_2 \cdot \dot{q}_1 \cdot \dot{q}_1 \cdot \sin(q_2) + \\ & m_2 \cdot g \cdot l_2 \cdot \cos(q_1 + q_2) + \dots \\ & f \cdot L_2 \cdot \cos(q_1 + q_2) \end{aligned} \quad (2.27)$$

where

I_i - is the driving torque actuated by human muscles, q_1, q_2 - are gradients of torque.

Here, τ_i is the driving torque actuated by human muscles.

For static postures all gradients in equations 2.24 and 2.25 will be equal zero.

Gradients of torque τ_1 with respect can be written as follows (Hollerbach, 1980):

$$\frac{\partial \tau_1}{\partial \theta_1} = - (m_2 g l_2 + f L_2) \sin(\theta_1 + \theta_2) - (m_1 g l_1 + m_2 g L_1 + f L_1) \sin \theta_1 \quad (2.28)$$

$$\frac{\partial \tau_1}{\partial \theta_2} = - m_2 L_1 l_2 (2 \sin \theta_2 \ddot{\theta}_1 + \sin \theta_2 \ddot{\theta}_2 + 2 \dot{\theta}_1 \dot{\theta}_2 \cos \theta_2 + \dot{\theta}_2^2 \cos \theta_2) - (m_2 g l_2 + f L_2) \sin(\theta_1 + \theta_2) \quad (2.29)$$

$$\frac{\partial \tau_1}{\partial \dot{\theta}_1} = - 2 m_2 L_1 l_2 \dot{\theta}_2 \sin \theta_2 \quad (2.30)$$

$$\frac{\partial \tau_1}{\partial \dot{\theta}_2} = - 2 m_2 L_1 l_2 \sin \theta_2 (\dot{\theta}_1 + \dot{\theta}_2) \quad (2.31)$$

$$\frac{\partial \tau_1}{\partial \ddot{\theta}_1} = I_1 + I_2 + m_1 l_1^2 + m_2 (L_1^2 + l_2^2 + 2 L_1 l_2 \cos \theta_2) \quad (2.32)$$

$$\frac{\partial \tau_1}{\partial \ddot{\theta}_2} = I_2 + m_2 l_2^2 + m_2 L_1 l_2 \cos \theta_2 \quad (2.33)$$

Explicit gradients of torque τ_2 :

$$\frac{\partial \tau_2}{\partial \theta_1} = - (m_2 g l_2 + f L_2) \sin(\theta_1 + \theta_2) \quad (2.34)$$

$$\frac{\partial \tau_2}{\partial \theta_2} = - m_2 L_1 l_2 (\sin \theta_2 \ddot{\theta}_1 - \dot{\theta}_1^2 \cos \theta_2) - (m_2 g l_2 + f L_2) \sin(\theta_1 + \theta_2) \quad (2.35)$$

$$\frac{\partial \tau_2}{\partial \dot{\theta}_1} = 2 m_2 L_1 l_2 \dot{\theta}_1 \sin \theta_2 \quad (2.36)$$

$$\frac{\partial \tau_2}{\partial \dot{\theta}_2} = 0 \quad (2.37)$$

$$\frac{\partial \tau_2}{\partial \ddot{\theta}_1} = I_2 + m_2 l_2^2 + m_2 L_1 l_2 \cos \theta_2 \quad (2.38)$$

$$\frac{\partial \tau_2}{\partial \ddot{\theta}_2} = I_2 + m_2 l_2^2 \quad (2.39)$$

Compared to the static free body, the following additional forces arise during dynamic motions:

- **Centrifugal forces** G_{cf-fa} and G_{cf-ua} equal to $G_c f = m \cdot (V^2/r)$, where m is the mass of a body part taking into account the mass of ballast weights, V is the speed of rotational motion, r is the distance from the shoulder joint to the CoM of the body part, and acting on the forearm and shoulder, respectively;
- **Inertia force** is G_{i-fa} and G_{i-ua} , where a is the acceleration of the movement of body segment;
- **Hydrodynamic force** $G_f r$, created by the pressure of water on the surface of the hand. The point of application of the conditional concentrated force is determined from the

condition that the moment created by it relative to the shoulder is equal to the moment of the distributed force, i.e.

In this thesis the high-speed dynamic motions were not assessed and only inertial forces were considered.

Human body mechanics of pushing and pulling

Pushing and pulling are common activities in the workplace. Such actions require repeated use of the shoulder, arm, entire hand, and only finger manipulations with a variable tolerance.

Pulling and pushing movements can be used in a sitting position by a fairly wide range of workers in various activities such as:

- Pushing and pulling sliding objects such as cardboard boxes on flat surfaces (such as a table);
- Pushing/pulling tools;
- Drawers use;
- Placing/removing objects inside containers.

Such motions are also the cause of many injuries, but comprehensive statistics on injuries associated with these activities are lacking. This may be due to the fact that injuries are not always clearly recorded, since injuries are divided into different categories, making them difficult to analyze. The most common injuries are those caused by overexertion (for example, back sprains). Slipping injuries are also often connected to pushing and pulling. Injuries to fingers and hands can be caused by being caught in, on, or between objects.

According to Majumder et al., 2018 , repeated pushing and pulling forces during prolonged work lead to a growing danger of MSD and injuries. These two common mode actions create bi-directional torque. Researchers have documented that constant or frequent use of hand tools requires the generation of high upper limb torque during push-pull, resulting in lower back and upper limb musculoskeletal complaints (Kuiper et al., 1999, Lin et al., 2003 Tiwari et al., 2010).

According to Tiwari et al., 2010, Chaffin, 1987, when performing isometric push-pull movements in the horizontal plane, the musculoskeletal system is overloaded and there remains a potential risk of accidents due to slipping forward or backward due to inertia. However, even though instruments which require rectilinear or rotational movements have a lower risk of slipping, the muscle load on the upper limbs is inevitable.

A numerical standard has not yet been developed for the analysis and application of pull and push motions in industry due to the complex nature of motion and the many factors that influence it.

The magnitude of the horizontal force developed during pulling and pushing is influenced by many factors:

- Human body mass and strength;
- Force application height;
- Direction of force application;
- Force application distance;
- Posture (leaning forward or leaning back);
- Friction with ground;
- Duration and distance of the push or pull.

According to the data indicated in “PushingPulling website”, 2017 the amount of force that the worker must apply, but the values do not match the weight of the objects that push and pull. Therefore, these values cannot be used as guidelines for weight limits that can be pushed or pulled in the workplace. According to “PushingPulling website”, 2017 these limits must be respected in work situations, especially when the worker is pushing/pulling, and when the arms are above the shoulders or below waist level and the force is applied at an angle. Higher forces can develop if the worker's body rests against a solid structure.

3 Data collection and analysis

3.1 Overview of data collection

The basis of this work involves the investigation of the body postures (including joint angles, torques, forces and CoM) of participants, their performance at the workplace, upper limb muscular fatigue, pushing/pulling motion studies and seated discomfort under HG. All the studies were based on physical experiments. These were all conducted under 1G and then repeated in a water tank to simulate HG ($\frac{1}{6}G$, in some cases under $\frac{1}{3}G$). Four different methods were used in these studies. In some studies, direct, indirect, subjective and observation methods were combined, providing a wider range of parameters to understand a phenomenon. This sub-chapter, was partially extracted and adapted from Volkova et al., 2022 in peer-reviewed Frontier in Physiology publication Volkova et al., 2022 devoted to "An empirical and subjective model of upper extremity fatigue under hypogravity".

Performance study description

Direct, indirect and subjective methods were used. The main tasks that the participants performed:

- assembly and disassembly of a block of several components;
- manipulations with the load - repetitive task (R) (lifting, lowering, displacement);
- work with controls (joystick, toggle switches);
- the issuance of information through a computer keyboard and writing on a sheet of paper.

The two research hypotheses were proposed. Hypothesis 1: $\frac{1}{6}G$ would change the posture of the upper body in comparison with 1G while performing the tasks. Hypothesis 2: $\frac{1}{6}G$ would increase performance of participants.

A total of fourteen volunteers participated in the study (seven males, seven females) 35 ± 5 years, height 1.75 ± 0.11 m, body mass 71.22 ± 17.01 kg. All participants were right-hand dominant; they reported having no current back pain. Experiments were conducted in two sets: in a water tank and out of water. During the experiments in the custom-made swimming pool, participants were seated with their heads out of the water. To reduce the impact of the parallax effect while working in underwater conditions, participants first performed tasks out of the water and then, after getting used to the task, performed them underwater. The ballasts used were selected for specific body parts, providing the required level of buoyancy, i.e., equivalent to gravity on the Moon. For the torso, a weight vest (Strength shop.ch, Switzerland) was used, and for the forearm and upper arm there were adjustable weights (Strength shop.ch, Switzerland). All participants were restrained at the level of the hips. All participants completed the tasks listed above within 5 minutes. All participants also completed a subjective assessment of the NASA Task Load Index (NAS-TLX) (Hart, 2006) immediately after completing each task. Data collection equipment included timer, stadiometer (NutriActivia, Minnesota, USA), bioelectrical impedance analysis scale (Nokia Health, Body +, China). A participant-adjusted chair was build from the Item profiles and components (Item, Germany).

Postural study description

An indirect and observational methods were applied. Static posture and dynamic, repetitive motions of participants were investigated, specifically in an outstretched arm task (S1), arm bent at the elbow task (S2), dynamic task (D) and repetitive task (R). The hypothesis was that HG would create a backward tilt of the upper body in comparison with 1G while performing the tasks.

The modeling of the biomechanics of static equilibrium in the workplace in HG ($\frac{1}{6}G$) conditions includes numerical models based on D'Alembert's principle. Additional mathematical modeling of the slow movements in the workplace in HG conditions was based on recursive Lagrange formulation (see Chapter 2). In the framework of this particular study, joint angles of the upper extremity (upper arm, forearm), spine, torques and forces of upper extremity and torques of the hips were investigated. The physical experiments were conducted in a water tank and out of water. During the experiments in the Swissub diving center (Pully, Switzerland), participants were seated with their heads out of water. The ballasts were distributed on different parts of the body of participants to create the necessary level of gravity, equivalent to the Moon. Furthermore, the workload and CoM of each participant was investigated. Participants in this experiment were thirty-two healthy adults without chronic problems of the musculoskeletal system (35 ± 5 years). Measurements were done in a specially prepared experimental set-up consisting of a (participant-adjusted) chair and operational loads for different tasks. All participants were restrained at the level of the hips and feet. Data collection equipment included timer, 20 kg digital load cell weight sensor with HX711 amplifier module (SparkFun Distributor, Switzerland), built into the experimental workplace and video cameras (GoPro 8, Woodman Labs, Inc. San Mateo, California, U.S), Arduino electronics (Arduino, Italy), bioelectrical impedance analysis scale (Nokia Health, Body +, China), stadiometer

(NutriActivia, Minnesota, USA). Softwares included: Openpose (version 1.4.0) (T. Simon et al., 2017 Cao et al., 2017, Cao et al., 2019, T. Simon et al., 2017, Wei et al., 2016) with GPU (GEFORCE GTX 2080, Nvidia Corp, Santa Clara, CA, USA), FFMPEG software (Newmarch, 2017) Adobe Lightroom Classic (Adobe Inc, San Jose, CA, USA), Agisoft Metashape 1.7.2 program (Agisoft LLC, St. Petersburg, Russia), Blender 2.8 (Blender Foundation, Amsterdam, Netherlands), MakeHuman 1.2.0 (open-source 3D characters maker) software, Arduino IDE 1.8.16 (Arduino Software). A participant-adjusted chair was build from the Item profiles and comfonents (Item, Germany).

Fatigue study description

The effect of HG on upper limb physical fatigue and the mental workload was evaluated in participants. The hypothesis was that HG would increase participant productivity, and at the same time reduce the weighted workload. Task Intensity- Endurance time curves were developed particularly for seated positions, during performance of static, dynamic and repetitive tasks. Here too, thirty-two healthy participants without chronic problems of the musculoskeletal system aged 33.59 ± 8.16 years took part. Fatigue models were constructed for tasks of varying intensity, using the data collected with direct methods.

These direct methods involved a timer and the use of hand dynamometer (Camry scale store, North America), back-leg-chest dynamometer (BLC) (Baseline, New York, USA), to measure hand and BLC muscle contractions based on a bioelectrical impedance analysis scale (Nokia Health, Body +, China) to determine body composition of each participants (weight, percentage of body fat, water percentage, muscle and bone mass), stadiometer (NutriActivia, Minnesota, USA). All participants also completed the NASA-TLX subjective mental workload assessment; this revealed their subjective workload level when executing different tasks. Softwares included: Agisoft Metashape 1.7.2 program (Agisoft LLC, St. Petersburg, Russia), Blender 2.8 (Blender Foundation, Amsterdam, Netherlands), MakeHuman 1.2.0 (open-source 3D characters maker) software. A participant-adjusted chair was build from the Item profiles and components (Item, Germany).

During the water tank experiments, all participants were seated and had their heads above water level. The participants performed a limited number of tasks, specifically: outstretched arm task (S1), arm bent at the elbow task (S2), dynamic task (D) and repetitive task (R) with operational loads (0.5 kg, 1kg, 3kg, 5 kg, 7 kg). All participants were restrained at the level of the hips and feet. A participant-adjusted chair was build from the Item profiles and components (Item, Germany).

Pushing and pulling motion study

The purpose of this experiment was to study the strength of the upper limbs in typical push-pull modes and to predict the limits of working during frequent or continuous work. Pushing and pulling motions were conducted in two different environments (1G and simulated with water $\frac{1}{6}G$). The hypothesis was that HG would reduce pushing/pulling participant strength

in comparison with 1G while performing the tasks. In this study, a total of fifteen men and women (35 ± 5 years) were recruited. Data collection equipment included a force plate and a custom-made experimental setup adapted for pushing/pulling motions under water and out of water. All participants did pushing/pulling tasks in a sitting posture in a participant-adjusted chair without backrest. All participants were restrained at the level of the hips and feet. Softwares included: Agisoft Metashape 1.7.2 program (Agisoft LLC, St. Petersburg, Russia), Blender 2.8 (Blender Foundation, Amsterdam, Netherlands), MakeHuman 1.2.0 (open-source 3D characters maker) software. A participant-adjusted chair was build from the Item profiles and components (Item, Germany).

Seated discomfort study description

The aim of this study was to further broaden current knowledge about comfort at workplace under HG. The two research hypotheses were proposed. Hypothesis 1: Decreasing gravity level will increase comfort of different body parts while participants are sitting and conducting station and dynamic tasks Hypothesis 2: The combination of an optimal seat angle can increase comfort of participants, specifically under HG.

The participants in this experiment were twenty-five healthy adults without chronic problems of the musculoskeletal system (35 ± 5 years). All participants conducted static (S) and dynamic tasks (D). Subjective methods included the use of a comfort survey assessing various body parts and a checklist of chair characteristics (Corlett et al., 1995). For this study, three chair configurations with different backrest angles were used. A participant-adjusted chair, including backrest was build from the Item profiles and components (Item, Germany).

3.2 Statistical methods

In order to determine the required number of participants for the experiments and avoid wasting limited resources on unnecessary samples, a size effect analysis was performed for all experiments. Data distribution was analyzed using Excel (Microsoft office, 2020) and statistical analysis package Stata 17 (StataCorp, California, US) and R software (R Core Team, USA). Statistical significance was defined at $\alpha = .05$. Continuous variables are presented as means and standard deviations. The defined thresholds were 0.2 (small effect), 0.5 (moderate effect), and 0.8 (large effect) (J. Cohen, 1992) between experimental groups. Body part masses and lengths were measured as per statistical data (Plagenhoef et al., 1983). The CoM of the body segments were also estimated this way. For example, for the forearm, shoulder and the whole body, CoM for males is equal 43.4%, 45.8% and 56.9 % respectively. The descriptive statistics of all participant anthropometric data (all experiments) are presented in Appendix Table A.8. Slight differences between female and male can be observed by age ($p=0.742$). Males were significantly taller and heavier ($p<0.001$). The following section details the size effect and statistical methods for each of the different experiments described in this chapter. The results of power analysis are described in the Appendix subsection A.1.2.

Performance study statistics

The performance study was conducted with fourteen participants in two levels of gravity. Five different tasks were assessed independently. This analysis suggests actual power 0.81 and fifteen participants as a correct number for experiments. All details for power analysis are presented in ("Data. Data for thesis", n.d.) The results for Shapiro-Wilk normality test are presented in Appendix Table A.9.

Postural study statistics

Postural studies included joint angles, torques, forces, and CoM variables. All participants completed two different tasks in two different environments (1G and $\frac{1}{6}$ G). Three measurements (average of the first 5 sec - 1 min) were taken for each participant at the beginning, middle and end of the experiment. The time interval for each task was chosen based on the total duration of work (endurance time) by each each participant. In the case of studying the influence of the environment and the task of postural variables, at least twelve participants are required with an actual power of 0.85. In this study, the number of participants per task was equal to the number of participants reported in the fatigue study statistics. Shapiro-Wilk test was conducted to verify the normality of the data, see Appendix Table A.10. All details for power analysis are presented in "Data. Data for thesis", n.d.

Fatigue study statistics

The model used for physical fatigue of upper extremity fatigue and mental workload assessment was empirical and subjective with three levels of gravity, six task intensities, and four types of tasks (outstretched arm (S1) - twenty two participants, arm bent at the elbow (S2) - twenty seven participants, dynamic (D) - twenty five participants and repetitive (R)- twenty six participants), with gender as an independent variable, and Endurance time (min), weighted workload WWL,%, hand and back-chest-leg muscle contraction (kg) as dependent variables.

The Endurance Time - Task intensity curves for all types of tasks were determined using the power model. R-squared values and power model coefficients were then investigated in accordance with these models. An assessment of distribution normality, p-values calculation, and one tailed paired samples t-test were conducted.

With all participants split into four separate groups, a post-hoc power analysis suggests a power of 0.88 for average-sized group effects. All details for power analysis are presented in "Data. Data for thesis", n.d.

Statistical analysis by means of a multivariate regression with correlation coefficients, standard errors and p-values assessment was conducted to investigate the level of significance of dependence between ET (min) and WWL,% and muscle contraction from the gravity level (1G, $\frac{1}{3}$ G and $\frac{1}{6}$ G), as well as the character of this dependence.

Pushing/pulling statistics

Pushing and pulling motions were assessed in two different environments (1G and $\frac{1}{6}$ G). This analysis assumes six participants as the correct number for these experiments with actual power equal 0.99. All details of power analysis are provided in the (“Data. Data for thesis”, n.d.). For descriptive statistical study, a box plot method was applied. It defined the five number summary: the minimum, the maximum and the sample average. All details for power analysis are presented in “Data. Data for thesis”, n.d.

Seated discomfort study statistics

The comfort study was conducted with three different configurations. Configuration 1 was tested by nine participants, configuration 2 was tested by eight participants, and configuration 3 was tested by eight additional participants in two levels of gravity. A mixed-design ANOVA test (as between-subjects) was used to investigate an impact of gravity changes on body comfort. An ordinal logistic regression model was used to obtain finer details of gravity impact on the comfort of various parts of the body. This analysis assumes an actual power of 0.85 and twenty-one participants as the correct number for these experiments. All details of power analysis are provided in the (“Data. Data for thesis”, n.d.). For the seated discomfort study, a box plot description was also applied.

The Table 3.1 shows all experiments and the methods used, the number of participants and the level of gravity tested. All details for power analysis are presented in “Data. Data for thesis”, n.d.

Table 3.1: Experiments summary. S1 - static task (outstretch arm task), D - dynamic task , R - repetitive task, S2-static task (arm bent at the elbow)

Experiment name	Method	Number of participants	G-level
Performance study	Direct, indirect, subjective	14	1G, $\frac{1}{6}$ G
Postural study	Indirect, observational	12	1G, $\frac{1}{6}$ G
Fatigue study	Direct, subjective	22- S1, 25- D, 26 - R, 27- S2	1G, $\frac{1}{6}$ G, $\frac{1}{6}$ G,
Pushing and pulling study	Direct, observational	6	1G, $\frac{1}{6}$ G
Seated discomfort study	Subjective	21	1G, $\frac{1}{6}$ G

3.3 Performance at the workplace

The aim of this study was to extend current knowledge about participant performance (work productivity, error rate) in a seated posture without backrest under 1G and HG, specifically ($\frac{1}{6}$ G). The experimental set up for this experiment is presented in Figure 3.1 and 3.2.



Figure 3.1: Experimental set up for performance at the workplace study (A) Basement preparation (B) Pool assembling (C) Participant conduct a performance related task

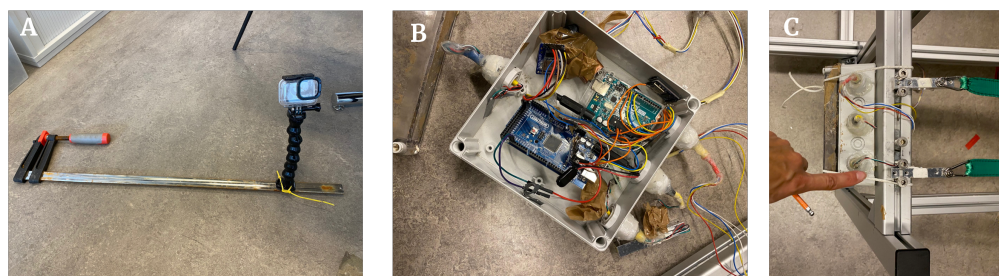


Figure 3.2: Details of the experimental set up for performance at the workplace study (A) Camera holder with protection for underwater recording (B) Electronics water proof box with components (C) Fixation of the box to the sitting part

3.3.1 Observational methods

The goal of this study was to identify predictors of task failure and understand the difference between these predictors in different environments 1G and $\frac{1}{6}$ G. An action plan to prevent these failures was subsequently developed. Visual observation of the participants was applied as a direct method of data collection. The participants during the experiment were observed and indicators related to their performance were noted. The video data were also analyzed. The following indicators were registered:

- The number of operations/motions performed in a certain time;
- The number of errors;
- The visual identification of the moments when the participants began to get tired/bored;
- Postural changes (angle between torso and vertical) in the beginning and in the end of tasks.

Postural studies were conducted with markerless motion capture method as well as with angle measurements on printed with goniometer in case the visibility was insufficient for the markerless motions capture method.

3.3.2 Subjective Methods

Originally developed for the aviation industry, the NASA-TLX scale was then applied to power plants, remote control systems, and space applications. This scale was used to assess a number of human factors: team collaboration (6%), fatigue (2%), tensivity (3%), experience (4%) and disability (1%) (Hart, 2006). NASA-TLX is based on independent subjective demands which are related to: Mental (MD), Physical (PD), and Temporal Demands (TD), Frustration (FD), Effort (ED), and Performance (PD). Before completing the task, participants were asked to read these subjective demands, and a detailed description thereof, see Appendix Figure A.3, and 100 point rating scale, Figure A.4. Each subjective demand of participants was weighted, resulting in a composite mental workload, see Equation 3.1.

In this study, the NASA-TLX (Hart and Staveland, 1988) scale was used for mental workload assessment of the participants, carried out immediately after the execution of each task under 1G and simulated $\frac{1}{6}G$, as well as $\frac{1}{3}G$. The benefit of this approach is that it reveals a specific demand of each participant. The benefit of this approach is that it reveals a specific demand of each participant.

NASA - TLX application consisted of two parts. In the first part, individual weighing of subjective demands through fifteen pairwise weighing occurred. Participants had to select, from each pair, the most appropriate subjective demand for the workload. The fifteen pairs for pairwise comparison included: MD or PD, MD or EF, PD or FR, PD or P, PD or TD, FR or MD, FR or EF, P or MD, P or TD, EF or PD, EF or P, TD or FR, TD or MD, TD or EF. The total number of selected specific subjective demands is referred to as task load index or $Weight_{demand}$. The calculation will be discussed below. The second part uses a 100-point range evaluation $Rating_{demand}$, for which the following questions were posed for all subjective demands (Hart, 2006):

- MD - How mentally demanding was the task?
- PD - How physically demanding was the task?
- TD - How hurried or rushed was the pace of the task?
- P - How successful were you in accomplishing what you were asked to do?
- EF - How hard did you have to work to accomplish your level of performance?
- FR - How insecure discouraged, irritated, stressed, and annoyed were you?

Each subjective demand of participants was weighted; this resulted in a composite mental workload, see Equation. The calculation of weighted workload is as follows:

$$WWL = \frac{\sum (Weight_{demand} \cdot Rating_{demand})}{15} \quad (3.1)$$

where $Weight_{demand}$ -task load index based on pairwise comparison of subjective demand (total 15 pairs), $Rating_{demand}$ - a total score of 0 corresponds to a very low subjective demand, a total score of 100 corresponds to a very high subjective demand.

3.4 Postural study

After initial experiments in the pool in the garden, it became possible to conduct experiments in a professional diving center Swissub in Pully, Switzerland, see Figure 3.3. The figure below shows photographs taken at Swissub. For this study indirect methods were applied.

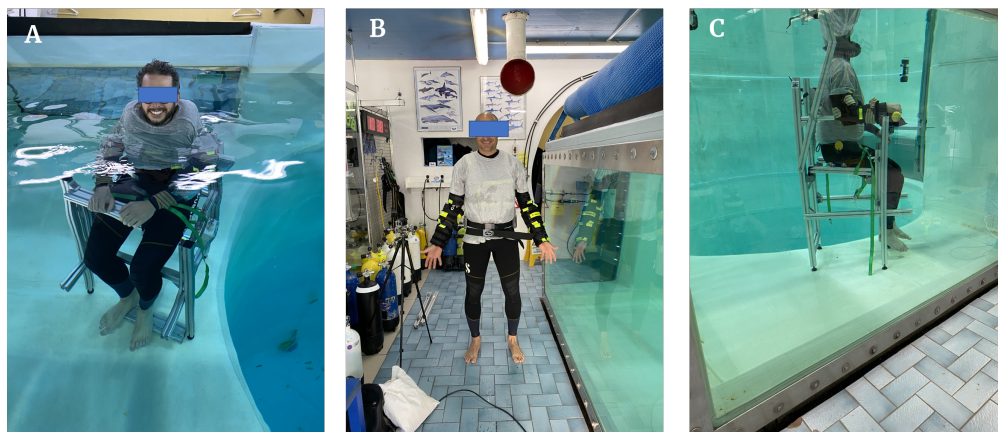


Figure 3.3: (A) Participant conducting the task in Swissub (B) Ballasts distribution on the participants body (C) Participant profile in the workplace. Backrest configuration test

3.4.1 Indirect methods

This study was performed with indirect methodology, see Chapter 1. Further information was taken and adapted from the peer-reviewed publication Volkova et al., 2022. An Empirical and Subjective Model of Upper Extremity Fatigue Under Hypogravity, Frontiers in physiology (special issue). In the scope of this study, static holding of weights, as well as dynamic motions were taken into account to show the principle of application of markerless motion capture methods and data processing steps. The camera calibration computation errors were based on bundle adjustment (pixel) and global registration [cm] computation (see sub-chapter 4.1). The calculation of markerless motion capture errors was based on percentage of correct keypoints (PCK), mean absolute error (MAE) as well as mean joint position errors (MPJPE) for global skeleton and particular joints for 2D recognition in 1G and simulated 1/6G in an underwater environment (see sub-chapter 4.3). The PCK results were not counted the invisible joints. An experimental setup is shown in Figure 3.4. The definition of the coordinate system is as follows: X is the antero-posterior axis, Y is the superior-inferior axis, Z is the right-left axis. The markerless motion capture is based on four Gopro 8 video cameras. The following parameters

of the cameras were used: 1,920x1,080 pixels at 30Hz. Openpose (version 1.4.0) was installed from GitHub and run with GPU. Then the JSON format output included twenty-five keypoints (see Figure 3.4 (B) of the participant's body that were stored for each frame and camera. The control points were annotated manually and then all cameras were calibrated with a Multiple view calibration tool script. Intrinsic and extrinsic data were then extracted and implemented for OpenPose 3D pose reconstruction. To verify the quality of joint recognition, the predictions with manually annotated joints were compared, and then the error of each joint was calculated. The total number of non-reading frames was also estimated.

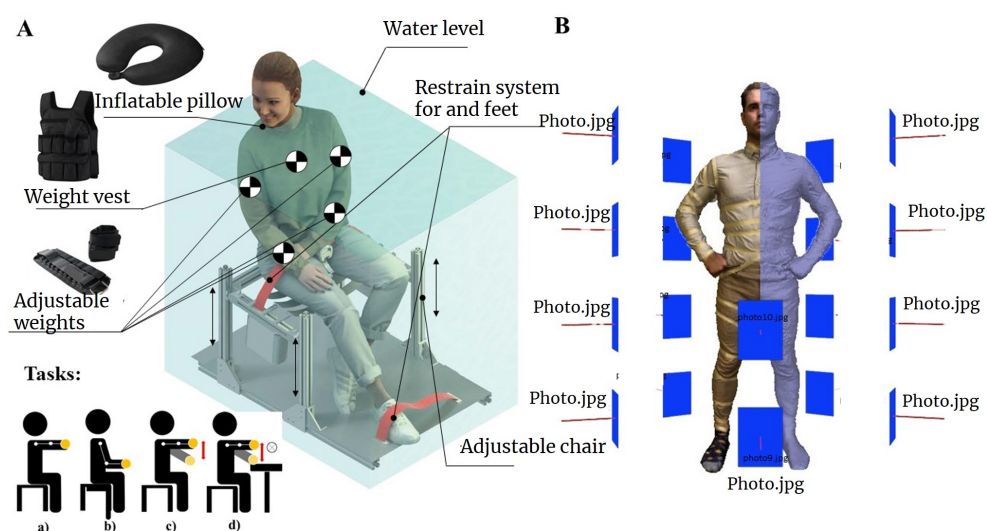


Figure 3.4: (A) Experimental setup. (B) Participant 3D scan example with a visual explanation of the principle of photogrammetry (Agisoft Metashape). Volkova, 2022. Creative Commons license

The experimental room light was used to synchronize data on all cameras. First, the cameras were started with the light off, and then the light was turned on by the experimenter before the start of the experiment and at the end of each task performed by the participant. Further, the useful frames could be easily detected manually for each camera with FFMPEG software (Newmarch, 2017). One of the start frames chosen was the synchronization frame. The total number of frames for each video camera was set to be equal after the synchronization frame was calculated. Frames with participants performing the tasks were manually selected. This method was used both for ground and underwater conditions, effectively replacing the "classical clap method". The first frame corresponds to taking a weight in one's hand at the start of the task and the last frame corresponds to the experimental protocol when the participant was tired and could no longer hold the weight in their hand. Due to the specific conditions of recording, some preliminary steps were implemented. For the videos recorded in an underwater environment, it was necessary to rework the white balance of the frames and create the necessary resolution (if for example the videos were recorded in vertical orientation). For these purposes, Adobe Lightroom Classic (Adobe Inc, San Jose, CA, USA) was

implemented and the Adobe Photoshop batch processing to automate the process for white balance adjustments, see Figure 3.5.



Figure 3.5: White balance adjustment and creating new resolution

The whole data processing steps is shown in Figure 3.6.

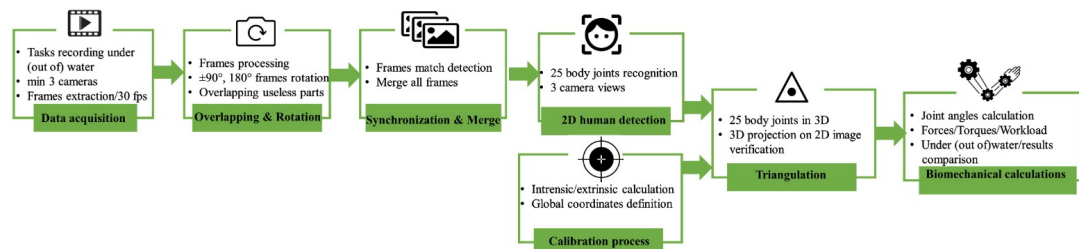


Figure 3.6: The scheme of data processing for 3D biomechanical computations

Some practical advises for camera calibration developed by CVLab (EPFL) and an example of points for annotation is presented in Appendix subsection A.1.1 and Figure A.8 .

Calibration

At this stage one has a set of image points for each calibration object in the images that will be used to calibrate the cameras. There are following steps to perform are as follows: estimation of the relative poses, concatenation, bundle adjustment and finally global registration. The various errors and the visual outputs indicate whether the algorithm converged to a good solution. The camera calibration theory is described in sub-chapter 2.2.

In order to calibrate the cameras, all frames must be synchronized. In a case study, this was preformed manually using light synchronization: after the cameras were turned on, the experimental room light was turned off and on three times. This method was used both for ground and underwater conditions, effectively replacing the "classical clap method". Then, frames containing similar scene information with respect to the light effect were selected as a starting point of the sequences

Running the multiple view calibration tool

To be able to run the calibration tool, the following prerequisites are required: numpy, scipy, imageio, matplotlib, OpenCV. At this point, a video depicts the pattern in different poses. The first step consists in extracting the video 30 fps frame which can be done as follows (Newmarch, 2017):

Listing 3.1: 30 fps frames extraction line code

```
1 ffmpeg ffmpeg -i video.mp4 -vf "fps=30" output/frame_%06d.jpeg
```

This frame rate is necessary for good synchronization of the frames of the three cameras and to improve the quality of triangulation.

Once all frames have been extracted, the calibration can be achieved using the script detailed in “Github”, 2022. allowing both intrinsic and extrinsic camera computations. This step is necessary for triangulation of 2D keypoints of the participant’s skeleton model and must be executed for every setup. The description here is limited to the main steps and results of calibration, as these are important parts of the markerless motion capture method.

To be able to run the calibration tool, the following prerequisites are required: numpy, scipy, imageio, matplotlib, OpenCV. At this point, a video depicts the pattern in different poses. The first step consists in extracting the video 30 fps frame which can be done as follows (Newmarch, 2017):

Listing 3.2: 30 fps frames extraction line code

```
1 ffmpeg ffmpeg -i video.mp4 -vf "fps=30" output/frame_%06d.jpeg
```

This frame rate is necessary for good synchronization of the frames of the three cameras and to improve the quality of triangulation.

Once all frames have been extracted, the calibration can be achieved using the script detailed in “Github”, 2022. allowing both intrinsic and extrinsic camera computations. This step is necessary for triangulation of 2D keypoints of the participant’s skeleton model and must be executed for every setup. The description here is limited to the main steps and results of calibration, as these are important parts of the markerless motion capture method.

Compute intrinsic parameters

For intrinsic computation, support by an 8 x 6 calibration checkerboard can be done with this command line, Listing 3.3 (“Github”, 2022):

Listing 3.3: Intrinsic computation line code

```
1 python compute_intrinsics.py --folder_images ./frames -ich 6 -icw 8 -s 30 -t 24 --debug
```

To be able to make the distortion function behave correctly, it is necessary to sample more

precise points and to better cover the corners of the image. To verify this monotonicity on the image and camera distribution views should be verified. If the results are not sufficient, it is possible to switch to the rational model with the option `-rm`. In the case study, rational model (rm) was not used because experimental cameras have low distortion and rm is suitable only for wider angle lenses.

Relative poses computation

This step is then followed by computation of relative poses. It allows one to build relative poses between pairs of pre-made looks described in `setup.json`. These views are then linked together to calculate the position of each camera relative to the first camera. The file named `landmarks.json` contains the exact image points for each view, which are used to calculate the basic matrices and poses. This file (`landmarks.json`) was calculated with the click point Jupiter notebook tool, described in “Github”, 2022. An example of the selected landmarks on a chair is shown in the Appendix in Figure A.8.

For landmarks computation, a tennis ball and chair structure was used as an object that could be seen from all views of the cameras. This approach was applied for underwater and out of water environments. The `intrinsics.json` file contains the internal settings for each view. The `filenames.json` file contains one image filename for each view; it is used for visualization purposes. Generally, for `filenames.json` it is enough to select one frame from the camera. See linecode 3.4 (“Github”, 2022):

Listing 3.4: Compute relative poses

```
1 python compute_relative_poses.py -s setup.json -i intrinsics.json -l landmarks.json -f
   filenames.json --dump_images
```

This should produce the RMS eprojection error and total reprojection error. It should not exceed 1 pixel, or calculations cannot be continued. The residual error and the sampson distance provide an indication of whether the estimated fundamental matrix and hence the relative pose fit the annotated image points.

Concatenation of relative poses

In this step, chains of all relative poses are used to obtain an estimate of the actual camera poses. To concatenate the relative poses and hence obtain the initial solution for the BA, the following command is executed. It takes the relative poses computed beforehand as input (“Github”, 2022).

Listing 3.5: Concatenate relative poses

```
1 python scripts/concatenate_relative_poses.py -s setup.json -r output/relative_poses/
2 relative_poses.json --dump_images
```

Bundle adjustment computation

BA calculation was performed by refining internal and external parameters and 3D points using the least squares method, as seen in Listing 3.6. BA line code. The camera rig is still up to scale at this point. The file "poses.json" is the output of the previous step ("Github", 2022).

Listing 3.6: Bundle adjustment

```
1 python bundle_adjustment.py -s setup.json -i intrinsics.json -e poses.json -l landmarks
  .json -f filenames.json --dump_images -c ba_config.json
```

There is an additional method for verifying the correct calibration. It uses a match of green dots manually selected through the Jupiter Notebook, (see "Github", 2022) script with red dots recognized by the algorithm. The last step is devoted to transformation of the local to global reference system.

Global registration

The poses and 3D points calculated using the bundle adjustment are not scaled correctly. In order to restore a rigid transformation between the poses computed by the bundle adjustment and the actual poses in world coordinates, the world coordinate position (minimum 4 non-coplanar points) of the image landmarks are needed. For this, a "landmarks_global.json" file is provided. The following command finds the rigid transform through the least-squares between two sets of points. Further, all poses calculated using the bundle adjustment are updated. The resulting updated poses are saved in "global_poses.json", see listing 3.7 ("Github", 2022).

Listing 3.7: Global registration

```
1 python global_registration.py -s setup.json -ps ba_poses.json -po ba_points.json -l
  landmarks.json -lg landmarks_global.json -f filenames.json --dump_images
```

At this step, the global coordinates related to the scene should be selected. Five points located on the experimental chair were selected. Because this experiment uses two different setups for the underwater and out-of-water experiments, the global coordinates for the two setups were different.

Body volume computation

This paragraph was extracted from a publication of the author of this manuscript, Volkova et al., 2022, *Frontier in Physiology* Volkova et al., 2022 "An empirical and subjective model of upper extremity fatigue under hypogravity".

The photogrammetrie approach of the Agisoft Metashape 1.7.2 program (Agisoft LLC, St. Petersburg, Russia) was used to estimate the entire torso volume (Jebur et al., 2018). A high-resolution camera (12 MP), lens length (4.25 mm), and f/1.8 were used to photograph the bodies of all participants, with 1,000 photos taken for each.

All models were created using DSM 114 = 10 cm/pixel resolution and high or medium dense cloud quality. To begin, a customized mesh of the participants' bodies was imported into Blender using photogrammetry. Then, for each body segment, a target mesh was created, and a boolean modifier^I with difference option was used to calculate the volume of a specific body segment (Freixas et al., 2006).

The volumes of each participant were scaled and corrected using a stadiometer (NutriActivia, Minnesota, USA) to account for their height. Proportional editing^{II} (Guevarra, 2020), which was needed to change an irregular mesh. When compared to the water displacement approach, the Boolean method with a combination of proportional editing functions yielded a result with a difference in the estimate of the 3D model of 5 cm³ for the full body volume.

The hand, forearm and shoulder volumes were assessed as follows. First, the hand up to the wrist was immersed and a mark was made with water level 1, then the hand was immersed up to the elbow and a new mark was made with water level 2, and then the hand was immersed in the cylinder with water along the shoulder and a new mark indicating level 3 was made. The difference between the water levels was then calculated. The shoulder volume is equal to the difference in water displacement between the level 3 and 2 marked when the upper arm and elbow are immersed. The forearm volume was calculated based on the difference in water level 2 and 1 noted when both elbow and wrist were immersed. The wrist hand volume was neglected as it is less than 1% of the total body volume. This can be included in the overall error estimation. The required mass of ballast weights to simulate lunar gravity will not exceed several tens of grams, which is less than the natural variability of the wrist parameters and will not distort its mass-inertial profile, which is usual for a human. Thus, the effects of HG do not affect the loading ability and fatigue of the hand, and also do not give significant amendments to the calculated loads on the rest of the skeleton.

From 2D recognition to triangulation The joint angles for performance study were evaluated with observational and indirect methods, while postural changes for postural study were assessed with indirect methods only.

The participants of the experiment were recorded on the camera in profile, and then frames were selected that captured the scenes when the participant was just starting to work and at the end of the task. These videos were filmed underwater and out of water. Further, frames with the necessary scenes were extracted and angles were measured using the Illustrator (Adobe, USA) method of measures. Such angles were fixed for all types of tasks envisaged by the experiment.

The joint angles for full postural fatigue relate experiments were evaluated using a custom-

^I**Boolean modifier** was used to conduct logical operations on complex 3D models. Intersect, difference, and union are examples of these operations. The difference option was used to compute the volume of a certain body segment. It allows to subtract the target mesh from the modified mesh so that anything outside the target mesh is kept

^{II}**Proportional editing** is a method of applying a scaling effect to selected model elements (such as mesh elements). This method is useful for smooth deformation of the mesh surface

made Matlab script, see Appendix A.5 and (“Figshare. Custom-made scripts”, 2022).

After camera calibration step, the final output of the global registration file '*global_poses.json*', and all 2D projections of the OpenPose 25-body joint model were obtained. In the next step, triangulation took place.

Triangulation was performed only for preselected scenes (dynamic and static). For correct triangulation, it is important that each folder with 2D data of the 25-body joint model has the same number of synchronized JSONs files.

In general, each camera recorded several scenes for one hour, and then all the data was processed in its entirety, without division into scenes that showed the tasks performed by the participants. The numbering for such files was from 0 to 30,000. Only after processing the data were the necessary scenes selected. For example, from 200 to 500, all other files, without a record of the executed task, were ignored.

Further, to calculate the necessary parameters, including the angles of deviation of body parts from the vertical, the center of mass, forces, torsion and forces, a custom made Matlab script used. This script reads input data in json format with dimension equal (760 x 25 x 3) received after triangulation calculation.

First of all, 2D skeletons were calculated. One frame with an image of a person represents the following document with 25 2D keypoints and confidence interval for each of them (joint) (“OpenCVdocs website”, 2022):

Listing 3.8: 2D keypoints - OpenPose output

```
1 { "version": 1.3, "people": [ { "person_id": -1, "pose_keypoints_2d"
   : [930.599, 174.189, 0.894699, ...], "face_keypoints_2d": [], "hand_left_keypoints_2d": [], "
   hand_right_keypoints_2d": [], "pose_keypoints_3d": [], "face_keypoints_3d": [], "
   hand_left_keypoints_3d": [], "hand_right_keypoints_3d": [] } ] }
```

The 2D skeletons were then triangulated into the final 3D json and this final output.json file was imported into the script adapted from (“OpenCVdocs website”, 2022).

Listing 3.9: Joints description

```
1 joints = [
2     "nose", "neck", "rshoulder", "relbow", "rwrist", "lshoulder", "lelbow", "lwrist", "midhip",
3     "rhip", "rknee", "rankle", "lhip", "lknee", "lankle", "reye", "leye", "rear", "lear", "
4     lbigtoe", "lsmalltoe", "lheel", "rbigtoe", "rsmalltoe", "rheel", "background",
5 ]
6
7 def draw_pose_(image_, pose, confidence=None):
8     joint_pairs = [ # ( 'nose ', 'leye ', color_joints [ 'red ' ] ),
9                     ( 'nose ', 'neck ', color_joints [ 'green ' ] ),
10                    ( 'neck ', 'lshoulder ', color_joints [ 'white ' ] ),
11                    ( 'neck ', 'rshoulder ', color_joints [ 'blue ' ] ),
```

```

11         ("neck", "midhip", color_joints["red"]),
12         ("midhip", "rhip", color_joints["orange"]),
13         ("midhip", "lhip", color_joints["cyan"]),
14         ("rhip", "rknee", color_joints["brown"]),
15         ("lhip", "lknee", color_joints["magenta"]),
16         ("lknee", "lankle", color_joints["purple"]),
17         ("rknee", "rankle", color_joints["grey"]),
18         ("lshoulder", "lelbow", color_joints["red"]),
19         ("lelbow", "lwrist", color_joints["orange"]),
20         ("rshoulder", "relbow", color_joints["green"]),
21         ("relbow", "rwrist", color_joints["blue"]),
22
23     ]

```

The following input data were taken into account in the Matlab script, see section Appendix A.5:

- Output data after triangulation calculation;
- Data with anthropometric indicators of participants, including (gender, age, weight of body parts of participants, inertial indicators for upper limbs, load level performed during the task and participant number);
- Data interval numbers that correspond to the problem under study, for example 200-500 (as it was explained above);
- Gravity level;
- Name of the output file;
- Participant number.

Joint angles assessment

The hypothesis for this study was that under HG a backward tilt of the upper body is observed, in comparison with 1G, while performing static and dynamic tasks. Body tilt is expressed through a change in joint profiles (angles, torques, position). The experiment involved 32 healthy participants aged 33.6 ± 8.2 years, on which vision-based 3D motion analysis was used to investigate joint profiles.

Joint angles can be found using markerless motion capture if all rigid links of the experiment participants are recognized at each moment of task performing. Specific rigid links can be considered as vectors and then angles between them can be easily calculated. The following are considered in this work, as illustrated in Figure 3.7:

- The angle between the axis Y and the position of the forearm/upper arm;
- The angle between the spine and axis Y (forward- backward, right- left);

- The angle between spine and thigh.

In this study, the angle between head and y-axis and neck and y-axis was not taken into account due to experimental limitations. The recording of the body of the participant was carried out only to the bottom of the neck.

Studying the differences of these joint angles in different conditions allows one to understand how the human body reacts under different loads in different environments.

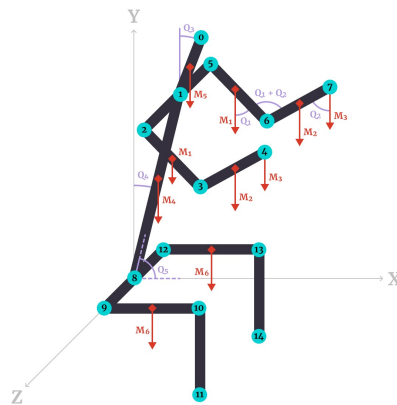


Figure 3.7: 3D skeleton model used for data processing

Joint forces and torques assessment

In this study, reaction forces on the seat as well as on the back of the seat were collected to investigate the forces. For this, custom made electronics units were designed, adapted for underwater experiments; see Figure 3.8.

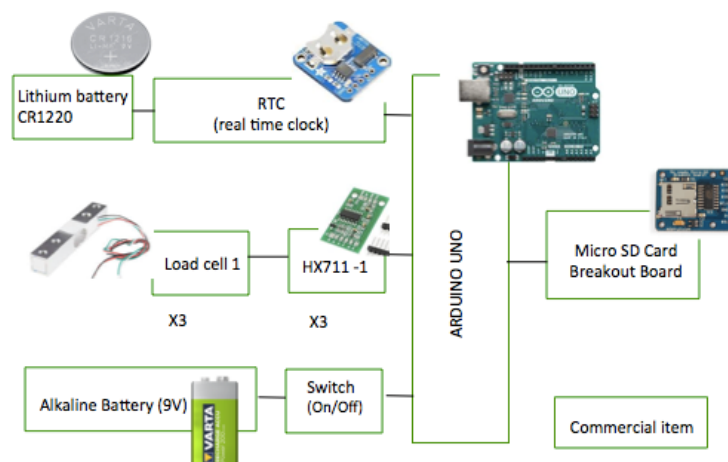


Figure 3.8: Block diagram for electronics box

It shows the block diagram for this electronics box and photo with all components. In Appendix Figure A.5, the electronics scheme for this box. The theoretical basis for this part is explained in Sub-chapter 2.1.

Workload estimation

To estimate the joint workload, e.g., at the shoulder or elbow, the ratio of the joint torque and the joint capacity are examined. The following equation can be used for workload calculation (Database et al., 1996):

$$Workload_{joint} = T_{joint} / J_{capacity},$$

where T_{joint} - is torque of the joint, and $J_{capacity}$ - is a physical joint capacity.

Joint capacity for extension/flexion of upper extremities is described in (Database et al., 1996).

CoM estimation

The dynamics of the human body's seated posture in a work environment under hypogravity has hardly ever been studied. Such a system can be modeled by tracking the center of mass, which accounts for important variables such as muscle activity. The difference between the whole-body system of thirty-two participants working under simulated $\frac{1}{6}G$ (Moon) and 1G (Earth) using measurements of static, dynamic, and repetitive actions was determined.

In this study, the center of mass (CoM) data for various body movements were obtained in the framework of a previous study (Volkova et al., 2022) devoted to the upper extremity fatigue of participants under hypogravity (HG). This study aimed to define the CoM of the body using a markerless method which is a relatively new method for evaluation along with 3D visualization methods. In general, the CoM shift can be measured using various methods, which are complex and time-consuming. Data on the location of the CoM of a person in a sitting position is necessary for various design and analysis tasks, in particular for the design of seats, restraint systems, and other human-centered products and environments. Also, the displacement of the center of mass is usually used to quantify the stability of the posture.

This study presents an analysis of the location of the CoM of the entire body concerning the hip joint of participants performing static, repetitive, and dynamic tasks in two different environments under 1G and $\frac{1}{6}G$.

Weighted sum of limb centers: CoM prediction of the participants is calculated as a weighted sum of the limb centers (Bachmann et al., 2019).

$$CoM = \frac{1}{M} \sum_{(i,j) \in Limbs} m_{ij} \frac{P_i + P_j}{2} \quad (3.2)$$

with $M = \sum_{(i,j) \in Limbs} m_{ij}$.

A custom made Matlab script for predicting the whole body CoM for a weighted sum of limb,

presented in Appendix A.5.

The assessment of CoM was conducted for 3D skeleton models extracted with indirect method (markerless motion capture). The location of the CoM of the participants in the sitting posture for each frame was observed. The CoM was calculated relative to the hip joint coordinated (pelvis).

3.5 Fatigue study

The aim of this research was to broaden further the current knowledge about upper extremity fatigue under HG.

First, a numerical model for the ballast calculation was developed, based on a simplified model of the human skeleton. In this model the masses of the various body parts of the participants, as well as CoM link of the body were calculated in accordance with (Plagenhoef et al., 1983). The length of the body parts and the distance between the joints of the body were measured. To estimate the body parts volume, the photogrammetrie method was used.

This study involved no use of electronics and sensors. All participants were strapped at the hips and legs. Using their specific anthropometry, each participant's legs were attached to the footrest, taking into account leg length from knee to foot in particular.

The results obtained were analyzed with Excel and statistical analysis package Stata 17 (StataCorp, California, US). Statistical significance was defined at $p < 0.01$ ^{III}. An exponential regression test was determined the Endurance Time - Task intensity curves for all types of tasks. Assessments of the normality of distribution, p-values calculation, t-test were then conducted. The standard residual errors are calculated and presented in a chapter 4.7.2. Continuous variables are presented as means and standard deviations.

In the water tank experiments, ballasts were added on different parts of the body of the participants. For the torso, a weight vest (Strength shop.ch, Switzerland) was used, and for the forearm and upper arm there were adjustable weights (Strength shop.ch, Switzerland). Upper limb and trunk ballast weights for participants were calculated as explained in Chapter 2.

3.5.1 Direct methods

Participants performed four different one-handed tasks: holding weights with an outstretched arm (S1), holding weights in an arm bent at the elbow (S2), slow dynamic motion (D), and repetitive motion (R). Since not all thirty-two participants were available for the same tasks, twenty-two participants were invited for task S1, twenty-seven conducted task S2, twenty-five conducted task D and twenty-six participants conducted task R. Six tasks of varying intensity

^{III}*** $p < 0.01$ – results are highly significant, ** $p < 0.05$ – results have moderate significance, * $p < 0.10$ – results have marginal significance

were investigated from 0.4 to 9 kg. The choice of maximum load depended on the participant's physical capabilities and on gender. All participants answered a questionnaire designed to assess their readiness for physical activity (Warburton et al., 2019), see Appendix Figure A.6.

As stated in the publication Volkova et al., 2022, the lead author of which is the author of this dissertation, all participants in the experiment received detailed oral instructions to perform the tasks. More difficult tasks, such as those that required repetition, were demonstrated via a video, and each participant could refer to the video instructions at any time during the exercise. Warm-up activities were completed by all participants to prepare them for physical activity. They lifted a 3 kg dumbbell fifteen times in their right hand for 5 minutes each time, with a 1-minute break in between. The tasks were carried out in 1 G first, then in the water tank.

Each participant's right-hand strength was recorded three times before and three times after the task with a hand digital dynamometer. The mean values were then assessed. A calibrated back-leg-chest (BLC) dynamometer was used in the same way. Back measurements were not taken due to the difficulties of simulating the tasks underwater.

These dynamometers measure isometric muscle strength in kilograms (kg) of force. All measurements were taken in a seated position; they took into account the position of the participant's limb (outstretched arm or arm bent at the elbow). For measurements with a BLC dynamometer, the chain length was adjusted to the participant's sitting height. This was done by asking the participant to sit on a chair and put their legs on the base of the BLC dynamometer, bent at 90 degrees. In all cases, tasks were performed until volitional failure. Participants were able to take micro-pauses (very short intermittent breaks between all tasks) equal to at least 1/5 of working time (Australia, 2011). In practice, rest breaks mainly result from a worker's personal feedback of sufficient free time to allow workers to complete an activity with relative comfort (Brown, 1994). This means that additional time was provided if needed by the participant to recuperate.

The speed of motions can play a crucial role in an underwater environment, and significant loads can occur from the water during fast movements. As defined in Chapter 2, $F_{res} = 47[\frac{cm}{s}]$ - the limit of motion speed of the participant's dynamic motions were designed in accordance with the found value and were approximately $10[\frac{cm}{s}]$ for a 3-second motion cycle. This resulted in a margin equal to 3.

3.5.2 Subjective method

For the fatigue study, the NASA-TLX assessment method was applied. See description in Sub-section 3.3.2.

3.6 Pushing/pulling study

In this study direct and observational methods of assessment were applied.

3.6.1 Direct methods

For this experiment, a custom-made wood structure was designed. It was adapted for underwater experiments, as seen in the block diagram in Figure 3.9 (A) and Figure 3.9 (B) with an experimental setup.

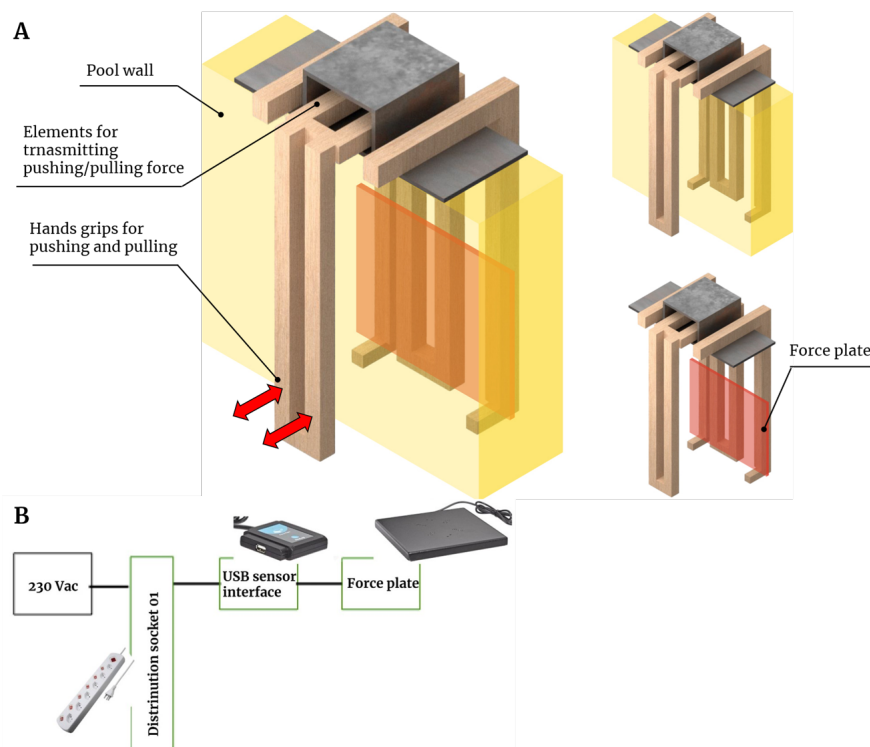


Figure 3.9: (A) Experimental set up for pushing/pulling experiment (B) Block diagram for pushing/pulling

Testing of muscle strength of the upper limb (isometric mode) carried out with the help of two hands and during the "pull-push" operations and was carried out for 60 s. Written informed consent was obtained and anthropometric parameters were measured for all the participants.

To quantify the strength of the hand-arm-shoulder complex, an isometric force test of two arms in static posture at a torque of 0 [Nm] on force plate (Neolog, USA) was recorded. The participants had to pull/push the wooden handles of the self-made installation with their hands with an emphasis at shoulder level in a horizontal direction. The experiment was carried without any verbal encouragement, while each participant was instructed to develop maximum voluntary strength during 60 [s]. Each participant was given a trial version before

the experiment.

The study was focused on maximum voluntary strength of the upper extremity complex only, so the inadvertent application of force by other parts of the body or the possibility of body weight contributing to greater strength by any participant was limited. Seating bench height was also adjusted individually for each participant to ensure optimal grip of the feet on the floor surface, as well as to limit the gravitational load on the back, which affects the development of strength.

3.7 Seated discomfort study

The aim of this research was to broaden further the current knowledge about comfort at workplace under HG. The proposed configurations (at least three) for two different work activities (static, dynamic) at the workplace in underwater with simulated HG ($\frac{1}{6}G$) environment for the comfort and biomechanical adaptability of the human body were analyzed.

Chairs configurations

Chair configurations were intended to be comfortable and suitable for HG conditions. Comfortable means that the impact of HG on the participants' bodies would be perceived in such a way that the loads and torques on the joints of the upper limbs, as well as on the spine, would be reduced and the participants would feel no discomfort sitting in the seat. See chair configurations below (Figure 3.10):

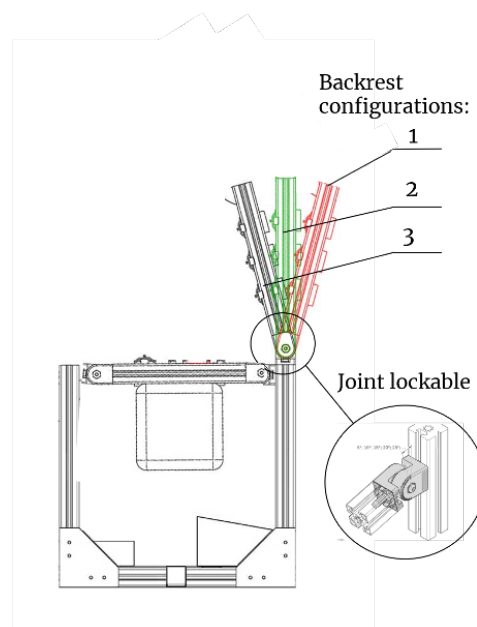


Figure 3.10: Side view of the experimental chair configurations

The following configurations were tested:

1. Configuration 1: Backrest inclination more than 90 degrees;
2. Configuration 2: Backrest inclination 90 degrees;
3. Configuration 3: Backrest forward inclination less than 90 degrees;

The chair was adjustable and all available reclining positions were easy to fix manually with the aid of a lockable joint. Each configuration was tested by five participants. During this experiment, additional data points for previous experiments were also collected. Then, based on the collected data, detailed seat-design procedures based on the analyzed activities were proposed.

3.7.1 Indirect methods

For indirect methods, markerless motion capture was selected. The details of this method were explained in sub-chapter 3.4.1.

3.7.2 Subjective methods

The subjective assessment was carried out with body part discomfort rating based on (Corlett, 1976), see a template for discomfort of different body parts evaluation in Appendix Figure A.7. The aim of this study was to understand how comfortable participants were throughout the experiment.

3.7.3 Observational methods

Observation and questionnaires were used as direct methods. Conversation with experiment participants during the tasks was audio-recorded. The aim of the investigation was to understand how participants felt and how their body adapted to HG and proposed chair configuration. An opinion about participants' preferences was also requested. This rating began by asking participants to mark their level of comfort (for different parts of the body (head, neck, shoulders, upper back, lower back, hips, feet) at the beginning and end of trials (Corlett et al., 1995). The following ratings were given for different levels of comfort in the rating:

- 1 - Uncomfortable;
- 2 - A certain discomfort;
- 3 - Some discomfort;
- 4 - Slight discomfort;
- 5 - Very comfortable.

4 Results

This chapter presents the main results of our study, including:

- performance at the workplace;
- postural studies (including joint angle, torques, forces, CoM assessment, workload);
- fatigue study;
- pushing/pulling study;
- seated discomfort study.

As an output of the synthesis of the results, a combinatorial study is proposed to better understand the effect of HG on biomechanics at the workplace.

This chapter start with camera calibration results because this is an important part of this study. All indirect methods were related to camera calibration and triangulation of the participants' 3D skeletons necessary for postural study.

4.1 Camera calibration results

In order to calibrate the cameras, all frames were synchronized. After that, the following steps were taken: estimation of the intrinsic parameters, relative poses, concatenation, bundle adjustment and finally global registration. The results of these steps are presented below.

Compute intrinsic parameters

For this step the following output should be obtained, see Figure 4.1:

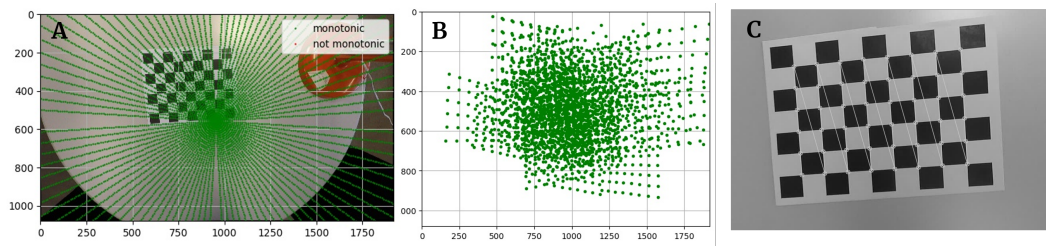


Figure 4.1: Intrinsic parameters computation. The visual results (A) Monotonicity (B) Camera views distribution on checkerboard. (C) 8 x 6 calibration checkerboard recognition.

The Figure 4.1 shows an example of correct visual results for intrinsic parameter calculation: monotonicity, camera views distribution on checkerboard, results of checkerboard recognition. Camera views dots evenly distributed over the checkerboard frame shows the correct capture of the checkerboard. Such results were calculated for each camera used for the experiments.

Relative poses computation

The relative posed results are shown in Figure 4.2:

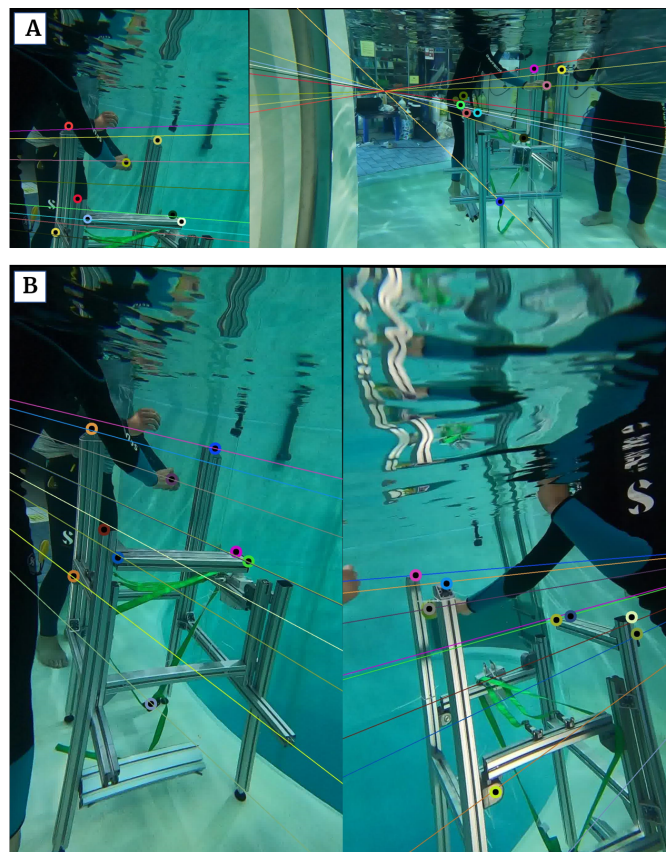


Figure 4.2: Relative poses results. (A) Views cam 1 and cam 2. (B) Views cam 1 and cam 3.

In this figure, all lines pierce the selected landmarks placed on the chair and this indicates that all landmarks were correctly recognized and all lines converge at the possible location of the camera.

Bundle adjustment computation

The output seen in Figure 4.3 should be obtained. Figure 4.3 (A) shows the confirmation of camera recognition. Recognition of camera 1 is confirmed by a green square superimposed on camera 1 and a blue square superimposed on camera 2. Camera 3 is not visible in these images.

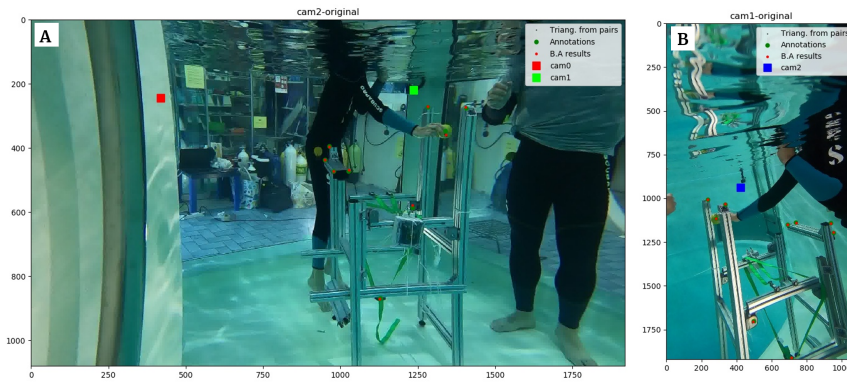


Figure 4.3: Bundle adjustment output. Confirmation of the position of the cameras. (A) View for cam 1. (B) View for cam 2.

Global registration

Figure 4.4 and 4.5 shows recognized by calibration algorithm blue global points:

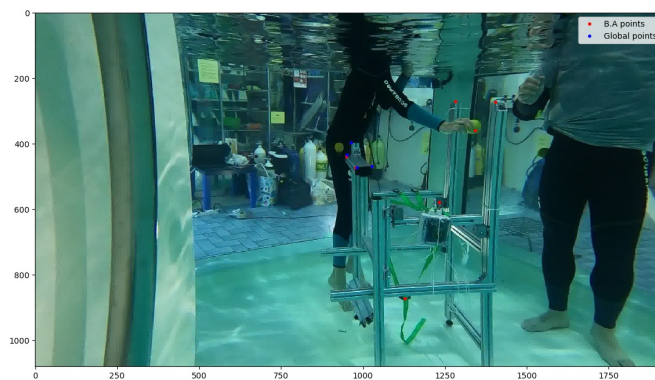


Figure 4.4: Global registration results. View cam 3.

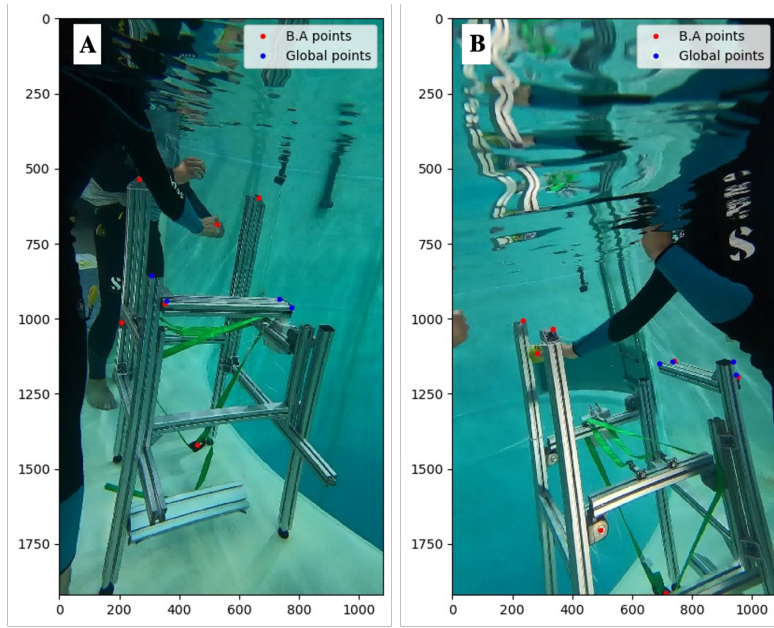


Figure 4.5: Global registration results. (A) View cam 1. (B) View cam 2.

If global points are located in preselected positions, corresponding to the three camera views, it means that calibration was successful and global registration will run correctly. The provided example shows a successful global registration.

Reprojection error results are presented in Table 4.1 and calibration errors (global registration) in Table 4.2.

Table 4.1: Bundle adjustment (BA) calibration errors

Field of computation	Camera 1	Camera 2	Camera 3
Bundle adjustment (1G) [pixel]	0.92	0.81	0.85
Bundle adjustment ($1/6G$) [pixel]	1.33	1.41	1.87

Table 4.2: Global registration errors

Field of computation	Mean error distance	Pair of view average error Mean (SD)
Global registration (1G) [cm]	1.31	0.41 (0.37)
Global registration ($1/6G$) [cm]	4.52	1.41 (1.87)

As can be seen from the data in the table the bundle adjustment error values do not exceed 5 pixels for all cameras, and the global registration reprojection error is less than 10 cm. Thus, these results are convenient for further steps.

4.2 Performance at the workplace

As seen in chapter 3, performance can be assimilated to the amount of work performed per unit of time. It includes elements such as productivity and error rates in a seated upright posture.

During data analysis with direct and indirect (proof of concept) methods a trend was found by which the torso of participants would tilt backward at the end of the tasks, while under 1G there is a tendency to tilt torso forward. The details of the indirect evaluation method are explained in Chapter 4.1 as this method was applied after the testing process of this method in workplace performance experiments. It is assumed that the moment of inertia did not greatly affect this deviation, since the largest operational load was 3 kg and the movement speed was relatively slow.

Figure 4.6 shows the results for torso inclination in degrees at the beginning and the end of repetitive tasks with 0.5 kg, 1 kg and 3 kg. The negative values means that torso tilts backward relative to the vertical, while positive values mean that the body tilts forward relative to the vertical.

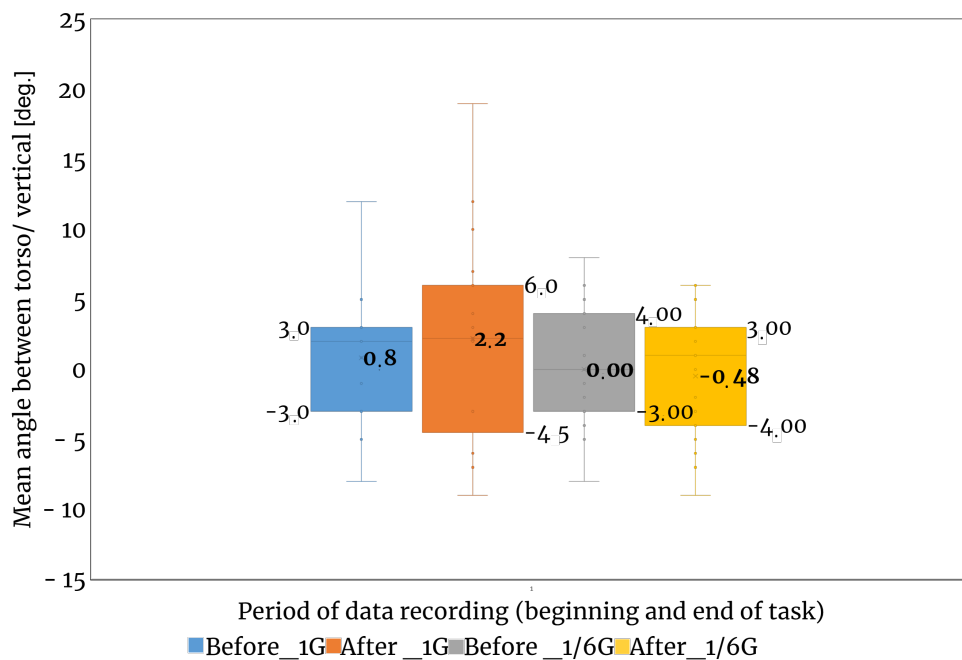


Figure 4.6: Body tilts angles results (negative value - tilt backward, positive value - tilt forward)

With observational methods, while defining the number errors for quantifiable tasks occurred during the task realization it was found that:

- Repetitive tasks (R) 1 error - 1G and 0 errors - $\frac{1}{6}$ G (Moon);

- Joystick (J) 2 errors - 1G and 0 errors $\frac{1}{6}$ G (Moon);
- Assembling (A) 4 errors - 1G and 1 error - $\frac{1}{6}$ G (Moon);

With subjective methods weighted workload values (see Figure 4.7) for all tasks were calculated and then each subjective demand was assessed separately.

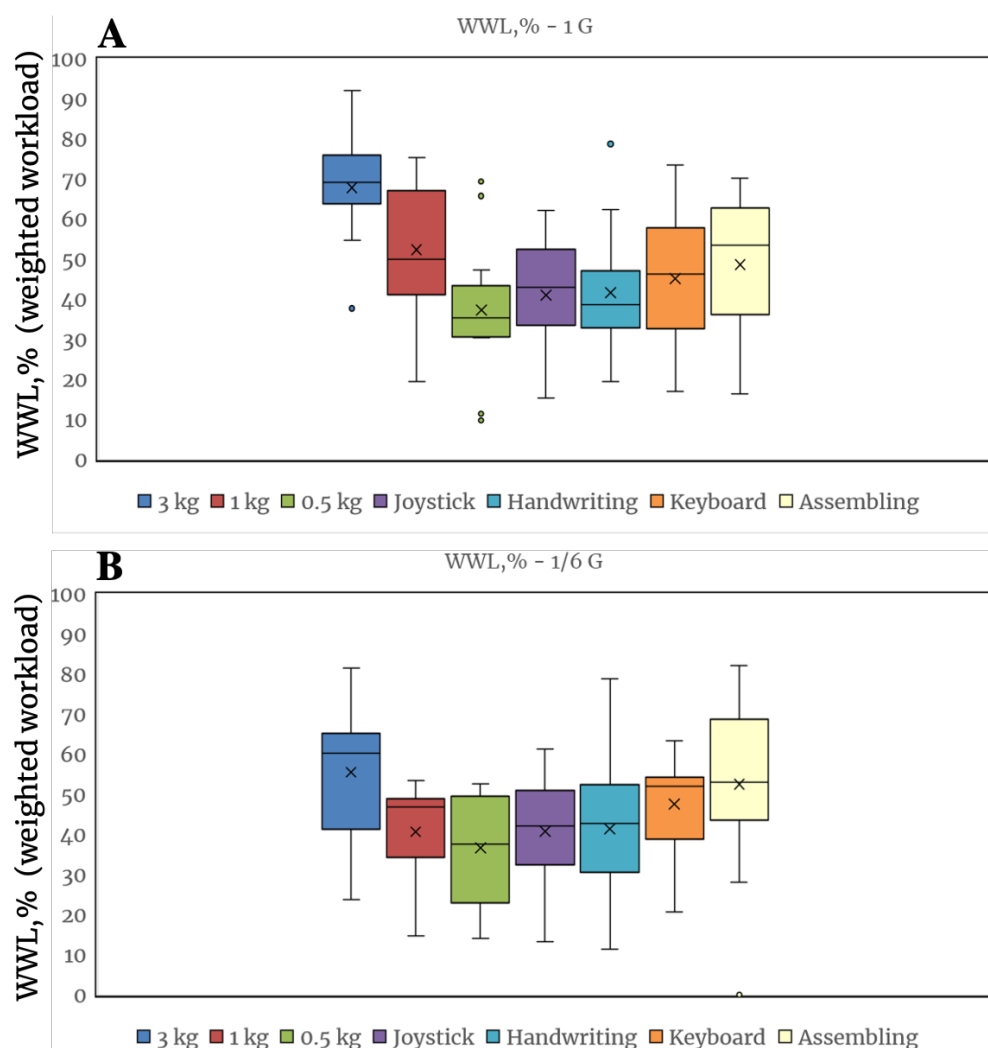


Figure 4.7: **(A)** WWL % for 1G. **(B)** WWL % for $\frac{1}{6}$ G. Tasks: work with keyboard (K), repetitive tasks (R) with 0.5 - 3 kg, tasks with joystick (J), task with text writing (W), task with assembling (A)

The descriptive statistics of females and males and mixed results for females/males are presented in Table 4.3 for 1G and $\frac{1}{6}$ G. From these tables it can be seen that the values of WWL, % are lower for $\frac{1}{6}$ G than for 1G for all tasks. In a separate study of the change in the WWL for males and females, it was noted that the WWL values are always higher in females for all

environments and for all tasks.

The results for PD, MD, Performance, EF, and FR are presented below (Table 4.3).

Table 4.3: Summary of NASA-TLX parameters for the tasks with keyboard (K), repetitive tasks (R) with 0.5 - 3 kg, tasks with joystick (J), task with text writing (W), task with assembling (A) for males and females. All values in table are means.

Task G-level	MD Mean	PD Mean	TD Mean	P Mean	EF Mean	FR Mean	WWL(%)
14 participants (males and females)							
R-1G (3 kg)	34.64	81.41	43.21	49.29	77.50	39.29	67.69
R-½G (3 kg)	28.57	61.42	41.07	40.00	59.29	28.57	55.43
R-1G (1 kg)	27.86	57.14	41.07	51.43	56.79	23.21	52.29
R-½G (1 kg)	26.07	34.64	35.00	46.43	33.93	15.00	40.64
R-1G (0.5 kg)	25.71	36.07	33.93	39.64	34.29	13.57	37.26
R-½G (0.5 kg)	21.79	22.86	34.29	43.57	26.79	13.21	36.57
J-1G	47.14	12.50	37.86	42.14	29.29	19.64	41.00
J-½G	46.07	14.64	37.86	43.21	31.43	23.93	40.74
W-1G	46.43	12.50	42.50	38.71	28.71	25.36	41.56
W-½G	43.93	14.64	35.00	41.43	35.71	22.86	41.40
K-1G	50.57	12.50	51.43	51.79	27.50	20.36	45.12
K-½G	53.57	14.64	43.21	48.21	35.00	33.57	47.50
A-1G	48.36	23.93	50.00	56.07	35.71	30.36	48.55
A-½G	45.36	29.29	53.21	59.29	49.29	42.14	52.48

Appendix Table A.11 shows the summary values for NASA-TLX survey for males and females separately. Below presented results of statistical analysis of all tasks. The impact of gravity level on the task related weighted workload was investigated. Shapiro-Wilk test was conducted to verify the normality of the data, see Appendix Table A.9. If the p value is greater than 0.05, this indicates a normal distribution of the data. The test showed that the data for all tasks are normally distributed. Table 4.4 - Table 4.6 show the results of statistical analysis of impact of gravity level change on WWL for all tasks for males and females separately.

Table 4.4: Statistical analysis of the repetitive tasks. F - females, M - Males.

	<i>Dependent variable:</i>					
	‘3_kg‘	‘1_kg‘	‘0.5_kg‘	‘3_kg‘	‘1_kg‘	‘0.5_kg‘
	(F)	(F)	(F)	(M)	(M)	(M)
‘G-level‘	69.24*** (17.24)	55.48*** (12.31)	36.86*** (11.58)	66.14*** (15.61)	49.10*** (12.55)	37.67*** (11.70)
Observations	14	14	14	14	14	14
R ²	0.55	0.61	0.44	0.58	0.54	0.44
Adjusted R ²	0.52	0.58	0.39	0.55	0.51	0.40
Residual Std. Error (df = 13)	45.61	32.58	30.65	41.30	33.21	30.96
F Statistic (df = 1; 13)	16.13***	20.30***	10.13***	17.96***	15.30***	10.36***

Note:

*p<0.1; **p<0.05; ***p<0.01

Table 4.5: Statistical analysis of the task with joystick and handwriting. F - females, M - Males.

	<i>Dependent variable:</i>			
	Joystick	Handwriting	Joystick	Handwriting
	(F)	(F)	(M)	(M)
‘G-level‘	44.43*** (13.86)	42.45*** (10.64)	37.57*** (10.56)	40.67** (15.16)
Observations	14	14	14	14
R ²	0.44	0.55	0.49	0.36
Adjusted R ²	0.40	0.52	0.45	0.31
Residual Std. Error (df = 13)	36.68	28.16	27.94	40.10
F Statistic (df = 1; 13)	10.27***	15.90***	12.66***	7.20**

Note:

*p<0.1; **p<0.05; ***p<0.01

Table 4.6: Statistical analysis of the tasks with keyboard and assembling. F - females, M - Males.

	<i>Dependent variable:</i>			
	Keyboard	Assembling	Keyboard	Assembling
	(F)	(F)	(M)	(M)
'G-level'	39.29** (14.19)	48.71*** (14.78)	50.95*** (14.26)	48.38** (17.53)
Observations	14	14	14	14
R ²	0.37	0.46	0.50	0.37
Adjusted R ²	0.32	0.41	0.46	0.32
Residual Std. Error (df = 13)	37.54	39.10	37.74	46.38
F Statistic (df = 1; 13)	7.67**	10.87***	12.76***	7.62**

Note:

*p<0.1; **p<0.05; ***p<0.01

A statistical analysis for all tasks showed that simulated HG significantly affects the performance of all participants for all listed above tasks. The results for the same tasks on the combined data for males and females are presented in Appendix Table A.12 and Table A.13.

4.3 Postural study

To investigate the joint profiles of participants (see Chapter 3, section 3.3), the markerless motion capture method was used. This method is based on the following steps: videos/frames synchronization, camera calibration, joint triangulation, joint angles and profile calculation.

The results of calculation of markerless motion capture errors was based on percentage of correct keypoints (PCK), mean absolute error (MAE) as well as mean joint position errors (MPJPE) for 2D skeleton recognition in 1G and simulated ½G in an underwater environment presented in a Table 4.7.

Table 4.7: Markerless motion capture errors

Error type	1G	½G
PCK	100	77
MPJPE [mm]	20.4	25.5
MAEx [mm]	4.3	9.1
MAEy [mm]	3.6	11.0

Note: PCK - percentage of correct keypoints, MAE - mean absolute error, MPJPE - mean joint position errors

4.3.1 Joint angles assessment

Studying the differences of joint angles in various conditions increases understanding of how the human body reacts under different loads in different environments. Shapiro-Wilk test was conducted to verify the normality of the data, see Appendix Table A.10. If the p value is greater than 0.05, this indicates a normal distribution of the data. The test showed that the data for all tasks are normally distributed.

Based on statistical analyzes, the effect of gravity level on the change in joint angles is not related to the task being performed, but to the gender of the experiment participant. The mean angles between spine and vertical and joint angles between upper arm and vertical under 1G and simulated HG for females and males separately are presented in Figure 4.9 and Figure 4.10 respectively.

All other results for females and males conducting dynamic and static tasks are presented in the Appendix Tables A.14 - A.23. The mean angles for spine inclination for 1G and HG are presented below (see Figure 4.8 and 4.9) for dynamic and static tasks for females and males respectively. The mean angles between upper arm and vertical for 1G and HG are presented on Figure 4.10 and 4.11 for dynamic and static tasks for females and males respectively.

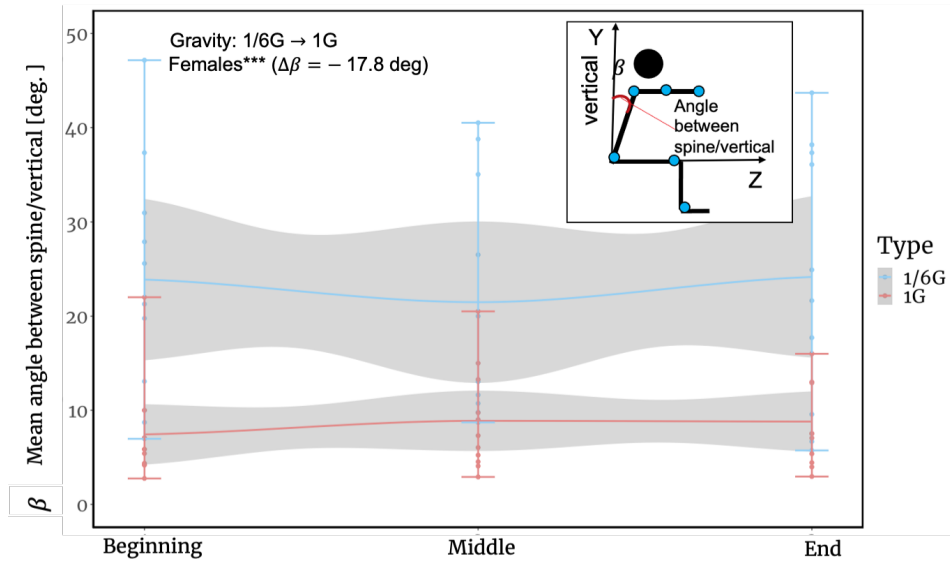


Figure 4.8: Mean angle between spine and vertical for static and dynamic tasks for females. Beginning, middle, end along the x-axis indicate the period of the experiment. CI, 95% - confidence interval.*** $p < 0.01$, ** $p < 0.05$, * $p < 0.10$.

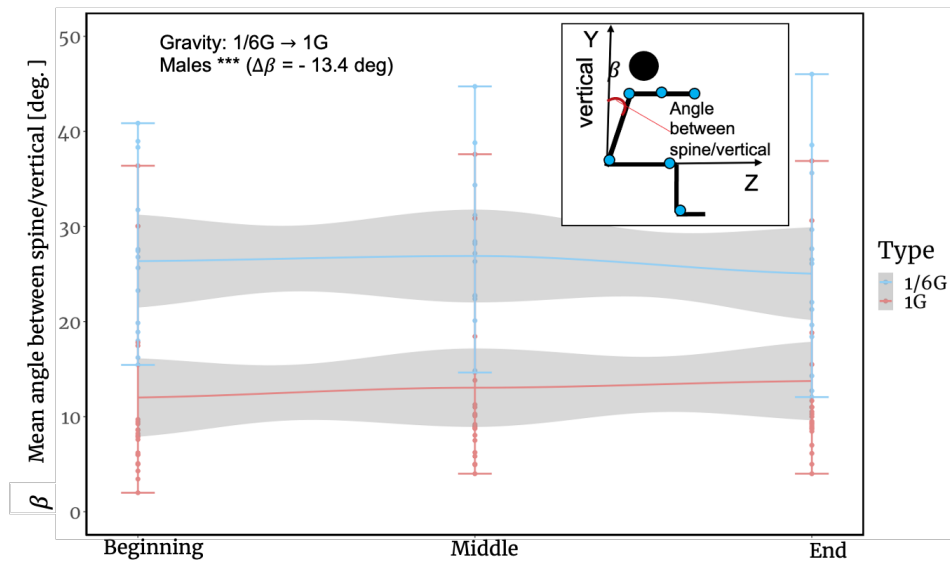


Figure 4.9: Mean angle between spine and vertical for static and dynamic tasks for males. Beginning, middle, end along the x-axis indicate the period of the experiment. CI, 95% - confidence interval.*** $p < 0.01$, ** $p < 0.05$, * $p < 0.10$.

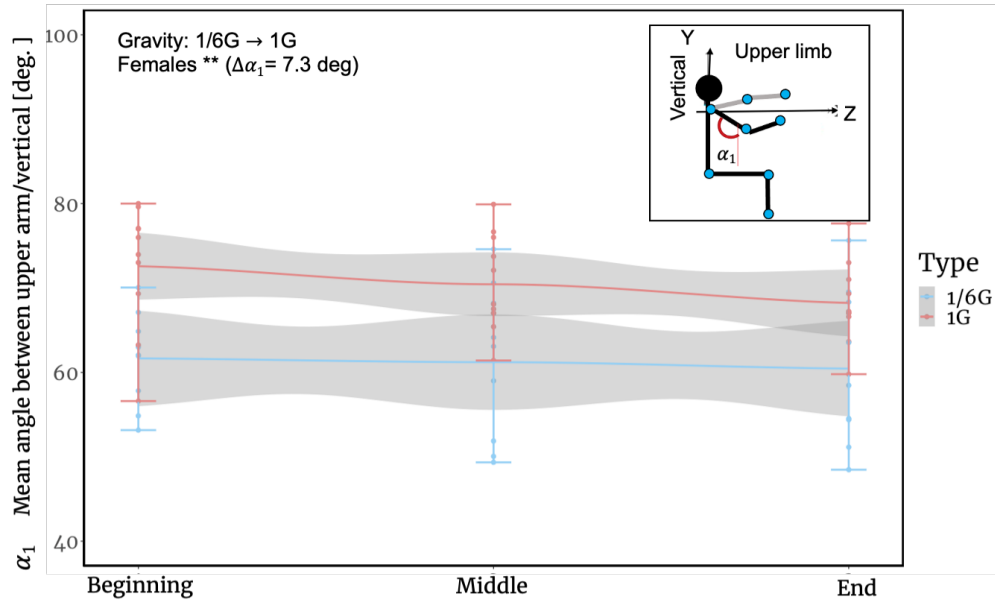


Figure 4.10: Mean angle between upper arm and vertical for static and dynamic tasks for females. Beginning, middle, end along the x-axis indicate the period of the experiment. CI, 95% - confidence interval. *** $p < 0.01$, ** $p < 0.05$, * $p < 0.10$.

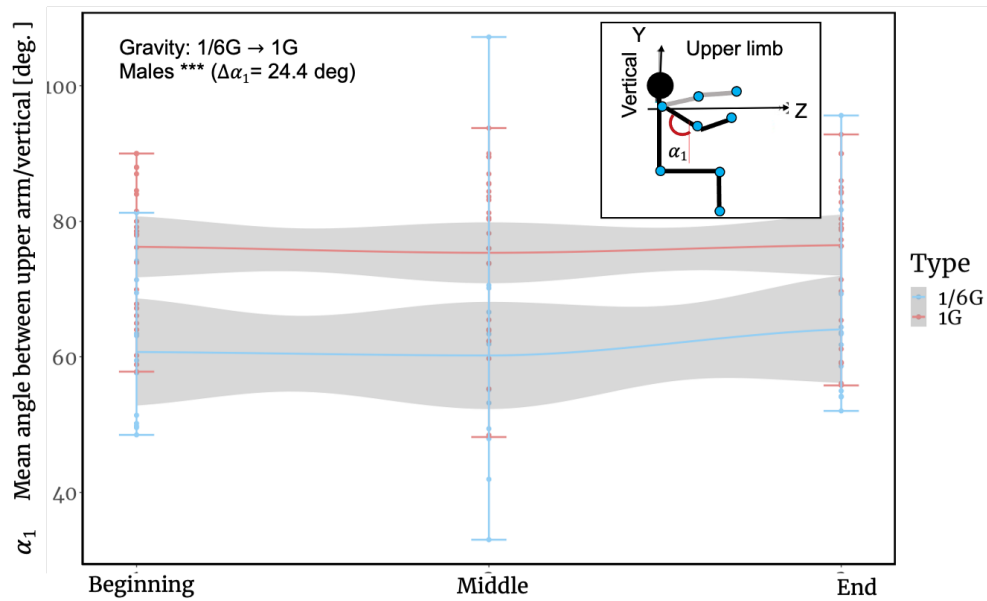


Figure 4.11: Mean angle between upper arm and vertical for static and dynamic tasks for males. Beginning, middle, end along the x-axis indicate the period of the experiment. CI, 95% - confidence interval. *** $p < 0.01$, ** $p < 0.05$, * $p < 0.10$.

From this analysis, a negative relation between backward body tilt and gravity level was found.

This provides new insights in understanding HG and proves useful for ergonomic analysis, especially for improving workplace design in HG environments.

4.3.2 Joint forces and torques assessment

The Tables below (see Table 4.8), show the results of joint forces and torques in the upper extremity (at the elbow and shoulder), for two different gravity levels 1G and $\frac{1}{6}$ G for 32 participants. It was found with recursive form of Lagrange motion equation. These results (mean and standard deviation) are presented for static tasks for males and females separately.

Table 4.8: Forces results projected in the vertical for shoulder and elbow for males and females for static task (S1). Torques results around horizontal axis for shoulder and elbow for males and females for static task (S1).

	Force shoulder [N]	Force elbow [N]	Torque shoulder [N·m]	Torque elbow [N·m]
S-1G (M)	56.22 (11.76)	29.82(10.28)	18.91 (8.18)	6.534 (2.79)
S-1G (F)	41.98(10.33)	26.52 (11.28)	14.92 (5.14)	5.11 (2.52)
S- $\frac{1}{6}$ G (M)	30.18(10.72)	25.91 (10.28)	9.03 (6.87)	5.07 (3.34)
S- $\frac{1}{6}$ G (F)	20.97(2.76)	10.61 (2.93)	2.347(1.44)	0.98(0.67)

Note: Results are Mean and standard deviation (SD). M - males, F - females. Prior to this experiment a simplified 2D assessment was conducted to give indications of potential effects.

Figure 4.12 shows the hip torque defined for static posture for 14 participants defined with D'Alembert's principle:

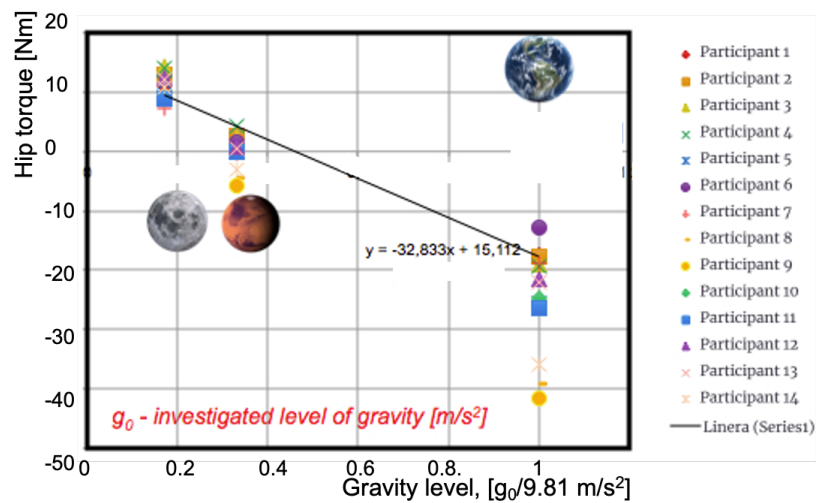


Figure 4.12: Hip torques values for different levels of gravity (Volkova et al., 2021). *Copyright International Astronautical federation (© 2021) From (Markerless motion capture method application for investigation of joint profiles in the workplace under simulated hypogravity) by (Volkova et.al.).*

The first data correlation for the Mars environment was numerically obtained on a small sample of six participants, while data for 1G and $\frac{1}{6}$ G were collected experimentally. Here more data will be needed under $\frac{1}{6}$ G (Mars) to confirm these curve fits.

It can be assumed that the positive and negative values of the torque are associated with the rotation of the participants' pelvis around horizontal axis with the participation of various muscles of the body. This can also be a good indicator of the direction of the participants' torso (thus, CoM) tilt. Using the magnitude of torques, it is possible to compare the load on these muscles under experimental conditions at HG and 1G. The experiment revealed a trend towards a linear relationship between particular joint (hip) torque and G level. As seen in the static hip torque estimation example, the body can lean forward or backward relative to the pelvis depending on the level of gravity.

4.3.3 Workload of the elbow/shoulder

The mean results for the workload of elbow and shoulder were calculated through the statistical method and the resulting torques values for elbow, shoulder and hip for 32 participants are presented. The summary results for all participants are shown in Table 4.9.

Table 4.9: Workload results for males and females. Results are mean and standard deviation (SD) in parentheses. M- males, F - females

	Workload shoulder [%]	Workload elbow [%]
S-1G (M)	0.46 (0.17)	0.19 (0.07)
S-1G (F)	0.48 (0.17)	0.19 (0.09)
S- $\frac{1}{6}$ G (M)	0.29 (0.21)	0.17 (0.12)
S- $\frac{1}{6}$ G (F)	0.11(0.08)	0.04 (0.03)

The above table show us the difference in the workload of shoulder and elbow of male and female for the simulated $\frac{1}{6}$ G, 1G gravity. A significant difference in the average workload values for a static task (4-5 times) can be observed.

4.3.4 CoM assessment

Figure 4.13 shows the 3D visualization skeleton generated in Matlab. All parts of the body are shown in the same figure. All results of the whole body CoM location are presented with respect to participants' hip joint (pelvic).

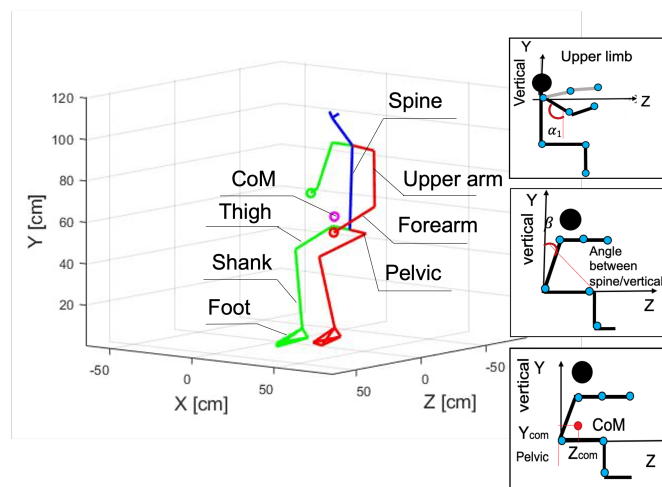


Figure 4.13: The whole body center of mass location and projection of assessed postures on YZ axis

The results for CoM mean values for Y and Z - axis for static and dynamic tasks for males and females reported separately, see Figures 4.14 - 4.17. All other results for females and males conducting dynamic and static tasks are presented in the Appendix Tables A.23 - A.26. The results of this analysis also showed that changing the environment from one to another significantly affects the change in the position of the CoM. As can be seen from the Figures 4.14 and Figure 4.16, the mean CoM/Pelvic Y - coordinate is shifted down by 5-7 cm under HG.

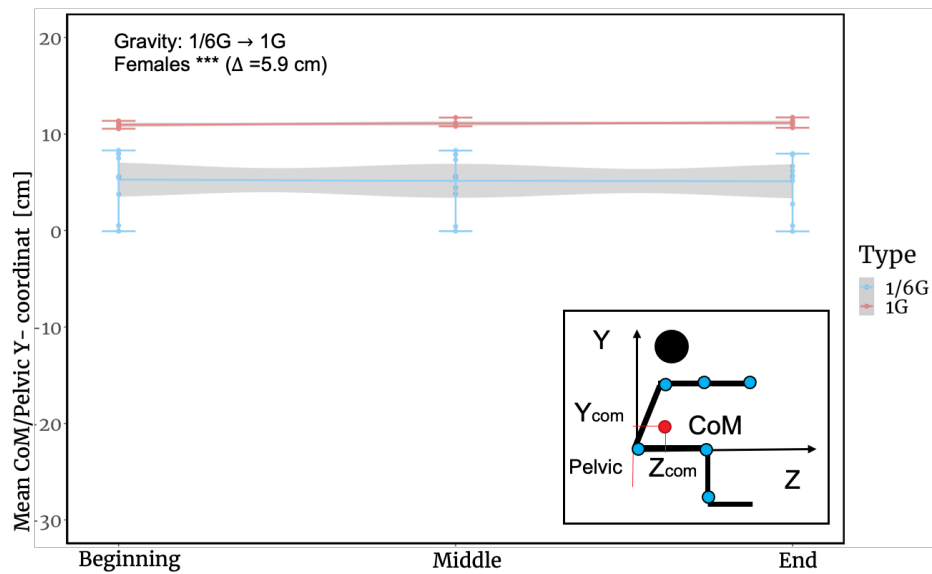


Figure 4.14: CoM mean values for Y axis for static tasks for females [cm]. Beginning, middle, end along the x-axis indicate the period of the experiment. CI, 95% - confidence interval. *** $p < 0.01$, ** $p < 0.05$, * $p < 0.10$.

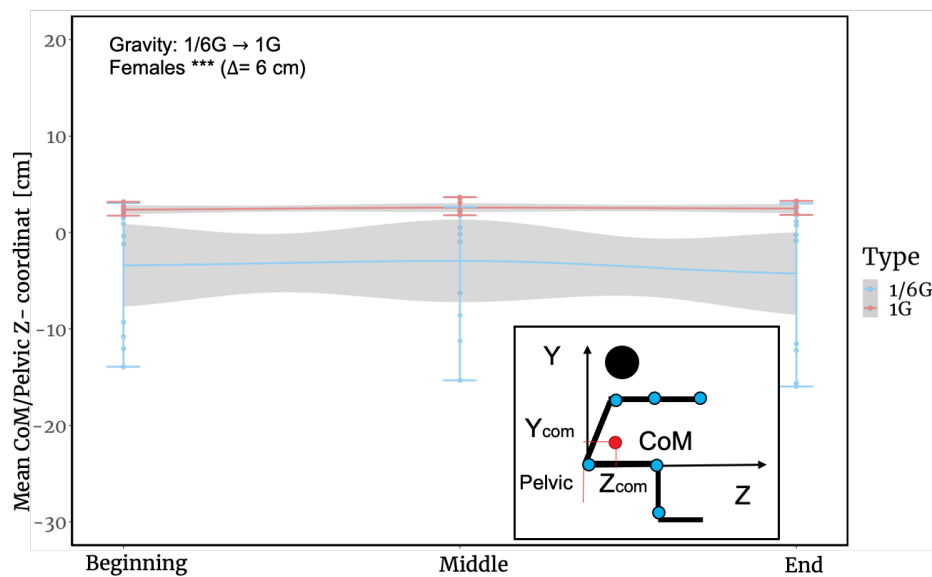


Figure 4.15: CoM mean values for Z axis for static tasks for females [H]. Beginning, middle, end along the x-axis indicate the period of the experiment. CI, 95% - confidence interval. *** $p < 0.01$, ** $p < 0.05$, * $p < 0.10$.

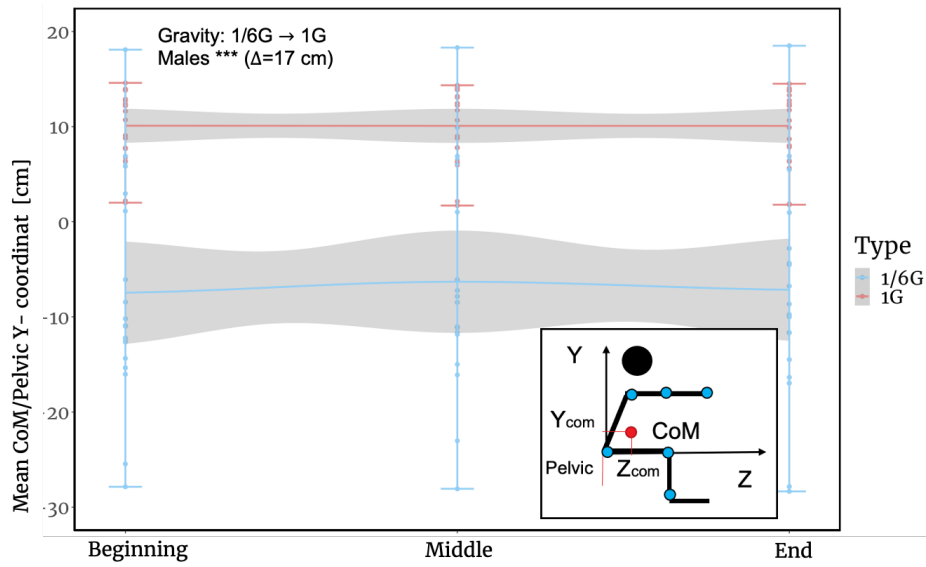


Figure 4.16: CoM mean values for Y - axis for static tasks for males [H]. Beginning, middle, end along the x-axis indicate the period of the experiment. CI, 95% - confidence interval. *** $p<0.01$, ** $p<0.05$, * $p<0.10$.

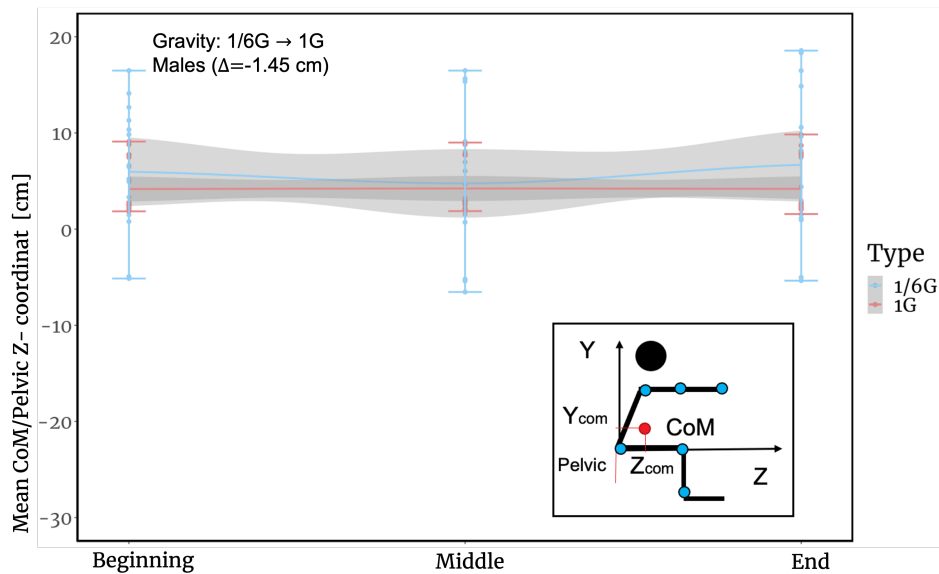


Figure 4.17: CoM mean values for Z - axis for static tasks for males [H]. Beginning, middle, end along the x-axis indicate the period of the experiment. CI, 95% - confidence interval. *** $p<0.01$, ** $p<0.05$, * $p<0.10$.

To calculate the total work and metabolic energy for lifting motions in the upper limbs with a 3kg load under simulated $\frac{1}{6}G$ and 1G, we need to know the following information: masses of all parts of the body, body segments trajectory, center of mass trajectory of the whole body,

speed of the motion, and isometric contraction force measured before and after motions. The trajectory of body segments as well as CoM of the body can be found with markerless motion capture. The modification applied to the calculation of various movement in the above case, originally intended by (Chappell and Klaus, 2013), follows the following assumptions:

- The external work is the change in the potential energy and kinetic energy of the CoM of the participant;
- The internal work is the change in the sum of the kinetic energy of a body segment (like an arm, for instance) relative to the CoM, and the rotational kinetic energy of the body rotating around the CoM.

Thus,

$$W_{int} = \sum (\Delta K \cdot E_{BS} + \Delta K \cdot E_{ROTCOM}) \quad (4.1)$$

W_{int} can be written as:

$$W_{int} = \frac{1}{2} \cdot m_{BS} \cdot v^2 + \frac{1}{2} \cdot m_{load} \cdot v^2 + \frac{1}{2} \cdot I_{BS} \cdot \omega^2 + \frac{1}{2} \cdot I_{load} \cdot \omega^2 \quad (4.2)$$

where $\frac{1}{2} \cdot m_{BS} \cdot v^2$ - Translational kinetic energy [J];

$\frac{1}{2} \cdot I \cdot \omega^2$ - Rotational kinetic energy [J];

v - speed of motion ([m/s];

I_{load} - moment of inertia of the operational load ([kg/m²];

I_{BS} - moment of inertia of the body part [kg/m²].

Equation for external work can be written as:

$$W_{ext} = \sum (\Delta K \cdot E_{com} + \Delta P \cdot E_{CoM}) \quad (4.3)$$

where

$$W_{ext} = \Delta(m \cdot g_{moon} \cdot h_{CoM} + \frac{(m_{BS} + m_{load}) \cdot v_{CoM}^2}{2}) \quad (4.4)$$

m_{BS} - Mass of the body segment (and operational load), [kg];

m_{load} - Mass of the body segment and external load, [kg];

v_{CoM} - Speed of center of mass of torso, [m/s];

h_{CoM} - Height of CoM above sitting part of the chair, [m];

g_{moon} - gravitational acceleration of the Moon, [m/s²].

Equation for internal work can be written as:

$$W_{tot} = W_{ext} + W_{int} \quad (4.5)$$

There is no significant difference between the upper limb inertia including ballasts required for the $\frac{1}{6}G$ simulation and without ballasts, so we can assume equivalent inertia values for the two environments.

$$m_{BS} = m_{fa} + m_{ua} + m_{tr} \quad (4.6)$$

where, m_{fa} - mass of forearm [kg];

m_{ua} - mass of upper arm [kg];

m_{tr} - mass of torso [kg];

m_h - mass of head [kg].

$$M_e = W_{tot} \cdot Efficiency + (F_{ISO} \cdot cost) \quad (4.7)$$

where KE_{com} - kinetic energy of the CoM of the participant, [J];

PE_{com} - potential energy of the CoM of the participant, [J];

W_{ext} - External work, [J];

W_{int} - Internal work, [J];

δK - change kinetic energy, [N];

KE_{BS} - change of the kinetic energy of a body segment, [J];

KE_{ROTCOM} - rotational kinetic energy of the body rotating around the CoM, [kg];

F_{ISO} - isometric muscle contraction, [N];

M_e - metabolic energy of human, [J];

Cost - cost of generating force from 0 to 1.

Efficiency - the coefficient of productivity of participant (subjective response can be considered).

It is assumed that the energy costs for the environment of the Moon will be higher due to the problem of stabilizing the body. But once a simple lifting motion is analyzed, the difference becomes less important. In this case, the same 0.5 force generation cost assumption can be applied to both environments.

4.4 Fatigue study

The details of the fatigue study described in peer-reviewed publication Volkova et al., 2022 devoted to "An empirical and subjective model of upper extremity fatigue under hypogravity" and a summary of the results are described in this sub-chapter. The aim of this study was to further broaden the current knowledge about upper extremity fatigue under HG. For 1G and $\frac{1}{6}$ G, empirical models of Endurance time- Task intensity were built for four different tasks : (S1), (S2), (D) and (R). The results described below confirm the hypothesis of an increase in the productivity of participants expressed by the endurance time (min) and a decrease in weighted workload under HG compared with 1G.

Fatigue curves for 1G, $\frac{1}{6}$ G

The power model has superior over exponential fit; this is the case for all data, for each task and for specific environments due to slightly greater R^2 (see Figures 4.18). Thus, power models were used for 1G and $\frac{1}{6}$ G comparisons. The constants b_0 , b_1 and R^2 values of power trendline equation for all models are provided in Table 4.10. According to the results, coefficients b_0 , vary greatly, while coefficients b_1 have quite similar values for 1G and $\frac{1}{6}$ G for males and females. The average values of the coefficient $b_1=0.86$ for males and $b_1=1.11$ for females for 1G, while the average values of $b_1=1.50$ for males and $b_1=1.61$ for females for $\frac{1}{6}$ G.

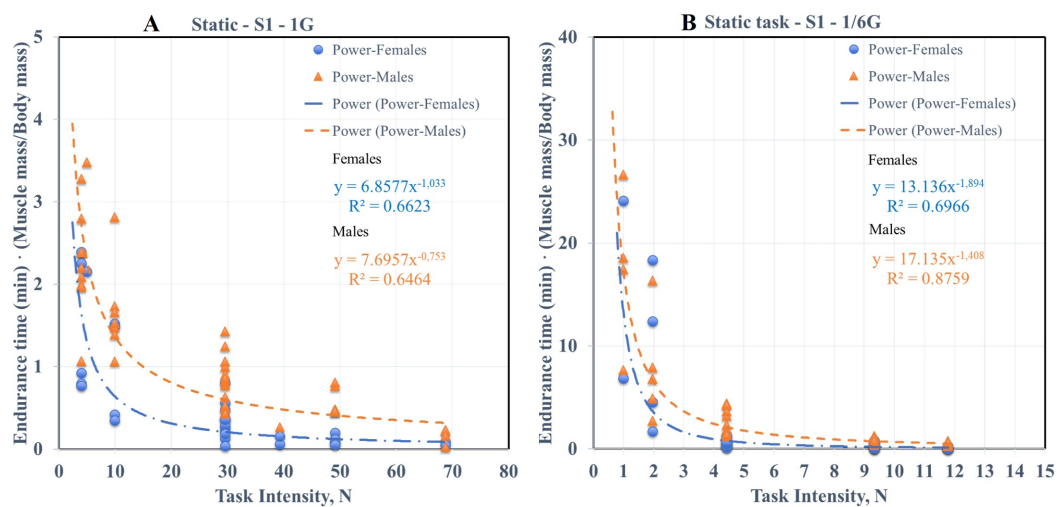
All models for all tasks have the average value $R^2=0.63$ for males and average value $R^2=0.62$ for females for 1G and average $R^2=0.77$ for males, average value $R^2=0.70$ for females conducting the tasks under $\frac{1}{6}$ G. The lower values of R^2 for 1G are most likely due to the fact that a smaller number of participants could work with loads of 5 and 7 kg. For example, 80% of females were unable to work with 5-7 kg load under 1G.

Consistent with all curves, ET (min) increased for simulated lunar gravity in comparison with 1G, see Table 4.10. The average ET (min) for 1 kg, 3 kg and 5 kg for all types of tasks was found to identify the growth rate. For a static task (S1) with a load of 1 kg, the ET of males increased 4.62 times and 6.53 times for females for $\frac{1}{6}$ G compared to 1G. For the same task with a load of 3 kg, the ET of males increased 3.11 times and 1.91 for females for $\frac{1}{6}$ G compared to 1G. And for a load of 5 kg, the ET of males increased 1.64 times and 2.14 for females for $\frac{1}{6}$ G compared to 1G. As can be seen from the given example, with increasing load, the ratio between ET (min) under $\frac{1}{6}$ G and 1G decreases ET values may have increased slightly for all tasks performed in water, as in water the weight of the operational loads have not been compensated to obtain a weight corresponding to the Moon or Martian gravity. The effect of inertia in water (lunar gravity simulation) and without water was almost the same. But by reducing the operational load weight due to the Archimedes force, it reduced the effect of inertia in the water.

Table 4.10: Power ($ET = b_o \cdot (\text{Task Intensity})^{b_1}$) model coefficients for Males (M)/Females (F)

Power Model	b_o	b_1	R^2	mn ET (min) load (1kg)	mn ET (min) load(3kg)	mn ET (min) load(5kg)
22 participants						
S1-1G	7.70/6.86	-0.75/-1.03	0.65 / 0.66	1.67/0.95	0.85/0.34	0.39/0.14
S1-1/6G	17.13/13.14	-1.40/-1.89	0.87/0.70	7.73/6.21	2.65/0.65	0.64/0.30
25 participants						
D-1G	8.72/7.79	-0.85/-1.02	0.62/0.69	1.30/0.80	0.79/0.35	0.28/0.08
D-1/6G	21.47/6.52	-1.50/-1.36	0.79/0.72	14.93/9.34	2.16/0.82	0.77/0.34
26 participants						
R-1G	26.10/38.65	-0.87/-1.34	0.61/0.56	6.39/2.54	1.93/0.72	0.75/0.21
R-1/6G	18.49/13.92	-1.30/-1.46	0.70/0.62	9.80/5.31	4.43/2.84	1.06/0.49
27 participants						
S2-1G	38.77/14.93	-0.98/-1.07	0.66/0.56	2.43/0.65	0.80/0.69	0.80/0.16
S2-1/6G	37.22/11.80	-1.81/-1.72	0.74/0.79	15.72/6.63	2.38/0.94	0.82/0.29
6 participants (M/F)						
S1-1G	1.56	-1.19	0.77	1.43	0.56	0.22
S1-1/6G	2.71	-1.32	0.72	2.62	0.77	0.32
S1-1/3G	7.89	-1.55	0.84	10.34	1.29	0.60
D-1G	1.57	-1.03	0.56	1.70	0.62	0.32
D-1/3G	3.38	-1.34	0.80	3.70	0.92	0.37
D-1/6G	5.49	-1.27	0.77	6.57	1.60	0.68
R-1G	5.25	-1.85	0.57	3.15	0.89	0.33
R-1/3G	6.64	-1.37	0.60	6.24	1.39	1.08
R-1/6G	10.20	-1.38	0.71	9.69	2.06	1.00
S2-1G	2.51	-0.94	0.52	4.26	1.20	0.51
S2-1/3G	6.12	-1.46	0.82	6.36	1.28	0.55
S2-1/6G	7.66	-1.47	0.85	9.55	1.37	0.69

Note: Task intensity is between 0.4-9 (kg) or 0.65-11.37 (N) (1/6G), 3.92-68.67 N (1G) , ET is in minutes. Volkova, 2022. Creative Commons license



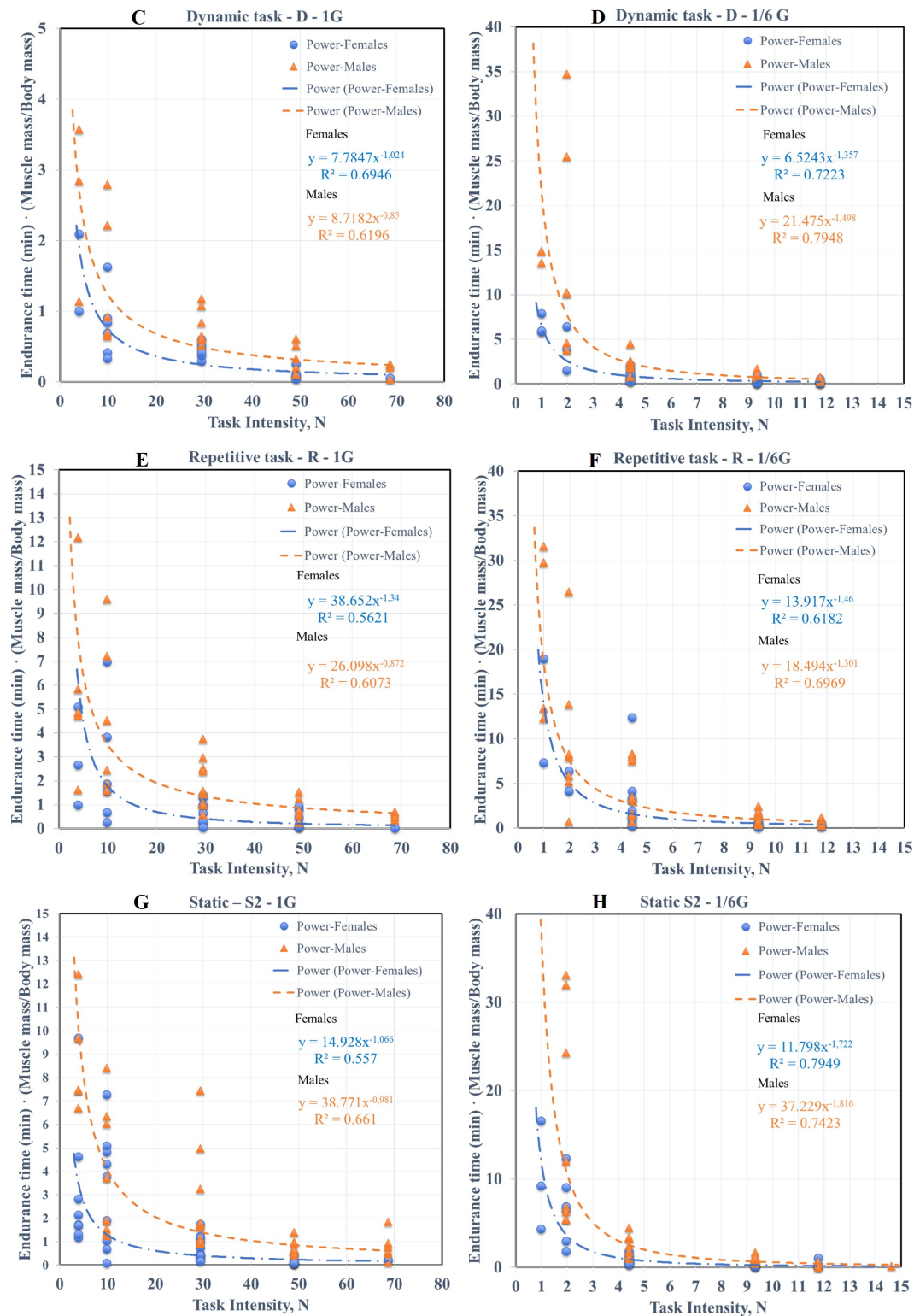


Figure 4.18: The ET power models (N = 520 studies, 6 task intensities, (A) - static task (S1) - 1G, (B) - static task (S1) 1/6G, (C) - dynamic task (SD) - 1G, (D) - dynamic task (D) - 1/6G, (E) - repetitive task (R) - 1G, (F) - repetitive task (R) - 1/6G, (G) - static task (S2) - 1G, (H) - static task (S2) - 1/6G. Volkova, 2022. Creative Commons license

Hand and BLC muscle contraction Table 4.11 shows the average values for all task intensities from 0.4 kg to 7 kg for hand (H) and back-leg-chest (BLC) strength measured for each participant before and after each task in an appropriate environment, 1G, $\frac{1}{3}$ G and $\frac{1}{6}$ G.

Table 4.11: (Hand BLC strength values of participants 1G, $\frac{1}{3}$ G, $\frac{1}{6}$ G for males/females.

G - level Task	H(Before) Mean (SD)	H (After) Mean (SD)	Δ (%) H	BLC (Before) Mean (SD)	BLC (After) Mean (SD)	Δ (%) BLC
22 participants						
S1-1G	48.84 /24.95 (2.92)/(1.82)	48.95/24.66 (2.05)/(2.09)	0.21/-1.21	7.81 /2.83 (0.83)/(0.16)	7.89 /2.43 (0.82)/(0.22)	0.99/-16.12
S1- $\frac{1}{6}$ G	47.30/26.28 (1.12)/(3.53)	45.86/24.82 (1.46)/(2.78)	-4.95/-4.91	NA	NA	NA
25 participants						
D-1G	46.02/22.15 (7.57)/(1.09)	45.49/20.84 (5.73)/(1.50)	-1.17/-6.29	8.03/2.55 (1.34)/(0.25)	8.01/2.18 (1.36)/(0.41)	-0.19/-16.41
D- $\frac{1}{6}$ G -	46.37/24.46 (2.61)/(5.10)	44.96/24.91 (1.13)/(5.10)	1.83/-3.14	NA	NA	NA
26 participants						
R-1G	48.47/23.79 (4.18)/(3.41)	47.41/22.65 (3.65)/(2.33)	-2.23/-5.04	8.57/2.88 (0.86)/(0.51)	8.13/2.65 (0.88)/(0.59)	-5.47/-8.87
R- $\frac{1}{6}$ G	44.00/22.96 (5.44)/(3.02)	43.75/22.15 (5.22)/(2.85)	-0.58/-3.64	NA	NA	NA
27 participants						
S2-1G	44.56/20.52 (3.52)/(1.21)	42.49/19.48 (2.39)/(0.71)	-4.87/-5.37	13.46/5.15 (1.22)/(1.49)	12.73/4.75 (1.61)/(1.36)	-5.73/-8.49
S2- $\frac{1}{6}$ G	43.27/22.03 (2.84)/(2.05)	41.70/20.67 (1.48)/(2.24)	-3.77/-6.61	NA	NA	NA
6 participants						
S1-1G	53.05/26.05	49.12/25.94	-8.00/-0.41	NA	NA	NA
S1- $\frac{1}{3}$ G	51.02/23.09	49.02/21.88	-4.09/-5.55	NA	NA	NA
D-1G	47.85/26.57	47.81/26.55	-0.08/-0.08	NA	NA	NA
D- $\frac{1}{3}$ G	51.04/25.07	49.55/24.51	-3.02/-2.29	NA	NA	NA
R-1G	51.22/27.42	46.93/24.50	-9.13/-11.91	NA	NA	NA
R- $\frac{1}{3}$ G	48.76/25.57	46.65/24.89	-4.53/-2.76	NA	NA	NA
S2-1G	46.76/24.76	42.63/22.29	-9.68/-11.10	NA	NA	NA
S2- $\frac{1}{3}$ G	48.75/23.42	47.15/22.89	-3.39/-2.33	NA	NA	NA

Note: Tasks: S1 -outstretched arm, S2- holding weights in an arm bent at the elbow, D - dynamic, R- repetitive. Task intensity equal to 0.4 - 9 kg. H- hand, BLC - back-leg-chest. All values are presented as mean and standard deviation (SD). NA - the values that could not be measured for logistic reasons of the experiment. Volkova, 2022. Creative Commons license

The percentage change in values after each task is calculated for hand and BLC muscle contraction to compare the results.

NASA-Task Load Index for 1G, $\frac{1}{2}$ G

To investigate the mental workload of participants in 1G and $\frac{1}{2}$ G, weighted workload (WWL) in %, as well as average values of MD, PD, TD, P, EF, FR are calculated with NASA-TLX, see Table 4.12. In this table one example of a study of the effect of 3 kg load on participants' mental workload was given. The results of the subjective questionnaire, taking into account the responses collected in the $\frac{1}{2}$ G simulation with 6 participants, are included.

In this study, it was found that all average values of WWL,% are lower for all type of tasks for males and females for simulated $\frac{1}{2}$ G compared to the data obtained under 1G. A 12% decrease was found in average value of WWL,% for static task (S1), 33% for dynamic task (D), 15% for repetitive task (R) and 23% for static task (S2) for males under $\frac{1}{2}$ G versus 1G. The average WWL,% values decreased for static task (S1) by 8%, for dynamic task (D) the values remained the same, for the repetitive task (R) the values increased by 4 % and for static task (S2) they increased by 12% for females in $\frac{1}{2}$ G compared to 1G. Correlation between the results remain to be investigated.

It is also important to investigate the impact of the different demands of weighted workload. In accordance with all presented data, physical demand (PD) and effort (EF) have the highest values for males and females.

The results of the weighted workload (WWL) and all 6 parameters included in the WWL for the three gravity levels are presented graphically in Figure A.9 in the Appendix.

The inertia of the operational load of more than 3 kg could affect the exponentially WWL. But more data was collected with participants who worked with loads equal or less than 3 kg. And most likely, the type of task influenced the WWL, since, for example, a static task with an outstretched hand and a dynamic task are considered the most physically-intensive. While the repetitive task with pauses allowed for periodic recovery during the task and thus the effort demand and physical demand were less and overall the final score WWL was less than for the static task.

Table 4.12: Summary of the calculated NASA-TLX parameters, Males (M)/Females (F)

Task G-level	MD mean	PD mean	TD mean	P mean	EF mean	FR mean	WWL(%)
22 participants							
S1-1G (M)	40.72	275.54	71.09	118.63	232.91	56.45	53.02
S1-1G (F)	49.77	264.69	102.92	101.08	252.61	49.08	54.67
S1-½G (M)	42.70	198.10	94.50	163.90	181.30	10.4	46.6
S1-½G (F)	75.00	226.67	145.78	120.67	179.44	8.11	50.37
25 participants							
D-1G (M)	47.00	279.60	30.10	148.50	286.00	87.10	58.55
D-1G (F)	35.20	303.80	64.90	105.70	204.60	14.30	48.57
D-½G (M)	73.00	187.90	82.00	108.90	134.60	0.40	39.12
D-½G (F)	12.25	231.25	107.75	143.75	214.50	21.50	48.73
26 participants							
R-1G (M)	115.00	190.22	132.11	130.89	197.89	9.89	51.73
R-1G (F)	48.09	285.09	75.45	92.73	194.45	44.64	49.36
R-½G (M)	92.50	167.00	106.50	126.00	158.50	6.00	43.77
R-½G (F)	54.30	215.80	142.10	135.80	184.20	39.40	51.44
27 participants							
S2-1G (M)	58.08	247.46	88.69	119.46	165.54	48.38	48.51
S2-1G (F)	58.92	318.58	125.58	118.42	272.75	12.92	60.48
S2-½G (M)	57.89	184.89	66.67	91.33	181.44	13.56	39.72
S2-½G (F)	59.64	269.64	127.00	151.00	211.36	11.64	55.35
6 participants							
S1-½G (M,F)	40.92	129.92	121.25	72.50	115.42	26.00	33.73
S1-1/3G (M,F)	31.36	150.90	89.09	147.27	142.27	40.90	40.12
S1-1G (M,F)	21.91	278.73	54.64	111.73	149.45	16.91	42.22
D-13G (M,F)	61.25	114.17	53.75	90.42	143.33	38.42	33.42
R-13G (M,F)	44.09	118.18	75.45	105.45	146.82	51.82	36.12
S2-13G (M,F)	49.50	97.00	68.50	74.50	130.00	40.80	30.69

Note: All values in table are means. The results for 6 participants are calculated only for the loads 0.5 kg, 1 kg, 3 kg, 5 kg, 7 kg for males and females). Volkova, 2022. Creative Commons license

Comparison 1G, ½G, ⅓G

Due to the low number of participants (3 males and 3 females), only a small amount of data was available to carry out a comparative analysis of the effect of gravity on participant's fatigue in ⅓G doing static, dynamic and repetitive tasks. Figure 4.19 (A) shows an example of the fatigue curves for 1G, ½G and ⅓G, where the fatigue curve for simulated lunar gravity is located above the curve for Martian gravity and Earth gravity. Only one power trend curve was built

due to this limited data, and the intensity of the task from 1 kg to 7 kg was taken into account. The values of b_0 , b_1 , R^2 mean muscle mass ET ratio of muscle mass [kg] and body mass [kg] of the participant for kg load, 3 kg and combined 5 and 7 kg loads for all types of tasks are presented in Table 4.10.

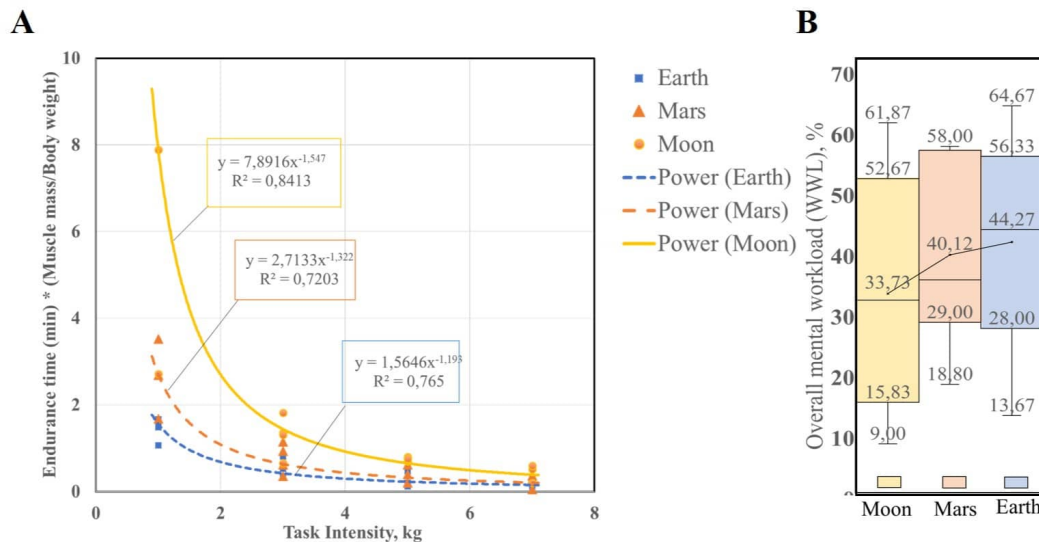


Figure 4.19: **(A)** Endurance time - gravity level dependence for static tasks for Earth, simulated Moon and Mars gravity levels. Task Intensity in kg. **(B)** Weighted workload (WWL, %) (example for static task (S1)), for males and females for loads (1 kg, 3 kg, 5 kg, 7 kg) - gravity level dependence. Volkova, 2022. Creative Commons license

The ratio was found between the mean ET (min) values for 1kg, 3 kg and 5-7 kg loads, normalized to the participants' ratio of muscle mass (kg) and body weight (kg) for $\frac{1}{6}G$ and $1G$, and then for $\frac{1}{3}G$ and $\frac{1}{6}G$. For static tasks (S1), the ratio between ET (min) for $\frac{1}{6}G$ and $1G$ is 4.10, and the ratio between ET(min) for $\frac{1}{3}G$ and $1G$ is 1.60. For dynamic tasks (D) the ratio between ET(min) for $\frac{1}{6}G$ and $1G$ is 2.87, and the ratio between ET (min) for $\frac{1}{3}G$ and $1G$ is 1.25. For repetitive tasks (R), the ratio between ET(min) for $\frac{1}{6}G$ and $1G$ is 2.82, and the ratio between ET(min) for $\frac{1}{3}G$ and $1G$ is 2.30.

To more fully understand this phenomenon, a NASA-TLX survey was conducted upon participant task completion. Figure 4.19 (B) shows the Box-and-whisker plots with outliers for Earth, simulated lunar and Martian gravity. For static tasks one can observe the normal distribution for $\frac{1}{6}G$, $\frac{1}{3}G$ and $1G$. According to the respective median values for each environment and each box plot it can be concluded that there is little difference between the three groups of data, but that a tendency for the workload to increase with increasing gravity is nonetheless evident. To investigate the level of significance of the dependence between ET (min) and WWL, % and muscle contraction from the gravity level ($1G$, $\frac{1}{3}G$ and $\frac{1}{6}G$), as well as the character of this dependence, statistical analysis by means of a least square regression was conducted.

Table 4.13 shows the ET (min) and WWL,% predictors for Static (S1) and dynamic (D), repetitive (R) and static (S2) tasks under 1G, $\frac{1}{3}$ G and $\frac{1}{6}$ G for males and females. A significantly positive relation between ET (min) and gravity level with a negative coefficient of correlation is observed for all tasks except repetitive one and moderate (for static (S1) task) and significantly positive relation (for (S2) and (D) tasks) between WWL, % with a positive coefficient of correlation. A moderation relation between hand muscle contraction force and gravity level was found only for static tasks.

Table 4.13: The ET (min) and WWL% predictors of different types of tasks under 1G, $\frac{1}{3}$ G, $\frac{1}{6}$ G, Males (M)/Females (F).

Task G-level	ET (min)	WWL%	(H) before (kg)	(H) after (kg)
		n = 131		
S1 (M/F)	-0.25 (0.08)**	0.03 (0.02)*	-0.22 (0.12)*	0.24 (0.13)**
		n=102		
D (M/F)	-0.33 (0.11)**	0.04 (0.02)**	-0.09 (0.11)	0.08 (0.12)
		n=115		
R (M/F)	-0.08 (0.06)	0.00 (0.02)	-0.14 (0.14)	0.01 (0.15)
		n=237		
S2 (M/F)	-0.09 (0.05)**	0.00 (0.01)**	0.03 (0.09)	-0.01 (0.09)

Note: *** $p < 0.001$, ** $p < 0.05$, * $p < 0.10$. Robust standard errors in parentheses. All models were estimated with least square regression.

4.5 Pushing and pulling study

The anthropometric data of males and females differed due to differences in physiology. These differences apparently influenced the strength developed by the participants during the experiment. In general, the pulling force was higher than the pushing force, with the males demonstrating greater strength. In simulated lunar gravity, restraint participants in the level of hips and feet demonstrated less force than on Earth. This is likely due to the friction reduction effect that occurs when participants perform underwater tasks. The stronger the pull down, the stronger the body sticks to the seat and the friction is higher.

Table 4.14 and Table 4.15 presents the mean value, maximum and minimum standard deviation and p-value of anthropometric parameters for both groups. It was noted that all parameters differed between males and females. This means that the anthropometric measures could influence the strength developed by both groups of participants during the experiments.

As can be seen from Figure 4.20 (A) and 4.20 (B) and Table 4.14-4.15, the strength developed by male were slightly higher than that of females. The average pull force in both groups was higher than the push force. In terms of seated push force, males showed a similar trend in

strength reduction after 30 seconds of force application.

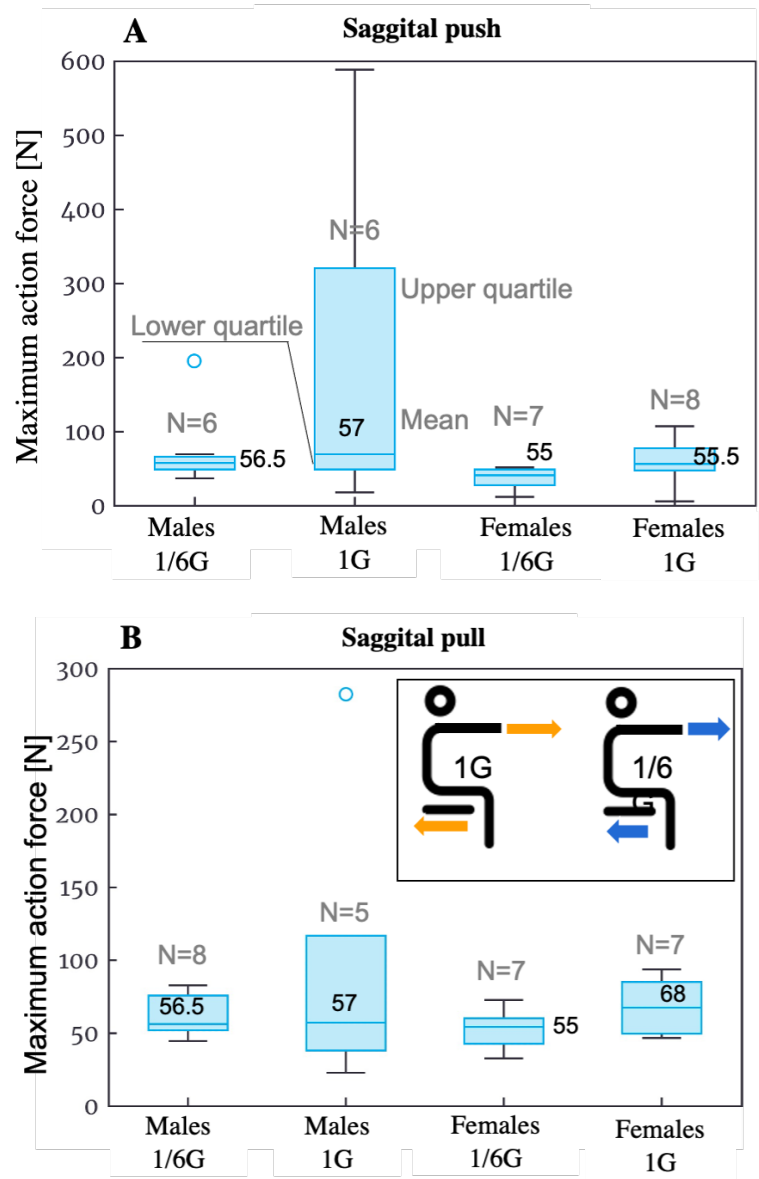


Figure 4.20: (A) Pushing force data box plot for 1G and 1/6G (B) Pulling force data box plot for 1G and 1/6G

Table 4.14: Maximum action pulling force descriptive statistics

	Male - 1/6 G	Male - 1G	Female - 1/6G	Female - 1G
Nbr participants	8	5	7	7
Median [N]	56.5	57	55	68
Mean/Max [N]	52.5 /76.5	38 /117.2	43.25 /60.0	50 /85.5

Table 4.15: Maximum action pushing force descriptive statistics

	Male - ½G	Male - 1G	Female - ½G	Female - 1G
Nbr participants	6	6	7	8
Median [N]	57	69.5	42	55.5
Min/Max [N]	49.0/6.0	49.0 / 321.0	27.0 / 46.5	48.0 / 77.5

4.6 Seated discomfort study

The results of the seated discomfort study are shown in Figure 4.21 below. These results are grouped according to the tested environment as well as design chair configuration 1 (nine participants), 2 (eight participants), and 3 (eight participants).

4.6.1 Average of all body parts

For an initial analysis, it was decided to average the comfort scores for all body parts into a single composite scalar score. A mixed-design ANOVA was used with the self-report time (before, after) as the within-subjects measure and task type (D), (R), (S) as the between-subjects measure, see figure 4.21.

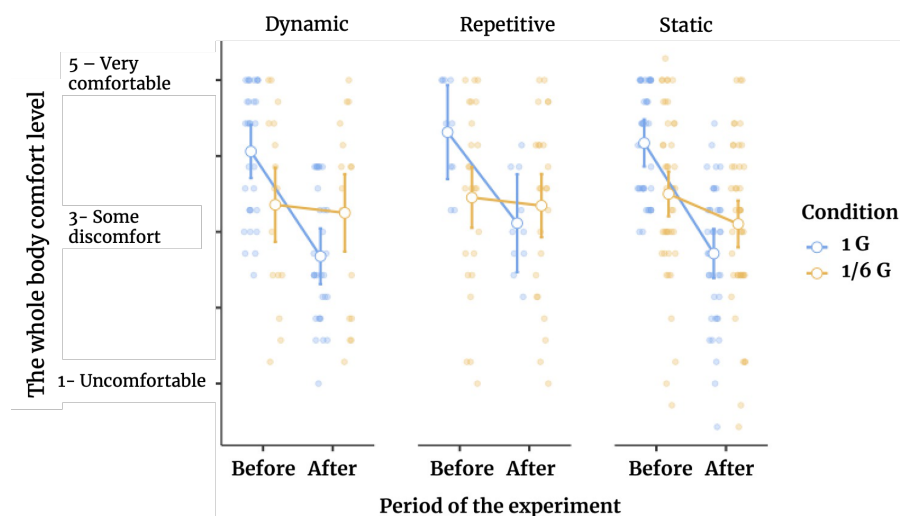


Figure 4.21: Overall body comfort under 1 G and ½G for dynamic (D), repetitive (R) and static (S) tasks for males and females. **Before** and **After** mean that the survey was conducted before/after the participant started/finished the task respectively

Each task was considered independent, even if coming from the same subject due to an unreliable number of repetitions (this is a limitation). It can be seen from Figure 4.21 that there is an accentuated decrease in comfort for all tasks (D), (R), and (S) when they are done

under 1G in comparison with $\frac{1}{6}$ G. The same does not occur when tasks are done under simulated HG in water, even though water might be more uncomfortable in the beginning.

These different changes with time are supported by a significant interaction between time and condition, see Table 4.16.

Table 4.16: Time and conditions factors impact on participants' body comfort

Within Subjects Effects						
	Sum of Squares	df	Mean square	F	p	η_p^2
Time	9.5119	1	9.5119	111.844	<0.001	0.413
Time \times Condition	5.1732	1	5.1732	60.827	<0.001	0.277
Time \times Task_type	0.2458	2	0.1229	1.445	0.239	0.018
Time \times Condition \times Task_type	0.0414	2	0.0207	0.244	0.784	0.003
Residual	13.5225	159	0.0859			

Note: df - degrees of freedom, F- variance ratio, p-value, η_p^2 - partial Eta squared (proportion of variance accounted by some effect)

A post-hoc analysis shows that the effect of time (i.e., the decrease) is indeed only significant for the land condition. (Tables 4.16 - 4.17 are with only the data from the land condition; p-values not corrected for 2 comparisons)

Table 4.17: A post-hoc analysis: Time and conditions factors impact on participant' body comfort

Within Subjects Effects						
	Sum of Squares	df	Mean square	F	p	η_p^2
Time	12.97	1	12.97	172.32	<0.001	0.68
Time \times Task_type	0.06748	2	0.033	0.448	0.641	0.011
Residual	5.87	78	0.07			

Note: df - degrees of freedom, F- variance ratio, p-value, η_p^2 - partial Eta squared (proportion of variance accounted by some effect)

The effect of time is not significant (barely, $p=0.052$) when we examine the water condition, see Table 4.18.

Table 4.18: The effect of time factor study of the participant' comfort

Within Subjects Effects						
	Sum of Squares	df	Mean square	F	p	η_p^2
Time	0.36	1	0.36	3.89	0.052	0.46
Time \times Task_type	0.22	2	0.10	1.16	0.31	0.028
Residual	7.65	81	0.09			

Note: df - degrees of freedom, F- variance ratio, p-value, η_p^2 - partial Eta squared (proportion of variance accounted by some effect)

The differences between conditions in the before and after are also significant, regardless of the tasks (see Tables 4.19 - 4.20). For the before measures, land comfort is significantly higher than water comfort, as illustrated below. However, for the after measures, comfort is significantly higher for the water than for the land.

Table 4.19: Impact of HG on the participants' body comfort (measures in the beginning of the experiment)

ANOVA- Total 1						
	Sum of Squares	df	Mean square	F	p	η_p^2
Time	0.18	2	0.09	0.37	0.689	0.005
Condition	4.27	1	4.27	17.38	<0.001	0.098
Task_type \times Condition	0.03	2	0.01	0.06	0.9	0.001
Residual	39.31	160	0.24			

Note: df - degrees of freedom, F- variance ratio, p-value, η_p^2 - partial Eta squared (proportion of variance accounted by some effect)

Table 4.20: Impact of HG on the participants' body comfort (measures in the end of the experiment)

ANOVA- Total 2						
	Sum of Squares	df	Mean square	F	p	η_p^2
Task type	0.53	2	0.26	1.00	0.36	0.012
Condition	1.27	1	1.27	4.80	0.030	0.029
Task_type \times Condition	0.13	2	0.06	0.23	0.78	0.003
Residual	42.53	160	0.26			

Note: df - degrees of freedom, F- variance ratio, p-value, η_p^2 - partial Eta squared (proportion of variance accounted by some effect)

4.6.2 Analysis for each body part comfort

To obtain finer detail in terms of comfort, since there is an overall effect where the task is done, but no effect of the task, each body part was tested separately. Here, an ordinal logistic regression model was used since the comfort scores are ordered natural numbers from 1 to 5. Alternatively, dependent variable were the "after" scores, and the model had the "before" scores as a covariate, to account for individual variation in initial comfort scores. The reference level was "land", meaning that the model Estimate represents how much the comfort in water changed when compared to land. Significant differences were found for effects on the neck, shoulder, upper back, lower back, hips and thigh (Table 4.21).

Table 4.21: Study of the influence of the gravitational factor on the comfort of different parts of the body of participants

Predictor	Estimate	SE	Z	p
Modem Coefficients - Neck_2				
Condition:				
1/6 - 1G	1.80	0.334	5.38	<0.001
Neck_1	1.75	0.227	7.70	<0.001
Modem Coefficients - Shoulder_2				
Condition:				
1/6 - 1G	2.48	0.357	6.94	<0.001
Shoulder_1	1.52	0.233	6.53	<0.001
Modem Coefficients - Upper back_2				
Condition:				
1/6 - 1G	2.52	0.367	6.85	<0.001
Upper back_1	1.81	0.235	7.68	<0.001
Modem Coefficients - Lower back_2				
Condition:				
1/6 - 1G	1.10	0.315	3.50	<0.001
Lower back_1	1.70	0.229	7.43	<0.001
Modem Coefficients - Hips/thighs_2				
Condition:				
1/6 - 1G	1.03	0.415	2.50	<0.001
Hips/thighs_1	3.38	0.412	8.19	<0.001

Note: SE - standard error, Z- critical values, p - significance level: * p<0.1; ** p<0.05; *** p<0.01

4.6.3 Effect of backrest angles on comfort

The different backrest angles used were analyzed as to whether they had any effect on the reported levels of comfort, see Figure 4.22.

Starting with the same strategy of averaging the comfort scores for all body parts into a single

composite scalar score and using a mixed design ANOVA with the self-report time (before, after) as the within-subjects measure and this time, backrest angle (1, 2, 3; see corresponding angles) as the between-subjects measure. Again, tasks for each backrest angle were considered independent, even if coming from the same subject.

There were no effects of the backrest angle on overall body comfort. All angles show similar levels of comfort for before and after measures.

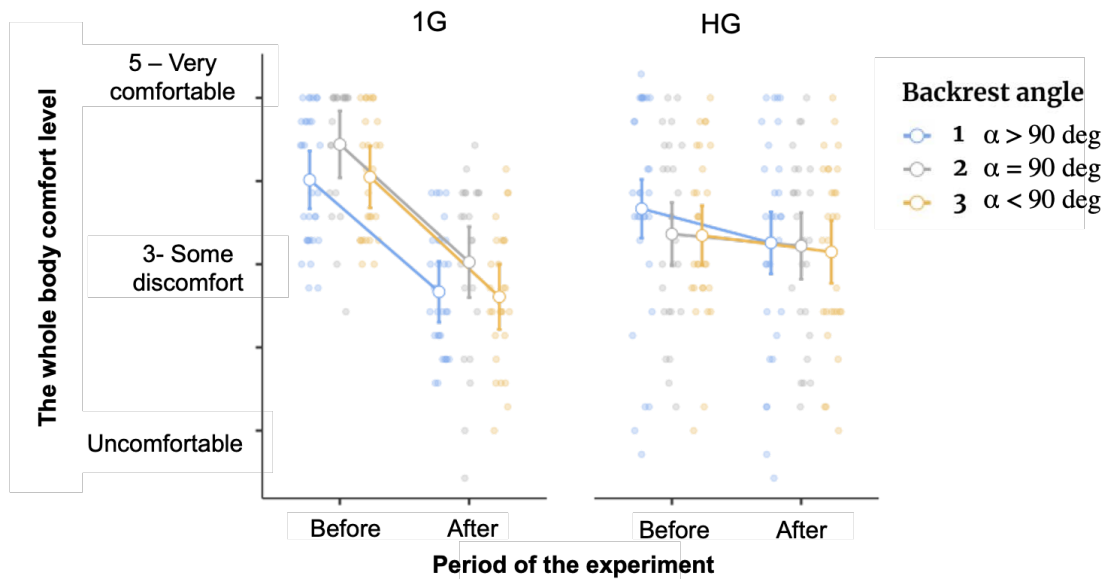


Figure 4.22: Backrest impact on overall body comfort under 1G (Left) and HG (Right). **Before** and **After** mean that the survey was conducted before/after the participant started/finished the task respectively

And this is confirmed by the lack of statistical significance on both the interaction between backrest angle and time (within subjects effects), and the main effect of Backrest angle (between subjects effects). Other relevant results are presented below, Tables 4.22 - 4.23. Testing only the differences in the after measures, using an ANOVA design, no significant differences were seen between backrest angles. Analysis for the body segments focused on neck, shoulder and upper back, because they are more sensitive to the gravity impact.

Table 4.22: Backrest angle impact on body segments comfort (ANOVA test)

Within subjects effects						
	Sum of Squares	df	Mean square	F	p	η_p^2
Time	13.41	1	13.41	106.65	<0.001	0.396
Time × Backrest angle	0.074	1	0.037	0.294	0.745	0.004
Residual	20.49	163	0.125			
Between subjects effects						
	Sum of Squares	df	Mean square	F	p	η_p^2
Backrest angle	0.596	2	0.298	0.711	0.009	0.413
Residual	68.38	163	0.42			
ANOVA - total_2						
Backrest angle	0.366	2	0.183	0.665	0.516	0.008
Residuals	45.11	0164	0.275	0	0	0

Note: df - degrees of freedom, F- variance ratio, p-value, η_p^2 - partial Eta squared (proportion of variance accounted by some effect)

Table 4.23: Backrest factor impact on the body segments comfort

Modem Coefficients				
Predictor	Estimate	SE	Z	p
Modem Coefficients - Neck_2				
Backrest angle:				
2 - 1	0.533	0.362	1.47	0.141
3 - 1	-0.190	0.345	-0.549	0.583
Neck_1	1.322	0.202	6.541	<0.001
Modem Coefficients - Shoulder_2				
Backrest angle:				
2 - 1	0.358	0.355	1.01	0.312
3 - 1	0.359	0.338	1.06	0.288
Shoulder_1	0.734	0.195	3.77	<0.001
Modem Coefficients - Upper back_2				
Backrest angle:				
2 - 1	0.249	0.355	0.701	0.483
3 - 1	-0.058	0.347	-0.168	0.867
Upper back_1	1.07	0.194	5.53	<0.001

Note: SE - standard error, Z- critical values, p - significance level: * p<0.1; ** p<0.05; *** p<0.01

4.7 Combinatorial study

Combinatorial study aims to identify common patterns for 1G and HG for performance, applied force, posture, fatigue and comfort and overcome extensions of existing ISO standards for workplace design.

The following are the results of statistical analyzes identified the level of significance of the influence of gravity and the task on all postural indicators (including center of mass) for all participants conducted static and dynamic tasks.

4.7.1 ISO standards selection

Results were verified in accordance with existing international standards. Each standard was studied separately.

ISO 11226:2000 - *Evaluation of static working postures* In this standard on the basis of endurance data, maximum holding periods for trunk inclination, head inclination, and upper arm elevation were determined.

The procedure for applying the standard begins with the determination of specific postural parameters, i.e. torso tilt, head tilt, neck flexion/extension, upper arm lift and joint extremes. In this standard, dependencies for the angles of inclination of the body during work on the duration of work for different parts of the body are built. Trunk inclination in relation to endurance time presented below, see Figure 4.23.

Here trunk posture should be evaluated for sitting posture as it is defined in ("ISO 11226.EPFL Cobaz site", 2000). This data was assessed with markerless motion capture method, see results subsection 4.3. Then the holding time for trunk inclination is assessed in the previous sub-chapters. Figure 4.23 presenting the dependencies extracted from ISO 11226:200 with plotted data points for simulated ½G for the same operational loads.

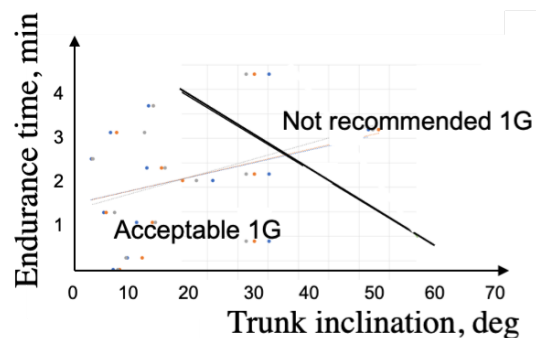


Figure 4.23: Maximum acceptable endurance time/trunk inclination with 1G data

During the experiments, the participants did not deviate more than 20 to 50 degrees from the vertical that for simulated reduced gravity, the duration of work increased significantly before the participant began to feel of fatigue. Under 1G participants did not deviate more than 10 to 20 degrees from the vertical that for simulated HG. Another difference is that for similar tasks, participants work longer in HG than in 1G, in which case the data points for the underwater environment are above the line, and thus fall into the "Not recommended" area.

As can be seen from the graph, the values for $\frac{1}{6}G$ go beyond the acceptable limits, but at the same time, the participants worked within the limits of their physical capabilities. It is supposed that it is necessary to define a new dependency graph for lunar and martian gravity.

In this case, for such conditions, it is necessary to perform additional studies towards the creation of new standards, taking into account the increased duration of work in lunar conditions and the changed angle of inclination of the body when performing various tasks. More data should be collected in order to further refine the model. Thus, the evaluation of holding/endurance time part can be extended for HG environment.

ISO 11228-2:2007 - *Ergonomics-manual handling - Part 2: Pushing and pulling*

In HG, the participants demonstrated less maximum action force than on Earth. This is likely due to the reduction in friction that occurs when participants perform underwater tasks. The ISO 11228-2:2007 "ISO 11228-2. EPFL Cobaz site", 2007 standard includes several tables of maximum force and different compressive load on spine when push and pull occur at different levels of the body ("ISO 11228-2. EPFL Cobaz site", 2007). The problem of friction may lead to the calibration of this standard.

ISO/CD 11228-3 - *Ergonomics-Manual handling - part 3: Handling of low loads at high frequency*

To analyze this standard, calculations were made for the same tasks (dynamic operational load lifting from 3 kg) performed by the participants in the experiment in two different environments.

It was further assumed that, according to the Borg scale, forces of different intensity were applied during almost half of the working cycle. For the task of operational loads under lunar conditions, the applied force can be averaged on a scale of 3 to 4. For terrestrial conditions, the same task will be more intense and can be scaled from 5 to 7. Also the body posture and recovery in the two different environments occurs in different way, due to changes in applied force, posture, duration of work (see the main components of OCRA checklist on Figure 1.19 ("ISO 11228-3. EPFL Cobaz site", 2007)).

4.7.2 Full variable analysis

The purpose of this analysis was to evaluate the relationship between variables associated with such experiments as the study of fatigue, comfort and posture and gravity level. The following variables were considered: angles between spine and vertical [deg.], angles between upper extremity and vertical [deg.], Y and Z CoM coordinates plots. Below in Tables 4.24-4.27 are presented the results for regression for all these variables for males and females separately for combined data sets for static and dynamic tasks. This is due to the fact that the primary statistical calculations showed that the gender of the participants in the experiments affects the change in the result, while the type of task almost does not affect the results. Statistical results related to calculated angles between spine and thigh and forearm and vertical, also results for split and combined data sets for males and females are given in Appendix Figure A.10- Figure A.13, table A.16- A.18, Table A.21-Table A.22.

Table 4.24: Mean angle between spine and vertical for static and dynamic tasks together [deg.].

	<i>Dependent variable: mean spine/vertical angle</i>	
	Males	Females
G-level	-13.45*** (3.61)	-17.81*** (2.87)
Task	-2.94 (3.55)	2.25 (2.88)
Constant	33.86*** (3.29)	24.96*** (2.57)
Observations	132	66
R ²	0.10	0.38
Adjusted R ²	0.09	0.36
Residual Std. Error	20.38	11.67
F Statistic	7.29***	19.53***

Note:

*p<0.1; **p<0.05; ***p<0.01

Table 4.25: Mean angle between shoulder and vertical for static and dynamic tasks together [deg.]

<i>Dependent variable: mean shoulder/vertical angle</i>		
	Males	Females
G-level	24.43*** (2.53)	7.34** (3.36)
Task	3.52 (2.50)	0.26 (3.37)
Constant	49.84*** (2.27)	60.15*** (3.00)
Observations	138	66
R ²	0.41	0.07
Adjusted R ²	0.41	0.04
Residual Std. Error	14.71	13.64
F Statistic	47.73***	2.39*

Note:

*p<0.1; **p<0.05; ***p<0.01

Table 4.26: Mean CoM coordinate Z- axis for static and dynamic tasks together [cm]

<i>Dependent variable: mean CoMz (in relation to pelvic on Z axis)</i>		
	Males	Females
G-level	-1.45 (1.50)	6.02*** (1.43)
Task	-2.17 (1.50)	0.44 (1.41)
Constant	6.67*** (1.28)	-3.77*** (1.20)
Observations	114	56
R ²	0.03	0.25
Adjusted R ²	0.01	0.22
Residual Std. Error	8.01	5.26
F Statistic	1.51	8.91***

Note:

*p<0.1; **p<0.05; ***p<0.01

Table 4.27: Mean CoM coordinate Y- axis pelvic for static and dynamic tasks together [cm]

<i>Dependent variable: mean CoMy (in relation to pelvic on Y axis)</i>		
	Males	Females
G-level	17.06*** (1.58)	5.87*** (0.57)
Task	3.17** (1.59)	-0.94 (0.57)
Constant	-8.47*** (1.35)	5.70*** (0.48)
Observations	114	56
R ²	0.52	0.67
Adjusted R ²	0.51	0.66
Residual Std. Error	8.45	2.11
F Statistic	60.01***	54.28***

Note:

*p<0.1; **p<0.05; ***p<0.01

All analyzes are carried out in such a way as to compare the influence of a certain environment ($\frac{1}{6}G$ and $1G$) on the measured indicators (angles, CoM). The values of the indicators were taken into account throughout the entire interval of the task performance by the participant, from the beginning of the task to its end, when the person was completely tired. Gravity level means gravity change from $\frac{1}{6}G$ to $1G$. By comparison the results, can be observed that the coefficients for the angles between the spine and the vertical, the angle between the upper arm and the vertical, the deviations of the CoM are very different depending on the environment. The value of p shows how large the deviation is in general $p<0.01$ or $p<0.05$, that proved the significance of this difference. And the indicator in brackets shows the standard error in the calculations.

5 Baseline for workplace design

This chapter includes a discussion related to all the results described in Chapter 4, and it also suggests options for extending the existing standards for terrestrial conditions for conditions of HG. Based on the analyzed data and standards, a workplace optimization approach is proposed and some recommendations are considered for designing a workplace under HG.

5.1 Interpretation of results

Since several experiments were carried out to identify the effect of HG on human movements and physiology, the interpretation of the results is carried out for each experiment separately.

5.1.1 Performance at the workplace

The results of a preliminary study of participants' performance in the HG and 1G workplace are presented in Sub-chapter 4.2. The results include an analysis of data collected by direct and subjective methods.

By subjective measurements, it was found that when working with an overload of $\frac{1}{6}G$, the torso of the participants deviated slightly backward compared to 1G. This may be due to the change in the position of the center of mass (CoM) in two different environments. There, the results provide an interesting direction for research. Further exploration of this finding was refined in postural study experiments.

In a Table 4.4 results were presented for all subjective demands such as mental demand (MD), physical demand (PD), temporal demand (TD), performance (P), effort (EF), frustration (FR), including the weighted workload indicator (WWL, %). It can be noted that, in general, all WWL, % indicators decreased for simulated HG in relation to 1G. For repetitive tasks for 3 kg, the indicator decreased by 12.26 %, for repetitive tasks for 1 kg by 11.65 %, for tasks with 0.5 kg by less than 1 %. Further, it can be noted that for tasks with a joystick, this remained almost unchanged and decreased by less than 1 %, for tasks with writing text, the indicator

also changed by less than 1 %, but for tasks with keyboard work, the indicator for simulated reduced gravity increased by 2.39 % and for assembly tasks, this indicator also increased by 8.93 %.

With a more detailed analysis of the subjective demands included in the WWL,% (see Table 4.3), it can be noted that for example, for repetitive tasks (R) with loads from 0.5 g to 3 kg, PD and EF significantly exceed all other indicators in general, why these indicators showed differences in the WWL, %. These results are consistent with research results devoted to the study of fatigue under HG discussed in sub-chapter 4.4: "Fatigue study". Regarding the joystick task, it was noticed that under $\frac{1}{6}G$ the MD decreased compared to 1G, while the performance (P) increased. Although the weighted workload is not very different for terrestrial and simulated conditions of lunar gravity, for $\frac{1}{6}G$, the MD and TD decreased, the P increased. For the keyboard task, the MD increased, while the TD and P decreased for lunar gravity compared to earth gravity. For the assembly task, MD decreased for $\frac{1}{6}G$ in comparison with 1G, while TD, P, and EF increased. The significant increase in WWL,% for the simulated lunar conditions for assembling the elements is also consistent with the fact that the participants in the experiment made more mistakes when performing this task in water than out of water. All of the listed tasks that were used to study the productivity of work can be divided into physics-related (repetitive task, work with joystick, handwriting) and precision-related tasks (assembling task, work with keyboard). Physics-related tasks became easier to perform in simulated lunar conditions as the weight of operational objects became lighter or it became easier to apply force on working objects. And indicators of physical demand and efficiency declined too. But the WWL score for tasks with assembling and working with the keyboard became higher for working in simulated lunar gravity, since the participants' bodies were probably less stable and more energy was released to complete the task. Since all participants completed the tasks first on land and then underwater, these changes in the WWL and the number of errors when performing the task underwater are unlikely to be related to the problem of participants instructing or training.

A separate study of the WWL, % parameters for males and females showed that, in general, the values for all tasks for women were higher than for men, except for tasks with a keyboard up to 1G. WWL in females was 11.7% lower than males under 1G. An important difference was also noted for the following tasks: Joystick WWL for females was 13.3% higher at $\frac{1}{6}G$ and 6.9% higher for 1G than for males, WWL recording work was 11.4% higher in females than males for $\frac{1}{6}G$ compared to 1G, and for WWL assembly work 15.5% higher for $\frac{1}{6}G$ compared to 1G for females than for males.

5.1.2 Postural study

This study aimed to examine the applicability of the markerless motion capture method for identification of the joint profile under simulated HG environment, especially in the aquatic environment.

These plots compare body posture under various gravity conditions, specifically at the initial stage, in the middle interval, and the final interval, when the state of fatigue was reached.

The results on body position change show that there is a tendency for the upper limbs of the human body and the trunk to tilt backward in the sitting position when performing static and dynamic tasks back under HG. This is especially "visible" at the end of the task, when the participant begins to be tired, as this deviation occurs gradually. In fact, such deviations are almost invisible to the naked eye. Therefore, the use of the markerless tracking method is an efficient way to capture such trends.

During the experiments involving a vision-based method, it was found that the inclination of the spine relative to the vertical deviated forward / backward by 20.83° at $\frac{1}{6}G$ compared with 1 G for females when performing static tasks, by 14.19° for females when performing dynamic tasks, for males by 7.97° with static tasks and by 18.92° for males conducting dynamic tasks. All of these deviations are indicative and strongly correlated with the impact of the level of gravity ($p < 0.01$).

Regarding the angles deviation between the spine and thigh, a significant correlation was found ($p < 0.01$) for males for static tasks, it is 13.18° , and for dynamic tasks 16.30° for $\frac{1}{6}G$ compared with 1G.

For the upper limbs, specifically forearm, significant correlation was found for males for dynamic tasks 27.57° and moderate correlation ($p < 0.05$) for dynamic tasks for females 4.78° . For upper arm it was observed that deviation was significant ($p < 0.01$) for females and for males, for static tasks for females deviation was 17.43° , for static tasks for males deviation was 22.5° , for males for dynamic tasks deviation was 21.28° .

It can be assumed that the angle between the forearm/upper arm and the vertical is slightly larger in simulated Moon gravity, probably because the total weight of the participant is reduced and the CoM can also be shifted; as seen in the static hip torque estimation example, the body can lean forward or backward relative to the pelvis. Also from these graphs, it can be seen that the angle of inclination of the torso of males and females is greater when simulating the gravity of the Moon than when under the gravity of the Earth when performing the same task. Apparently, even under load, the body tends to take a neutral position in which the person straightens their back and the upper limbs are slightly raised.

The same trend was observed with CoM deviation, which confirms the calculations of the deviation of the angles of the torso and upper limbs of the participants in the experiment. For Y (vertical axis) there was a significant deviation for all tasks ranging from 4-20 cm in males in static tasks and in females in static and dynamic tasks. For the Z-axis (horizontal), only one significant correlation was observed for CoM deviation in males in static tasks at 3-7 cm. A difference was observed in the stabilization of the body on Earth and the simulated lunar gravity. In lunar simulated gravity, participants' bodies are less stable even with a restraint system, and this should be taken into account when developing workplace design guidelines.

Biomechanical methods (D'Alembert's principle) also validated this observation. It was found during the first experiments devoted to hip torque values computations. A tendency was revealed for a linear dependence between particular joint (hip) torque and G level. The mathematically calculated values of the hip joint for the gravity of Mars still require experimental verification. The positive and negative values of the torque are related to the rotation of the pelvis of the participants with the involvement of different muscles of the body. This can also be a good indicator of the inclination direction of the participants' torso and thus the CoM. The negative value of torque was associated with clockwise rotation of pelvic and body tilt backward and positive value of torque was associated with counterclockwise pelvis rotation and forward body tilt.

It was identified that, when the anthropometrical and kinematic data of the participants is known, it is possible to calculate the value of the torque in the joint, which is a measure of the load on the muscles with the markerless motion capture method. It was reasoned that with its positive value, which corresponds more likely to the forward tilt of the participant, this moment is created mainly by the gluteal muscles. With a negative value, the corresponding tilt backward without significant support on the back involves the iliac-lumbar muscles. The assessment of the hip joint was carried out by the biomechanical method, taking into account the reaction of the seat support.

For shoulder and forearm force, $\frac{1}{6}G$ values were found to be higher for static and dynamic tasks. This difference ranges from 1.15 to 5. For shoulder and forearm torques, values found for $\frac{1}{6}G$ environment are higher for static and dynamic tasks. This difference ranges from 1.15 to 4.

Having data on the value of the torque, it is possible to compare the load on these muscles under experimental conditions with HG and with Earth gravity with a different load mass. It is also possible to directly correlate this load with the load that occurs in other poses. Thus, the moment created in the hip joint by the gluteal muscles during sitting can be correlated with the moment created by leaning forward, etc.

By analogy with the hip, similar dependencies can be recorded for other joints. In the general case, the equivalent loads for different muscles and joints are different, which leads to a different fatigue profile and the need for different recreational and training procedures for the conditions of terrestrial gravity, MG, and the HG of the Moon and Mars.

The workload study results under $\frac{1}{6}G$, $\frac{1}{3}G$ and 1G show the difference in the workload of shoulder and elbow of male and female for the simulated Moon gravity on the top and Earth gravity on the bottom. A significant difference in the values 6 -7 times for a static task between simulated lunar and Earth gravity can be observed.

It can be concluded that in simulated lunar gravity, participants can work longer than in terrestrial gravity until their hands become tired. It can be seen that the angle between the forearm and the vertical is slightly more important in the conditions of $\frac{1}{6}G$. This is probably

due to a decrease in the total weight of the participants and a shift in the CoM. From these graphs, it can also be concluded that the torso angle is greater when simulating $\frac{1}{6}G$ than in normal gravity when performing the same task. From these results, it is possible to conclude that there is a tendency for the body of the carriers to deviate backward under the conditions of lunar gravity, compared with 1G.

5.1.3 Fatigue study

Some of the conclusions in this sub-chapter have been drawn from the publication of the author of this dissertation Volkova et al., (2022) "An empirical and subjective model of upper extremity fatigue under hypogravity" published in *Frontier in Physiology*.

This first study Volkova et al., 2022 not only provided insight into the effect of HG ($\frac{1}{6}G$ and $\frac{1}{3}G$) on data such as ET (min) of the upper extremities of participants and their mental workload, but also contributes to a better understanding of the relationship between upper-limb physical fatigue and mental workload when participants perform tasks under HG.

HG increases a participant's productivity by reducing overall physical fatigue expressed in ET (min) compared to Earth's gravity, as seen in the results. This was confirmed by a defined significant positive ($p=0.002$) relationship between Endurance time and gravity level ($\frac{1}{6}G$, Moon, $\frac{1}{3}G$, Mars, 1G) with negative coefficient for male and female participants for a static task. Increasing gravity thus reduces endurance time (ET) (min). In addition, a general decrease in mental workload is observed under the same conditions. A moderate relation ($p<0.1$) between weighted workload and gravity level exists, with a positive coefficient for male and female participants for the same task. One can note a possible relationship between lower p-values for mental stress to each participant's individual understanding and interpretation of the survey. Increasing gravity increases the mental workload. Variables such as hand muscle contraction after task, displayed good correlation with gravity level as well, a trend which was observed for both dynamic and repetitive tasks.

For all participants, it was seen that power function better matched the data of ET (min) - Task Intensity, but without specification of upper limb joints. This finding supports other studies (Rohmert, 1960, Monod and Scherrer, 1965, Huijgens, 1981, Sato et al., 1984, Rohmert et al., 1986, Sjøgaard, 1986). A number of authors have used the exponential model (Manenica, 1986, Matthijsse et al., 1987, Rose et al., 2000).

Focusing on the twenty-two participants conducting Static task (S1), the principal findings related to ET [min], mental workload and contraction force results. ET increased by an average of 3.54 times for females and 3.14 for males under $\frac{1}{6}G$, in comparison with 1G. It was seen that a division of data for males and females into separate data sets resulted in a better curves fit and higher R^2 . This relates to the difference in physical capacities between participants by gender, as well as to their anthropometry. Another interesting finding is related to the ratio value between the average ET (min) values for loads of 1 kg, 3 kg and 5-7 kg, normalized to

the ratio of muscle mass [kg] and body weight [kg] of participants, measured under $\frac{1}{6}G$ and 1G. This is systematically higher for males than for females due to the greater sensitivity of females to loads, especially under 1G. For example, performance of the task with a load of 5 kg is possible for most males, but completion is rare for females, leading to a large gap in ET results. If under 1G and underwater measurements of ET [min] for males are on average two times higher than for females, a greater difference for females results. The dynamic (D), repetitive (R) and static (S2) tasks showed similar trends and relations

With the same twenty-two participants it was found that under $\frac{1}{6}G$, mental workload decreased by an average of 1.15 times for males and 1.08 for females in comparison with 1G for the static tasks (S1). The WWL,% for females were higher than for males due to the female's higher sensitivity to the loads and weaker physical strength. Physical and effort demand have the highest impact on the weighted workload which is consistent with (Brown, 1994). According to (Xu et al., 2018), the "control of movement is a kind of mental activity that can cause mental fatigue", because increased effort by the participant is required to complete the task following increasing physical fatigue. According to (Rubio et al., 2004) there is a high correlation of NASA-TLX with performance, and in the results of this study it increases with reduction of the gravity level; yet the physical demand and effort significantly reduced when gravity level was reduced.

Estimated averages of muscle contraction force indicate a greater reduction in physical strength under $\frac{1}{6}G$ than 1G. This is consistent with participants' ability to work longer; their ET is higher in a simulated $\frac{1}{6}G$ environment due to lower loads and the weight of the participants themselves. Overall, a greater decrease in hand strength after doing all tasks under 1G and $\frac{1}{6}G$ was shown for all participants. The same pattern is seen for the BLC measurements. An increase in muscle contraction after the tasks is very rare, possibly due to non-compliance by participants with the instructions for using anemometers or to individual characteristics of participants.

To turn to the assessment of muscle contractions of the hand and back-chest-legs before and after the tasks, a higher change in % for $\frac{1}{6}G$ than for 1G was observed due to all participants generally working longer at $\frac{1}{6}G$ and thus becoming weaker in terms of upper limb strength. An increase in muscle contraction after the tasks is very rare, possibly due to non-compliance by participants with the instructions for using dynamometers or to individual characteristics of participants.

For six participants it was found that under $\frac{1}{6}G$, ET increased by a factor of 1.60 and ET increased by a factor of 4.10 and mental workload decreased by a factor of 1.26 for males and females in comparison with 1G; for the dynamic (D), repetitive (R) and static (S2) tasks the same trend was found. In spite of a pattern of increasing ET [min] with decreasing gravity, such results do not fully converge with experimental group results containing more participants. Thus, an experiment with a higher number of participants with a simulation of reduced gravity and the same tasks is recommended in order to increase reliability of the data.

Little research has focused on the state of upper extremities under HG in comparison with lower extremities. The results of this study conducted in the frame of this research are consistent with the lower limb study under HG (Richter et al., 2017). The authors studied the effect of simulated HG on jumping and running subjects, and it was found that ground reaction forces and mechanical work in the reduced gravity conditions decreased compared to 1G. Reduced gravity below 0.4 G is insufficient to support musculoskeletal and cardiopulmonary systems for a long period of time. Fatigue study (Lauer et al., 2018) confirmed the reduction in water of mechanical load on the shoulder by up to 75%. This is also seen in our findings: since all movements were performed in water, even though each participant was given additional ballasts to make the body heavier, the total body weight still remained 6 or 3 times ($\frac{1}{6}G$, $\frac{1}{3}G$ respectively) lighter than under 1G.

Other studies focused on lower extremities under HG, but the results of this study demonstrate the importance of studying upper extremities as well. This is essential for short term and long-term missions and regular work on the moon. These results can guide considerations when designing tasks for specific environments under HG. Currently, however, the ergonomics of astronauts' movements in HG conditions have not been extensively studied and additional relevant data are necessary.

An empirical and a subjective model for physical fatigue of upper extremity fatigue and mental workload assessment is proposed in this study, with three levels of gravity, six task intensities, and four types of tasks (outstretched arm (S1), arm bent at the elbow (S2), dynamic (D) and repetitive (R), with gender as an independent variable, and Endurance time [min], mental workload, hand and back-chest-leg muscle contraction as dependent variables. Excellent agreement between experimental data and subjective data is shown. With ET [min] assessment, a reduction in participant performance was found with increased gravity level for task types. With mental workload assessment, the workload in $\frac{1}{6}G$ is lower than in 1G for the same tasks. In an additional test with comparison of impact of 1G, $\frac{1}{3}G$, $\frac{1}{6}G$ on six participants' physical strength constituency and a certain linearity were noted, expressed by increasing the physical fatigue and workload with gravity level increasing. Finally, all the models showed that the level of physical fatigue and mental stress for the simulated gravity of Mars is between levels estimated during the experiments under 1G and $\frac{1}{6}G$. An empirical fatigue model with a subjective assessment tool is recommended to provide a better understanding of the phenomena; such a tool is sufficient for prediction of fatigue curves for a particular task. Application of subjective mental workload assessment can be critical for workplaces equipped with human-machine systems designed to ensure higher levels of comfort, performance, and safety. The model developed could assess physically limiting situations in industry in 1G and HG to propose alternative solutions. It can also be used to analyze upper extremity fatigue and could be implemented for predictions of fatigue as well as musculoskeletal disorders during long-term missions. The motions with extension and ulnar deviation should be investigated during future experiments.

Physical fatigue data under HG can be useful for studying body posture because without an

appropriate gravitational load stimuli, bones and muscles become vulnerable. This data makes it possible to design and optimize workplace and manual operations, a relationship addressed by very few studies. This model can be applied to tasks that are still in the design phase. Furthermore, an application to digital human modelling can be made, since experimental data for modelling and further predictions are required. This will lead to the development of new guidelines as well as standards for workplace design under HG and it will also have a positive impact on physical exercise recommendations to increase fatigue under HG.

5.1.4 Pushing and pulling study

Assessment of human strength is an important step in developing ergonomic recommendations for workers/astronauts who will be involved in manual loading and unloading. Thus, this study attempted to assess push and pull motions of upper limb using tools, and to predict working strength limits in frequent or continuous work.

The results of the test study showed that the power costs were slightly higher in terrestrial conditions than in water, taking into account the simulated lunar gravity. This is most likely due to general instability, human body conditions $\frac{1}{6}G$ and the need to introduce an additional support to apply full force to perform the exercise. The pushing/pulling force on Earth is bigger due to the friction effect that occurs when participants perform the tasks underwater. Friction is caused by gravity, which attracts the body of the participants in the experiment: the stronger the pull down, the stronger the human body (sitting part of the body) sticks to the seat.

The obtained data on the force helps in the development of a work schedule both on Earth and in conditions of reduced gravity. The predictive model can potentially be used to develop engineering recommendations for tool design in the workplace for long-term tasks.

5.1.5 Seated discomfort study

ANOVA analysis concluded that doing the tasks under $\frac{1}{6}G$ has a smaller degrading effect on comfort. In sum, changes in comfort (smaller decrease in discomfort due to the task) in the water (under $\frac{1}{6}G$) were mainly located in the neck, shoulder, and upper back. These changes can be seen as smaller decreases in the discomfort associated in the task that can be seen in the initial analysis.

Concerning the study of the backrest impact on overall comfort it was found that there were no effects of the backrest angle on overall comfort level. This is confirmed by the lack of statistical significance on both the interaction between backrest angle and time (within subjects effects), and the main effect of backrest angle (between subjects effects). However, testing different workplace designs is an integral part of optimizing the design for human combat mechanics. Further consideration of the effect of different design configurations on biomechanics and human fatigue is necessary. For example, the handrails, armrests, floor panels, as well as

velcro footrests, grooved flooring, and footrests can be tested that were used on NASA's Apollo lunar rovers cite ("NASA website", 1972).

5.1.6 Combinatorial study

While human factors and ergonomics standards do not guarantee proper workplace design, they can help provide clear requirements and guidelines for design. This can form the basis of a good ergonomic design. By setting the requirements for working conditions to prevent unnecessary human error, such standards contribute to the safety and comfort of workers.

Standards is a combination of available practical and academic knowledge are relatively easy for professional designers to use and incorporate into the design process; most of these standards are available to the general public and other interested parties (Karwowski et al., 2021). This certainly contributes to the dissemination and popularization of knowledge about the human factor and ergonomics among non-specialists.

At the moment, there are no existing standards that clearly indicate what requirements should be applied for the design of workplaces in an environment other than the Earth, for example Moon and Mars. However, the knowledge gained experimentally during the completion of this dissertation helped to build empirical models that can be correlated with existing standards. For example, the results of postural experiments could help to understand in which direction to calibrate the standard according to ISO 11226:2000 - "Evaluation of static working postures". Data collected in the framework of the experiment on physical fatigue with a hand contraction force measurements, as well as experimental data on pushing and pulling maximum actin force, the standard for example ISO 11228-3 - "Manual handling: Handling of low loads at high frequency" and ISO 11228-2:2007 - "Manual handling, pushing and pulling" respectively can be calibrated by the coefficient defined during experiments. Subsequently, the proposed design optimization approach with further extension of existing standards creates new designs.

5.1.7 Markerless motion capture

Motion capture has become popular and robust in comparison with optical or inertial measurement methods. Marker-based motion capture methods are inconvenient for participants to carry, especially while doing dynamic, long-duration tasks in an underwater environment. Using suits for motion capture is also not possible in high-speed conditions with wide base-lines. Nakano et al., 2020 defined marker-based motion capture methods joint identification and markerless methods as having a relatively small difference and the mean absolute error (MAEx) equal to 51.25 mm, MAEy equal to 35.99 mm and MAEz equal to 43.63 mm for elbow joint for dynamic motions (walk, jump, throw). In the case examined here, the tracking failures were completely eliminated by manually digitizing the correct position of the joints. By training the algorithm on data adapted to the scene or environment, this manual work can be greatly reduced.

Thus, such results convincingly show that this method deserves to be tried in scientific fields and especially in such specific environments as described in this study. The quality of 2D pose tracking conducted with OpenPose and the quality of camera calibration affects the accuracy of 3D pose estimation; accordingly, one must initially ensure that there are no errors in recognition at the initial stages. Possible sources of error can be the data processing itself, or an incorrect time synchronization of cameras.

Firstly, markerless motion capture techniques can improve the efficiency of experiments and speed up data collection. In addition, it helps to conduct non-invasive research on participants such as long-term water trials.

Such solutions are significantly cheaper compared to sensors-based methods and this can largely increase the amount of collected data and, accordingly, the results. Secondly, such methods can be applied to tasks that are still at the design stage. This is directly related to the design of lunar and Martian bases, since there are still no clear recommendations and decisions on how astronauts will conduct operations.

By applying these methods in practice, it was found that joint torque and joint work are ideal candidates for assessing exercise and task intensity. Thirdly, during the study of joint profiles using markerless methods, it was found that different muscles work differently at different gravity levels. This can lead to a change in the body position at workplace. Under conditions of terrestrial gravity, the extremities of humans are more functional, while under Moon gravity the trunk is more functional. This is supported by other studies conducted in the aquatic environment. Since there may be various kinds of errors associated with prediction capacities, the verification of the results obtained should be carried out in real conditions (for example, a parabolic flight campaign).

5.2 Optimization approach for workplace design under $\frac{1}{6}G$ and $\frac{1}{3}G$ conditions

This subsection is intended to open discussion around a new methodology based on the workplace optimization approach that might fit for the integration/assessment of the human factor in representations of habitats in HG. Such a methodology can be implemented to reduce the risks of the human factor during long duration (LD) space missions to maintain the desired quality of life and safety. This approach was discussed in detail in the article devoted to the problems of optimization of habitats under HG conditions, "Multi-objective optimization for habitats in extreme environments" presented at IAC-2019 in Washington D.C., United States (Volkova et al., 2019). In this chapter, only the general elements extracted from this paper are addressed.

In SanSoucie et al., 2009 devoted to the "Lunar habitat design optimization and analysis", scientists found that efficient optimization techniques are required for habitat design. They propose to use genetic algorithms for different problem-solving: structural, environmen-

tal (heat, radiation) etc. Other scientists, Sumini et al., 2018 in the paper multi-objective optimization (MOO) "MOO for Structural Design of Lunar Habitats" proposed to use such optimization for the structural design problem of the habitat shell. They define the objectives of optimization through the minimization of transportation, construction costs, minimization of the radiation effect and micrometeorites on the habitat shell. The Pareto frontier was used to determine effectiveness of the structure. In this paper, in situ resource utilization reinforced concrete is examined as a potential candidate for future design solutions. In Mars One assessment of the technical feasibility of its project mission (Do et al., 2016) authors analyse it with an iterative analysis approach, which simulates the mission architecture. The initial goal of the Mars One project was to build the first human colony on Mars. The authors found that the proposed technologies, life support, and entry, descent, and landing are not functional for such a mission. Also, the growth area of Mars One should be increased to be able to feed the crew, and atmospheric processors should be increased as well. The required design improvements were defined by solving the MOO problem. The detailed analysis of human factor and ergonomics for LD missions to the Moon/Mars through the MOO approach was not found, because as mentioned above, it was mainly focused on engineering aspects.

The scheme for a methodological framework of the optimization approach is presented in Figure 5.1. The ergonomic assessment and workplace design validation must be done in the final stage of the design process. During this assessment, the working loads and type of the tasks impact on biomechanics should also be analyzed.

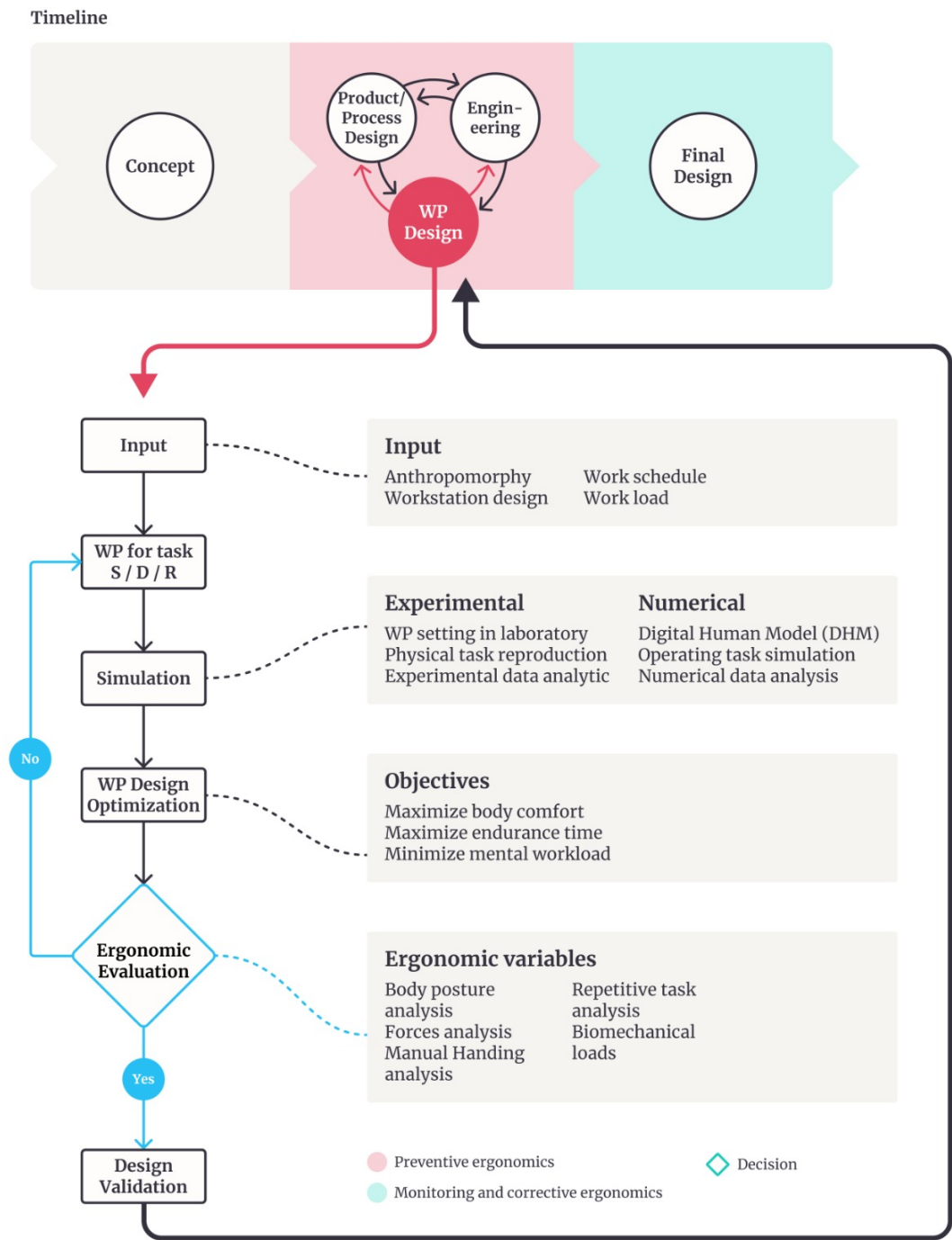


Figure 5.1: Proposed optimization approach for biomechanics-based workplace design

One of the first steps that should be taken is screening of relevant factors. This can be done based on intuition of the designer or based on verified data from relevant fields. Then the

optimization process can be based on three main steps:

- Initial data collection;
- Anthropomorphic metric data definition (weight, statures). Because anthropometry directly influences working activity, it must be taken into account in the design process to avoid overloads in the human body;
- Definition of MOO with Pareto frontier based body joint torques, joint angles, comfort level of the body parts, physical fatigue, contraction force. For the numerical model for defined task and scenario motions should be predicted. The motion prediction is based on pre-measured motion data because it helps to predict the motions with high accuracy.

The Pareto frontier of human performance/posture/fatigue/comfort/workload can be determined based on the following steps:

- Initial sampling data points collection during the experimental data. Each point corresponds to the specific human posture and task;
- Pareto optimal solution search by solving the defined equations.

Below is an example of a mathematical expression for optimizing task design to improve subjective comfort and increase endurance time when participants work with different design configurations:

$$\{f_{1,k}(\mathbf{x}), f_{2,k}(\mathbf{x}), \dots, f_{ET,k}(\mathbf{x})\} \rightarrow \min \quad (5.1)$$

$$x_i^L \leq x_i \leq x_i^U \quad (i = 1, 2, \dots, n) \quad (5.2)$$

$$g_l(\mathbf{x}) \leq 0 \quad (l = 1, 2, \dots, nC) \quad (5.3)$$

where x_i^L and x_i^U the lower and upper limits of the design variables;

$g_l(\mathbf{x})$ constraint;

nC denotes the number of constraints.

Such an optimization problem must be solved first for each participant separately, and then the same problem can be solved for a group of participants when a trend is visible. For example, in the automotive industry, designers group people according to anthropometric parameters. Medium-sized people prefer to sit more in a neutral position, while large-sized people prefer to sit with their legs extended forward, people with small body prefer to sit upright and close to a table or workplace.

The intention is to use the following input data: place observation, task maneuver, workstation design, work environment, work schedule, and the workload for tasks described above. This approach demonstrates multiple main variables necessary for workplace design optimization. The workplace design is created based on human-workplace interaction simulation model and engineering aspects. The participants tasks (in terms of their complexity) should be defined e.g.: operating a computer, operation of a glovebox, operation of a robotic system, assembly and maintenance tasks.

As soon as the design variables of the workplace are considered (including environmental and working task variables), ergonomic variables analysis, and detailed workplace design can be implemented. Ergonomic variables are related to scenario creation in a laboratory with working activity (tasks). At this moment, motion-capture systems or physical measurements methods can be implemented. Alternatively, virtual reality scenarios can be used instead of real laboratories. DHM can imitate the activity motion details. For such models, numerical data - postures, forces, joint torques, etc. - should be implemented. It is crucial to study the following human factors related to repetitive tasks: postures, manual handling, applied forces.

The framework aims to take into account design and, most importantly, ergonomic variables (related to the human body parameters). For such procedure numerical simulation and DHM as a supporting tool for design validation should be implemented. DHM is a computed added model with the physical and anthropometric characteristics of a human. Different softwares can be considered for validation purposed, such as JACK, Anybody, APOLIN, CAR, CYBERMAN, ERGOMAN, etc. can be used.

With the help of the calculation of the joint torques, angles, coordinates, forces for all body parts, the physical workload of the human body can be estimated. Different software estimates different number of joints. Inverse kinematics allows for identification of the momentum and forces of the joints during the animation. The following steps can describe this process:

- Collect the data, employing motion capture tools (coordinates of the joints);
- Develop a 2D/3D numerical model of motion that can simulate the analyzed task;
- Export body posture data from 2D/3D model, including joint angles, torques, forces at each frame/time step;
- Conduct risk assessment of performed motions/postures, using existing and suitable for space-related field risk assessment tools (or others);
- Identify problematic motions/postures and prepare workplace modifications that can potentially reduce identified risk and repeat 2D/3D numerical model step.
- Realize the design modifications of the workplace and repeat this procedure. Conditions of optimization should be satisfied. In this case, assessment tools such as, for example, rapid upper limb assessment (RULA) equation (Takala et al., 2010).

These assessments are applied to the DHM and represent a continuous improvement. To rate each motion, posture, force/load, the risk assessment tool can be utilized (Hignett and McAtamney, 2000; McAtamney and Corlett, 1993). At the end of this process, the total risk assessment, based on RULA, the rating can be created for a whole working operation process. Additional input can be considered: gender, percentile stature, anthropometric diversity. When ergonomics-based hypotheses are made, then the appropriate variables should be included in the analysis and computations. The basic ergonomic requirements, such as e.g., biomechanics and ergonomics-related international or space-related standards, should be respected. The following are examples of common ergonomic variables:

- Workers allocation;
- Body posture analysis;
- Forces analysis;
- Manual handling analysis;
- Repetitive task analysis;
- Biomechanical loads.

According to this approach, when ergonomics is considered as a design parameter, the workplace become human-centered. When optimization is complete, the choice of the optimal ergonomic aspects should be done to start the next phase of the design generation procedure. Physiological muscle fatigue can be calculated through typical load capacity model with a recalculation to the actual load in the selected force diagram. Muscle fatigue can be measured, for example with a dynamometer. Also, the degradation/restore posture after standing/sitting/lying can be analyzed. The workplace design can be validated based on ergonomic evaluation experimentally and/or numerically.

Physiological measures can be taken with a dynamometer or force plate, electromyogram, electroencephalographic measure, electrocardiogram, or eye fixation. Sometimes indirect physiological measures can be implemented when some parameters can be estimated numerically through software simulations or biomechanical calculations, as described in the (Song et al., 2010).

Below is an approach to optimizing the workplace based on the data collected during the experiments. The optimization functions were: to minimize the fatigue (maximize the endurance time) of the participants and at the same time to minimize discomfort in the workplace. The numbers 1, 2, 3 refer to the three backrest angles that are optimized for these functions. The following is an example of applying this approach on data collected during experiments in two environments 1G and $\frac{1}{6}G$.

In this study problem, an assessment of the physical fatigue of the upper limbs with a certain load in relation of ergonomic workplace design for sitting posture under 1G and HG. A procedure for determining the optimal solutions to ergonomic design problems, in this case the effect of seat back tilt on the subjective comfort of the experiment participants was proposed. The results of this experiment are explained in Sub-chapter 4.6 - "Seated discomfort study".

Muscle load assessment is formulated as a MOO problem, and optimal solutions are obtained for each participant. Subjective comfort ratings are also used to support optimal design decisions. The optimization results suggest that the proposed assessment more fully reproduces the mental and physical state of the participants in the experiment than the separate use of muscle loads.

This example limits the required comfort level from 3 (some discomfort) to 5 (very comfortable) for all body parts (the objective is to minimize discomfort). For the endurance time of the work, it is necessary to choose solutions so that the participants work for as long as possible, but not at the expense of comfort, see Figures 5.2 and Figure 5.3.

The same approach applies to $\frac{1}{2}G$.

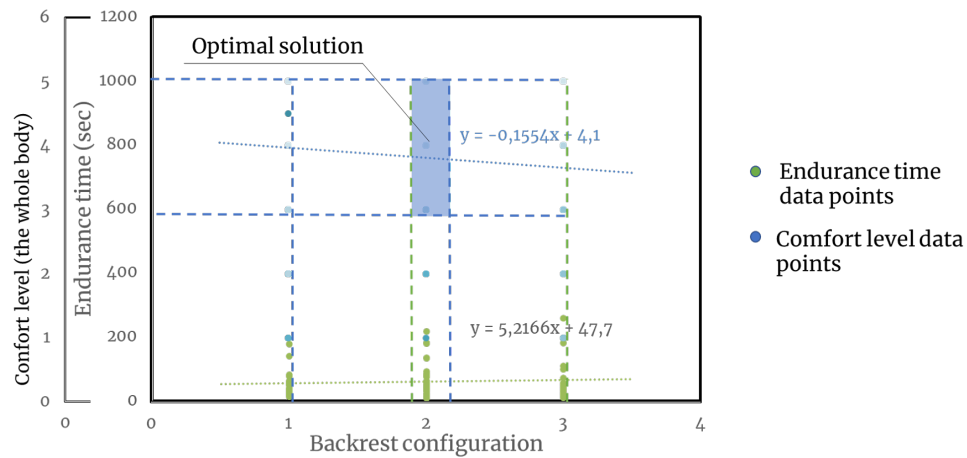


Figure 5.2: Optimal solution for backrest inclination, 1G. 1 - backrest inclination more than 90 degrees, 2 - backrest inclination 90 degrees, 3 - backrest inclination less than 90 degrees

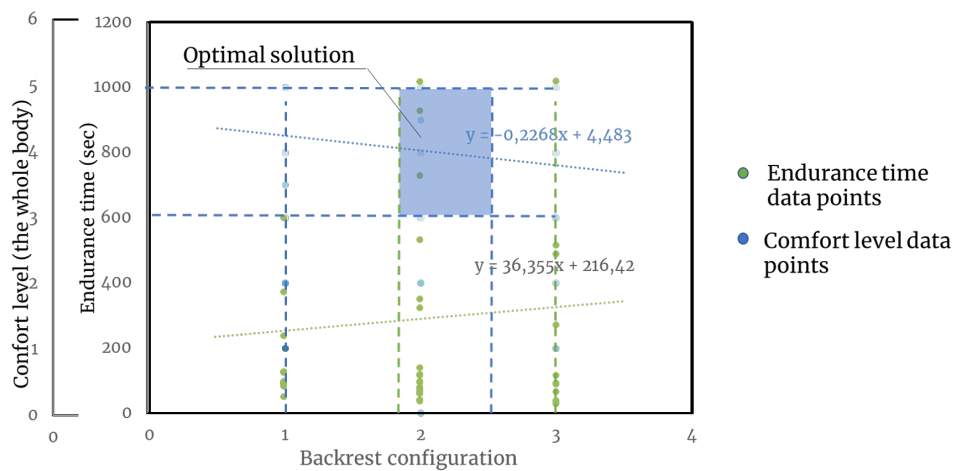


Figure 5.3: Optimal solution for backrest inclination, $\frac{1}{2}G$. 1 - backrest inclination more than 90 degrees, 2 - backrest inclination 90 degrees, 3 - backrest inclination less than 90 degrees

Comparing the plots, it can be seen that despite the fact that there are similar trends for comfort level and endurance time changes, there may be more options for design. Since the decrease in comfort is not as rapid as for 1G, with the same configurations, and endurance time is much longer than on the ground. Under 1G, the increase in endurance time is not so

rapid, but the comfort level decreases quickly enough. To depict this approach the solution of the optimization problem was solved by a graphical method and additional data are needed for the numerical solution of this problem.

This, it is essential take HG into account during workplace optimization. In the numerical model adapted to HG, it is also essential to take into account not only the effect of gravity level on the weight but also corrections for rotation and impulse loads under the conditions.

The risk of poor workplace design is related to the lack of human-centered design. Analyzing the root cause of the inefficiencies of such workplace design in HG is necessary. Such a design should be implemented throughout the design process. One of the most efficient approaches, from the point of view of this thesis, is to create a good ergonomic design with integrated biomechanical modeling based on MOO. This should also include safety and human performance concerns, as well as quality and productivity. A good human-centered design will increase the efficiency of safety and operation of all workplace components and should as a consequence have a positive impact on cost.

5.3 Extension of the 1G standards for HG conditions

Workplace accidents are an unfortunate reality in many industries. Accidents can be avoided by teaching people new skills, providing safety training, and following established standards and guidelines. There are currently no strictly established standards for design under HG. Missing knowledge in HG design must be completed before astronauts go to the Moon or Mars. Before global missions into space, it is necessary to conduct as many tests as possible, working out guidelines and standards to reduce the number of potential injuries and deaths. Haste before the implementation of large space projects has more than once led to the loss of lives. The development of standards based on empirical research can therefore help to overcome such situations and reduce risks.

This dissertation has focused on supporting the creation of standards under HG. The focus was on standards related to posture and effort as these are fairly well-developed standards for 1G environments and some best practices can be learned to develop new ones.

Ergonomics standards do not guarantee proper workplace design, but they can help define clear design requirements and guidelines. This can form the basis of a good ergonomic design. In this way, such standards can safeguard the security and comfort of workers by establishing guidelines or requirements for optimal working conditions and the prevention of unnecessary human error.

The evaluation procedure of ISO 11226 standard considers different body segments and joints independently in one or two steps. The main sections of ISO 11226 date to 1993/1994. Thus, this standard is based on the ergonomic knowledge and opinions of the experts at the time (Delleman et al., 2004).

The maximum endurance time for all participants was estimated based on the relationship between torso tilt. Endurance data were taken from previous studies of the author of the thesis, which were consistent with studies such as (Volkova et al., 2022).

With the help of the analysis, it became clear that the proposed method for assessing the risks of a worker in the workplace is not fully suitable for work under HG conditions. In this regard, additions to this standard may be proposed. For example, an additional number of experiments can be conducted to build a new empirical relationship to meet the operating conditions on the Moon and Mars. The Figure 5.4 (B) shows the assumption of such a change. A similar plots can be assumed for upper limbs inclination vs endurance time. It is also recommended that future similar international standards for assessment of working postures include at least more information on retention/recovery modes.

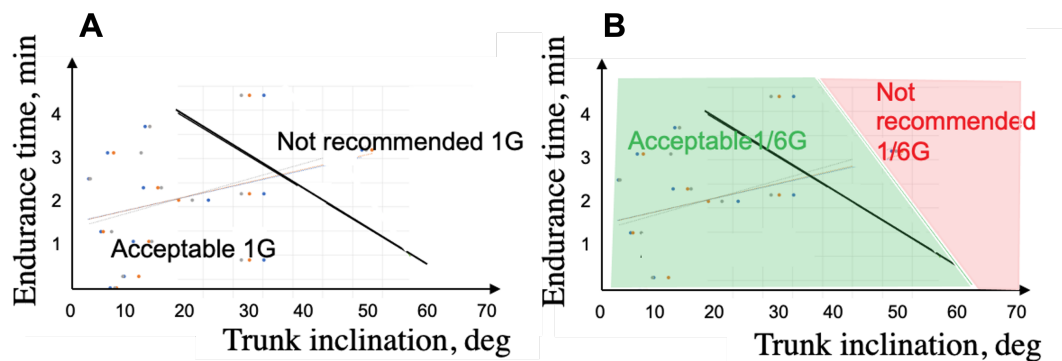


Figure 5.4: Proposed standard extension. (A) ISO 11226 example for 1G (B) ISO 11226 extension for HG

Standard ISO 11228-2:2007 - *Ergonomics-manual handling - Part 2: Pushing and pulling*. According to the experimental results obtained, the following recommendations can be considered for extending this for the HG environment:

- Maximum acceptable forces for one/two-handed pushing pulling can be calibrated by coefficient 1.2 as a minimum (**ISO 11228-2:2007**). This coefficient was defined during pushing and pulling experiment conducted under 1G and simulated $\frac{1}{6}G$;
- The angle of the shoulder joint (degrees) can change during the push-pull motion on the Moon due to the friction difference (see Figure 5.5), which can result in a different compressive load on the operators's lumbar-sacral spine segment L5/S1. Different angles of the shoulder joint with the same action force can lead to different compression loads. The difference can be 3-7 times;
- Basic force limits when pulling or pushing at different height can be modified to due to the changes of environment and posture.

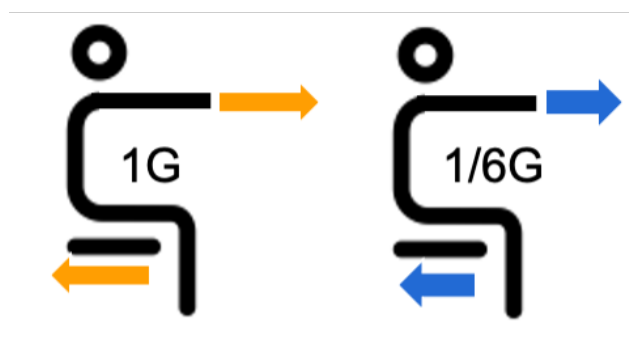


Figure 5.5: Pushing scheme under 1G (Left). Pushing scheme under HG (Right).

Standard ISO/CD 11228-3 - *Ergonomics-Manual handling - part 3: Handling of low loads at high frequency* can also be calibrated due to different contraction forces, body position (spine, upper limb position/inclination) and different recovery processes in two different environments.

As a result, in OCRA assessment can be give the final result of orange for 1G and green for simulated lunar conditions. Despite the fact that these results are quite in line with the standard's requirements, it is important to note that a person will feel more tired in simulated lunar conditions than in terrestrial ones, after already performing the same cycle until fatigue.

Some standards that take into account human metabolic rate can also be calibrated, for example, ISO 7142 - *Ergonomics of the thermal environment*. The increase in metabolic rate during dynamic activity on the Moon/Mars compared to Earth's gravity may affect the pre-astronaut recruitment process, as the cardiovascular capabilities of each individual and the requirements of the task performed in a particular environment provide the abilities needed to complete the workload. Also, metabolic rate prediction allows estimating the number of astronauts needed to complete a particular task.

5.4 Workplace design recommendations

Thanks to a comprehensive study and comparison of the task performance of experiment participants in terrestrial, simulated lunar and Martian conditions, some recommendations for designing a workplace in HG conditions can be suggested.

As reported in Chapter 4, the pressure on the seat of the workplace is quite low in underwater environment, even if some ballast is distributed on the participant's bodies. The fact is that the body is much lighter in the water and buoyancy appears. In underwater environment, point contact begins to play a role rather than the area of contact of the body with the surface of the chair. In this case, large and solid structure over the entire surface and elements for the seated part is redundant.

For example, during the experiment, participants sat on two or three thin fabric supports. This thickness was sufficient for these conditions: the participants felt quite comfortable. For earthly conditions, however, it was on the verge of comfort. Due to the need for one stable point of contact for the body, it is not always easy to find balance in water conditions, so fastening at the hips and back is necessary to stabilize the body, especially for dynamic tasks.

It has also been observed during experiments and confirmed by tests the theory that a person tends to straighten up in water. And when designing, it is important to take into account such a neutral position of the body to create forms that repeat the neutral shape of a person.

Neutral posture under HG identification

The neutral position of the body (NPP) is the position that the human body naturally takes in any condition of stay; when adopting such a position, almost no special muscular effort is required. The NPP has already been determined for MG. Initially, such studies were carried out for the Skylab experiments in the 1980s. Following these studies, Man and System Integration standards were created with respect to anthropometry and biomechanics. Previous studies have noted that crew members in microgravity assumed a conspicuous posture with arms raised, shoulders apart, knees bent with marked hip flexion and plantar flexion of the foot (Mount et al., 2003). Further, such studies were carried out on the STS.57 shuttle and international space station (Mount et al., 2003).

In the frame of this research an observational study was conducted for neutral posture investigation under HG. This observation is based both on the obtained results of calculating the kinematics of the participants in the experiments and on a survey of the participants about their feelings.

It was observed that the participants of the experiment involuntarily lean back slightly when performing tasks in the workplace. And to complete the tasks, the participants had to make efforts to stabilize the body. The Figure 5.6 shows the sitting position on the land and suggested sitting posture in HG.

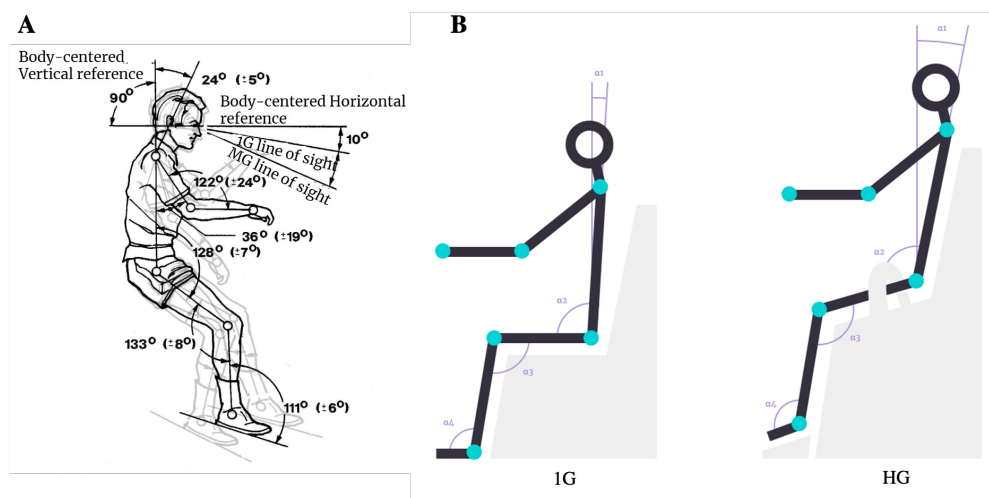


Figure 5.6: **(A)** Neutral posture under MG Source: NASA-STD-3000 Christensen et al., n.d. Republished with permission of SAE International, from Design study for an Astronaut's workstation, Vogler, Andreas, SAE Technical paper series, 2005-01-3050, copyright 2022; permission conveyed through Copyright Clearance Center, Inc. **(B)** Neutral posture under 1G (Left) and suggested neutral posture under HG (Right)

For such a change in body position, the following recommendations can be made to improve the design of the workplace for HG conditions:

- It is recommended to provide fasteners for the case at the level of the pelvic or even the shoulders, like the pilots of the aircraft. This will greatly stabilize the body for precise tasks in the workplace;
- It is recommended to provide footrests with ribbed surface and a slight slope. This will help create additional support for the body and stability;
- It is recommended to provide for the tilt of the seat and the back of the cross that repeat the neutral position of the body. This will help reduce muscle tension and stress on the back;
- The task should therefore be designed in such a way that these risk factors are avoided. Activities for pushing/pulling tasks should also be varied so as to allow adequate recovery time.

Workplace design recommendations for pushing and pulling tasks

If the workplace is planned to perform pulling and pushing tasks, then its design should be such as to reduce the potential risks from performing the task (Jacobs, 2004). The following can be considered for workplace design recommendations for pushing and pulling tasks:

- The workplace should be large enough to allow full manoeuvre;
- Footrests, sitting part, and table surfaces should be covered with ribbed material to increase friction;
- For dynamic and high-load tasks, including pulling and pushing tasks, the workplace must be equipped with a backrest and additional fastenings for the feet to avoid loss of stability during the tasks;
- Stacking heights should be restricted to improve visibility;
- Doors should be opened automatically instead of manually to reduce the frequency of initial pushes and pulls;
- Regarding the fact that such forces as, for example, forces from pushing and pulling in water are slightly less than on land, then it would seem that additional supports, for example for the back, may be necessary.

Applied forces to the objects/equipment should always be considered in relation to posture. Improper posture can increase required strength due to decreased postural stability. Changing the posture to suit can decrease or increase the required strength. For example, leaning forward requires lower strength and stability requirements than upright postures. It is important to choose the right height and design of the handle for pushing and pulling. This may increase the likelihood of full horizontal force application. Increasing friction between the seat or floor can also help maintain effective posture. For conditions on the Moon and Mars, it is important to have a ribbed surface, velcro or even magnet on the working surfaces for the most efficient pulling and pushing motions.

Prevention of Muscular Overload It is important to minimize static and repetitive muscular work. Some occasional heavy dynamic work phases can help to maintain physical fitness. Engaging in regular physical exercise, whether during or outside working hours, increases the worker's muscular and cardio-respiratory capacities. Although preventing muscular overload is a challenge if a worker's general physical capacities are lacking, worker-adapted training contributes to higher performance and reduction of the sensitivity to muscular loads.

6 Discussions and conclusions

This thesis focuses on the need to develop recommendations for the design of workplaces based on human biomechanics, with a specific interest in sitting workplaces and handling areas in hypogravity (HG) (specifically Moon $\frac{1}{6}G$ and Mars $\frac{1}{3}G$). Such workplaces could be used in long-term space missions in order to maximize worker performance and minimize the risks of musculoskeletal injuries. The research objective is to formalize a baseline workplace design based on best practices for the tasks: operating a computer and assembling of various finished products, as well as manual handling operations. The recommendations for the design, maintenance, and usage of this workplace in different gravity conditions (1G, $\frac{1}{6}G$, $\frac{1}{3}G$) are provided. Future directions of this research are also described. Physical experiments conducted in an underwater environment simulate HG conditions. This work may have a significant impact on workplace design for both Earth and Space projects.

6.1 General discussion

While the current focus of space exploration efforts lies in the development of space settlements and how to get to Mars or beyond, the human body response to HG conditions remains largely understudied. The effects on the human body stemming from the loss of loading and stimulation provided by gravity on the surface of Earth can be dire. This gravity reduction can potentially lead to health problems of the crew. In fact, research has identified serious biomedical risks arising from the absence of gravity during transit to Mars or during the long-term exposure of the human body to HG on the lunar or Mars surface. This thesis is devoted to providing a better understanding of this research problem. The focus lies on workplace design guidelines that can have a direct impact on the health, productivity, and well-being of a crew. Data collected from direct, indirect, subjective, and observational methods with experimental participants, and analyzing performance, fatigue, postural changes and comfort at the workplace, resulted in suggests options for extending standards, with subsequent recommendations and guidelines for workplace design in HG conditions.

Addressing such issues helps to reduce overall research and development costs, as well as

crew injuries and time requirements arising in currently ongoing as well as future space exploration programs. The accuracy of the simulation and calculations of HG simulated in aquatic environment may be affected by several potential errors. These include the estimation of body volume (3D body scan error), error of calculation of ballast weight distributed on the body of participants, inertia of ballasts and operational loads, friction, water temperature impact on the psychological and physiological state of participants, and transparency of the water which could affect the recognition of the human body or parts of the body. Also potential errors can be related to the errors of markerless motion capture algorithm, camera calibration (bundle adjustment, global registration), mean absolute error of keypoints and percentage of correct keypoints. Thus, all calculations and results presented here should be verified with other robust methods and platforms. Currently the most effective method in terms of cost and accuracy is simulation of HG under space flight-analogue conditions or suspension system.

6.2 Synthesis of research

The originality of this work lies in it being the first time that performance, posture, muscle fatigue and comfort of a participant was estimated depending on the load in conditions of HG at the workplace in a sitting posture, and that methods for using these data in calculation models were then proposed. In addition, modeling the biomechanics of the upper limbs at the workplace in conditions of HG is a new direction of research and there is still a lack of knowledge in this area.

HG simulation in underwater conditions is challenging for a number of reasons. The necessity of designing individual volume, the need for mass and volume-adapted adjustable weights for each segment of the participants, and the possibility to conduct only slow motions are challenges. In addition, there is the inertia of the ballasts, and time limitations for conducting experiments due to water temperature (max 1h of work underwater in diving suit is possible). Another issue is that this cross-disciplinary subject study combines biomechanics, physiology, engineering, ergonomics and computer vision aspects. This last aspect requires a good understanding of camera calibration mechanisms and precise techniques remain a challenge. The representation of normative human strength and endurance time (ET) for motion, as well as postural study, performance and comfort predictions had not been extensively researched under HG.

The preliminary subjective study of performance at the workplace showed that when working with an overload of $\frac{1}{6}$ G, the torso of participants deviated slightly backward compared to 1G. This may be due to the change in the position of the CoM in two different environments. These results provided an interesting direction for research. Further exploration of this finding was refined in postural study experiments. Subjective studies showed the decrease of weighted workload for the simulated HG in relation to 1G for repetitive tasks with loads on average of 3 kg, work with joystick and handwriting. At the same time subjective studies showed the increase of weighted workload for the simulated HG in relation to 1G for assembling task

and work with keyboard. These results are consistent with the results of a postural study at the workplace under HG previously discussed in (Volkova et al., 2022). Postural research was conducted because static force exertions should always be considered in relation to posture. In case of dynamic motions, like opening a drawer body fixation, friction and inertia should be considered. Unsuitable postures may decrease the required force as they increase the postural workload or decrease postural stability.

The results on body position change show that there is a tendency for the upper limbs of the human body and the trunk to tilt backward in the sitting position when performing static and dynamic tasks back under HG. Gravity change made a significant ($p < 0.01$) change in torso inclination, as well as upper extremities inclination. The use of the markerless tracking method captured these "invisible" to the eye trends at the end of the task, when the participant began to be tired, as this deviation occurs gradually.

It can be assumed that the body, even under load, tends to take a neutral position in which the person straightens their back and the upper limbs are slightly raised. The same trend was observed with CoM deviation, which confirms the calculations of the deviation of the angles of the torso and upper limbs of the participants in the experiment. For the vertical axis there was a significant deviation ($p < 0.01$) for all tasks for males in static tasks and in females in static and dynamic tasks. For the horizontal axis, only one significant correlation was observed for the significant ($p < 0.01$) CoM deviation in males in static tasks. This can be related to postural stability underwater and adaptation of the whole body to the new environment.

During fatigue study experiments, two trends were found in the empirical models, associated with different strength capabilities by gender. First, a significant positive ($p = 0.002$) relation was seen between endurance time and gravity level with a negative coefficient for males and females for a static task. Second, a marginal relation ($p < 0.1$) between weighted workload and gravity level with a positive coefficient for males and females was found for the same task. This trend was also observed for dynamic and repetitive tasks. It was, thus, concluded that the proposed objective method, combined with subjective assessment, can be useful for investigating human fatigue.

Experiments on the study of comfort in a sitting position in the workplace, when performing static and dynamic tasks, showed that there is a significant comfort increase in different parts of the body, especially the back ($p < 0.01$), neck ($p < 0.01$), upper and lower back ($p < 0.01$) with decreasing gravity level.

The proposed design optimization approach based on the measurement of human muscular fatigue and subjective comfort as a function of workload in HG conditions and design parameters leads to design solutions for biomechanics-centered design at the workplace under HG. The proposed data-based design optimization approach of the experiments, with a further extension of existing human factor standards, opens new design possibilities that in the future may well be recognized by a wider range of professionals in the field of workplace design.

The combination of multidisciplinary data can be scaled more generally to working space ergonomics under HG. With this data, it is possible to design and optimize workplace and manual operations. Because physical fatigue is included in the model, such workplace design requires less effort. This also has the potential of reducing repetitive strain injuries and musculoskeletal disorders which are common in numerous workplace situations and which contribute to absenteeism and thus additional costs for the workforce.

This study helps to fill the knowledge gap and validate static/dynamic contraction ET (fatigue level) models for all major joints (elbow, shoulder, etc.). These models can be relevant to ergonomic applications under HG conditions and help identify potential sources for injury under HG. This study could also support muscle fatigue (MF) study in an 1G environment, as there is still ongoing work about which the static contraction ET model provides the most accurate fatigue prediction.

Parabolic flight experiments may help to validate measurements captured in the aquatic environment. It is because underwater experiments presents a lower-cost approach but is also less representative than parabolic flights. Parabolic flight could ensure that all potential errors and inaccuracies can be eliminated for future experiments focused on the study of the upper part of the body in HG. Such experiments may also help identify deviations from mathematical modeling (the lowest-cost approach) and further apply this knowledge to predict similar and more complex movements with increased accuracy.

In conclusion, one of the main issues addressed in the current study was the issue of fatigue and associated fatigue identification parameters such as postural condition, performance, and comfort of different body parts of the participants in HG simulation. While legacy standards for workplace ergonomics and biomechanics may still be relevant, they are barely amenable to conclusions from experimental results. In this regard, cumulative experiments have been shown to be a solution for obtaining valuable information from multiple tests combining performance, postural exploration, fatigue, and comfort parameters. By combining several studies into one, it is possible to significantly reduce the time, sampling, and analysis required to extract information from devices.

This study attempted to provide models of fatigue and posture in HG and better understand the effects of HG on human physiology. The research conducted for this thesis may lead to the development of new standards for the design of work and living spaces within HG.

6.3 Limitations of this thesis

In the frame of this thesis, experiments were conducted that focused on assessment of participant performance, body postures (including joint angles, torques, forces and CoM changes) at the workplace, upper extremity muscular fatigue, pushing/pulling motion studies and seated discomfort under HG. Each of these studies has limitations and the main ones for each experiment are discussed below.

6.3.1 Performance at the workplace

This was one of the first studies and carried out as a proof-of-concept in the very beginning of this research. A simplified apparatus for registering movement underwater was used to obtain the initial data and develop motion analysis algorithms; a home-based swimming pool was used to simulate the HG environment. Additionally, all electronics were used in test mode to prepare for more global experiments. Under such conditions, it was difficult to collect reliable data because of the poor visibility in underwater conditions, which was mainly caused by poor lighting or the turbidity of the water. It was also found that the recognition did not function to its fullest potential because of the black color of the diving suits during the experiment. New tests with different bright colors were carried out to compare the motion recognition quality of the participants. Another limitation of this experiment was the sample size and duration of the tasks, as well as the quantity of selected tasks. Finally, self-reported data can be considered as a limitation of this study, because it can rarely be independently verified.

6.3.2 Postural study

While the results of the experiments on this topic were consistent with those on fatigue, and also in good agreement with the approaches of the European standards for ergonomics, there were still some limitations. In general, these are associated with the limited number of motions analyzed. This study focused on the analysis of only static and dynamic motions, while the fatigue studies also investigated repetitive tasks and additional types of static tasks. This is because of the large amount of video data and the complexity of processing the data collected with three cameras for the postural study. Other relevant limitations are outlined in the muscular fatigue study limitations section. Another limitation is related to the markerless motion capture OpenPose model, because the skeleton model lacks detail on the participant's back and is represented by a straight line segment. Therefore, additional studies should be carried out to test the influence of the back on the displacement of the CoM. Validation is recommended for all defined empirical dependencies between the angles, forces, torques, subjective responses and workload of participants with parabolic flights that are adapted to specific environments. The study of fatigue on posture is a novel method of exploration of a participant's fatigue states under HG. Martian gravity can be suggested for the next experiments related to this research direction. Validation of numerically predicted hip torques under $\frac{1}{3}G$ with a larger number of participants is recommended.

6.3.3 Fatigue study

While some valuable results were obtained, there were several limitations to the fatigue study. The main limitation arose from variations in age, anthropometry and in carrying out asymmetric tasks. To determine these effects, it is important that future studies analyze younger and older, as well as weaker and stronger populations. Symmetric tasks should also be investigated. In addition, it is recommended to validate $\frac{1}{3}G$ fatigue curve with a larger number of participants.

is recommended. Finally, the validation of all defined empirical and subjective models with parabolic flights or suspension system adapted to specific environments can be suggested for the next experiments. Finally, more intensive motions (less than 47 cm/s) in underwater enrolments could be tested during future experiments to assess the impact of HG.

6.3.4 Pushing and pulling study

This was a proof-of-concept study for which a custom-made wooden structure was designed. It is recommended that higher-quality test items be designed and a larger sample size used to be able to find significant relationships from the data. Additionally, tests under Martian gravity are recommended.

6.3.5 Combinatorial study

Although the combinatorial studies allowed for a better understanding of human biomechanics at the workplace under HG, further research on this topic is needed. This is necessary both to validate the obtained results with another method, and for further study of human movements in the workplace with a large number of operational tools. Experiments that take into account the interaction of people in the workplace are also recommended, with a minimum of two people rather than isolated movements of individuals.

In this study, one main design parameter was proposed for testing, but additional design configurations may be considered, such as head support, restraint system handrail and armrests design. The method proposed here for workplace optimization may work better given the greater amount of data obtained from experiments testing new design criteria. This is also due to the fact that the proposed method makes it possible to monitor the movement of the center of mass of the participants in the experiment and, as noted earlier, the inertial rotation around the CoM can be a potentially significant factor for motion studies under HG. The existing DHM is limited to modeling such phenomena

6.3.6 Seated discomfort study

The main limitation of this study is the reliability of self-reported data. In the future, it is recommended that joint experiments be conducted not only with subjective but also with objective data such as, for example, postural data collected with vision-based methods. An increased number of participants or additional configurations of the workplace could also be assessed.

6.4 Ethical issues

All data was anonymized in line with the Swiss Federal Official Responsible for Data Protection and Transparency. All ethical approvals were obtained from the ethics committee of both organizing sides. All participants signed a consent form approved by the EPFL ethics committee. All anonymized recordings and data of the subjects were stored on the hard drive/server of the Space Innovation at EPFL and protected by a password.

The generating, processing, and storing data in this project do not pose a particular data security risk. The analysis was conducted on workstations in the EPFL-domain.

Data storage and preservation. Data were stored for a year after the experiment. Data are accessible after applying for a revision of the Ethical approval.

Data sharing and reuse. All the ongoing data were not shared. All relevant data were available from the principal investigator upon request and after approval from the ethical committee. Several statistical results or analyses can be published in peer-reviewed scientific journals. No pictures of participants were published. All unpublished data will be stored at data repository 12 months after the end of the experiment.

6.5 Future works

This subsection is intended to open discussion on future directions that may be taken following this study, including the conducting global experiments under HG environment in a neutral buoyancy/hydrolaboratory (pool), conducting parabolic flight experiments to verify the results of experiments conducted underwater, neutral posture studies under HG in a sitting and standing positions, further improvement of computer vision in underwater conditions, application of innovative methods for HG simulation, further assessment of workplace optimization problems.

6.5.1 The whole habitat experiments under HG

Future direction involves conducting global experiments under an HG simulation environment with a large number of tasks and various objects to detect human biomechanics, as well as physiological and subjective responses under HG. Experimental studies of this type could be carried out according to separate programs and methods onboard an Il-76MDK, Airbus A-300 Zero-G, or G-Force One, in neutral buoyancy/hydrolaboratory (pool) settings and in the simulator of a suspension system on Earth, i.e., Simulator "Voshod-2" or analogs. Representatives of relevant organizations interested in the results should also participate in the study. Models proposed for experiments should preliminarily be land tested and approved by the principal investigator and university or administrative/ethical committee to conduct research experiments under the necessary conditions. The concept of experimental study assumes that the measurements will be carried out onboard aircraft associated with the numerical models

(because they have the highest reliability), with the study of the dynamics of movements under conditions of HG and with definition of a scheme of weights for other types of experiments. Because such experiments are limited in time, weight and size, only specially selected objects would be involved in the environment.

Unlike an aircraft cockpit cabin, in a neutral-buoyancy/hydrolaboratory, an entire habitat can be constructed and relatively long experiments can be conducted. However, experiments on aircraft can be challenging and require calculations for the distribution of weights for each segment of the body according to a validated numerical biomechanics model. To further develop the research of this dissertation, additional experiments analyzing working conditions should be carried out in more spacious conditions, e.g., at the neural buoyancy facility of the European Astronaut Centre in Germany. Under such conditions, a wider range of test conditions can be explored. A number of operating conditions are recommended for study. Simulation objects can include adjustable furniture such as seats, beds, desks and sanitary fixtures. The detailed list of the experimental objects for a particular study can be defined by the experimental plan. Potential task maneuvers (typical activity) for the experiments are listed below:

- Tasks at the workplace conducted in a standing position;
- Tasks that require a regular transition from a sitting to a standing position;
- Tasks involving pushing and pulling in a standing posture;
- Tasks at the workplaces with different configurations (seats, backrests, stripes);
- Tasks with opening and closing hatches;
- Symmetric tasks conducted with both hands.

The following working tools could be tested: control panels, control levers, steering wheels, tactile screens and production-line equipment. New experimental tasks could involve multiple people, which would enable the assessment of human interaction and decision-making problems. Additionally, full immersion of the head may be an alternative to experiments with partial immersion. In this case, professional divers who feel comfortable underwater are recommended when selecting participants for the experiments. Immersion should be carried out in the following conditions:

- Water temperature 28–30 degrees;
- Participants should be allowed to self-dive in open water (if they have a diver certificate);
- Participants must be accompanied by rescue divers (by two divers for one participant); During the working day, a total immersion of not more than 2 h is allowed, and the duration of continuous immersion is no more than 1 h. A simultaneous plunge of 15 people maximum is allowed (including rescue divers).

Experiments on a suspension system on Earth are the cheapest and most efficient; however, they cannot be used inside the habitat or accurately reproduce the biomechanics of humans in HG. Therefore, their use is assumed for the development of specific operations carried out in reduced gravity and research around the functionality of individual objects of study.

Experimental setup proposal

A mockup of a workplace for sitting, lying, and standing postures and a restraint system should be installed in the underwater environment. The mockup of the furniture must have mesh surfaces that interact with the participant, this is to avoid a reduction in Archimedean force, which does not act on the contact area because of a lack of pressure. The mockup must be equipped with strain gauges that measure the forces on the contact surfaces as well as contact sensors to determine the area of contact with the supporting surface. Additionally, it should have moisture-proof strain gauges and touch sensors that are capacitive with contact closure as contact sensors.

The video equipment should be placed around the workplace in the underwater environment. This allows for recording the entire body of the participant or several experiments at the same time. It is recommended to use good illumination and interferometry to improve measurement accuracy. Additionally, it is recommended that the time resolution of the recording sensor readings be set to one second. Calibration must be performed to ensure the operation of video equipment underwater. It is important to provide corrections for the refractive index and absorption coefficient, as well as increased dispersion. It should be noted that the proposed experimental equipment would require the use of low-voltage power supplies and certification of the insulation of devices according to electrical safety rules.

6.5.2 Parabolic flight experiments for validation purposes

Experiments of this type were designed for the ESA CORA program in the frame of this research but were postponed because of time constraints and COVID-19 related issues. These or analogous experiments can be conducted for validation of those conducted in the underwater environment. The details of the experiments are provided below and in the Appendix, Section A.3.

The proposed experiment using a parabolic flight intends to measure endurance time (ET), a main variable related to MF evaluation, through a series of high-load/short-duration tasks under HG with hand-held weights carried in various static/dynamic postures. To date, these experiments have been modeled mathematically and further validated in aquatic environments adapted to HG. This unique type of experiment under spaceflight-analog conditions would be able to realize three objectives:

- Collect high-quality data in a representative HG environment;

- Identify and understand deviations with mathematical simulations and aquatic environment testing to advance experimental capabilities for measuring upper extremity body MF in HG conditions (including inertial effects);
- Compare several workplace design options suitable for HG to provide recommendations and guidelines for improved design.

Such experiments may significantly contribute to HG research and effects on crew energy and time requirements, thus paving the way for cost-efficient and practical designs for manned infrastructure and hardware in space. Data collection equipment can include force plates, dynamometers, load cells built into the experimental workplace and video cameras. Load cells and force plates help calculate the reaction forces of the participants at the workplace. These measurements would be performed continuously. Hand dynamometers would be used to measure the maximum strength of the hand and forearm muscles. This measurement should take place before and after the completion of each proposed task by the participant.

Video data would be used for upper extremity joint angles, displacement changes during the study. A multi-camera setup would capture the body of objects in 360 degrees. All this data is necessary to estimate the participants' upper extremity body fatigue. These recordings would need to be performed continuously. Upper extremity body fatigue is understood as time processes and represents the functional capacity of the wrist, elbow, shoulder of the participant as a result of the action (task with operational loads in hand).

Measuring the effects of fatigue - the experiments would be performed in accordance with Rhomert's curves defined for example by (Rohmert, 1960) or recent study of (Volkova et al., 2022) and at given intervals of time. After static/dynamic holding tasks of different intensity (loads variation) and duration, the maximum strength still available could be compared with the maximum strength measured before the test. For each participant, the specific intensity (load) would be defined according to their individual capacities.

Mathematically predicted joint profiles with D'Alembert's principle and Lagrangian formulation (joint angles and torques) should be validated under spaceflight-analog conditions. However, the differences in values may be associated with the disadvantages of conducting experiments in an aquatic environment.

It is still challenging to simulate a HG environment, especially dynamic motion, because of inertia changes. Different factors can make an impact on "real" value measurements: the impact of water resistance on movement, intrusive attachment of the ballast to the trunk, forearm, upper arm, and movements faster than 47 cm/s .

Depending on the potential availability and conditions, a minimum of one and a maximum of six participants between the ages of 30 and 50 are recommended for participation in the experiment. All participants should correspond to the criteria (age 35 ± 5 years, height $180 \pm 5\text{ cm}$ (male) and $170 \pm 5\text{ cm}$ (female), weight $78 \pm 7\text{ kg}$ (male) and $60 \pm 5\text{ kg}$ (female) and be

healthy according to the physical activity readiness questionnaire (Warburton et al., 2019). It is advisable to invite the same participants who participated in the land and aquatic experiments.

Proposed sitting postures with weight holding:

- Sitting position with ischial support, without resting back on a chair;
- Sitting position with ischiosacral support;
- Sitting position with ischiofemoral support.

During realization of the motions (tasks) described in the previous paragraph, all participants would be filmed by 6 GOPRO HERO 8 cameras (or its analogous) installed around the experimental setup are necessary to apply a markerless computer vision approach for efficient data extraction. Additionally, a Kinect XBOX ONE or LiDAR-based camera (a camera that uses a laser to determine the distance between the camera and an object/surface) should be used for video data recording and for further motion capture studies. Then, evaluation of the subjective weighted workload would be realized based on the NASA-TLX approach.

Chairs type 1 Parabolic flight company/Aircraft supplier could potentially provide one aircraft chair for sitting upright postures studies. An aircraft chair with ten flexible pressure sensors (load cells) placed on the seat adapted for sitting postures is presented in Figure 6.1. The collected data would include video data, weight of the participants, reaction forces from the legs, and hand strength. This setup helps to validate the dependencies obtained during aquatic experiments (joint torques, joint angles, and joint-specific statistical fatigue).

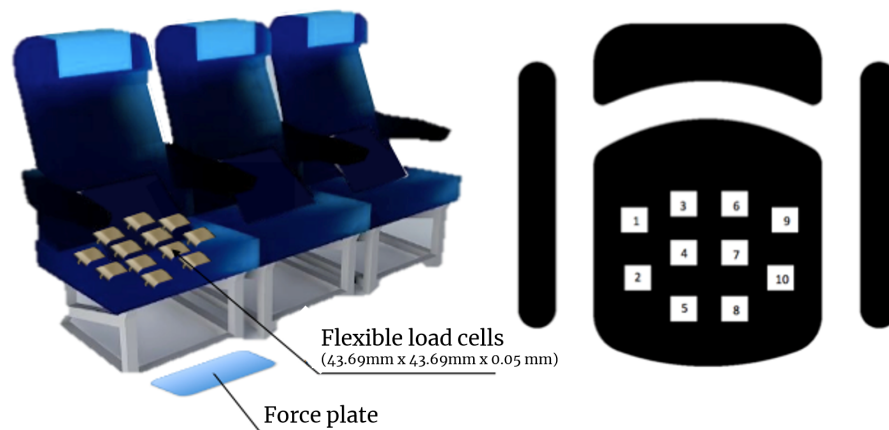


Figure 6.1: (A) A general view of the chair. (B) Sensor distribution on the seat. Sensors were numbered from one to ten

Chairs type 2 (two chairs - rack)

Two different configurations for the chairs integrated into the rack allow for study of the effects of backrest recline on the human body (chair 1) and the effects of forward tilt seating, as seen in Figure 6.2 and Figure 6.3. The seats attached to the strain gauges would be sewn in 8 lines, with 2 layers of trampoline net integrated under the seats for safety reasons. The collected data would include video data, weight of the participants, reaction forces from the legs, and hand strength. This experiment would validate dependencies obtained during an aquatic experiment (joint torques, joint angles) and compare these design options of a workplace suitable for HG. Additionally, this study should verify the hypothesis related to the reduction of muscle activity and changes in the intervertebral discs. In chair 2 (backward tilt), a reverse decrease in lumbar lordosis compared to other seated positions and an increase in gluteal tension as well as a decrease in intervertebral discs pressure and lumbar muscle activity can be verified. Previous studies by Pynt, 2015 demonstrated the evidence of these effects under Earth gravity.

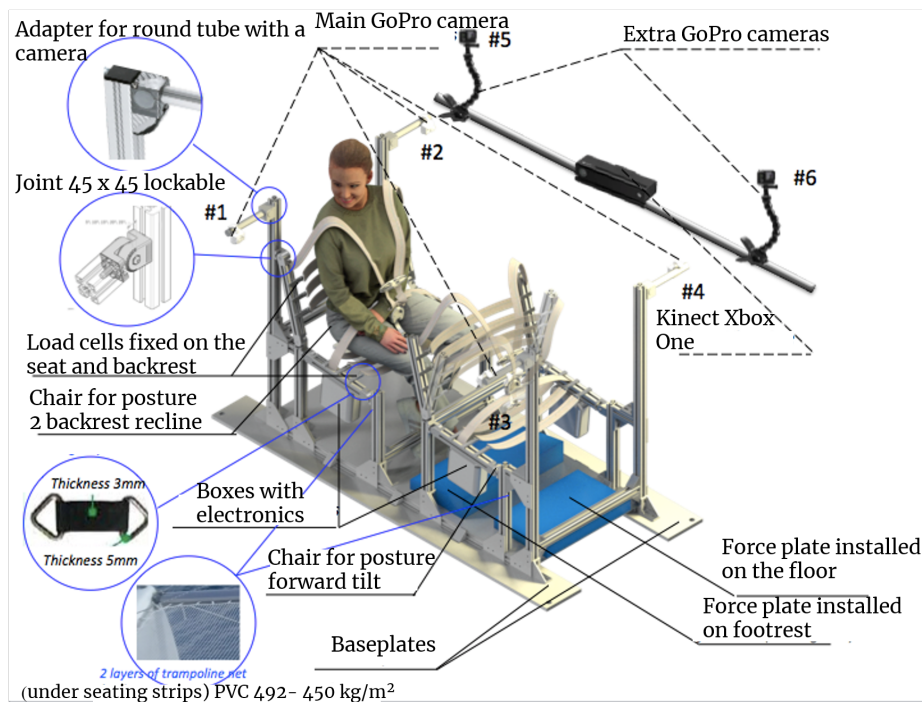


Figure 6.2: General view of the rack with two mounted chairs with explanation

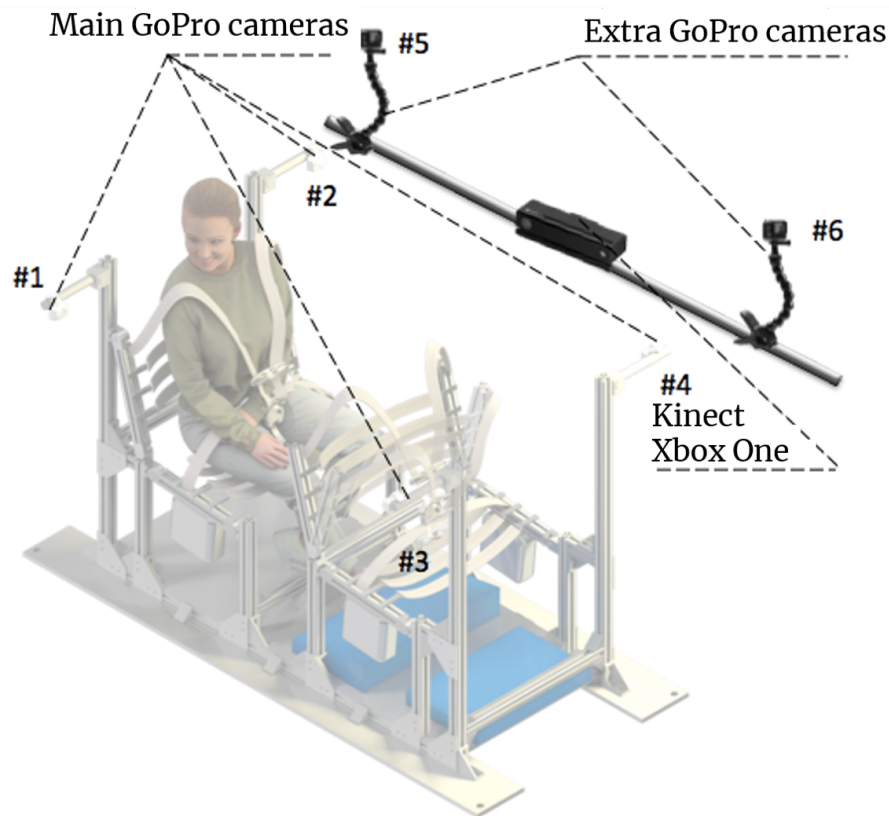


Figure 6.3: Layout of cameras on the rack and around the rack

Experimental setup proposal

Due to multiple person recognition, each participant would be assigned an individual code, called a tracking tag, to help identify the specific participant. The code would need to be placed on the participants' outerwear. Post-processing analysis would only include participants with their personal code. The experimental setup is presented in Figure 6.2 and Figure 6.3. A standard chair as well as a rack-chair system equipped with seat belts would be provided for participants, and during experiments, all three participants would be prompted to sit in the chairs buckled up. Three cameras installed around a standard chair would record the motions of the first participant.

At least four cameras mounted on a cylindrical bar with an adaptor fixed to the vertical profiles would record the motions of the third and fourth participants (see Figure 6.3). For all three postures, a force plate would measure the reaction forces of the feet. In the case of the second posture (pelvis tilted backward), the force plate would be installed on the footrest, which would be inclined 10 degrees. Before and after each parabola (during a hypergravity maneuver), the grip strength of each participant would be measured and recorded via a digital hand

dynamometer.

Once the rack is attached to the cabin and a standard aircraft chair is prepared for the experiment, in-flight operations would commence. The study is divided into three different flights to be completed during the flight campaign. Thus, there are three experiments per flight conducted by three participants (flight operators). For each new flight, the three experiments would be repeated with three new participants. Once in-flight operations start, the experiment would be switched. After the first warming parabola, three sets for $\frac{1}{3}G$, $\frac{1}{6}G$ and MG each are performed with a 1 min (or more) separation between parabolas on the same set.

6.5.3 Neutral posture under HG identification

Further identification of the neutral position of the human body in a sitting position under hypogravity at the workplace to maintain and improve human performance on the Moon and Mars is recommended.

6.5.4 Computer vision in underwater conditions

Further application of computer vision in underwater conditions is possible with the participation of only one camera and LiDAR. Using computer vision underwater is quite a labor-intensive task. When using conventional cameras, at least three cameras are needed but more cameras should be used to improve accuracy. The number of cameras also depends on the area of the scene being filmed and the visibility of all people and objects on the scene. Because of new computer vision technologies, such as LiDAR cameras, it is possible to apply new approaches to filming and it is important to speed up data processing. The LiDAR camera is recommended for new research due to the ability to film with a single camera. With the help of a laser, light is reflected from the object being filmed, which could help in the future to create a 3D image of the object being filmed.

6.5.5 New methods of HG simulation

New methods of simulating HG can be developed, e.g., by using a robotic arm such as the Kuka robot. Experiments have already been carried out to fully compensate $1G$ with the help of such a robotic arm. By analogy, weight on earth can be compensated to simulate the weight on the Moon or Mars. Thus, the robot can accompany the movements of the human hand according to a given scenario, and then, these movements could be analyzed using the above computer vision methods.

6.5.6 Workplace optimization based on fatigue and postural study

Little is currently known about the impact of HG (specifically, $\frac{1}{6}G$ - $\frac{1}{3}G$) on the participant's body in the built environment. There is also no established baseline for design of living and

working places.

It is essential to take into account HG during optimization of workplace design. In the numerical model adapted to the HG, not only the effect of the gravity level on the weight, but also corrections for rotation and impulse loads under the conditions, must be taken into account. New optimization functions could be considered for such optimization, for example, physiology-related, or muscle-contraction related.

The risk of poor workplace design is related to the lack of human-centered design. Analyzing the root cause of the inefficiencies of such workplace design in HG conditions is needed. Such a design should be implemented throughout the design process. One of the most efficient approaches, from the point of view of this author, would be to create a good ergonomic design with integrated biomechanical modeling based on the MOO. This should also include safety and human performance concerns, as well as quality and productivity. A good human-centered design increases the efficiency of safety and operation of all workplace components and should as a consequence have a positive impact on cost.

A An appendix

A.1 Supplementary figures and tables

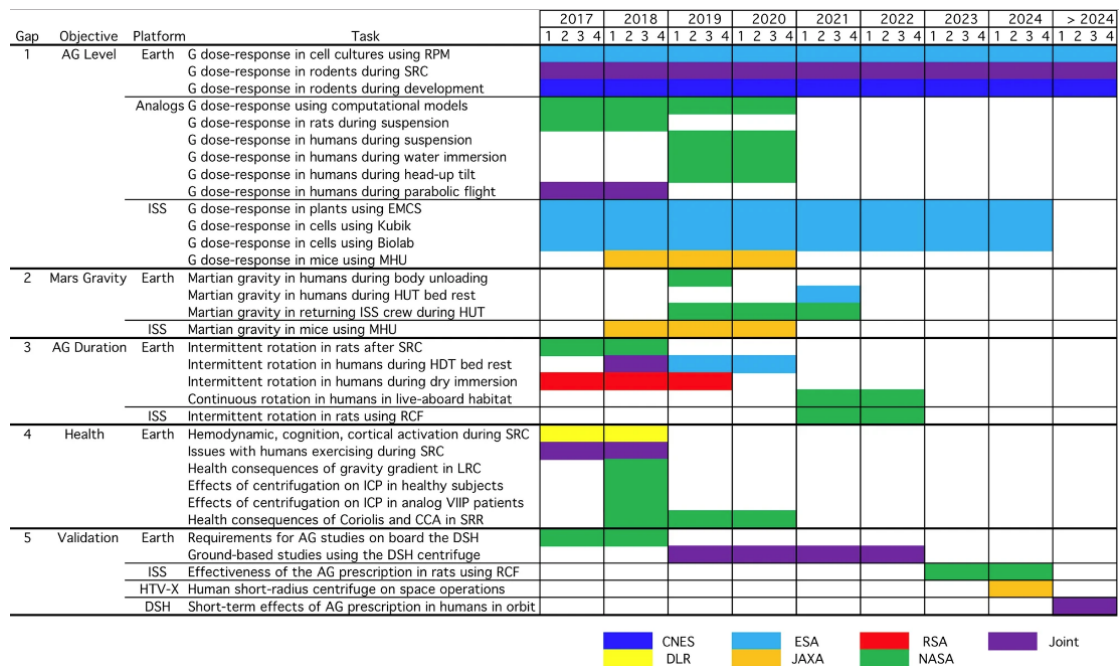


Figure A.1: The international road map of artificial gravity research summarizes the current and future research activities of different countries on artificial AG (Clément, 2017). Copyright © 2017, Clement, Creative commons license CC BY

	Footloops	Skylab Food Table Restraints	MIR Seat Restraints	Munich Space Chair	FLOW
Positive Characteristics	Light and cheap mounted anywhere, where needed fast fixation wide reach	Good stabilization Can be stowed away easily	Simple, clear system Quick fixation	Good and comfortable fixation for long-duration and high precision work	Good and comfortable fixation for long-duration and high precision work Fast ingress
Negative Characteristics	Foot muscles stabilize whole body, Difficult to used for high precision work	Only one dedicated use Only in combination with footloops	Uncomfortable Stay in the way when not used	Set up time, Relatively big storage volume Stays in the way, if not used	TBD
Interface with space station	4	2	2	4	8
weight	10	5	4	6	7
volume	10	8	5	4	8
modularity	7	4	2	4	8
flexibility	10	2	2	6	10
Simple to use	10	6	10	8	10
Ingress/egress time	9	8	9	9	10
Short-term comfort	8	8	6	10	10
Long-term comfort	4	6	1	10	10
Correct posture for tasks	4	8	2	10	10
reach	10	6	4	8	8
TOTAL (110)	86	63	47	79	99

Figure A.2: Chairs comparison (Vogler, 2005). Comparative evaluation of upper thigh restraint systems compared to foot loops. Scores from 1-10 have been given on estimation by the author. *Republished with permission of SAE International, from Design study for an Astronaut's workstation, Vogler, Andreas, SAE Technical paper series, 2005-01-3050, copyright 2022; permission conveyed through Copyright Clearance Center, Inc.*

Table A.1: Cons and pros of markerless motion capture method

Markerless	With markers
<p>Pros</p> <ul style="list-style-type: none"> • Easy to use • High precision • Easy to process the data <p>Cons</p> <ul style="list-style-type: none"> • Occasional errors due to appearance ambiguities can confuse background objects with persons • Requires sufficient light 	<p>Pros</p> <ul style="list-style-type: none"> • No false positives, more reliable as long as sufficient number of markers are placed, and these remain in their designed locations <p>Cons</p> <ul style="list-style-type: none"> • Can't be scaled to crowds and un-cooperative settings • Difficult to use in, e.g., underwater conditions and on most clothing (astronaut suites that can't be modified, loose clothing, or due to sweating) • Doesn't work in most practical scenarios, where the subject's body comes in contact with other surfaces and physical contact would dislocate or detach markers

Table A.2: Organizational Structure of ISO TC 159 "Ergonomics" (Karwowski et al., 2021)

Organizational Structure of ISO TC 159 "Ergonomics"	
Committee	Title
TC 159/SC 1: Ergonomic guiding principles	
TC 159/SC 1/WG 1	Principles of the design of work systems
TC 159/SC 1/WG 2	Ergonomic principles related to mental work
TC 159/SC 1/WG 4	Usability of everyday products
TC 159/SC 3: Anthropometry and biomechanics	
TC 159/SC 3/WG 1	Anthropometry
TC 159/SC 3/WG 2	Evacuation of working postures
TC 159/SC 3/WG 4	Human physical strength: manual handling and force limits
TC 159/SC 3/WG 5	Ergonomic procedures for applying anthropometry and biomechanics ?
TC 159/SC 4: Ergonomics of human-system interaction	
TC 159/SC 4/WG 1	Fundamentals of controls and signaling methods
TC 159/SC 4/WG 2	Visual display requirements
TC 159/SC 4/WG 3	Control, workplace, and environmental requirements
TC 159/SC 4/WG 5	Software ergonomics and human-computer dialogues
TC 159/SC 4/WG 6	Human-centered design processes for interactive systems
TC 159/SC 4/WG 8	Ergonomic design of control centers
TC 159/SC 5: Ergonomics of the physical environment	
TC 159/SC 5/WG 1	Thermal environments
TC 159/SC 5/WG 2	Lighting environments
TC 159/SC 5/WG 3	Danger signals and communication in noisy environments

Note: TC- technical committee; SC - subcommittee; WG - working group. *Copyright (Taylor Francis Group, LLC © 2021) From (Handbook of standards and guidelines in human factors and ergonomics) by (Karwowski, Waldemar and Szopa, Anna and Soares, Marcelo M/Crc Press). Reproduced by permission of Taylor and Francis Group, LLC, a division of Informa plc.*

Table A.3: Organizational Structure of CEN/TC 122 (Karwowski et al., 2021)

Organizational Structure of CEN/TC 122	
Working Group	Title
CEN/TC 122/WG 1	Anthropometry
CEN/TC 122/WG 2	Ergonomic design principles
CEN/TC 122/WG 3	Surface temperatures
CEN/TC 122/WG 4	Biomechanics
CEN/TC 122/WG 5	Ergonomic of human-computer interaction
CEN/TC 122/WG 6	Signals and controls
CEN/TC 122/WG 8	Danger signals and speech communication in noisy environments
CEN/TC 122/WG 9	Ergonomics of personal protective equipment
CEN/TC 122/WG 10	Ergonomic design principles for the operability of mobile machinery
CEN/TC 122/WG 11	Ergonomics of the thermal environment
CEN/TC 122/WG 12	Integrating ergonomic principles for machinery design

Note: CEN - european committee for standardization ; TC -technical committee ; WG - working group. Copyright (Taylor Francis Group, LLC © 2021) From (*Handbook of standards and guidelines in human factors and ergonomics*) by (Karwowski, Waldemar and Szopa, Anna and Soares, Marcelo M/Crc Press). Reproduced by permission of Taylor and Francis Group, LLC, a division of Informa plc.

Table A.5: Part of published CEN standards for ergonomics

Published CEN Standards for Ergonomics		
CEN Reference	Title	ISO Standard
EN ISO 10075-1:2017	Ergonomic principles related to mental workload - Part 1: General issues and concepts, terms, and definitions	ISO 10075:1991
EN ISO 10075-2:2000	Ergonomic principles related to mental workload - Part 2: Design principles	EN ISO 10075-2:1996
ENV 6385:1990	Ergonomic principles of the design of work systems	ISO 6385:2016
EN ISO 6385:2016	Ergonomic principles in the design of work systems	ISO 6385:2016
Anthropometries and biomechanics		
EN 1005-1:2001	Safety of machinery - Human physical performance - Part 1: Terms and definitions	
EN 1005-2:2003	Safety of machinery - Human physical performance - Part 2: Manual handling of machinery and component parts of machinery	
EN 1005-3:2009	Safety of machinery - Human physical performance - Part 3: Recommended force limits for machinery operation	
EN 13861:2011	Safety of machinery - Guidance for the application of ergonomics standards in the design of machinery	
EN 547-1:2009	Safety of machinery - Human body measurements - Part 1: Principles for determining the dimensions required for openings for whole-body access into machinery	

Note: Copyright (Taylor Francis Group, LLC © 2021) From (*Handbook of standards and guidelines in human factors and ergonomics*) by (Karwowski, Waldemar and Szopa, Anna and Soares, Marcelo M/Crc Press). Reproduced by permission of Taylor and Francis Group, LLC, a division of Informa plc.

Table A.6: ISO Standards for ergonomics guiding principles (Karwowski et al., 2021)

ISO Standards for ergonomics guiding principles	
Reference Number	Title
ISO 6385:2016	Ergonomic principles in the design of work systems
ISO 10075:1991	Ergonomic principles related to mental workload-General terms and definitions
ISO 10075-2:1996	Ergonomic principles related to mental workload-Part 2: Design principles
ISO/FDIS 10075-3	Ergonomic principles related to mental workload-Part 3: Principles and requirements concerning methods assessing mental workload
ISO/CD 20282-1	Ease of operation of everyday products-Part 1: Context of use and user characteristics
ISO/CD TS 20282-2	Ease of operation of everyday products-Part 2: Test method

Note: Copyright (Taylor Francis Group, LLC © 2021) From (Handbook of standards and guidelines in human factors and ergonomics) by (Karwowski, Waldemar and Szopa, Anna and Soares, Marcelo M/Crc Press). Reproduced by permission of Taylor and Francis Group, LLC, a division of Informa plc.

Table A.7: Functional factors in sitting (Corlett et al., 1995)

Functional Factors in Sitting
The task
Seeing
Reaching
Exerting forces
The sitter
Support weight
Resist accelerations
Under-thigh clearance
Trunk-thigh angle
Leg loading
Spinal loading
Neck/arms loading
Abdominal discomforts
Stability
Postural changes
Long-term use
Acceptability
Comfort
The seat
Seat height
Seat shape
Backrest shape
Stability
Lumbar support
Adjustment range
Ingress/egress

Note: Copyright (Taylor Francis Group, LLC © 2005) From (Evaluation of human work) by (John R. Wilson and Nigel Corlett). Reproduced by permission of Taylor and Francis Group, LLC, a division of Informa plc.

Item	Endpoints	Description
Mental demand	1 - 10 Low / High	How much mental and perceptual activity was required (e.g., thinking, deciding, calculating, remembering, looking, searching, etc.)? Was the task easy or demanding, simple or complex, exacting or forgiving?
Physical demand	1 - 10 Low / High	How much physical activity was required (e.g., pushing, pulling, turning, controlling, activating, etc.)? Was the task easy or demanding, slow or brisk, slack or strenuous, restful or laborious?
Temporal demand	1 - 10 Low / High	How much time pressure did you feel due to the rate or pace at which the tasks occurred? Was the pace slow and leisurely or rapid and frantic?
Performance	1 - 10 Good / Poor	How successful do you think you were in accomplishing the goals of the task set by the experimenter (or yourself)? How satisfied were you with your performance in accomplishing these goals?
Effort	1 - 10 Low / High	How hard did you have to work (mentally and physically) to accomplish your level of performance?
Frustration level	1 - 10 Low / High	How insecure, discouraged, irritated, stressed and annoyed versus secure, gratified, content, relaxed and complacent did you feel during the task?

Figure A.3: The description of the subjective demands of the NASA-TLX survey (Rubio et al., 2004). *Republished with permission of BLACKWELL PUBLISHING, from Evaluation of Subjective Mental Workload: A Comparison of SWAT, NASA-TLX, and Workload Profile Methods, International Association of Applied Psychology/Rubio et al. , copyright 2022*

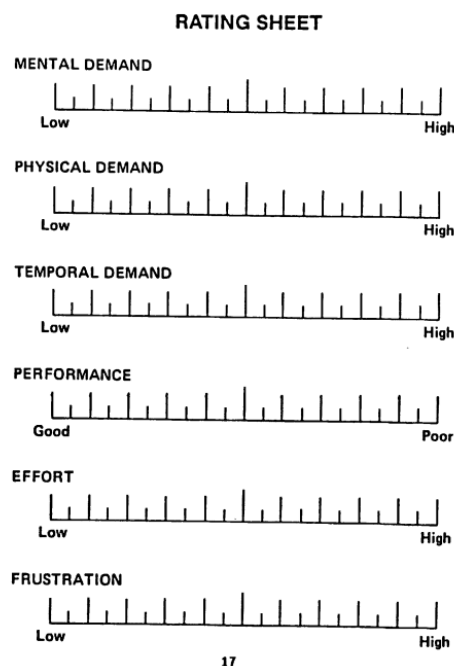


Figure A.4: NASA-TLX 100 points rating scale (Rubio et al., 2004). *Republished with permission of BLACKWELL PUBLISHING, from Evaluation of Subjective Mental Workload: A Comparison of SWAT, NASA-TLX, and Workload Profile Methods, International Association of Applied Psychology/Rubio et al. , copyright 2022*

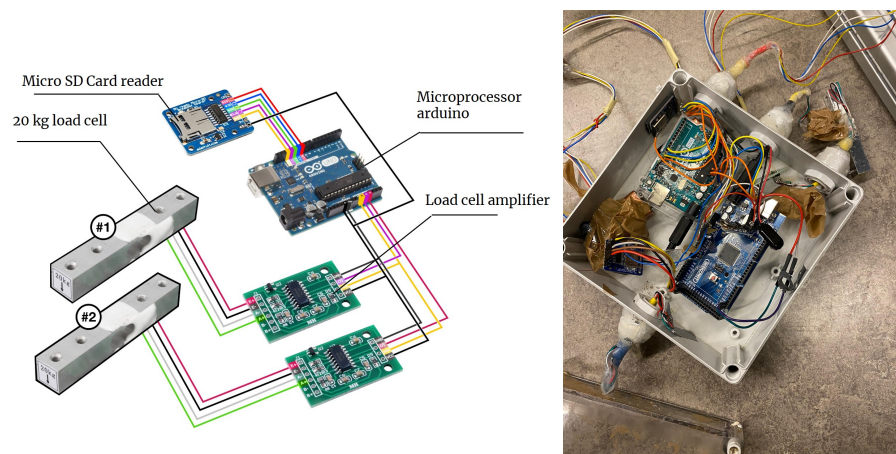


Figure A.5: Scheme of electronic for sitting part reaction force recording

GENERAL HEALTH QUESTIONS		
Please read the 7 questions below carefully and answer each one honestly: check YES or NO.	YES	NO
1) Has your doctor ever said that you have a heart condition <input type="checkbox"/> OR high blood pressure <input type="checkbox"/> ?	<input type="checkbox"/>	<input type="checkbox"/>
2) Do you feel pain in your chest at rest, during your daily activities of living, OR when you do physical activity?	<input type="checkbox"/>	<input type="checkbox"/>
3) Do you lose balance because of dizziness OR have you lost consciousness in the last 12 months? Please answer NO if your dizziness was associated with over-breathing (including during vigorous exercise).	<input type="checkbox"/>	<input type="checkbox"/>
4) Have you ever been diagnosed with another chronic medical condition (other than heart disease or high blood pressure)? PLEASE LIST CONDITION(S) HERE:	<input type="checkbox"/>	<input type="checkbox"/>
5) Are you currently taking prescribed medications for a chronic medical condition? PLEASE LIST CONDITION(S) AND MEDICATIONS HERE:	<input type="checkbox"/>	<input type="checkbox"/>
6) Do you currently have (or have had within the past 12 months) a bone, joint, or soft tissue (muscle, ligament, or tendon) problem that could be made worse by becoming more physically active? Please answer NO if you had a problem in the past, but it does not limit your current ability to be physically active. PLEASE LIST CONDITION(S) HERE:	<input type="checkbox"/>	<input type="checkbox"/>
7) Has your doctor ever said that you should only do medically supervised physical activity?	<input type="checkbox"/>	<input type="checkbox"/>

Figure A.6: The 2020 Physical Activity Readiness Questionnaire for Everyone (PAR-Q+) (Warburton et al., 2019)

Body part	Trial 1		Trial 2		Trial 3	
	Beg	End	Beg	End	Beg	End
Head						
Neck						
Shoulders						
Upper back						
Lower back						
Hips/thighs						
Feet						

Figure A.7: Template for comfort survey (Corlett, 1976). Note: Copyright (Taylor & Francis Group, LLC © 2005) From (Evaluation of human work) by (John R. Wilson and Nigel Corlett). Reproduced by permission of Taylor and Francis Group, LLC, a division of Informa plc.

A.1.1 Camera calibration

This section was developed with a support of CVLab documentation (“Github”, 2022).

Setting up the camera for intrinsics estimation:

(a) The camera must be in the same mode/configuration as in the the final system, that is to say, the same zoom, focus, aperture, resolution, etc. should be used. If the camera will be used in video mode in the final system, it should be used in the same mode here as well. (b) Auto-focus, auto-stabilization or other such features that dynamically alter the geometry of the image must be disabled.

Preparing the calibration pattern

(a) Print the calibration pattern with the highest resolution and by making sure the squares have the correct aspect ratio. (b) Glue the pattern on a solid flat surface. Keep in mind that the quality of the pattern influences the calibration.

Acquisition of the calibration images

(a) Move either the pattern or the camera in order to acquire a set of images from different viewpoints. If the camera is in video mode, move it slowly to avoid blur.

(b) The pattern should be completely visible in the image but this is not a strict requirement as the algorithm discards images that are not usable.

(c) The pattern depicted in the image set should cover the whole image frame with variations in the pose/viewpoint. Special care should be taken with the corners of the image.

Calibration

(a) At this stage there is a set of calibration images that can be readily used with this tool.

(b) After calibration, the various errors and the visual outputs indicate whether the algorithm converged to a proper solution. If this is not the case, there are several actions that can be undertaken to solve it.

Some practical tips for bundle adjustment setup are explained below:

Setting up the camera for extrinsic estimation:

(a) The positions of the cameras during the calibration must be the same as in the final system. A new calibration of the extrinsics is required every time a camera move.

(b) The cameras must have the same mode/configuration as in the final system, that is to say, the same zoom, focus, aperture, resolution, etc.

(c) Auto-focus, auto-stabilization or other such features that dynamically alter the geometry of

the image must be disabled.

Data acquisition:

- (a) The procedure requires a set of synchronized images/videos depicting.
- (b) The images have to be annotated with the positions of the objects. The more precise the annotations the better the calibration.



Figure A.8: Landmarks preparation step

A.1.2 Statistical analysis

Required number of participants for fatigue study

Our experiment was planned for 4 independent groups, each undergoing 2 different conditions. G*Power 3.1.9.7 was used to calculate the necessary total sample size (power analysis) to observe an average size effect with a Type I error rate of 0.05 ($\alpha=0.05$) and a power of 0.95 ($1-\beta=0.95$) for: i) the effect of the interaction between group and condition; ii) for the effect of group; iii) and for the effect of condition. We expect the results from different conditions to be somewhat correlated ($r=0.4$) and assume that sphericity assumptions are met.

Results for the power analysis for the interaction term shows that total of 76 subjects (to be split evenly between 4 groups) are required to observe a significant average size interaction

with a Type I error rate of 0.05 ($\alpha=0.05$) and a power of 0.95 ($1-\beta=0.95$).

Results for the power analysis for the effect of Group shows that a total of 132 subjects (to be split evenly between 4 groups) are required to observe a significant average size interaction with a Type I error rate of 0.05 ($\alpha=0.05$) and a power of 0.95 ($1-\beta=0.95$). If we aim for a power of 0.8 ($1-\beta=0.8$), 82 subjects would be necessary.

Results for the power analysis for the effect of Condition shows that a total of 36 subjects are required to observe a significant average size interaction with a Type I error rate of 0.05 ($\alpha=0.05$) and a power of 0.95 ($1-\beta=0.95$).

Post hoc analysis - power for 100 participants

Post hoc analysis for 100 subjects indicate that an average sized interaction term can be detected with a power > 0.95 , an average sized effect of group can be detected with a power of 0.88, and that an average sized effect of condition can be detected with a power > 0.95 .

The power analysis and size effect for other experiments are described in “Data. Data for thesis”, n.d.

Table A.8: Descriptive statistics for the main characteristics of the participant. BMI - body mass index

Study variable	Total (N=32)		Male (N=18)	Female (N=14)	p-value
	Mean (SD)	Min/Max	Mean (SD)	Mean (SD)	
Age (year)	33.59 (8.16)	25/55	34 (9.62)	33.07 (6.11)	0.742
Height (m)	1.75 (0.11)	1.54/1.95	1.83 (0.07)	1.66 (0.06)	<0.001
Body mass (kg)	71.22 (17.01)	43.8/114.10	82.92 (13.02)	56.19 (5.95)	<0.001
BMI (kg/m ²)	22.91 (3.78)	16.09/37.43	24.83 (3.77)	20.43 (1.93)	<0.001
Muscle mass (kg)	53.64 (12.51)	35.10/75.80	63.3 (7.38)	41.22 (2.60)	<0.001
Body fat (%)	19.67 (6.29)	8.50/36.40	17.77 (6.46)	22.11 (5.32)	0.046
Body fat (kg)	14.18 (6.75)	5.36/41.53	15.38 (8.23)	12.65 (3.93)	0.227
Body water (%)	54.74 (6.13)	30.30/66.00	56.89 (4.52)	51.98 (6.94)	0.032
Body water (kg)	38.99 (9.97)	17.85/55.28	46.74(4.94)	29.02 (3.86)	<0.001
Bone mass (kg)	2.87 (0.65)	2.00/4.00	3.37 (0.38)	2.23 (0.12)	<0.001
Upper arm (m)	0.34 (0.04)	0.25/0.40	0.35 (0.33)	0.32 (0.03)	0.007
Forearm (m)	0.28 (0.03)	0.20/0.33	0.30 (0.02)	0.25 (0.02)	<0.001
V torso (dm ³)	37.00 (11.00)	28.00/61.00	44.71 (6.93)	27.00 (4.42)	<0.001
V upper arm (dm ³)	2.00 (0.80)	0.8/3.8	2.70 (0.67)	1.48 (0.38)	<0.001
V forearm (dm ³)	1.00 (0.30)	0.4/2.00	1.37 (0.20)	0.72 (0.16)	<0.001

Note: BMI - body mass index

Table A.9: Shapiro-Wilk normality test results for males and females. Performance study experiment. W - test statistic

Task	W	p-value
R - 3 kg	0.95	0.20
R - 1kg	0.95	0.31
R - 0.5 kg	0.97	0.81
Joystick	0.96	0.45
Handwriting	0.95	0.24
Keyboard	0.96	0.37
Assembling	0.96	0.39

Table A.10: Shapiro-Wilk normality test results for females/males and females. Postural study experiment. W - test statistic

Task	W	p-value
Spine/vertical - 1G	0.86/0.74	0.01/0.01
Spine/vertical - $\frac{1}{6}$ G	0.92/0.95	0.05/0.14
Spine/tight - 1G	0.92/0.89	0.03/0.01
Spine/tight - $\frac{1}{6}$ G	0.92/0.95	0.04/0.48
CoM-Y-Pelvic - 1G	0.96/0.88	0.46/0.01
CoM-Y-Pelvic - $\frac{1}{6}$ G	0.85/0.95	0.01/0.03
CoM-Z-Pelvic - 1G	0.92/0.72	0.09/0.01
CoM-Z-Pelvic - $\frac{1}{6}$ G	0.80/0.95	0.01/0.07
Forearm/vertical - 1G	0.83/0.92	0.01/0.01
Forearm/vertical - $\frac{1}{6}$ G	0.92/0.98	0.07/0.78
Upper arm/vertical - 1G	0.96/0.94	0.36/0.01
Upper arm/vertical - $\frac{1}{6}$ G	0.96/0.92	0.38/0.01

A.2 Supplementary results

Table A.11: Summary of the calculated NASA-TLX parameters for the tasks with keyboard (K), repetitive tasks (R) with 0.5 - 3 kg, tasks with joystick (J), task with text writing (W), task with assembling (A) Males (M)/Females (F). All values in table are means.

Task	MD	PD	TD	P	EF	FR	WWL(%)
G-level	Mean	Mean	Mean	Mean	Mean	Mean	
7 participants				(Males)			
R-1G (3 kg)	47.14	81.43	38.57	50.00	76.43	37.14	66.14
R-1/6 G (3 kg)	34.29	54.29	36.46	44.29	55.71	30.00	54.00
R-1G (1 kg)	31.43	57.14	35.71	43.57	55.71	27.14	49.10
R-1/6G (1 kg)	31.43	30.00	39.29	42.86	32.86	18.57	41.14
R-1G (0.5 kg)	30.71	35.71	37.86	31.43	29.29	15.00	37.67
R-1/6 G (0.5 kg)	27.14	14.29	42.86	38.57	24.29	17.14	36.33
J-1G	47.86	10.00	37.86	30.00	23.57	23.57	37.57
J-1/6G	46.43	5.71	21.43	32.14	29.29	23.57	34.10
W-1G	44.29	10.00	45.71	27.14	30.71	32.86	40.67
W-1/6G	53.57	5.71	42.86	31.43	39.39	34.29	47.10
K-1G	58.57	10.00	57.14	45.71	28.57	25.71	50.95
K-1/6G	51.43	5.71	42.14	37.86	35.71	44.29	46.67
A-1G	51.43	22.86	55.71	51.43	34.29	41.43	48.38
A-1/6G	50.00	39.29	60.71	65.71	61.43	53.57	60.24
7 participants				(Females)			
R-1G (3 kg)	22.14	81.43	47.86	48.57	78.57	41.43	69.24
R-1/6 G (3 kg)	22.86	68.57	45.71	35.71	62.86	27.14	56.86
R-1G (1 kg)	24.29	57.14	46.43	59.29	57.86	19.29	55.48
R-1/6G (1 kg)	20.71	39.29	30.71	50.00	35.00	11.43	40.14
R-1G (0.5 kg)	20.71	36.43	30.00	47.86	39.29	12.14	36.86
R-1/6 G (0.5 kg)	16.43	31.43	25.71	48.57	29.29	9.29	36.81
J-1G	46.43	15.00	37.86	54.29	35.00	15.71	44.43
J-1/6G	45.71	23.57	54.29	54.29	33.57	24.29	47.38
W-1G	48.57	15.00	39.29	50.29	26.71	17.86	42.45
W-1/6G	34.29	23.57	27.14	51.43	32.14	11.43	35.71
K-1G	42.86	15.00	45.71	57.86	26.43	15.00	39.29
K-1/6G	55.71	23.57	44.29	58.57	34.29	22.86	48.33
A-1G	46.43	25.00	44.29	60.71	37.14	19.29	48.71
A-1/6G	40.71	19.29	45.71	52.86	37.14	30.71	44.71

Table A.12: Statistical analysis of repetitive tasks with 3 kg, 1 kg and 0.5 kg for males and females

	<i>Dependent variable: WWL</i>		
	'3_kg'	'1_kg'	'0.5_kg'
'G-level'	67.69*** (11.41)	52.29*** (8.65)	37.26*** (8.08)
Observations	28	28	28
R ²	0.57	0.58	0.44
Adjusted R ²	0.55	0.56	0.42
Residual Std. Error (df = 27)	42.71	32.36	30.23
F Statistic (df = 1; 27)	35.17***	36.54***	21.27***
Note:	*p<0.1; **p<0.05; ***p<0.01		

Table A.13: Statistical analysis of the performance study tasks - Part II

	<i>Dependent variable: WWL</i>			
	Joystick	Handwriting	Keyboard	Assembling
'G-level'	41.00*** (8.58)	41.56*** (9.09)	45.12*** (9.94)	48.55*** (11.25)
Observations	28	28	28	28
R ²	0.46	0.44	0.43	0.41
Adjusted R ²	0.44	0.42	0.41	0.39
Residual Std. Error (df = 27)	32.09	34.01	37.17	42.09
F Statistic (df = 1; 27)	22.86***	20.91***	20.62***	18.62***
Note:	*p<0.1; **p<0.05; ***p<0.01			

The information describing the different subjective demands for 6 participants for 3 levels of gravity (1G, 1/3G and 1/6G) for static tasks (S1) was also added below.

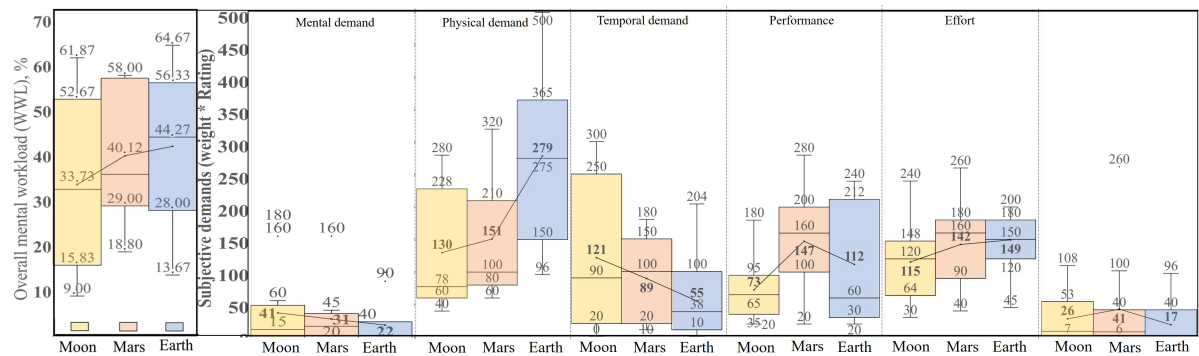


Figure A.9: Weighted workload (WWL,%) and subjective demands components (example for static task (S1)), for males and females for loads (1 kg, 3 kg, 5 kg, 7 kg) - gravity level dependence for static tasks extracted from supplementary materials of (Volkova et al., 2022). Volkova, 2022. Creative Commons license

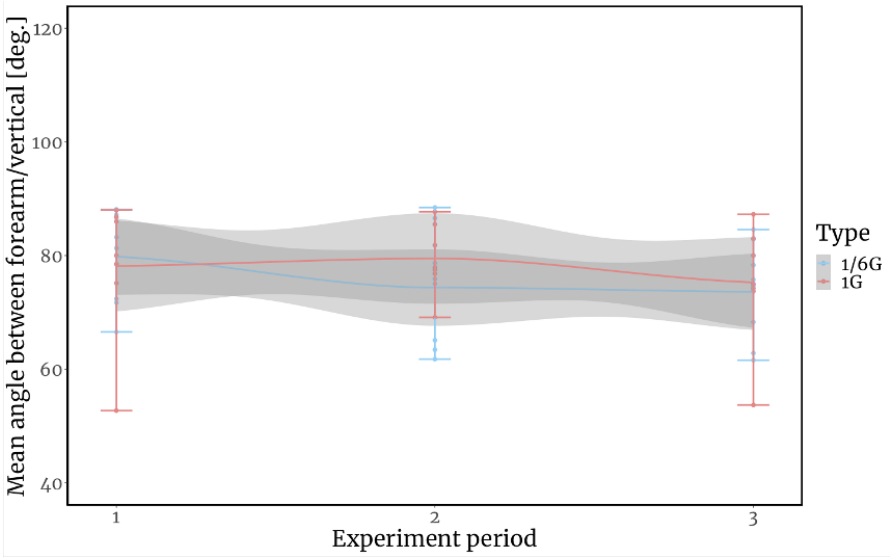


Figure A.10: Results for mean angle between forearm and vertical for females static and dynamic tasks. Experiment period: 1 - means the beginning of the experiment, 2- means the middle of the experiment, 3 means the end of the experiment. Confidence interval 95%

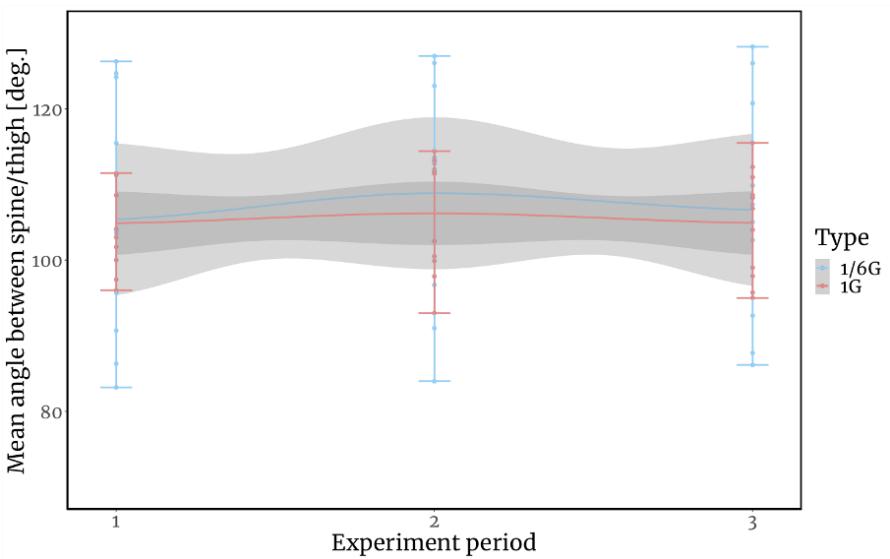


Figure A.11: Results for mean angle between spine and thigh for females static and dynamic tasks. Experiment period: 1 - means the beginning of the experiment, 2- means the middle of the experiment, 3 means the end of the experiment. Confidence interval 95%

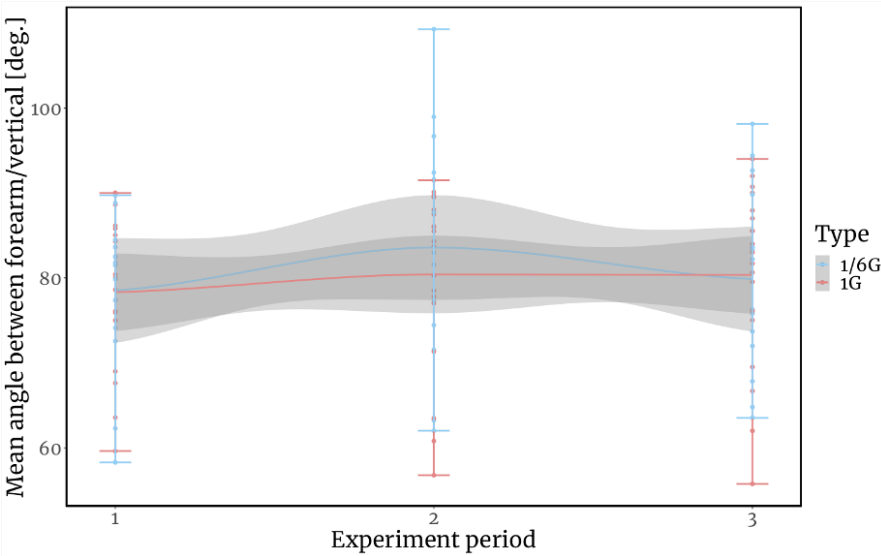


Figure A.12: Results for mean angle between forearm and vertical for males static and dynamic tasks. Experiment period: 1 - means the beginning of the experiment, 2- means the middle of the experiment, 3 means the end of the experiment. Confidence interval 95%

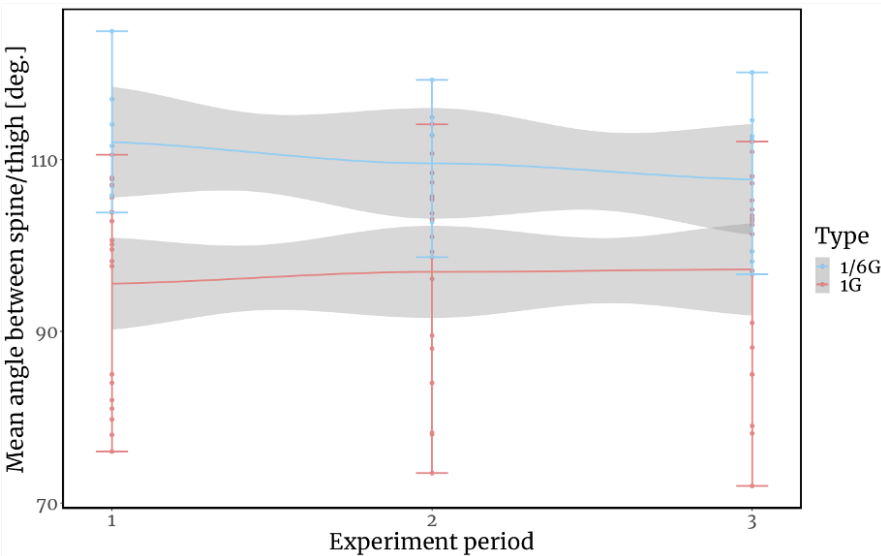


Figure A.13: Results for mean angle between spine and thigh for females static and dynamic tasks. Experiment period: 1 - means the beginning of the experiment, 2- means the middle of the experiment, 3 means the end of the experiment. Confidence interval 95%

Table A.14: Mean angle between spine and vertical for males and females separately [degrees]

	<i>Dependent variable: mean spine/vertical angle</i>			
	Static	Dynamic	Static	Dynamic
	Female	Female	Male	Male
G-level	-20.83*** (3.97)	-14.19*** (4.13)	-7.97 (4.98)	-18.92*** (5.17)
Constant	28.72*** (2.81)	23.14*** (2.92)	27.69*** (3.83)	37.10*** (3.97)
Observations	36	30	66	66
R ²	0.45	0.30	0.04	0.17
Adjusted R ²	0.43	0.27	0.02	0.16
Residual Std. Error	11.90	11.31	19.90	20.65
F Statistic	27.56***	11.81***	2.56	13.39***

Note:

*p<0.1; **p<0.05; ***p<0.01

Table A.15: Mean angle between spine and vertical for males and females together [degrees]

	<i>Dependent variable: mean spine/vertical angle</i>	
	Static	Dynamic
G-level	-12.61*** (3.55)	-17.41*** (3.77)
Gender	-5.83 (3.69)	-11.45*** (4.03)
Constant	30.43*** (3.03)	36.20*** (3.16)
Observations	102	96
R ²	0.13	0.23
Adjusted R ²	0.11	0.21
Residual Std. Error	17.73	18.25
F Statistic	7.13***	13.68***

Note:

*p<0.1; **p<0.05; ***p<0.01 .

Table A.16: Mean angle between spine and thigh [degrees] for static and dynamic tasks together

	<i>Dependent variable: mean spine/thigh angle</i>	
	Males	Females
G-level	-14.23*** (3.06)	1.81 (3.40)
Task	0.96 (2.66)	2.89 (3.41)
Constant	109.09*** (3.21)	101.93*** (3.04)
Observations	84	66
R ²	0.22	0.02
Adjusted R ²	0.21	-0.02
Residual Std. Error	11.89	13.80
F Statistic	11.71***	0.50

Note:

*p<0.1; **p<0.05; ***p<0.01

Table A.17: Mean angle between spine and thigh for males and females separately [degrees]

	<i>Dependent variable: mean spine/thigh angle</i>			
	Static	Dynamic	Static	Dynamic
	Female	Female	Male	Male
G-level	-0.33 (5.19)	4.38 (4.18)	-13.18*** (2.99)	-16.30** (6.34)
Constant	105.90*** (3.67)	100.65*** (2.96)	109.35*** (2.44)	110.84*** (5.84)
Observations	36	30	45	39
R ²	0.001	0.04	0.31	0.15
Adjusted R ²	-0.03	0.003	0.29	0.13
Residual Std. Error	15.57	11.45	9.47	14.29
F Statistic	0.004	1.10	19.37***	6.60**

Note: *p<0.1; **p<0.05; ***p<0.01

Table A.18: Mean angle between spine and thigh for males and females together [degrees]

	<i>Dependent variable: mean spine/thigh angle</i>	
	Static	Dynamic
G-level	-7.09** (2.95)	-3.97 (3.88)
Gender	3.99 (2.91)	4.42 (3.61)
Constant	105.29*** (2.74)	100.40*** (3.96)
Observations	81	69
R ²	0.10	0.06
Adjusted R ²	0.08	0.03
Residual Std. Error	12.85	13.78
F Statistic	4.51**	2.02

Note:

*p<0.1; **p<0.05; ***p<0.01

Table A.19: Mean angle between shoulder and vertical for males and females separately [degrees]

	<i>Dependent variable: mean shoulder/vertical angle</i>			
	Static	Dynamic	Static	Dynamic
	Female	Female	Male	Male
G-level	17.43*** (3.53)	-4.78 (5.30)	27.57*** (3.43)	21.28*** (3.69)
Constant	55.36*** (2.49)	66.20*** (3.75)	51.58*** (2.58)	51.61*** (2.78)
Observations	36	30	69	69
R ²	0.42	0.03	0.49	0.33
Adjusted R ²	0.40	-0.01	0.48	0.32
Residual Std. Error	10.58	14.51	14.14	15.20
F Statistic	24.44***	0.81	64.46***	33.23***

Note:

*p<0.1; **p<0.05; ***p<0.01 .

Table A.20: Mean angle between shoulder and vertical for males and females together [degrees]

	<i>Dependent variable: mean shoulder/vertical angle</i>	
	Static	Dynamic
G-level	24.05*** (2.59)	13.29*** (3.26)
Gender	-1.52 (2.72)	1.04 (3.53)
Constant	53.57*** (2.16)	56.13*** (2.67)
Observations	105	99
R ²	0.46	0.15
Adjusted R ²	0.45	0.13
Residual Std. Error	13.17	16.03
F Statistic	43.67***	8.33***

Note:

*p<0.1; **p<0.05; ***p<0.01

Table A.21: Mean angle between forearm/vertical for males and females separately [degrees]

	<i>Dependent variable: mean forearm/vertical angle</i>			
	Static	Dynamic	Static	Dynamic
	Female	Female	Male	Male
G-level	10.01** (3.70)	-2.80 (5.12)	2.77 (4.29)	5.65 (3.67)
Constant	78.71*** (2.62)	83.55*** (3.62)	81.72*** (3.23)	74.87*** (2.76)
Observations	36	30	69	69
R ²	0.18	0.01	0.01	0.03
Adjusted R ²	0.15	-0.02	-0.01	0.02
Residual Std. Error	11.10	14.01	17.67	15.13
F Statistic	7.33**	0.30	0.42	2.36

Note:

*p<0.1; **p<0.05; ***p<0.01 .

Table A.22: Mean angle between forearm/vertical for males and females together [degrees]

	<i>Dependent variable: mean forearm/vertical angle</i>	
	Static	Dynamic
G-level	5.28* (3.10)	3.06 (3.01)
Gender	0.77 (3.25)	4.29 (3.26)
Constant	80.30*** (2.58)	76.33*** (2.47)
Observations	105	99
R ²	0.03	0.03
Adjusted R ²	0.01	0.01
Residual Std. Error	15.78	14.86
F Statistic	1.46	1.31

Note:

*p<0.1; **p<0.05; ***p<0.01

Table A.23: Mean CoM coordinate Z - axis for males and females separately [cm]

	<i>Dependent variable: mean CoMz (in relation to pelvic on Z axis)</i>			
	Static	Dynamic	Static	Dynamic
	Female	Female	Male	Male
G-level	5.52** (2.05)	6.59*** (2.01)	1.21 (2.86)	-3.84*** (1.17)
Constant	-3.13** (1.30)	-4.01*** (1.31)	3.17 (2.02)	7.87*** (0.83)
Observations	30	39	54	60
R ²	0.21	0.31	0.003	0.16
Adjusted R ²	0.18	0.28	-0.02	0.14
Residual Std. Error	5.49	5.07	10.51	4.54
F Statistic	7.26**	10.75***	0.18	10.71***

Note: *p<0.1; **p<0.05; ***p<0.01 .

Table A.24: Mean CoM coordinate Z- axis for males and females together [cm]

	<i>Dependent variable: mean CoMz (in relation to pelvic on Z axis)</i>	
	Static	Dynamic
G-level	2.71 (2.00)	-0.74 (1.14)
Gender	-4.43** (2.08)	-7.23*** (1.24)
Constant	0.65 (1.38)	3.91*** (0.93)
Observations	84	86
R ²	0.08	0.29
Adjusted R ²	0.06	0.27
Residual Std. Error	9.08	5.26
F Statistic	3.50**	17.04***

Note:

* p<0.1; ** p<0.05; *** p<0.01

Table A.25: Mean CoM coordinate Y- axis pelvic for males and females separately [cm]

	<i>Dependent variable: mean CoMY (in relation to pelvic on Y axis)</i>			
	Static	Dynamic	Static	Dynamic
	Female	Female	Male	Male
Type1G	6.68*** (0.94)	4.95*** (0.57)	13.50*** (2.58)	20.26*** (1.84)
Constant	4.43*** (0.59)	6.08*** (0.37)	-3.52* (1.82)	-10.07*** (1.30)
Observations	30	39	54	60
R ²	0.64	0.76	0.35	0.68
Adjusted R ²	0.63	0.75	0.33	0.67
Residual Std. Error	2.51	1.43	9.47	7.12
F Statistic	50.85***	76.51***	27.41***	121.39***

Note:

* p<0.1; ** p<0.05; *** p<0.01 .

Table A.26: Mean CoM coordinate Y- axis pelvic for for males and females together [cm]

	<i>Dependent variable: mean CoMy (in relation to pelvic on Y axis)</i>	
	Static	Dynamic
G-level	11.13*** (1.74)	15.71*** (1.51)
Gender	4.99*** (1.81)	9.33*** (1.64)
Constant	-2.34* (1.38)	-7.80*** (1.17)
Observations	84	86
R ²	0.36	0.62
Adjusted R ²	0.34	0.61
Residual Std. Error	7.90	6.97
F Statistic	22.83***	66.48***

Note:

* p<0.1; ** p<0.05; *** p<0.01

A.3 Parabolic flight campaign

The pilot's seat should serve one purpose - to achieve maximum comfort. It should not cause any inconvenience, rather, its tasks include providing the necessary support for the hips, lower back, and back, not only in a state of relaxation and careful observation, but also in the case of vigorous activity. At the same time, the completeness of support should not limit freedom of movement. The ideal option is a mechanized seat with a remote electric control function, which creates the most comfortable position for each pilot. In the back of the seat, a special, easily accessible compartment stores a life jacket.

Participants will do the following motions during 1 Martian parabola (35 sec): 10 sec - static holding varying weights; 10 sec - lifting and lowering the varying weights; 10 sec - lifting and lowering of defined weight; 2 lunar parabolas (2 x 25 sec): 8 sec - static holding of varying weights per parabola; 8 sec - lifting and lowering varying weights per parabola; 8 sec - lifting and lowering of defined weight per parabola; 12/13 weightless parabolas (12 x 22 sec): 22 sec - static holding of the varying weights per 4 parabolas; 22 sec - lifting and lowering the varying weights per 4 parabolas; 22 sec - lifting and lowering of defined weight per 4 parabolas;

The scenario described above is based on a commercial flight program with a limited number of low-gravity parabolas. If we have the opportunity to participate in a scientific flight with 10

parabolas with lunar gravity and 10 parabolas with Martian gravity, then this will help increase the amount of data and, accordingly, increase the accuracy of the built models based on the collected data.

Flight Here, the fundamentals of the validation are tested. Just before the flight, a 3 min camera calibration will be done inside the plane. Then, load cell data, video data, reaction force data and acceleration data would be measured for 3 participants during flight. After the flight, the data will be verified on the ground. If the data for any subject was not correctly recorded for technical or other reasons, then the same subject will be invited to the second flight. Otherwise, 3 new participants will be invited to the second flight.

Flight 2 This flight will begin after carefully instructing new participants on how the experiment will be conducted and on the results of the first flight. During the second flight, experiments equivalent to the first flight will be conducted. If some part of the experiment was not performed during the first flight, then it will be carried out in priority during the second flight.

Flight 3 Equivalent to Flight 2 The supplementary materials for this experiment as well as structure and budget computations for these experiments are provided in Appendix and data sharing link.

A.4 Codes/scripts

Code 1 Extract JPEG frames from MP4 files with ffmpeg.

```

1 Extract JPEG frames from MP4 files with ffmpeg.
2
3 import subprocess
4 from pathlib import Path
5
6 FFMPEG_EXECUTABLE: str = ("C:path\\ffmpeg")
7
8
9 def process(input_path: Path) -> None:
10     """
11     Extract JPEG frames from MP4 files with ffmpeg.
12     :param input_path: directory containing MP4 files, will be processed
13       recursively
14     """
15     for file_name in input_path.iterdir():
16
17         if file_name.is_dir():
18             # Process directory recursively.
19             process(file_name)
20
21         elif file_name.is_file() and file_name.name.lower().endswith(".mp4"):
22             # Create directory and execute ffmpeg.
23             prefix: str = file_name.name[:-4]
24             output_file: Path = (
25                 file_name.parent / prefix / ("frame" + "_%06d.jpg"))
26             output_file.mkdir(exist_ok=True, parents=True)
27             command: str = (f"{FFMPEG_EXECUTABLE} -i {file_name} -vf fps=30 {output_file}")
28             print(command)
29             subprocess.run(command.split(" "), shell=True)
30
31 if __name__ == '__main__':
32     import sys
33
34     if len(sys.argv) < 2:
35         print("Fatal: please, specify input directory path.")
36         print(f"Usage: python {sys.argv[0]} <input directory>")
37         exit(1)
38
39     process(Path(sys.argv[1]))

```

A.5 Matlab script

Code 2 Main file for Matlab computation and Plot skeleton in Matlab

```

1  %% Computing shoulder moments
2  moments = joints2moment(jointAngles, participantName, g, pathMass);
3
4  %% Computing workload
5  workload = joints2workload(jointAngles, participantName, g, pathMass);
6
7  %% Merging all tables and saving to csv
8  totalTT = synchronize(jointAngles, com, moments, workload);
9  writetimetable(totalTT, "output\output_S1_hammer_280621.csv");
10
11  %%%%%%%%%%%%%%%%%%%%%%%%%%%%%%%%%%%%%%%%%%%%%%%%%%%%%%%%%%%%%%%%%%%%%%%%%
12  %% PLOT SKELETON (MATLAB) %%
13  %%%%%%%%%%%%%%%%%%%%%%%%%%%%%%%%%%%%%%%%%%%%%%%%%%%%%%%%%%%%%%%%%%%%%%%%%
14  function plotSkeleton(jointPosition, com, frameIdx)
15      segmentList = readtable("input\segmentListForPlotting.csv");
16
17      figure(10)
18      clf
19      hold on
20      axis equal
21      for j = 1:size(segmentList,1)
22          startJoint = squeeze(jointPosition(frameIdx, segmentList.jointStart(j)+1, :));
23          endJoint = squeeze(jointPosition(frameIdx, segmentList.jointEnd(j)+1, :));
24          seg = [startJoint endJoint]';
25          plot3(seg(:,3), seg(:,1), seg(:,2), segmentList.style{j}, 'Linewidth',2)
26      end
27
28      plot3(com.Z(frameIdx), com.X(frameIdx), com.Y(frameIdx), 'om', 'Linewidth',2)
29
30      az = 111.6425;
31      el = 16.5364;
32      xlim([-100 100]);
33      ylim([-100 100]);
34      zlim([-20 140]);
35      view(az,el);
36      grid on
37      xlabel("Z [cm]", 'FontSize',14)
38      ylabel("X [cm]", 'FontSize',14)
39      zlabel("Y [cm]", 'FontSize',14)
40
41  end

```

Code 3 JSON parser for Matlab computation

```

1 %% Parsing data or parsing multiple data files
2
3 % jsonFile = "output_R_3_060821.json";
4 jsonFile = "input\output_S1_hammer_280621.json";
5 rawData = jsonParser(jsonFile);
6
7 %% Getting specific time intervals
8 startFrames = [1878];
9 endFrames = [2876];
10 participantName = 26 ;
11 g = 9.81;
12 framrate = 1;
13
14 [data, timespace] = getTimeIntervals(startFrames, endFrames, rawData, "cam0", framrate);
15
16 %% Computing desired joint angles
17 jointAngles = joints2angles(data, timespace);
18
19 %% Computing center of mass
20 pathMass = "input\Participant_SUMMARY_data_full_full.csv";
21 com = joints2com(data, timespace, pathMass, participantName);
22
23 %%
24 plotSkeleton(data, com, 1)
25 %% Plot a skeleton
26 showAllFrames = false;
27 saveVideo = false;
28 if showAllFrames
29     for i = 1:size(data,1)
30         plotSkeleton(data, com, i);
31
32         if saveVideo
33             F(i) = getframe(gcf);
34             drawnow
35         end
36     end
37     if saveVideo
38         % create the video writer with 1 fps
39         writerObj = VideoWriter('comTest_filteredLimb.avi');
40         writerObj.FrameRate = 10;
41         % set the seconds per image
42         % open the video writer
43         open(writerObj);
44         % write the frames to the video
45         for i=1:length(F)
46             % convert the image to a frame
47             frame = F(i) ;
48             writeVideo(writerObj, frame);
49         end
50         % close the writer object
51         close(writerObj);
52     end
53 end

```

Code 4 JSON parser for Matlab computation

```
1 function inputData = jsonParser(path)
2     % Read the whole json file
3     fid = fopen(path);
4     raw = fread(fid, inf);
5     str = char(raw');
6     fclose(fid);
7
8     % Parse it
9     inputData = jsondecode(str);
10
11     % Either pose 3d is cell
12     idxList = [];
13     if iscell(inputData.pose_3d)
14         % disp("Cell detected. Proceeding to reshape...")
15         for i = 1:length(inputData.pose_3d)
16             if all(size(inputData.pose_3d{i}) == [25,3])
17                 idxList = cat(1,idxList,i);
18             end
19         end
20         tmp = inputData.pose_3d(idxList);
21         pose_3d = shiftdim(cat(3,tmp{:}),2);
22         idx_frames = inputData.idx_frames(idxList);
23         inputData.pose_3d = pose_3d;
24         inputData.idx_frames = idx_frames;
25     end
26
27 end
```

Code 5 Shoulder and elbow Workload for Matlab computation - Part I

```

1 function workload = joints2workload(jointAngles, participantName, g, pathMass)
2     allParticipantData = readtable(pathMass);
3     participantData = allParticipantData(find(allParticipantData.Name == participantName, 1), :);
4
5     comCoef = readtable("input\comCoef.csv");
6     IDX_GENDER = find(ismember(comCoef.Gender, participantData.Gender),1);
7
8     if participantData.Handedness == "left"
9         teta_1 = jointAngles.shoulder2vertL;
10        teta_2 = jointAngles.forearm2vertL;
11    elseif participantData.Handedness == "right"
12        teta_1 = jointAngles.shoulder2vertR;
13        teta_2 = jointAngles.forearm2vertR;
14    else
15        error("Unexpected handedness " + participantData.Handedness)
16    end
17
18    I_1 = participantData.Inertia_UpperArm;
19    I_2 = participantData.Inertia_ForeArm;
20    m_1 = participantData.UpperArm;
21    m_2 = participantData.ForeArm;
22    L_1 = participantData.length_UpperArm; % converting to meters
23    L_2 = participantData.length_ForeArm;% converting to meters
24    l_1 = L_1*comCoef{IDX_GENDER,"coef_UpperArm"}/100; % converting from percentage
25    l_2 = L_2*comCoef{IDX_GENDER,"coef_ForeArm"}/100; % converting from percentage
26    f = participantData.HandLoad;
27
28
29    q_1 = 90 - teta_1;
30    q_2 = -(teta_2 - teta_1);
31
32    q_1_ = gradient(q_1, seconds(jointAngles.Properties.TimeStep));
33    q_2_ = gradient(q_2, seconds(jointAngles.Properties.TimeStep));
34    q_1__ = gradient(q_1_, seconds(jointAngles.Properties.TimeStep));
35    q_2__ = gradient(q_2_, seconds(jointAngles.Properties.TimeStep));
36
37    torqueShoulder = ( ...
38        (I_1 + I_2 + m_1*l_1*l_1 + m_2*(L_1*L_1 + l_2*l_2 + 2*L_1*l_2*cos(q_2)))*q_1__ + ...
39        (I_2 + m_2*l_2*l_2 + m_2*L_1*l_2*cos(q_2))*q_2__ - ...
40        2*m_2*L_1*l_2*q_1_*q_2_*sin(q_2) - ...
41        m_2*L_1*l_2*q_2_*q_2_*sin(q_2) + ...
42        m_2*g*l_2*cosd(q_1 + q_2) + ...
43        m_1*g*l_1*cosd(q_1) + ...
44        m_2*g*L_1*cosd(q_1) + ...
45        f*L_2*cosd(q_1 + q_2) + ...
46        f*L_1*cosd(q_1));
47
48    torqueElbow = ( ...
49        (I_2 + m_2 * l_2 * l_2) * q_2__ + ...
50        (I_2 + m_2 * l_2 * l_2 + m_2 * L_1 * l_2 * cos(q_2)) .* q_1__ + ...
51        m_2 * L_1 * l_2 * q_1_ .* q_1_ .* sin(q_2) + ...
52        m_2 * g * l_2 * cosd(q_1 + q_2) + ...
53        f * L_2 * cosd(q_1 + q_2));

```

Code 6 Shoulder and elbow Workload for Matlab computation -Part II

```

1  wh = participantData.WeightGround / participantData.Height ^2;
2  age = participantData.Age;
3  if participantData.Gender == "Female"
4      gender = 0;
5  else
6      gender = 1;
7  end
8
9  flexion_e_l = -(age * 0.11) + (gender * 10.63) + (wh * 0.05) + 19.66;
10 flexion_e_r = -(age * 0.13) + (gender * 11.24) + (wh * 0.07) + 22.78;
11 flexion_s_l = -(age * 0.12) + (gender * 10.68) + (wh * 0.24) + 14.68;
12 flexion_s_r = -(age * 0.17) + (gender * 16.26) + (wh * 0.17) + 23.35;
13
14 if gender == 0 % Female
15     m_1 = 0.0255 * participantData.WeightGround;
16     m_2 = 0.0138 * participantData.WeightGround;
17 elseif gender == 1
18     m_1 = 0.0271 * participantData.WeightGround;
19     m_2 = 0.0162 * participantData.WeightGround;
20 else
21     error("Invalid gender")
22 end
23
24
25 if participantData.Handedness == "right"
26     tetta_1 = jointAngles.shoulder2vertR;
27     tetta_2 = jointAngles.forearm2vertR;
28 elseif participantData.Handedness == "left"
29     tetta_1 = jointAngles.shoulder2vertL;
30     tetta_2 = jointAngles.forearm2vertL;
31 else
32     error("Invalid handedness")
33 end
34
35 a_2 = participantData.length_UpperArm;
36 a = a_2/2;
37 c = participantData.length_ForeArm;
38 b = c/2;
39 m_3 = participantData.HandLoad;
40
41
42
43 if participantData.Handedness == "right"
44     workload_shoulder = torqueShoulder / flexion_s_r;
45     workload_elbow = torqueElbow / flexion_e_r;
46 elseif participantData.Handedness == "left"
47     workload_shoulder = torqueShoulder / flexion_s_l;
48     workload_elbow = torqueElbow / flexion_e_l;
49 else
50     error("Invalid handedness")
51 end
52
53 workload = array2timetable([workload_shoulder, workload_elbow], ...
54     'RowTimes', jointAngles.Time, ...
55     'VariableNames', ["workload_shoulder", "workload_elbow" ]);
56 end

```

Code 7 Torques - Part I

```

1 function momentsTable = joints2moment(jointAngles, participantIndex, g, pathMass)
2
3     allParticipantData = readtable(pathMass);
4     participantData = allParticipantData(find(allParticipantData.Name == participantIndex, 1), :);
5     comCoef = readtable("input\comCoef.csv");
6     IDX_GENDER = find(ismember(comCoef.Gender, participantData.Gender),1);
7
8     if participantData.Handedness == "left"
9         teta_1 = deg2rad(jointAngles.shoulder2vertL);
10        teta_2 = deg2rad(jointAngles.forearm2vertL);
11    elseif participantData.Handedness == "right"
12        teta_1 = deg2rad(jointAngles.shoulder2vertR);
13        teta_2 = deg2rad(jointAngles.forearm2vertR);
14    else
15        error("Unexpected handedness " + participantData.Handedness)
16    end
17
18    I_1 = participantData.Inertia_UpperArm;
19    I_2 = participantData.Inertia_ForeArm;
20    m_1 = participantData.UpperArm;
21    m_2 = participantData.ForeArm;
22    L_1 = participantData.length_UpperArm; % converting to meters
23    L_2 = participantData.length_ForeArm;% converting to meters
24    l_1 = L_1*comCoef{IDX_GENDER,"coef_UpperArm"}/100; % converting from percentage
25    l_2 = L_2*comCoef{IDX_GENDER,"coef_ForeArm"}/100; % converting from percentage
26    f = participantData.HandLoad;
27
28
29    q_1 = pi/2 - teta_1;
30    q_2 = -(teta_2 - teta_1);
31
32    q_1_ = gradient(q_1, seconds(jointAngles.Properties.TimeStep));
33    q_2_ = gradient(q_2, seconds(jointAngles.Properties.TimeStep));
34    q_1__ = gradient(q_1_, seconds(jointAngles.Properties.TimeStep));
35    q_2__ = gradient(q_2_, seconds(jointAngles.Properties.TimeStep));
36
37    torqueShoulder = ( ...
38        (I_1 + I_2 + m_1*l_1*l_1 + m_2*(L_1*L_1 + l_2*l_2 + 2*L_1*l_2*cos(q_2)))*q_1__ + ...
39        (I_2 + m_2*l_2*l_2 + m_2*L_1*l_2*cos(q_2))*q_2__ - ...
40        2*m_2*L_1*l_2*q_1_*q_2_*sin(q_2) - ...
41        m_2*L_1*l_2*q_2_*q_2_*sin(q_2) + ...
42        m_2*g*l_2*cos(q_1 + q_2) + ...
43        m_1*g*l_1*cos(q_1) + ...
44        m_2*g*L_1*cos(q_1) + ...
45        f*L_2*cos(q_1 + q_2) + ...
46        f*L_1*cos(q_1));
47
48    torqueElbow = ( ...
49        (I_2 + m_2 * l_2 * l_2) * q_2__ + ...
50        (I_2 + m_2 * l_2 * l_2 + m_2 * L_1 * l_2 * cos(q_2)) .* q_1__ + ...
51        m_2 * L_1 * l_2 * q_1_ .* q_1_ .* sin(q_2) + ...
52        m_2 * g * l_2 * cos(q_1 + q_2) + ...
53        f * L_2 * cos(q_1 + q_2));

```

Code 8 Torques - Part II

```

1  m_t = participantData.TotalTrunk;
2  m_u_a = participantData.UpperArm;
3  m_fa = participantData.ForeArm;
4  m_h = participantData.Head;
5  if participantData.Handedness == "left"
6      f_R = 0;
7      f_L = participantData.HandLoad;
8  elseif participantData.Handedness == "right"
9      f_R = participantData.HandLoad;
10     f_L = 0;
11 end
12 L_t = participantData.length_Trunk;
13 L_u_a = participantData.length_UpperArm;
14 L_fa = participantData.length_ForeArm;
15 L_h = participantData.length_Neck;
16 l_t = L_t*comCoef{IDX_GENDER,"coef_TotalTrunk"}/100;
17 l_u_a = L_u_a*comCoef{IDX_GENDER,"coef_UpperArm"}/100;
18 l_fa = L_fa*comCoef{IDX_GENDER,"coef_ForeArm"}/100;
19
20 teta_t = deg2rad(jointAngles.spine2vert);
21 teta_u_a_L = deg2rad(jointAngles.shoulder2vertL);
22 teta_fa_L = deg2rad(jointAngles.forearm2vertL);
23 teta_u_a_R = deg2rad(jointAngles.shoulder2vertR);
24 teta_fa_R = deg2rad(jointAngles.forearm2vertR);
25 teta_h = deg2rad(jointAngles.neck2vert);
26
27 staticTorqueHip = ...
28     m_t *g*(l_t*sin(teta_t)) ...
29     + m_h *g*(L_t*sin(teta_t) + L_h*sin(teta_h)) ...
30     + m_u_a*g*(L_t*sin(teta_t) + l_u_a*sin(teta_u_a_L)) ...
31     + m_u_a*g*(L_t*sin(teta_t) + l_u_a*sin(teta_u_a_R)) ...
32     + m_fa*g*(L_t*sin(teta_t) + L_u_a*sin(teta_u_a_L) + l_fa*sin(teta_fa_L)) ...
33     + m_fa*g*(L_t*sin(teta_t) + L_u_a*sin(teta_u_a_R) + l_fa*sin(teta_fa_R)) ...
34     + f_L *g*(L_t*sin(teta_t) + L_u_a*sin(teta_u_a_L) + L_fa*sin(teta_fa_L)) ...
35     + f_R *g*(L_t*sin(teta_t) + L_u_a*sin(teta_u_a_R) + L_fa*sin(teta_fa_R));
36
37
38 forceHip = (g*(m_t + m_h + m_u_a*2 + m_fa*2) + f_L + f_R)*ones(size(torqueElbow));
39 forceShoulder = (g*(m_u_a + m_fa) + f)*ones(size(torqueElbow));
40 forceElbow = (g*(m_fa) + f)*ones(size(torqueElbow));
41
42 momentsTable = array2timetable([torqueShoulder, torqueElbow, staticTorqueHip, forceHip, \
43 forceShoulder,
44 forceElbow], ...
45     'RowTimes', jointAngles.Time, ...
46     'VariableNames', ["torqueShoulder", "torqueElbow", "staticTorqueHip", "forceHip", \
47     "forceShoulder",
48     "forceElbow"]);
49 end

```

Code 9 CoM computation in Matlab

```

1 function comTable = joints2com(jointPosition, timespace, pathMass, participantName)
2     % jointPosition : jointPosition table such that
3     % <frames>x<joints>x<coord>
4     % timespace : row times to use for timetable creation
5     % pathMass : path (including file name) to sement mass table
6     % participantIndex : index in the segment mass table (Excel colum B has
7     % participant index 1)
8
9     % Dimension in which the frames are stored in jointPosition table
10    DIM_FRAME = 1;
11
12    % Maximal allowable segment length. If any segment is longer than this
13    % then COM is considered as invalid
14    MAX_SEGMENT_LENGTH = 150; % cm
15
16    % Reading data
17    massAll = readtable(pathMass);
18    segmentList = readtable("input\segmentList.csv");
19    comCoef = readtable("input\comCoef.csv");
20
21    % Extracting participant mass
22    mass = massAll(find(massAll.Name == participantName, 1), :);
23    mTot = mass.WeightGround;
24
25    % Choosing propoer COM coef
26    IDX_GENDER = find(ismember(comCoef.Gender, mass.Gender),1);
27
28
29    % Memory allocation
30    com = zeros(size(jointPosition, DIM_FRAME),3);
31    comPelvic = zeros(size(jointPosition, DIM_FRAME),3);
32    comPelvicNorm = zeros(size(jointPosition, DIM_FRAME),3);
33
34    % For all frames
35    for i = 1:size(jointPosition, DIM_FRAME)
36        % For all segments
37        for j = 1:size(segmentList,1)
38            % Get segment name with out "left" or "right"
39            if contains(segmentList.segName(j), "Right")
40                tmp = segmentList.segName{j};
41                segName = string(tmp(1:end-length('Right')));
42            elseif contains(segmentList.segName(j), "Left")
43                tmp = segmentList.segName{j};
44                segName = string(tmp(1:end-length('Left')));
45            else
46                segName = string(segmentList.segName{j});
47            end
48
49            % Get mass, start and end of segment
50            mSeg = mass.(segName);
51            if ismember("coef_" + segName, comCoef.Properties.VariableNames)
52                coef = comCoef(IDX_GENDER,:).("coef_" + segName);
53            else
54                coef = 0;
55            end

```

Code 10 CoM computation in Matlab

```

1  startJoint = squeeze(jointPosition(i, segmentList.jointStart(j)+1, :));
2      endJoint = squeeze(jointPosition(i, segmentList.jointEnd(j)+1, :));
3  if norm(startJoint - endJoint) > MAX_SEGMENT_LENGTH % If any segment is longer than 1m
4      com(i,:) = [NaN, NaN, NaN];
5      break; % If any segment was not detected ,
6      %then the computation of the COM is not possible
7      end
8
9      % Add contribution to center of mass
10     com(i,:) = com(i,:) + mSeg/mTot*( ...
11         startJoint' + coef*(endJoint' - endJoint'));
12     end
13     comPelvic(i,:) = com(i,:) - squeeze(jointPosition(i, 9, :))';
14     comPelvicNorm(i,:) = comPelvic(i,:)./mass.Height ;
15 end
16
17 % Storing data in a Timetable
18 comTable = array2timetable([com, comPelvic, comPelvicNorm], 'RowTimes',timespace,\\
19     'VariableNames',
20     ["X","Y","Z","X_pelvic","Y_pelvic","Z_pelvic","X_pelvicNorm",\\
21     "Y_pelvicNorm","Z_pelvicNorm" ]);
22 end

```

Code 11 Time intervals computation in Matlab

```

1 function [dataOut, timespace] = getTimeIntervals(startFrames, endFrames, data, reference, framerate)
2     % startFrames : list of idx of start frames of interval
3     % endFrames : list of idx of end frames of interval
4     % data : as returned by json parser
5     % reference : name of time reference field ("ace0", "ace1" ...)
6     % framerate : in Hz, nbr of frames per seconds
7
8     totalTimeSpace = [data.idx_frames.(reference)];
9
10    if isempty(startFrames)
11        dataOut = data.pose_3d;
12        timespace = seconds(totalTimeSpace/framerate);
13    else
14
15        startIdx = zeros(size(startFrames));
16        endIdx = zeros(size(startFrames));
17
18        for i = 1:length(startFrames)
19            startIdx(i) = find(totalTimeSpace >= startFrames(i),1);
20            endIdx(i) = find(totalTimeSpace >= endFrames(i),1) -1;
21        end
22
23        dataOut = [];
24        idxspace = [];
25        for i = 1:length(startIdx)
26            dataOut = cat(1, dataOut, data.pose_3d(startIdx(i):endIdx(i),:,:));
27            idxspace = cat(1, idxspace, totalTimeSpace(startIdx(i):endIdx(i))');
28        end
29
30        timespace = seconds(idxspace/framerate);
31    end
32 end

```

Code 12 Joint angles computation in Matlab

```

1 function jointAnglesTable = joints2angles(jointPosition, timespace)
2     % jointPosition : jointPosition table such that
3     % <frames>x<joints>x<coord>
4     % timespace : row times to use for timetable creation
5
6     % Dimension in which the frames are stored in jointPosition table
7     DIM_FRAME = 1;
8
9
10    % Angle is defined with :
11    % "name", joint idx start, joint idx middle (where the angle is), joint idx end
12    % if joint idx is -1 then it refers to vertical toward down
13    % if joint idx is -2 then it refers to vertical toward up
14    % if joint idx is -3 then it refers to vertical toward up projected in
15    % the ZY-plane
16    % if joint idx is -4 then it refers to vertical toward up projected in
17    % the XY-plane
18    % joint 25 is average between 10 and 13
19    ANGLELIST = {
20        "head2vert", 0, 1, -2;
21        "head2vert_forward", 15, 17, -3;
22        "head2vert_sideways", 15, 17, -4;
23        "neck2vert", 0,1, -2;
24        "neck2vert_forward", 0,1, -3;
25        "neck2vert_sideways", 0,1, -4;
26        "spine2vert", 1, 8, -2;
27        "spine2vert_forward", 1, 8, -3;
28        "spine2vert_sideways", 1, 8, -4;
29        "spine2tight", 1, 8, 13;
30        "forearm2vertL", 7, 6, -1;
31        "forearm2vertR", 4, 3, -1;
32        "shoulder2vertL", 6, 5, -1;
33        "shoulder2vertR", 3, 2, -1;
34    };
35
36
37    % Memory allocation
38    jointAngles = zeros(size(jointPosition,DIM_FRAME), size(ANGLELIST, 1));
39
40    % For all desired angles
41    for i = 1:size(ANGLELIST,1)
42        % For all frames
43        for j = 1:size(jointPosition, DIM_FRAME)
44            % Get start, middle and end joint position
45            jointStart = squeeze(jointPosition(j, ANGLELIST{i, 2} + 1, :));
46            jointMiddle = squeeze(jointPosition(j, ANGLELIST{i, 3} + 1, :));
47            if ANGLELIST{i,4} == -1 %angle to downward vertical
48                jointEnd = jointMiddle + [0; -1; 0];
49            elseif ANGLELIST{i,4} == -2 %angle to upward vertical
50                jointEnd = jointMiddle + [0; 1; 0];
51            elseif ANGLELIST{i,4} == -3 %forward
52                jointAngles(j,i) = atand(jointStart(1)/jointStart(2));
53                continue

```

Code 13 Joint angles computation in Matlab

```

1      elseif ANGLELIST{i,4} == -4 %sideways
2          jointAngles(j,i) = atand(jointStart(3)/jointStart(2));
3          continue
4      elseif ANGLELIST{i,4} == 25
5          jointEnd = (squeeze(jointPosition(j, 10, :)) + squeeze(jointPosition(j, 13, :)))/2;
6          else
7              jointEnd = squeeze(jointPosition(j, ANGLELIST{i, 4} + 1, :));
8          end
9      % Define the two segment originating from the middle joint
10         seg1 = jointStart - jointMiddle;
11         seg2 = jointEnd - jointMiddle;
12
13         % Computing the 360 degrees angle using cross product definition and
14         % dot product definition
15         jointAngles(j,i) = atan2d(norm(cross(seg1, seg2)), dot(seg1, seg2));
16
17
18     end
19 end
20 % Converting to table
21 jointAnglesTable = array2timetable(jointAngles, 'RowTimes',timespace, 'VariableNames',\
22 string(ANGLELIST(:,1)));
23 end

```

Bibliography

- Abouelkhair, F., & Duprey, S. (2012). Assessing shoulder posture ergonomics thanks to a finite element analysis. *Computer methods in biomechanics and biomedical engineering*, 15, 348–349.
- Adams, C. M. (2002). Sociokinetic analysis as a tool for optimization of environmental design.
- Aghevli, A., Bachmann, A., Bresina, J., Greene, K., Kanefsky, B., Kurien, J., McCurdy, M., Morris, P., Pyrzak, G., Ratterman, C., et al. (2006). Planning applications for three mars missions with ensemble. *International Workshop on Planning and Scheduling for Space*.
- Alizadehkhayat, O., Fisher, A., Kemp, G., & Frostick, S. (2007). Strength and fatigability of selected muscles in upper limb: assessing muscle imbalance relevant to tennis elbow. *Journal of Electromyography and Kinesiology*, 17(4), 428–436.
- Alqahtani, F. M. A., Banks, J., Chandran, V., & Zhang, J. (2019). Detection and tracking of faces in 3d using a stereo camera arrangements. *International Journal of Machine Learning and Computing*, 9(1), 35–43.
- Andersson. (1974). Lumbar disc pressure and myoelectric back muscle activity during sitting. i. studies on an experimental chair. *Scandinavian Journal of Rehabilitation Medicine*, 6(3), 104–114.
- Andersson. (1975). The sitting posture: an electromyographic and discometric study. *Orthopedic Clinics of North America*, 6(1), 105–120.
- Annett, J. (2002). Subjective rating scales in ergonomics: a reply. *Ergonomics*, 45(14), 1042–1046.
- ApolloSaturn website. (2017). <https://www.apollosaturn.com/Website-II/The-Apollo-Spacecraft>
- Aritan, S. (2012). Biomechanical measurement methods to analyze the mechanisms of sport injuries. *Sports injuries* (pp. 19–26). Springer.
- Associates, W., Associates), A. R. P. (, Scientific, S. A., & Office, T. I. (1978). *Anthropometric source book: anthropometry for designers* (Vol. 1). National Aeronautics; Space Administration, Scientific; Technical ...
- Australia, S. W. (2011). *Hazardous manual tasks: code of practice*. Australian Government-Safe Work Australia.
- Axpe, E., Chan, D., Abegaz, M. F., Schreurs, A.-S., Alwood, J. S., Globus, R. K., & Appel, E. A. (2020). A human mission to mars: predicting the bone mineral density loss of astronauts. *PloS one*, 15(1), e0226434.

- B, A. (1948). Standing and sitting posture. *Stockholm: AB Nordiska Bokhandeln*.
- Bachmann, R., Spörri, J., Fua, P., & Rhodin, H. (2019). Motion capture from pan-tilt cameras with unknown orientation. *2019 International Conference on 3D Vision (3DV)*, 308–317.
- Balci, R., & Aghazadeh, F. (2004). Effects of exercise breaks on performance, muscular load, and perceived discomfort in data entry and cognitive tasks. *Computers & Industrial Engineering*, 46(3), 399–411.
- Baque, P., Remelli, E., Fleuret, F., & Fua, P. (2018). Geodesic convolutional shape optimization. *International Conference on Machine Learning*, 472–481.
- Barratt, M. R., & Pool, S. L. (2008). *Principles of clinical medicine for space flight*. Springer Science & Business Media.
- Bauby, C., & Kuo, A. (2000). Stabilization of lateral motion in passive dynamic walking. *Journal of Biomechanics*, 33, 1433–1440.
- Bendix, T., & Biering-Sørensen, F. (1983). Posture of the trunk when sitting on forward inclining seats. *Scandinavian Journal of Rehabilitation Medicine*, 15(4), 197–203.
- Bennett, H. E. (1928). *School posture and seating: a manual for teachers, physical directors and school officials*. Ginn.
- Blackshear, W., & Gapcynski, J. (1977). An improved value of the lunar moment of inertia. *Journal of Geophysical Research*, 82(11), 1699–1701.
- Blanchonette, P. (2010). Jack human modelling tool: a review.
- Bock, O. (1996). Grasping of virtual objects in changed gravity. *Aviation, space, and environmental medicine*, 67(12), 1185–1189.
- Bouchard, D. R., & Trudeau, F. (2007). Reliability of the assessment of the oxygen/heart rate relationship during a workday. *Applied Ergonomics*, 38(5), 491–497.
- Bradski, G. (2000). The OpenCV Library. *Dr. Dobbs's Journal of Software Tools*.
- Branton, P., & Grayson, G. (1967). An evaluation of train seats by observation of sitting behaviour. *Ergonomics*, 10(1), 35–51.
- Braune, C. W. (1889). *The center of gravity of the human body as related to the equipment of the german infantry*. S. Hirtel.
- Brown, I. D. (1994). Driver fatigue. *Human factors*, 36(2), 298–314.
- Bruno Garza, J. L., & Young, J. G. (2015). A literature review of the effects of computer input device design on biomechanical loading and musculoskeletal outcomes during computer work. *Work*, 52(2), 217–230.
- Bush, T. R., & Gutowski, P. E. (2003). An approach for hip joint center calculation for use in seated postures. *Journal of Biomechanics*, 36(11), 1739–1743.
- Cao, Z., Hidalgo Martinez, G., Simon, T., Wei, S., & Sheikh, Y. A. (2019). Openpose: realtime multi-person 2d pose estimation using part affinity fields. *IEEE Transactions on Pattern Analysis and Machine Intelligence*.
- Cao, Z., Simon, T., Wei, S.-E., & Sheikh, Y. (2017). Realtime multi-person 2d pose estimation using part affinity fields. *Proceedings of the IEEE conference on computer vision and pattern recognition*, 7291–7299.

- Cappozzo, A., Catani, F., Leardini, A., Benedetti, M., & Della Croce, U. (1996). Position and orientation in space of bones during movement: experimental artefacts. *Clinical biomechanics*, 11(2), 90–100.
- Caron, O., Faure, B., & Brenière, Y. (1997). Estimating the centre of gravity of the body on the basis of the centre of pressure in standing posture. *Journal of biomechanics*, 30(11-12), 1169–1171.
- Celentano, J., Amorelli, D., & Freeman, G. (1963). Establishing a habitability index for space stations and planetary bases. *Manned Space Laboratory Conference*, 139.
- Cente, N. J. S. (1966). Manned space center, preliminary technical data for earth orbiting space station: standards and criteria. *MSC-EA-R-66-1, NASA TMX59700. Houston*, 2.
- Cerveri, P., Pedotti, A., & Ferrigno, G. (2004). Evolutionary optimization for robust hierarchical computation of the rotation centres of kinematic chains from reduced ranges of motion the lower spine case. *Journal of biomechanics*, 37(12), 1881–1890.
- Chaffin, D. B. (1987). Manual materials handling and the biomechanical basis for prevention of low-back pain in industry—an overview. *American Industrial Hygiene Association Journal*, 48(12), 989–996.
- Chaffin, D. B. (2007). Human motion simulation for vehicle and workplace design. *Human Factors and Ergonomics in Manufacturing & Service Industries*, 17(5), 475–484.
- Chaffin, D. B., Andersson, G. B., & Martin, B. J. (2006). *Occupational biomechanics*. John Wiley & sons.
- Chaffin, D. B., Schutz, R. K., & Snyder, R. G. (1972). *A prediction model of human volitional mobility*. Society of Automotive Engineers.
- Chany, A.-M., Marras, W. S., & Burr, D. L. (2007). The effect of phone design on upper extremity discomfort and muscle fatigue. *Human factors*, 49(4), 602–618.
- Chappell, S. P., & Klaus, D. M. (2013). Enhanced simulation of partial gravity for extravehicular activity. *Journal of Human Performance in Extreme Environments*, 10(2), 1.
- Chéronnet, L. (1950). The french chair. *The Burlington Magazine*, 92(565), 112–115.
- Chou, R., & Shekelle, P. (2010). Will this patient develop persistent disabling low back pain? *Jama*, 303(13), 1295–1302.
- Christensen, J. M., McBarron, J. W., McConville, J. T., Pogue, W. R., Williges, R. C., & Woodson, W. E. (n.d.). Man-systems integration standards nasa-std-3000, volume ii revision b, july 1995.
- Clauser, C. E., McConville, J. T., & Young, J. W. (1969). *Weight, volume, and center of mass of segments of the human body* (tech. rep.). Antioch Coll Yellow Springs OH.
- Clément, G. (2011). *Fundamentals of space medicine* (Vol. 23). Springer Science & Business Media.
- Clément, G. (2017). International roadmap for artificial gravity research. *npj Microgravity*, 3(1), 1–7.
- Cmulab website. (2022). https://cmu-perceptual-computing-lab.github.io/openpose/web/html/doc/md_doc_02_output.html
- Cohen, J. (1992). Statistical power analysis. *Current directions in psychological science*, 1(3), 98–101.

- Cohen, M. M. (2008). Testing the celentano curve: an empirical survey of predictions for human spacecraft pressurized volume. *SAE International Journal of Aerospace*, 1(2008-01-2027), 107–142.
- Colombini, D. (2002). *Risk assessment and management of repetitive movements and exertions of upper limbs: job analysis, ocr risk indices, prevention strategies and design principles*. Elsevier.
- Colyer, S. L., Evans, M., Cosker, D. P., & Salo, A. I. (2018). A review of the evolution of vision-based motion analysis and the integration of advanced computer vision methods towards developing a markerless system. *Sports medicine-open*, 4(1), 1–15.
- Cooper, G. E., & Harper, R. P. (1969). *The use of pilot rating in the evaluation of aircraft handling qualities*. National Aeronautics; Space Administration.
- Corlett. (1976). A technique for assessing postural discomfort. *Ergonomics*, 19(2), 175–182.
- Corlett, E., & Eklund, J. (1984). How does a backrest work? *Applied Ergonomics*, 15(2), 111–114.
- Corlett, Wilson, J. R., & CORLETT, N. (1995). *Evaluation of human work*. CRC Press.
- d'Alembert, J. L. R. (1743). *Traité de dynamique*. David l'ainé.
- Data. data for thesis. (n.d.).
- Database, T. N. I. M. S. N. et al. (1996). Muscular weakness assessment: use of normal isometric strength data. *Archives of Physical Medicine and Rehabilitation*, 77(12), 1251–1255.
- Davenport, E., CONGDON, S., & PIERCE, B. (1963). The minimum volumetric requirements of man in space. *Summer Meeting*, 250.
- Davidson, B. S., Madigan, M. L., & Nussbaum, M. A. (2004). Effects of lumbar extensor fatigue and fatigue rate on postural sway. *European journal of applied physiology*, 93(1), 183–189.
- De Kok, J., Vroonhof, P., Snijders, J., Roullis, G., Clarke, M., Peereboom, K., van Dorst, P., & Isusi, I. (2019). Work-related musculoskeletal disorders: prevalence, costs and demographics in the eu. *European Agency for Safety and Health at Work*, 1.
- De Leva, P. (1996). Adjustments to zatsiorsky-seluyanov's segment inertia parameters. *Journal of biomechanics*, 29(9), 1223–1230.
- Delleman, N. J., Haslegrave, C. M., & Chaffin, D. B. (2004). *Working postures and movements*. CRC press.
- Dempster, W. T. (1955). *Space requirements of the seated operator; geometrical, kinematic, and mechanical aspects of the body with special reference to the limbs* (tech. rep.). Michigan State Univ East Lansing.
- Do, S., Owens, A., Ho, K., Schreiner, S., & De Weck, O. (2016). An independent assessment of the technical feasibility of the mars one mission plan–updated analysis. *Acta Astronautica*, 120, 192–228.
- Drescher, E. (1929). Arbeitssitz und arbeitplatz. *Reichsarbeitsblatt III*, 159–75.
- Dul, J., De Vlamming, P., & Munnik, M. (1996). A review of iso and cen standards on ergonomics. *International Journal of Industrial Ergonomics*, 17(3), 14.
- Dumas, R., Cheze, L., & Verriest, J.-P. (2007). Adjustments to mcconville et al. and young et al. body segment inertial parameters. *Journal of biomechanics*, 40(3), 543–553.

- Dumas, R., & Wojtusich, J. (2018). Estimation of the body segment inertial parameters for the rigid body biomechanical models used in motion analysis. in: müller b., wolf s.(eds) handbook of human motion.
- Dunk, N. M., & Callaghan, J. P. (2005). Gender-based differences in postural responses to seated exposures. *Clinical biomechanics*, 20(10), 1101–1110.
- Dunk, N. M., Kedgley, A. E., Jenkyn, T. R., & Callaghan, J. P. (2009). Evidence of a pelvis-driven flexion pattern: are the joints of the lower lumbar spine fully flexed in seated postures? *Clinical biomechanics*, 24(2), 164–168.
- Encyclopedia of occupational Health and safety website. (2011). <https://www.iloencyclopaedia.org/part-iv-66769/ergonomics-52353/physical-and-physiological-aspects/item/487-muscular-work>
- ESA website. (2022). https://www.esa.int/Science_Exploration/Human_and_Robotic_Exploration/Exploration/Human_health_and_performance
- Fee, M. S. (2014). The role of efference copy in striatal learning. *Current opinion in neurobiology*, 25, 194–200.
- Fick, R. (1911). *Handbuch der anatomie und mechanik der gelenke: t. spezielle gelenk-und muskelmechanik* (Vol. 3). G. Fischer.
- Figshare. custom-made scripts. (2022). <https://figshare.com/s/4c918f38e7b7f39d98e6>
- Fitts, P. M. (1954). The information capacity of the human motor system in controlling the amplitude of movement. *Journal of experimental psychology*, 47(6), 381.
- Floyd, W., & Roberts, D. (1958). Anatomical and physiological principles in chair and table design. *Ergonomics*, 2(1), 1–16.
- Fraser, T. M. (1966). *The effects of confinement as a factor in manned space flight* (tech. rep.).
- Freixas, M., Grau, S., & Silva, D. (2006). Boolean operations in open-source blender project. *SIACG*, 159–167.
- Frey Law, L. A., & Avin, K. G. (2010). Endurance time is joint-specific: a modelling and meta-analysis investigation. *Ergonomics*, 53(1), 109–129.
- Fu, K. S., Gonzalez, R., & Lee, C. G. (1987). *Robotics: control sensing. vis.* Tata McGraw-Hill Education.
- Gallasch, E., Rafolt, D., Moser, M., Hindinger, J., Eder, H., Wießpeiner, G., & Kenner, T. (1996). Instrumentation for assessment of tremor, skin vibrations, and cardiovascular variables in mir space missions. *IEEE transactions on biomedical engineering*, 43(3), 328–333.
- Gardenweb. (2022). <http://gardenweb.ru/rabochee-sidene>
- Garg, A., Hegmann, K., Schwoerer, B., & Kapellusch, J. (2002). The effect of maximum voluntary contraction on endurance times for the shoulder girdle. *International journal of industrial ergonomics*, 30(2), 103–113.
- Github. (2022). https://github.com/cvlab-epfl/multiview_calib
- Gore, D., JR, MARTIN, D., & TRUST, R. (n.d.). Space shuttle orbiter habitability and its extensibility. *Conference on Large Space Platforms: Future Needs and Capabilities*, 1669.
- Gower, J., & Dijksterhuis, G. (n.d.). Procrustes problems. 2004. *Non cité*.
- Guevarra, E. T. M. (2020). Blending with blender: the modeling workspace. *Modeling and animation using blender* (pp. 87–115). Springer.

- Hamilton, D. R. (2008). Cardiovascular disorders. *Principles of clinical medicine for space flight* (pp. 317–359). Springer.
- Harrison, D. D., Harrison, S. O., Croft, A. C., Harrison, D. E., & Troyanovich, S. J. (1999). Sitting biomechanics part i: review of the literature. *Journal of manipulative and physiological therapeutics*, 22(9), 594–609.
- Hart, S. G. (2006). Nasa-task load index (nasa-tlx); 20 years later. *Proceedings of the human factors and ergonomics society annual meeting*, 50(9), 904–908.
- Hart, S. G., & Staveland, L. E. (1988). Development of nasa-tlx (task load index): results of empirical and theoretical research. *Advances in psychology* (pp. 139–183). Elsevier.
- Hartley, R., & Zisserman, A. (2013). Multiple view geometry in computer vision (cambridge university, 2003). *C1 C3*, 2.
- Hartley, R., & Zisserman, A. (2003). *Multiple view geometry in computer vision*. Cambridge university press.
- Hartvigsen, J., Leboeuf-Yde, C., Lings, S., & Corder, E. H. (2000). Is sitting-while-at-work associated with low back pain? a systematic, critical literature review. *Scandinavian journal of public health*, 28(3), 230–239.
- Haslegrave, C. (1986). Characterizing the anthropometric extremes of the population. *Ergonomics*, 29(2), 281–301.
- Häuplik-Meusburger, S. (2011). *Architecture for astronauts: an activity-based approach*. Springer Science & Business Media.
- Hedge, A. (2016). *Ergonomic workplace design for health, wellness, and productivity*. CRC Press.
- Hignett, S., & McAtamney, L. (2000). Rapid entire body assessment (reba). *Applied ergonomics*, 31(2), 201–205.
- Hill, S. G., Iavecchia, H. P., Byers, J. C., Bittner Jr, A. C., Zaklade, A. L., & Christ, R. E. (1992). Comparison of four subjective workload rating scales. *Human factors*, 34(4), 429–439.
- Hofstetter, W., de Weck, O., & Crawley, E. (2005). 9.1. 3 modular building blocks for manned spacecraft: a case study for moon and mars landing systems. *Incoase International Symposium*, 15(1), 1296–1312.
- Holden, K., Wilmington, R., & Whitmore, M. (1991). Cursor control device evaluations for space station freedom: a summary. *LESC-29974*.
- Hollerbach, J. M. (1980). A recursive lagrangian formulation of manipulator dynamics and a comparative study of dynamics formulation complexity. *IEEE Transactions on Systems, Man, and Cybernetics*, 10(11), 730–736.
- Huijgens, J. (1981). A model for quantifying static load, incorporating muscle fatigue. *Biomechanics Symposium, Boulder, CO*, 22–24.
- Imbeau, D., Farbos, B. et al. (2006). Percentile values for determining maximum endurance times for static muscular work. *International Journal of Industrial Ergonomics*, 36(2), 99–108.
- Ippel, M. J. (1996). Cognitive task load and test performance. *Proc. 38th Ann. Conf. of the Intern. Military Testing Association (IMTA)*, 304–314.
- ISO. (2004). <http://www.iso.org/iso/en/ISOOnline.openpage>
- ISO 11226.EPFL Cobaz site. (2000). <https://viewerbdc.afnor.org/pdf/viewer/QzRzLo8jTnc1>

- ISO 11228-2. EPFL Cobaz site. (2007). <https://viewerbdc.afnor.org/pdf/viewer/QCbUMBoDSmQ1>
- ISO 11228-3. EPFL Cobaz site. (2007). <https://viewerbdc.afnor.org/pdf/viewer/JwIoc7w66Fo1>
- ISS wikipedia. (2022). https://en.wikipedia.org/wiki/International_Space_Station
- Jacobs, P. (2004). Kodak's ergonomic design for people at work. *Professional Safety*, 49(3), 49.
- Jäger, M., Jordan, C., Theilmeier, A., & Luttmann, A. (2001). Dortmunder lumbalbelastungsstudie 2: ermittlung und beurteilung vergleichbarer tätigkeiten hinsichtlich der körperhaltung und der wirbelsäulenbelastung bei verschiedenen beruflichen tätigkeiten. *Forschungsbericht: Hauptverband der gewerblichen Berufsgenossenschaften (HVBG)*.
- Jebur, A., Abed, F., & Mohammed, M. (2018). Assessing the performance of commercial agisoft photostan software to deliver reliable data for accurate 3d modelling. *MATEC Web of Conferences*, 162, 03022.
- Jian, M., Qi, Q., Dong, J., Yin, Y., Zhang, W., & Lam, K.-M. (2017). The ouc-vision large-scale underwater image database. *2017 IEEE International Conference on Multimedia and Expo (ICME)*, 1297–1302.
- Kane, T. R., & Levinson, D. A. (1985). *Dynamics, theory and applications*. McGraw Hill.
- Kapandji, A., & Kapandji, I. A. (2007). *The physiology of the joints: the upper limb. volume one*. Churchill Livingstone.
- Karhu, O., Kansi, P., & Kuorinka, I. (1977). Correcting working postures in industry: a practical method for analysis. *Applied ergonomics*, 8(4), 199–201.
- Karol, S., & Robertson, M. M. (2015). Implications of sit-stand and active workstations to counteract the adverse effects of sedentary work: a comprehensive review. *Work*, 52(2), 255–267.
- Karwowski, W., Szopa, A., & Soares, M. M. (2021). *Handbook of standards and guidelines in human factors and ergonomics*. Crc Press.
- Keegan, J. J. (1962). Evaluation and improvement of seats. *Industrial medicine & surgery*, 31, 137–148.
- Keegan, J. J. (2005). Alterations of the lumbar curve related to posture and seating. *Ergonomics: The history and scope of human factors*, 1, 339.
- Kelly, T. (1964). Apollo lunar module.
- Kennedy, K., Touns, L., & Smitherman, D. (2007). Lunar habitation strategies. *AIAA SPACE 2007 Conference & Exposition*, 6275.
- Kilbom. (1987). Short-and long-term effects of extreme physical inactivity. a review. *Selected papers from the International Scientific Conference on Work with display units* 86, 219–228.
- Kilbom. (1994). Repetitive work of the upper extremity: part ii—the scientific basis (knowledge base) for the guide. *International journal of industrial ergonomics*, 14(1-2), 59–86.
- Kim, J. H., Aulck, L., Trippany, D., & Johnson, P. W. (2015). The effects of work surface hardness on mechanical stress, muscle activity, and wrist postures. *Work*, 52(2), 231–244.
- Kirk, B. J., Trajano, G. S., Pulverenti, T. S., Rowe, G., & Blazeovich, A. J. (2019). Neuromuscular factors contributing to reductions in muscle force after repeated, high-intensity muscular efforts. *Frontiers in physiology*, 10, 783.

- Knutsson, B., Lindh, K., & Telhag, H. (1966). Sitting—an electromyographic and mechanical study. *Acta Orthopaedica Scandinavica*, 37(4), 415–428.
- Kosmadoudi, Z., Lim, T., Ritchie, J., Louchart, S., Liu, Y., & Sung, R. (2013). Engineering design using game-enhanced cad: the potential to augment the user experience with game elements. *Computer-Aided Design*, 45(3), 777–795.
- Kroemer. (1971). Seating in plant and office. *American Industrial Hygiene Association Journal*, 32(10), 633–652.
- Kroemer, K. H., Kroemer, H. J., & Kroemer-Elbert, K. E. (2010). Engineering anthropometry. *Engineering physiology* (pp. 265–330). Springer.
- Krzywicki, H. J., & Chinn, K. S. (1967). Human body density and fat of an adult male population as measured by water displacement. *The American journal of clinical nutrition*, 20(4), 305–310.
- Kuchera, M. L. (1995). Gravitational stress, musculoligamentous strain, and postural alignment. *SPINE-PHILADELPHIA-HANLEY AND BELFUS-*, 9, 463–463.
- Kuiper, J. I., Burdorf, A., Verbeek, J. H., Frings-Dresen, M. H., Van Der Beek, A. J., & Viikari-Juntura, E. R. (1999). Epidemiologic evidence on manual materials handling as a risk factor for back disorders: a systematic review. *International Journal of Industrial Ergonomics*, 24(4), 389–404.
- Kumar, S. (2001). Theories of musculoskeletal injury causation. *Ergonomics*, 44(1), 17–47.
- Kwon, B., Roffey, D., Bishop, P., Dagenais, S., & Wai, E. (2011). Systematic review: occupational physical activity and low back pain. *Occupational medicine*, 61(8), 541–548.
- Lalitharatne, T. D., Hayashi, Y., Teramoto, K., & Kiguchi, K. (2012). A study on effects of muscle fatigue on emg-based control for human upper-limb power-assist. *2012 IEEE 6th International Conference on Information and Automation for Sustainability*, 124–128.
- Lanczos, C. (1970). The variational principles of mechanics, vol. 4. *Courier Corporation*.
- Lappe, M., Hoffmann, K.-P. et al. (2000). Optic flow and eye movements. *International review of neurobiology*, 29–50.
- Lauer, J., Vilas-Boas, J. P., & Rouard, A. H. (2018). Shoulder mechanical demands of slow underwater exercises in the scapular plane. *Clinical Biomechanics*, 53, 117–123.
- Laurig, W., & Vedder, J. (1998). Encyclopedia of occupational health and safety.
- Laws, C. J., Berg-Johansen, B., Hargens, A. R., & Lotz, J. C. (2016). The effect of simulated microgravity on lumbar spine biomechanics: an in vitro study. *European Spine Journal*, 25(9), 2889–2897.
- Lay, W., & Fisher, L. (1940). *Riding comfort and cushions* (tech. rep.). SAE Technical Paper.
- Le Veau, B. (1977). Biomechanics of human motion by williams, marian and lissner h r.
- Leach, C., & Rambaut, P. (1977). Biochemical responses of the skylab crewmember: an overview. *JOHNSTON, RS; DIETLEIN, LF Biomedical Results from Skylab (NASA SP-377)*. Washington: US Government Printing Office.
- Lee, S. (2021). Risk of cardiovascular adaptations contributing to adverse mission performance and health outcomes.
- Lee, S., Stenger, M. B., Laurie, S. S., & Macias, B. R. (2017). Risk of cardiac rhythm problems during spaceflight.

- Li, K. W., & Lee, C.-L. (1999). Postural analysis of four jobs on two building construction sites: an experience of using the owas method in taiwan. *Journal of Occupational Health*, 41(3), 183–190.
- Li, X., Han, S., Gül, M., Al-Hussein, M., & El-Rich, M. (2018). 3d visualization-based ergonomic risk assessment and work modification framework and its validation for a lifting task. *Journal of Construction Engineering and Management*, 144(1), 04017093.
- Lin, J.-H., Radwin, R. G., Fronczak, F. J., & Richard, T. G. (2003). Forces associated with pneumatic power screwdriver operation: statics and dynamics. *Ergonomics*, 46(12), 1161–1177.
- Lis, A. M., Black, K. M., Korn, H., & Nordin, M. (2007). Association between sitting and occupational lbp. *European Spine Journal*, 16(2), 283–298.
- Liu, J. Z., Brown, R. W., & Yue, G. H. (2002). A dynamical model of muscle activation, fatigue, and recovery. *Biophysical journal*, 82(5), 2344–2359.
- Lohman, T. G., Roche, A. F., Martorell, R., et al. (1988). *Anthropometric standardization reference manual*. Human kinetics books.
- Lueder. (1992). *Seating, posture and ergonomics, in sweer*. Chiropractic Family Practice: A clinical manual, Gaithersburg, Maryland: Aspen Publishing, Section 21.
- Lueder, R., & Noro, K. (1994). *Hard facts about soft machines: the ergonomics of seating*. CRC Press.
- Ma, L., Chablat, D., Bennis, F., & Zhang, W. (2009). A new simple dynamic muscle fatigue model and its validation. *International journal of industrial ergonomics*, 39(1), 211–220.
- Ma, L., Chablat, D., Bennis, F., Zhang, W., Hu, B., & Guillaume, F. (2011). A novel approach for determining fatigue resistances of different muscle groups in static cases. *International Journal of Industrial Ergonomics*, 41(1), 10–18.
- Majeske, C., & Buchanan, C. (1984). Quantitative description of two sitting postures: with and without a lumbar support pillow. *Physical therapy*, 64(10), 1531–1533.
- Majumder, J., Kotadiya, S. M., Sharma, L. K., & Kumar, S. (2018). Upper extremity muscular strength in push–pull tasks: model approach towards task design. *Indian journal of occupational and environmental medicine*, 22(3), 138.
- Manenica, I. (1986). A technique for posterial load assessment. the ergonomics of working postures. edited by n. corlett, j. wilson, i. manenica.
- Marton, T., Rudek, F., Miller, R., & Norman, D. (1971). Handbook of human engineering design data for reduced gravity conditions.
- Mathworkds website. (2022). <https://fr.mathworks.com/matlabcentral/answers/143618-correcting-lens-distortion-during-camera-calibration>
- Matthijsse, P. C., Hendrich, K. M., Rijnsburger, W. H., Woittiez, R. D., & Huijing, P. A. (1987). Ankle angle effects on endurance time, median frequency and mean power of gastrocnemius emg power spectrum: a comparison between individual and group analysis. *Ergonomics*, 30(8), 1149–1159.
- McAtamney, L., Aickin, C., Caple, D., Caponecchia, C., & Mackey, M. (2016). Challenges and future research opportunities with new ways of working. *Ergonomic Workplace Design for Health, Wellness, and Productivity*, 353.

- McAtamney, L., & Corlett, E. N. (1993). Rula: a survey method for the investigation of work-related upper limb disorders. *Applied ergonomics*, 24(2), 91–99.
- McConville, J. T., Clauser, C. E., Churchill, T. D., Cuzzi, J., & Kaleps, I. (1980). *Anthropometric relationships of body and body segment moments of inertia* (tech. rep.). ANTHROPOLOGY RESEARCH PROJECT INC YELLOW SPRINGS OH.
- McGill, S. M. (1997). The biomechanics of low back injury: implications on current practice in industry and the clinic. *Journal of biomechanics*, 30(5), 465–475.
- Merfeld, D. M. (1996). Effect of spaceflight on ability to sense and control roll tilt: human neurovestibular studies on sls-2. *Journal of Applied Physiology*, 81(1), 50–57.
- Meyer, J., Arnrich, B., Schumm, J., & Troster, G. (2010). Design and modeling of a textile pressure sensor for sitting posture classification. *IEEE Sensors Journal*, 10(8), 1391–1398.
- Miller, D. I., Nelson, R. C., & Montoye, H. J. (1975). *Biomechanics of sport* (Vol. 7). LWW.
- Minenko, V., Bykovsky, S., & Semenenko, (2017). Cockpit comfort level of the descent capsule-shaped vehicles. *Aerospace Scientific Journal*, 3(2), 17–33.
- Mital, A., Nicholson, A. S., & Ayoub, M. M. (2017). *A guide to manual materials handling*. CRC Press.
- Monod, H., & Scherrer, J. (1965). The work capacity of a synergic muscular group. *Ergonomics*, 8(3), 329–338.
- Morabito, J., Penkala, S., & Coxon, K. (2021). Workplace musculoskeletal problems in occupational therapy students. *BMC Public Health*, 21(1), 1–12.
- Morant, G. M. (1947). *Dimensional requirements for seats in raf aircraft*. Institute of Aviation Medicine.
- Morey-Holton, E. R. (2003). The impact of gravity on life. *Evolution on planet earth* (pp. 143–159). Elsevier.
- Mount, F. E., Whitmore, M., & Stealey, S. L. (2003). *Evaluation of neutral body posture on shuttle mission sts-57 (spacehab-1)* (tech. rep.).
- Nachemson, A. (1970). Intravital dynamic pressure measurements in lumbar discs: a study of common movements, maneuvers and exercises. *Scand J Rehabil Med*, 1, 1–40.
- Nagatomo, E., Kouzaki, M., & Ishihara, A. (2014). Effects of microgravity on blood flow in the upper and lower limbs. *Aerospace Science and Technology*, 34, 20–23.
- Nakano, N., Sakura, T., Ueda, K., Omura, L., Kimura, A., Iino, Y., Fukushima, S., & Yoshioka, S. (2020). Evaluation of 3d markerless motion capture accuracy using openpose with multiple video cameras. *Frontiers in sports and active living*, 2, 50.
- Naqvi, A. (1994). Study of forward sloping seats for vdt workstations. *Journal of human ergology*, 23(1), 41–49.
- NASA website. (1972). https://www.hq.nasa.gov/alsj/a17/A17_LunarRover2.pdf
- NASA. apollo news reference. section: crew personal equipment cpe1-16. (1972). https://www.hq.nasa.gov/alsj/LM05_Crew_Personal_Equipment_ppCPE1-16.pdf
- NASA. ergonomic chair website. (2022). <https://spinoff.nasa.gov/spinoff1997/ch2.html>
- Neufert, E., & Neufert, P. (2012). *Architects' data*. John Wiley & Sons.
- Newmarch, J. (2017). Ffmpeg/libav. *Linux sound programming* (pp. 227–234). Springer.

- Newton, I. (2009). *Philosophiae naturalis principia mathematica* (Vol. 62). Jussu Societatis Regiae ac typis Josephi Streater, prostant venales apud Sam ...
- Nicogossian, A. E., Doarn, C. R., & Hu, Y. (2016). Evolution of human capabilities and space medicine. *Space physiology and medicine* (pp. 3–57). Springer.
- Nishanth, R., Muthukumar, M., & Arivanantham, A. (2015). Ergonomic workplace evaluation for assessing occupational risks in multistage pump assembly. *International Journal of Computer Applications*, 113(9).
- Nussbaum, M. A., & Zhang, X. (2000). Heuristics for locating upper extremity joint centres from a reduced set of surface markers. *Human Movement Science*, 19(5), 797–816.
- Occhipinti, E. (1998). Ocra: a concise index for the assessment of exposure to repetitive movements of the upper limbs. *Ergonomics*, 41(9), 1290–1311.
- Oman, C. M., Pouliot, C. F., & Natapoff, A. (1996). Horizontal angular vor changes in orbital and parabolic flight: human neurovestibular studies on sls-2. *Journal of Applied Physiology*, 81(1), 69–81.
- Ong, S., Pang, Y., & Nee, A. (2007). Augmented reality aided assembly design and planning. *CIRP annals*, 56(1), 49–52.
- OpenCVdocs website. (2022). https://docs.opencv.org/3.4/d7/d4f/samples_2dnn_2openpose_8cpp-example.html
- Orwoll, E. S., Adler, R. A., Amin, S., Binkley, N., Lewiecki, E. M., Petak, S. M., Shapses, S. A., Sinaki, M., Watts, N. B., & Sibonga, J. D. (2013). Skeletal health in long-duration astronauts: nature, assessment, and management recommendations from the nasa bone summit. *Journal of bone and mineral research*, 28(6), 1243–1255.
- Osokin, D. (2018). Real-time 2d multi-person pose estimation on cpu: lightweight openpose. *arXiv preprint arXiv:1811.12004*.
- O'Sullivan, P., Dankaerts, W., Burnett, A., Chen, D., Booth, R., Carlsen, C., & Schultz, A. (2006). Evaluation of the flexion relaxation phenomenon of the trunk muscles in sitting. *Spine*, 31(17), 2009–2016.
- O'Sullivan, P., Twomey, L., Allison, G., Sinclair, J., Miller, K., & Knox, J. (1997). Altered patterns of abdominal muscle activation in patients with chronic low back pain. *Australian journal of physiotherapy*, 43(2), 91–98.
- Ozsoy, B., Ji, X., Yang, J., Gragg, J., & Howard, B. (2015). Simulated effect of driver and vehicle interaction on vehicle interior layout. *International Journal of Industrial Ergonomics*, 49, 11–20.
- Parow, W. (1864). Studien über die physikalischen bedingungen der aufrechten stellung und der normalen krümmungen der wirbelsäule. *Archiv für pathologische Anatomie und Physiologie und für klinische Medizin*, 31(2), 223–255.
- Parsons, K. (1995). Ergonomics and international standards: introduction, brief review of standards for anthropometry and control room design and useful information. *Applied Ergonomics*, 26(4), 239–247.
- Perino, M. A. (2005). Moon base habitation and life support systems. *MOON BASE: A Challenge for Humanity, 1 st Workshop, Venice, may, 26*.

- Petro, A. (2000). Transfer, entry, landing, and ascent vehicles. *WJ Larson, & LK Pranke, Human Spaceflight: Mission Analysis and Design*, 391–420.
- Pheasant, S., & Haslegrave, C. (1996). Anthropometry, ergonomics and the design of work.
- Plagenhoef, S., Evans, F. G., & Abdelnour, T. (1983). Anatomical data for analyzing human motion. *Research quarterly for exercise and sport*, 54(2), 169–178.
- Poston, A. (2004). *Index of government standards on human engineering design criteria, processes, and procedures. version 1* (tech. rep.). DEPARTMENT OF DEFENSE HUMAN FACTORS ENGINEERING TECHNICAL ADVISORY GROUP ...
- PushingPulling website. (2017). <https://www.ccohs.ca/oshanswers/ergonomics/push1.html>
- Pynt, J. (2015). Rethinking design parameters in the search for optimal dynamic seating. *Journal of bodywork and movement therapies*, 19(2), 291–303.
- Rando, C. M., & Schuh, S. V. (2008). Lunar and mars exploration: the autonomy factor. *38th International Conference on Environmental Systems*.
- Redgrave, J. N., Moore, L., Oyekunle, T., Ebrahim, M., Falidas, K., Snowdon, N., Ali, A., & Majid, A. (2018). Transcutaneous auricular vagus nerve stimulation with concurrent upper limb repetitive task practice for poststroke motor recovery: a pilot study. *Journal of Stroke and Cerebrovascular Diseases*, 27(7), 1998–2005.
- Reid, G. B., & Nygren, T. E. (1988). The subjective workload assessment technique: a scaling procedure for measuring mental workload. *Advances in psychology* (pp. 185–218). Elsevier.
- Reynolds, R. J. (2019). Human health in the lunar environment. *Lunar science* (p. 7). IntechOpen.
- Richter, C., Braunstein, B., Winnard, A., Nasser, M., & Weber, T. (2017). Human biomechanical and cardiopulmonary responses to partial gravity—a systematic review. *Frontiers in physiology*, 8, 583.
- Riley, N., & Bilodeau, M. (2002). Changes in upper limb joint torque patterns and emg signals with fatigue following a stroke. *Disability and rehabilitation*, 24(18), 961–969.
- Roffey, D. M., Wai, E. K., Bishop, P., Kwon, B. K., & Dagenais, S. (2010). Causal assessment of occupational sitting and low back pain: results of a systematic review. *The Spine Journal*, 10(3), 252–261.
- Rohmert, W., Wangenheim, M., Mainzer, J., Zipp, P., & Lesser, W. (1986). A study stressing the need for a static postural force model for work analysis. *Ergonomics*, 29(10), 1235–1249.
- Rohmert, W. (1960). Ermittlung von erholungspausen für statische arbeit des menschen. *Internationale Zeitschrift für angewandte Physiologie einschließlich Arbeitsphysiologie*, 18(2), 123–164.
- Rohmert, W. (1984). Das belastungs-beanspruchungs-konzept. *Zeitschrift für arbeitswissenschaft*, 38(4), 193–200.
- Romero-Franco, N., Fernández-Dominguez, J. C., Montaña-Munuera, J. A., Romero-Franco, J., & Jiménez-Reyes, P. (2019). Validity and reliability of a low-cost dynamometer to assess maximal isometric strength of upper limb: low cost dynamometry and isometric strength of upper limb. *Journal of sports sciences*, 37(15), 1787–1793.

- Roscoe, A. H., & Ellis, G. A. (1990). *A subjective rating scale for assessing pilot workload in flight: a decade of practical use* (tech. rep.). ROYAL AEROSPACE ESTABLISHMENT FARNBOROUGH (UNITED KINGDOM).
- Rose, L., Ericson, M., & Ortengren, R. (2000). Endurance time, pain and resumption in passive loading of the elbow joint. *Ergonomics*, 43(3), 405–420.
- Rubio, S., Diaz, E., Martin, J., & Puente, J. M. (2004). Evaluation of subjective mental workload: a comparison of swat, nasa-tlx, and workload profile methods. *Applied psychology*, 53(1), 61–86.
- Rudisill, M., Howard, R., Griffin, B., Green, J., Toups, L., & Kennedy, K. (2008). Lunar architecture team: phase 2 habitat volume estimation: "caution when using analogs". *Earth & space 2008: engineering, science, construction, and operations in challenging environments* (pp. 1–11).
- Ryan, C. G., Dall, P. M., Granat, M. H., & Grant, P. M. (2011). Sitting patterns at work: objective measurement of adherence to current recommendations. *Ergonomics*, 54(6), 531–538.
- Saha, S. K., & Schiehlen, W. O. (2001). Recursive kinematics and dynamics for parallel structured closed-loop multibody systems. *Mechanics of Structures and Machines*, 29(2), 143–175.
- Saibene, F., & Minetti, A. E. (2003). Biomechanical and physiological aspects of legged locomotion in humans. *European journal of applied physiology*, 88(4), 297–316.
- Salvendy, G. (2012a). *Handbook of human factors and ergonomics*. John Wiley & Sons.
- Salvendy, G. (2012b). *Handbook of human factors and ergonomics* (Vol. 144). John Wiley & Sons.
- SanSoucie, M. P., Hull, P. V., & Tinker, M. L. (2009). Lunar habitat design optimization and analysis. *Habitation*, 12(1), 79–85.
- Sato, H., Ohashi, J., Iwanaga, K., Yoshitake, R., & Shimada, K. (1984). Endurance time and fatigue in static contractions. *Journal of human ergology*, 13(2), 147–154.
- Savitsky. (1972). *Wind load on structures*.
- Schaub, K., Berg, K., & Wakula, J. (1997). Postural and workplace related influences on maximal force capacities. *IEA*, 97, 219–221.
- Schede, F. (1935). *Grundlagen der körperlichen erziehung*. Enke.
- Schoberth, H. (2013). *Sitzhaltung· sitzschaden sitzmöbel*. Springer-Verlag.
- Schulthess, W. (1907). Die pathologie und therapie der ruckgratsverkrümmungen. *HandBuch der Orthopadischen Chirurgie*.
- Schwartz, J. (2005). Rew exploration vehicle. *NASA Concept Exploration and Refinement Study*.
- Seo, J., Lee, S., & Seo, J. (2016). Simulation-based assessment of workers' muscle fatigue and its impact on construction operations. *Journal of Construction Engineering and Management*, 142(11), 04016063.
- Sforza, P. M. (2015). *Manned spacecraft design principles*. Elsevier.
- Shackel, B., Chidsey, K., & Shipley, P. (1969). The assessment of chair comfort. *Ergonomics*, 12(2), 269–306.
- Shapiro, L. (2019). *Embodied cognition*. Routledge.

- Sherwood, B., & Capps, S. (1990). Long duration habitat trade study: space transfer concepts and analyses for exploration missions. *NASA Study Contract NAS8-37857 for Marshall Space Flight Center. Huntsville, AL: Boeing Aerospace and Electronics.*
- Simon, M., Bobskill, M., & Wilhite, A. (2012). Historical volume estimation and a structured method for calculating habitable volume for in-space and surface habitats. *Acta Astronautica*, 80, 65–81.
- Simon, T., Joo, H., Matthews, I., & Sheikh, Y. (2017). Hand keypoint detection in single images using multiview bootstrapping. *Proceedings of the IEEE conference on Computer Vision and Pattern Recognition*, 1145–1153.
- Sjøgaard, G. (1986). Intramuscular changes during long-term contraction. *The ergonomics of working postures*, 136–143.
- Snyder, R. G., Chaffin, D. B., & Schutz, R. K. (1972). *Link system of the human torso* (tech. rep.). MICHIGAN UNIV ANN ARBOR HIGHWAY SAFETYRESEARCH INST.
- Song, G., Zhuang, D., & Wanyan, X. (2010). Biomechanical human model of pilot operation posture. *2010 3rd International Conference on Biomedical Engineering and Informatics*, 3, 1146–1150.
- Spivak, S. M., & Brenner, F. C. (2018). *Standardization essentials: principles and practice*. CRC Press.
- Staffel, F. (1884). Zur hygiene des sitzens. *Zbl F Allg Gesundheitspflege*, 3, 403–421.
- States, R. A. (1997). Two simple methods for improving the reliability of joint center locations. *Clinical Biomechanics*, 12(6), 367–374.
- Straßer, H. (1913). Die rumpfhaltungen. *Lehrbuch der muskel-und gelenkmechanik* (pp. 244–320). Springer.
- Sumini, V., Wald, S., Mueller, C., Chesi, C., & Weck, O. L. d. (2018). Multiobjective optimization for structural design of lunar habitats. *Earth and space 2018: engineering for extreme environments* (pp. 169–182). American Society of Civil Engineers Reston, VA.
- Summerskill, S., Marshall, R., Cook, S., Lenard, J., & Richardson, J. (2016). The use of volumetric projections in digital human modelling software for the identification of large goods vehicle blind spots. *Applied ergonomics*, 53, 267–280.
- Tafforin, C., & Bichi, A. (1996). Global analysis of scientific data from the three experimental campaigns for european manned space infrastructure. *SAE transactions*, 536–545.
- Takala, E.-P., Pehkonen, I., Forsman, M., Hansson, G.-Å., Mathiassen, S. E., Neumann, W. P., Sjøgaard, G., Veiersted, K. B., Westgaard, R. H., & Winkel, J. (2010). Systematic evaluation of observational methods assessing biomechanical exposures at work. *Scandinavian journal of work, environment & health*, 3–24.
- Tichauer, E. (1971). A pilot study of the biomechanics of lifting in simulated industrial work situations. *Journal of Safety Research*, 3(3), 98–115.
- Tiwari, P., Gite, L., Majumder, J., Pharade, S., & Singh, V. (2010). Push/pull strength of agricultural workers in central india. *International Journal of Industrial Ergonomics*, 40(1), 1–7.
- Torres, Y., & Viña, S. (2012). Evaluation and redesign of manual material handling in a vaccine production centre's warehouse. *Work*, 41(Supplement 1), 2487–2491.

- Triggs, B., McLauchlan, P. F., Hartley, R. I., & Fitzgibbon, A. W. (1999). Bundle adjustment—a modern synthesis. *International workshop on vision algorithms*, 298–372.
- Tsang, P. S., & Velazquez, V. L. (1996). Diagnosticity and multidimensional subjective workload ratings. *Ergonomics*, 39(3), 358–381.
- Uusitalo, A., Mets, T., Martinmäki, K., Mauno, S., Kinnunen, U., & Rusko, H. (2011). Heart rate variability related to effort at work. *Applied ergonomics*, 42(6), 830–838.
- Vogler, A. (2005). Design study for an astronaut's workstation. *SAE transactions*, 529–540.
- Volkova, T. (2017). New generation of orbital station. *Master thesis, Moscow Institute of Architecture (State Academy)-ENSA Paris la Vilette, Moscow-Paris*, 120.
- Volkova, T., Nicollier, C., & Gass, V. (2022). An empirical and subjective model of upper extremity fatigue under hypogravity. *Frontiers in physiology. Research topic: Investigation of the Inter-Individual Variability of Physiological Responses to Changes in Activity Levels-, gravity Loading-, Nutritional Status, Pharmaceuticals and Exposure to Radiation*, 13.
- Volkova, T., Nicollier, C., & Gass, V. (2019). Defining best design practices for safety and comfort in moon and mars habitats. *conference proceeding 70th International Astronautical Congress (IAC), Washington D.C., United States, 21-25 October 2019*.
- Volkova, T., Nicollier, C., & Gass, V. (2021). Markerless motion capture method application for investigation of joint profiles in the workplace under simulated hypogravity. *conference proceeding International Astronautical Federation. Global Space Exploration Conference (GLEX 2021), St Petersburg Russian Federation, 14-18 June 2021*.
- von Meyer, H. (1853). Das aufrechte stehen. *Arch Anat Physiol*, 9–44.
- Wang, S., Tang, H., Wang, B., & Mo, J. (2021). A novel approach to detecting muscle fatigue based on semg by using neural architecture search framework. *IEEE Transactions on Neural Networks and Learning Systems*.
- Warburton, D. E., Jamnik, V., Bredin, S. S., Shephard, R. J., & Gledhill, N. (2019). The 2020 physical activity readiness questionnaire for everyone (par-q+) and electronic physical activity readiness medical examination (eparmed-x+): 2020 par-q+. *The Health & Fitness Journal of Canada*, 12(4), 58–61.
- Wei, S.-E., Ramakrishna, V., Kanade, T., & Sheikh, Y. (2016). Convolutional pose machines. *CVPR*.
- Wettig, J. (2002). New developments in standardisation in the past 15 years—product versus process related standards. *Safety science*, 40(1-4), 51–56.
- Williams, M. M., Hawley, J. A., Mckenzie, R. A., & van Wijmen, P. M. (1991). A comparison of the effects of two sitting postures on back and referred pain. *Spine*, 16(10), 1185–1191.
- Winkel, R., & Rgensen, K. (1986). Evaluation of foot swelling and lower-limb temperatures in relation to leg activity during long-term seated office work. *Ergonomics*, 29(2), 313–328.
- Winter, D. A. (2009). *Biomechanics and motor control of human movement*. John Wiley & Sons.
- Womersley, L., & May, S. (2006). Sitting posture of subjects with postural backache. *Journal of manipulative and physiological therapeutics*, 29(3), 213–218.

- Wong, A. Y., Chan, T. P., Chau, A. W., Cheung, H. T., Kwan, K. C., Lam, A. K., Wong, P. Y., & De Carvalho, D. (2019). Do different sitting postures affect spinal biomechanics of asymptomatic individuals? *Gait & posture*, 67, 230–235.
- Woodhull, A., Maltrud, K., & Mello, B. (1985). Alignment of the human body in standing. *European journal of applied physiology and occupational physiology*, 54(1), 109–115.
- Xia, T., & Law, L. A. F. (2008). A theoretical approach for modeling peripheral muscle fatigue and recovery. *Journal of biomechanics*, 41(14), 3046–3052.
- Xiang, Y., Arora, J. S., & Abdel-Malek, K. (2009). Optimization-based motion prediction of mechanical systems: sensitivity analysis. *Structural and Multidisciplinary Optimization*, 37(6), 595–608.
- Xu, R., Zhang, C., He, F., Zhao, X., Qi, H., Zhou, P., Zhang, L., & Ming, D. (2018). How physical activities affect mental fatigue based on eeg energy, connectivity, and complexity. *Frontiers in neurology*, 9, 915.
- Young, J. W., Chandler, R. F., Snow, C. C., Robinette, K. M., Zehner, G. F., Loftberg, M. S., et al. (1983). *Anthropometric and mass distribution characteristics of the adult female*. (tech. rep.). Civil Aerospace Medical Institute.
- Zabihhosseinian, M., Holmes, M. W., & Murphy, B. (2015). Neck muscle fatigue alters upper limb proprioception. *Experimental brain research*, 233(5), 1663–1675.
- Zatsiorsky, V. (1990). Methods of determining mass-inertial characteristics of human body segments. *Contemporary Problems of Biomechanics*.
- Zemp, R., Fliesser, M., Wippert, P.-M., Taylor, W. R., & Lorenzetti, S. (2016). Occupational sitting behaviour and its relationship with back pain—a pilot study. *Applied ergonomics*, 56, 84–91.
- Zhang, Z. (2000). A flexible new technique for camera calibration. *IEEE Transactions on pattern analysis and machine intelligence*, 22(11), 1330–1334.

TATIANA VOLKOVA

Nationality: Russian

 (+41) 766358746

Date of birth: 24/05/1989

 **Email address:** tatiana.volkova@epfl.ch

 **Address:** EPFL I-VP SIU PPH 338, Station 13, 1015 Lausanne (Switzerland)

ABOUT ME

My interdisciplinary technical skills, hands-on work and limitless passion have assisted me in solving complex and unpredictable problems.

WORK EXPERIENCE

PhD- Principal Investigator - Lausanne *Space Innovation/Swiss Federal Institute of Technology/EDCE* [15/05/2018 – Current]

- Conducting research on human biomechanics in the workplace under simulated moon gravity
- Conducting participant-based experiments in a neutral buoyancy facility
- Teaching assistant in Space Mission Design & Operations (Prof. C. Nicollier - ESA astronaut). Main disciplines: flight dynamics, propulsion, rendezvous, interplanetary missions.

Turnkey Biotech Plant Manager - Lyon/Moscow *Boccard* [01/03/2015 – 31/07/2017]

- Provided project management
- Performed technical solutions and design consulting
- Developed a new French business unit in Russia.

Sustainability Engineer - Paris *La Maison Passive* [01/01/2014 – 30/11/2014]

- Analyzed French design office and architectural solutions
- Optimized building energy performance (residential buildings and individual houses)
- Performed a building lifecycle analysis.

Thermal Performance Engineer - Moscow *Roscosmos company* [01/09/2009 – 01/09/2011]

- Analyzed space technology thermal performance
- Conducted structural analysis & simulations (Ansys)
- Prepared industry-based Master degree.

EDUCATION AND TRAINING

MEng: Technological Innovation, Engineering & Entrepreneurship - Paris *Ecole Polytechnique (I'X)* *Final grade: A* [01/09/2012 – 06/06/2014]

Graduate internship in Setec Batiment, Paris. Position: building physics and healthy indoor environment engineer

MEng: Aerospace engineer - Constructor/ MEcon : Economist - Manager - Moscow
Bauman Moscow State Technical University (Bauman MSTU). Final grade: A [01/09/2006 – 31/07/2012]

Dual degree. Space vehicles and Carrier Rockets / Economics and management of high-tech industry (space-related)

Additional education. Pilot student for single-engine airplane, PPL/A- Lausanne
Ecuvillens Aeroclub [01/02/2020 – Current]

Additional education. MArch: Architect - New generation orbital stations - Moscow/Paris
Moscow Architectural Institute (MARKHI)/ENSA Paris la Villette [01/09/2015 – 31/07/2017]

LANGUAGE SKILLS

Mother tongue(s): **Russian**

Other language(s):

French,

English

LISTENING C2 READING C2 WRITING C2

LISTENING C2 READING C2 WRITING C2

SPOKEN PRODUCTION C1 SPOKEN INTERACTION C1 SPOKEN PRODUCTION C1 SPOKEN INTERACTION C1

DIGITAL SKILLS

Microsoft Office / MathCad / TRNSYS / IESVE / Blender 2.8 / Revit / AutoCAD / Rhinoceros Grasshopper / OpenCV / Adobe InDesign / Python / MATLAB / ANSYS / Lightroom / C++

HOBBIES AND INTERESTS

Aviation PPL (A), open water diving (PADI Level 2), athletics, painting